MODIFICATION OF SURFACES WITH THIN ORGANIC FILMS BY REACTION WITH ARYLDIAZONIUM SALTS

A thesis

submitted in partial fulfillment

of the requirements of the Degree of

Doctor of Philosophy in Chemistry

in the

University of Canterbury

by

Joshua (Josua) Lehr

2010

Acknowledgements

I would like to thank Prof Alison Downard for her encouragement, guidance and support during the years of my PhD. I am also indebted to Prof Bryce Williamson for his valuable feedback on my work. A thank you must also go to all the (past and present) members of our research group, as well as the rest of the staff of the Department of Chemistry at the University of Canterbury.

I am grateful to all the staff and students in the Department of Electrical Engineering at the University of Canterbury for access to, and assistance with, their facilities. I would also like to thank the MacDiarmid Institute for making these facilities available. I am grateful to all my family and friends for their support. I am indebted to the Tertiary Education Commission, University of Canterbury, and the MacDiarmid Institute for PhD scholarships.

Table of Contents

Abstract i

Abbreviations ii

Publications iv

Chapter 1. Introduction 1

1.1 Properties of Carbon Surfaces Used 1

1.1.1 Glassy Carbon 1

1.1.2 Pyrolyzed Photoresist Films 4

1.2 Dediazoniation of Aryldiazonium Salts 7

1.3 Covalent Surface Modification using Aryldiazonium Salts 9

1.3.1 Electro-Induced Modification using Aryldiazonium Salts 9

1.3.2 Spontaneous Modification using Aryldiazonium Salts 18

1.3.3 Applications of Surfaces Modified using Aryldiazonium Salts 21

1.4 Aims 27

1.5 References 28

Chapter 2. General Experimental Methods 44

2.1 Introduction 44

2.2 Chemicals and Preparative Methods 44

2.2.1 Solutions 44

2.2.2 Preparation of Tetrabutylammonium Tetraflouroborate Electrolyte 44

2.2.3 Synthesis of Aryldiazonium Salts 45

2.2.4 Synthesis of Citrate-Capped Gold Nanoparticles 45

2.3 Surface Preparation 45

2.3.1 Glassy Carbon 45

2.3.2 Pyrolyzed Photoresist Film 46

2.3.3 Gold Surfaces 46

2.4 Electrochemistry 47
2.4.1 Instrumentation 47
2.4.2 Electrochemical Cells and Electrodes 47
2.5 Atomic Force Microscopy 49
2.5.1 Instrumentation 49
2.5.2 Imaging 49
2.5.3 *Film Thickness Measurements* 49
2.5.4 Determination of Surface Roughness 51
2.6 Scanning Electron Microscopy 51
2.7 Optical Microscopy 51
2.8 Water Contact Angle Measurements 52
2.9 X-Ray Photoelectron Spectroscopy 52
2.10 Atomic Absorption Spectroscopy 52
2.11 General Surface Modification Procedures 53
2.11.1 Electrochemical Modification of Surfaces 53
2.11.2 Spontaneous Modification of Surfaces 53
2.12 Data Analysis and Software 54
2.12.1 Determination of Charge and Electrochemical Surface Concentration 54
2.12.2 Software 55
2.13 References 56

Chapter 3. Modification of Glassy Carbon with Electro-Active Films by Electro-Reduction of Aryldiazonium Salts 57

3.1 Introduction 57
3.2 Experimental 58
3.3 Modification of GC with NP Films 59
3.3.1 Electro-Reduction of NBD at GC 59
3.3.2 Effect of NP Modification on Redox Probe Voltammetery of $Fe(CN)_6^{3-}$ 60
3.3.3 Electrochemistry of NP Modified GC 61
3.4 Modification of GC with NPOH Films 66

3.4.1 Electro-Reduction of HNBD at GC 66
3.4.2 Electrochemistry NPOH Modified GC 69
3.5 Modification of GC with AQ Films 70
3.5.1 Electro-Reduction of Anthraquinone Diazonium Cation at GC 71
3.5.2 Electrochemistry of AQ Modified GC 72
3.5.3 Stability of Redox Electrochemistry of AQ Modified GC 75
3.6 Conclusion 76
3.7 References 78

Chapter 4. Modification of Carbon Surfaces by Spontaneous Reaction of Aryldiazonium Salts 81

4.1 Introduction 81
4.2 Experimental 82
4.3 Spontaneous Modification of GC with NP Films 83
4.3.1 Electro-Reduction of NP Films Spontaneously Attached to GC 83
4.3.2 OCP Behavior of GC during Modification with NP Films 88
4.4 Spontaneous Modification of PPF with NP Films 92
4.4.1 Electro-Reduction of NP Films Spontaneously Attached to PPF 92
4.4.2 Atomic Force Microscope Film Thickness Measurements 98
4.4.3 Atomic Force Microscope Surface Roughness Analysis 101
4.4.4 Water Contact Angle Measurements 101
4.4.5 Stability of Spontaneously Prepared NP Films to Sonication 102
4.4.6 OCP Behavior of PPF during Modification with NP Films 103
4.5 Spontaneous Modification of PPF with CP Films 105
4.5.1 Water Contact Angles of CP Modified PPF 105
4.5.2 $Fe(CN)_6^{3-}$ Redox Probe Voltammetry of CP Modified PPF 106
4.5.3 Potential of Reduction of CBD 107
4.6 Conclusion 108
4.7 References 110

Chapter 5. Modification of Gold Surfaces by Spontaneous Reaction of Aryldiazonium Salts 114

5.1 Introduction 114
5.2 Experimental 117
5.3 Spontaneous Modification of Gold with NP Films 118
5.3.1 Effect of Solvent on Modification 118
5.3.2 Effect of Immersion Time on Surface Concentration of NP Films 120
5.3.3 XPS Characterization of NP and Reduced NP Films 122
5.3.4 AFM Film Thickness Measurements 124
5.3.5 Packing Density of NP Films 125
5.4 Role of the Gold Surface in NP Film Formation Process 126
5.4.1 OCP Behavior during NP Film Formation 126
5.4.2 Electrochemical Investigation of Gold Oxide Formation 129
5.4.3 AAS Investigation of Gold Ion Formation 131
5.5 Stability of Spontaneously Prepared NP Films at Gold 132
5.5.1 Stability in Vacuum 133
5.5.2 Stability to Sonication 133
5.6 Spontaneous Modification of Gold with CP and MP Functionalities 134
5.6.1 Potential of Reduction Peak for Various Aryldiazonium Salts at Gold 135
5.6.2 Spontaneous Modification of Gold with CP Films 136
5.6.3 Spontaneous Modification of Gold with MP Films 137
5.7 Conclusion 138
5.8 References 140

Chapter 6. Patterning Surfaces by Microcontact Printing Using Aryldiazonium Salts 144

6.1 Introduction 144
6.2 Experimental 146

6.3 Microcontact Printing of NP Films on PPF 149
6.3.1 Electro-Reduction of Printed NP Films 149
6.3.2 Effect of Printing Time on Surface Concentration 150
6.3.3 AFM Thickness Measurements of Printed NP Films 152
6.3.4 Density of Printed NP Films 154
6.3.5 Patterning of NP Films on PPF by μCP 155
6.4 Microcontact Printing of AP Films on PPF 156
6.4.1. Electrochemistry of Printed AP Films 156
6.4.2 Patterning of AP Films on PPF by μCP 157
6.5 Microcontact Printing CP Films on PPF 158
6.5.1 Printing of CP Films 159
6.5.2 Coupling of NA onto Printed CP Films 159
6.5.3 Patterning of CP Films on PPF by μCP 162
6.6 Preparation of Multi-Component Systems on PPF 163
6.6.1 Multicomponent Surfaces by the Fill-In Method 165
6.6.2 Multicomponent Surfaces by the Build-Up Method 165
6.7 Microcontact Printing on Gold 168
6.7.1 Printing of NP Films 169
6.7.2 Patterning of Gold Surfaces 170
6.8 Microcontact Printing on Silicon 172
6.8.1 Spontaneous Modification of Silicon with NP Films 172
6.8.2 Printing of NP Films on Silicon 172
6.8.3 Patterning of Silicon Surfaces 173
6.9 Microcontact Printing on Copper 174
6.10 Conclusion 175
6.11 References 177

Chapter 7. Covalent Attachment of Glucose Oxidase Hydrogel to Carbon Electrodes 181

7.1 Introduction 181

7.2 Experimental 185
7.2.1 Materials and Reagents 185
7.2.2. Preparation of Hydrogels 186
7.2.3. Immersion of Hydrogel Electrodes Samples in Phosphate Buffer 186
7.2.4 Electrochemical Determination of Enzymatic Activity 186
7.2.5 Modification via Reduction of Aryldiazonium Salts 187
7.2.6 Coupling of GOx to CP Modified Surfaces 187
7.2.7 Step Profilimetry 188
7.3 Activity and Stability of Physisorbed GOx Hydrogels 188
7.3.1 Dependence of Catalytic Activity on Glucose Concentration 188
7.3.2 Effect of Curing Time of Hydrogel on Enzymatic Activity 190
7.3.3 Long Term Stability of Activity of Physisorbed Hydrogels 194
7.4 Covalent Attachment of Glucose Oxidase Hydrogels 198
7.4.1 Covalent Attachment of Hydrogel using CP Films 198
7.4.2 Covalent Attachment of Hydrogel using AP Films 200
7.5 Stability of Activity of Covalently Attached GOx Hydrogels 201
7.5.1 *Stability to Immersion* 201
7.5.2 Stability to Sonication 203
7.6 Conclusion 204
7.7 References 206

Chapter 8. Conclusion 209

Abstract

In this work, the modification of conducting substrates with thin (nanometer thick) aryl films via reaction with aryldiazonium salts was investigated. Two methods were used: modification by electro-reduction of the aryldiazonium salts and modification by spontaneous reaction of aryldiazonium the salts with the surface at open circuit potential. The majority of the studies were undertaken using *p*-nitrobenenze diazonium salt, which gives electro-active nitrophenyl (NP) films at the surface that can be detected and characterized by cyclic voltammetry.

Films prepared spontaneously on carbon and gold electrodes at open circuit potential were characterized by electrochemistry, atomic force microscopy (AFM), X-ray photoelectron spectroscopy (XPS) and water contact angle measurements. At both carbon and gold, spontaneous modification proceeds via electron transfer from the surface to the diazonium salt. Furthermore, on both types of surface, spontaneously prepared NP films were found to be loosely packed multilayers of less than 5 nm in thickness.

The spontaneous reaction was utilized for the patterning of carbon, gold, silicon and copper surfaces by microcontact printing (μCP) with diazonium salts. The presence of spontaneously formed films upon printing was confirmed by cyclic voltammetry and AFM. The films were demonstrated to be useful for the tethering of further molecules to the surface. Patterns prepared by μCP were imaged using scanning electron microscopy (SEM) and condensation figures. The preparation of two-component systems, with different chemical functionalities attached to different, well-defined, regions of the surface, was demonstrated.

The optimization of the long term activity of glucose oxidase hydrogels by covalent attachment of the hydrogels to modified carbon electrodes was investigated. Covalent attachment was demonstrated, but the resulting electrode-hydrogel surfaces did not show long-term activities superior to those for physisorbed hydrogels. It is suggested that the limiting factor for long-term hydrogel activity is not adhesion of the hydrogel to the surface, but degradation of enzymatic activity by H_2O_2.

Abbreviations

AAS	Atomic absorption spectroscopy
ABD	*p*-Aminobenzene diazonium chloride
AP	*p*-Aminophenyl
APOH	*p*-Hydroxyaminophenyl
ACN	Acetonitrile
AFM	Atomic force microscope
Aq	Aqueous
AQ	Anthraquinone
CA	Current amplification
CBD	*p*-Carboxybenzene diazonium tetrafluoroborate salt
CNT	Carbon nanotube
CP	*p*-Carboxyphenyl
EAS	Electrophilic aromatic substitution
EDC	*N*-ethyl-*N*'-(3-dimethylaminopropyl) diimide hydrochloride
FcOH	Ferrocene methanol
GC	Glassy carbon
GOx	Glucose oxidase
HNBD	4-Hydroxy-3-nitrobenzene diazonium tetrafluoroborate salt
HOPG	Highly ordered pyrolytic graphite
IRRAS	Infrared reflectance absorption spectroscopy
μCP	Microcontact printing
MBD	*p*-Methoxybenzene diazonium tetrafluoroborate salt
MP	*p*-Methoxyphenyl
MQ	Milli Q water
NA	*p*-Nitroaniline
NBD	*p*-Nitrobenzene diazonium tetrafluoroborate salt
NHS	*N*-hydroxysuccinimide
NP	*p*-Nitrophenyl
NPOH	*o*-Nitrophenol

OCP	Open circuit potential
PB	Phosphate buffer
PDMS	Poly(dimethylsiloxane)
PEGDGE	Poly(ethylene glycol) diglycidyl ether
PPF	Pyrolyzed photoresist film
SAM	Self-assembled monolayer
SCE	Saturated calomel reference electrode
SEM	Scanning electron microscope
TOF-SIMS	Time-of-flight secondary-ion mass spectroscopy
XPS	X-ray photoelectron spectroscopy

Publications

Publications resulting from work described in this thesis

Garrett, D.J.; Lehr J.; Miskelly, G.M.; Downard, A. J., Microcontact Printing Using the Spontaneous Reduction of Aryldiazonium Salts. *Journal of the American Chemical Society*; **2007**, 129, 15456-15457.

Lehr, J.; Williamson, B.E.; Flavel, B.S.; Downard, A. J., Reaction of Gold Substrates with Diazonium Salts in Acidic Solution at Open-Circuit Potential. *Langmuir*; **2009,** 25**,** 13503-13509.

Lehr, J.; Williamson, B.E.; Barrière, F.; Downard, A.J.; Dependence of Catalytic Activity and Long-Term Stability of Enzyme Hydrogel Films on Curing Time, *Bioelectrochemistry,* **2010,** 79 142-146.

Lehr, J.; Garrett, D.J.; Paulik, M.; Flavel, B.S.; Brooksby, P.A; Williamson, B.E; and Downard, A.J, Patterning of Carbon, Metal and Semiconductor Substrates with Thin Organic Films by Microcontact Printing with Aryldiazonium Salt Inks, in preparation for submission to *Analytical Chemistry.*

Other Publications

Flavel, B.S.; Garrett, D.J.; Lehr, J.; Shapter, J.G.; Downard, A.J.; Chemically immobilised carbon nanotubes on silicon: Stable surfaces for aqueous electrochemistry, *Electrochimica Acta*, **2010**, 55, 3995-4001.

Chapter 1. Introduction

The modification of surfaces with thin films incorporating specific chemical functionalities has been a significant area of research over the past few decades. Applications of modified surfaces in molecular electronics, the development of sensors, fabrication of catalytic surfaces, and cell studies have motivated this research.[1-5] The most widely used method of surface modification with thin organic films is the formation of self assembled monolayers (SAMs) using thiol chemistry. This method of modification has been shown to proceed at number of metal surfaces, including Au, Ag, Cu, and Pd. The resulting molecular layers are often well defined monolayers.[1, 6, 7] Silanes have also been used to modify SiO_2 surfaces giving stable monolayers.[8, 9]

In recent years, the modification of surfaces via reduction of aryldiazonioum salts has received considerable attention.[10-12] The resulting films are often strongly bound to the surface via a covalent bond between the surface and the modifier, and generally exhibit higher stability than the SAMs formed using thiol chemistry. Diazonium cation chemistry been used to modify a large number of carbon, metal and semiconductor surfaces.[11] In this thesis, the mechanism of formation, characteristics, and some possible applications of diazonium salt derived films are investigated.

1.1 Properties of Carbon Surfaces Used

The majority of the work described in this thesis has been conducted at carbon surfaces. It is therefore appropriate to review the structure and characteristics of the carbon surfaces used.

1.1.1 Glassy Carbon

Since it was first produced in the 1960s glassy carbon (GC) has become a commonly used material in electrochemistry. GC is generally produced from polymeric resins, such as

polyacrylonitrile or phenol/formaldehyde polymers, by heating (generally under pressure) to temperatures between 1000 and 3000 ºC. This process is referred to as 'carbonization' or 'pyrolysis'. The result is a hard, conductive carbon material that is impermeable to solution.[13-16] GC is available commercially in many forms such as disks, plates, rods and crucibles.

Considerable research aimed at elucidating the structure of GC has been undertaken. Jenkins and coworkers initially proposed that the structure of GC consists of entangled graphitic aromatic ribbons.[13] A different model has been put forward by Oberlin, who has proposed that GC consists of crumpled graphite-like sheets.[16] These two models are often seen to be contradictory. However, as Gopel and coworkers have pointed out[17], Oberlin's model can be seen as complementary to that of Jenkins, giving a detailed account of the structure of the entangled ribbons. In this view the ribbons are composed of stacked planar aromatic structures (graphene sheets, Figure 1.1). This model predicts that GC contains both basal-plane and edge-plane carbon sites.[17]

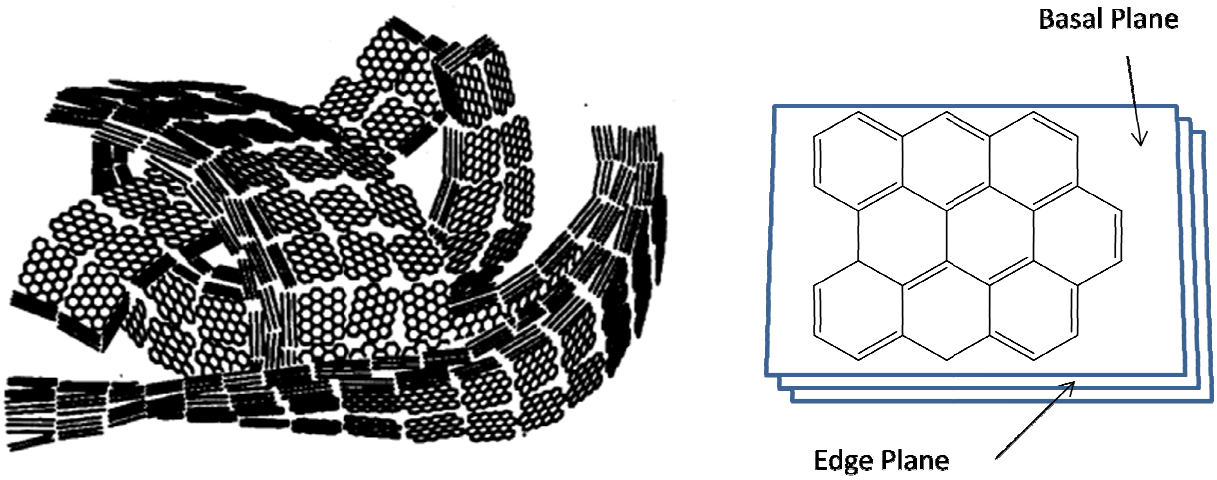

Figure 1.1. Proposed structure of glassy carbon. Reproduced from reference 17.

Graphene edge-plane sites exist in two general forms: zigzag sites (Figure 1.2 (a)) and armchair sites (Figure 1.2 (b)). Figure 1.2 (c) shows specific chemical functionalities believed to be present at the edges of graphene sheets. A significant number of these are oxygen containing, including carboxylic acid, phenol, ketone, and quinone groups.[17-20] However there is also evidence for oxygen-free carbon edge sites.[21-23] The existence of free 'σ-dangling bonds' at

graphene edge planes has been proposed;[24] however these are unlikely to be stable under ambient conditions.[25] It has also been proposed that hydrogen saturated sites are present at graphic edge planes, although complete saturation of the edge plane is inconsistent with significant experimental data.[25] Radovic and Bockrath have proposed that a significant number of the graphene edge sites are carbene- and carbyne-like functionalities (Figure 1.2 (a) and (b)), which theoretical calculations reveal should be stable in ambient conditions.[23]

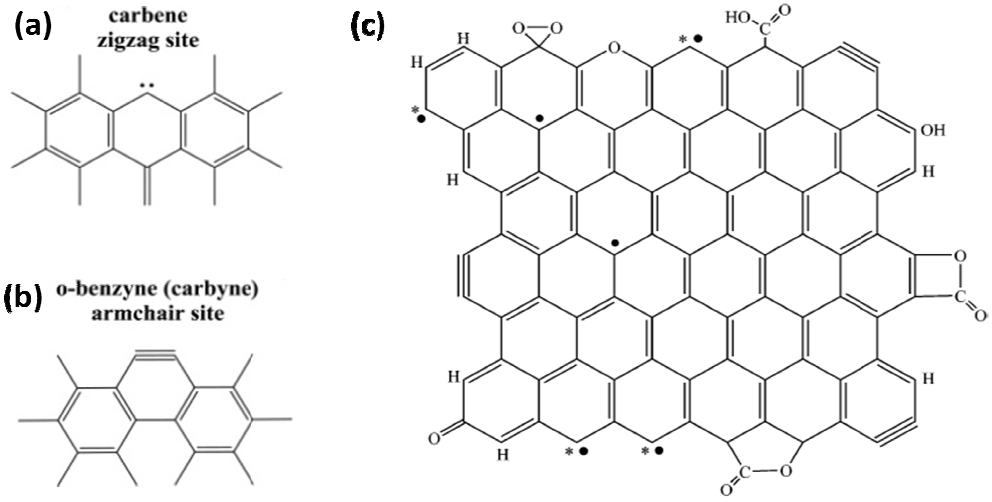

Figure 1.2. Functionalities present on glassy carbon edge plane. Reproduced from reference 23.

More recently Harris has observed the presence of fullerene-like components when GC was analyzed using high resolution transmission electron microscopy, and hence, proposed a fullerene-like microstructure.[15] In this view, GC is composed of broken or imperfect fullerene-related fragments with pentagons and heptagons distributed randomly throughout sheets of hexagons.[15] Due to the broken nature of the fullerene fragments this model also predicts the presence of carbon edge planes.

Heterogeneous rate constants for common redox systems have been shown to be significantly higher at edge-plane-rich GC than at highly ordered pyrolytic graphite (HOPG), which has relatively few edge plane sites.[26] Furthermore, treatment of HOPG, to expose more edge planes, has been shown to lead to faster rates of electron transfer.[26, 27] Hence, electron transfer is generally believed to be much faster at the edge plane sites than at the basal plane sites of GC.

However, scanning micropipet experiments, recently carried out by Unwin and coworkers on HOPG, suggest that the basal plane electron transfer activity is much greater than generally thought.[28].

Treatment of GC prior to use is important for obtaining reproducible electrodes surfaces. Several pretreatment methods have been reported in the literature. The most common of these are electrochemical pretreatment and mechanical polishing.[17, 29-33] Electrochemical pretreatment, generally consisting of anodization (sometimes followed by cathodization) in aqueous conditions, leads to increased capacitance and oxidation of the edge plane sites.[17, 29-31] Mechanical polishing is generally carried out by polishing the GC electrodes on a cloth with ~1 μm particle size alumina or diamond paste, followed by sonication in an appropriate solvent to remove the polishing agent. The procedure does not lead to an increase in capacitance or surface oxygen functionalities,[17] and therefore was used as the pretreatment method for GC electrodes in this thesis. The reported root-mean square surface roughness (rms) of polished GC ranges from (4.1 ± 0.1)[34] to (44 ± 6)[35] nm.

1.1.2 Pyrolyzed Photoresist Films

Pyrolyzed photoresist film (PPF) was first prepared by Kinoshita and coworkers in the late 1990s.[36] The preparation method consists of spin coating Novalak type photoresist onto silicon pieces, and then heating in a nitrogen atmosphere to pyrolyze the photoresist. Pyrolysis has been investigated by heating to maximum temperatures between 600 and 1100 ºC. The properties of the resulting PPF depend on the temperature that the pyrolysis is carried out at. Thermal gravimetric analysis shows considerable weight loss between 150 and 450 ºC, believed to be associated with the loss of H_2O, CO, and CO_2 from the photoresist.[36, 37] Further weight loss at higher temperatures has been assigned to aromatization.[37] Significant shrinkage was also observed upon pyrolysis, with the photoresist film thickness decreasing from 6-8 μm to ~1-2 μm.[36-38] Atomic force microscopy measurements have shown a rms surface roughness for PPF pyrolysed at ~1000 ºC of 0.2 to 0.5 nm;[38, 39] much lower than polished GC (see previous Section).

High resolution transmission electron microscopy of PPF pyrolysed at 1100 ºC has shown the presence of graphite-like nanocrystals with an average crystallite size of 2.8 nm.[36, 37] Raman spectroscopy of PPF shows two distinct bands; a D band at ~1360 cm^{-1}, and an E_{2g} band at ~1580 cm^{-1}. The D band is assigned to the breakage of symmetry at graphitic edge planes, while the E_{2g} band has been assigned to graphitic basal planes.[26, 37, 38] Hence, a larger D/E_{2g} integrated intensity ratio is indicative of a more disordered structure containing smaller graphitic crystals and a higher proportion of edge plane sites to basal plane sites.[37, 38, 40] HOPG has a D/E_{2g} ratio of 0.0027 to 0.012, indicative of a low proportion of edge planes.[40] Polished GC has a much larger D/E_{2g} ratio of 1.53 to 1.93, indicative of a significantly greater number of edge planes.[40] Precise D/E_{2g} ratios have not been reported for PPF. However, visual inspection of published Raman spectra of PPF surfaces[37, 38] suggests D/E_{2g} ratios similar to, or greater than, those for GC, indicative of a high proportion of edge plane sites and a small crystallite size, consistent with the microscopy data above. The D/E_{2g} ratio was found to be constant when different 10 µm areas were sampled along a 900 µm line, suggesting a uniform microstructure across the PPF surface.[37] However, the D/E_{2g} ratio was seen to increase with increasing pyrolysis temperature up to 1100 ºC, indicating that the number of edge planes increases, and the crystallite size decreases, with increasing pyrolysis temperature.[38]

An X-ray photoelectron spectroscopy (XPS) study of the chemical composition of a PPF surface revealed an oxygen/carbon (O/C) ratio of 2.3 (±0.5) % after pyrolysis at 1000 ºC in forming gas (95% N_2 + 5% H_2). This is lower than for polished GC which, in the same study, was found to have an O/C ratio of 6.7 (±0.5) %.[39] It has been suggested that PPF's low O/C ratio is due to the presence, during heating, of hydrogen, which would react with trace oxygen thus preventing oxidation of the surface.[39] The oxidation of PPF after exposure to air has also been shown to be much less rapid than for heat treated GC.[37] The XPS-determined O/C ratio decreases between 500 and 600 ºC, with no change observed above 600 ºC. However, the O_{1s} peak consists of two components: one at a binding energy of ~231 eV assigned to C-O oxygen, and one at ~233 eV assigned to the C=O oxygen. As the pyrolysis temperature was increased from 500 ºC to 1100 ºC, the C=O signal increased at the expense and the C-O signal, suggesting more surface oxygen is present in carbonyl form for PPF pyrolyzed at high temperatures.[38]

Pyrolysis temperature also has an effect on the sheet resistance of PPF, which decreases with maximum pyrolysis temperature from > 700 Ω square^{-1} at 600 ºC to < 60 Ω square^{-1} at 1100 ºC.[36, 37] Hence, PPF pyrolyzed at higher temperatures (> 1000 ºC) is more suitable for electrochemical applications than PPF pyrolyzed at lower temperatures.

The rate of electron transfer at PPF surfaces has been investigated with $Ru(NH_3)_6^{3+/2+}$ and $Fe(CN)_6^{3-/4-}$ redox probe voltammetry. $Ru(NH_3)_6^{3+/2+}$ is an outer-sphere redox probe, which is relatively insensitive to surface species at carbon, whereas $Fe(CN)_6^{3-/4-}$ is a surface-sensitive inner-sphere redox probe.[41] The separations between the oxidation and reduction peaks (ΔE_p) in the cyclic voltammograms of both $Ru(NH_3)_6^{3+/2+}$ and $Fe(CN)_6^{3-/4-}$ were found to be smaller for PPF pyrolyzed at higher temperatures, indicating faster electron transfer between the surface and the redox species in solution.[36, 37] This can be attributed to the decrease in resistance and filling in of the band-gap during pyrolyisis.[37] Cyclic voltammetry has also shown a relatively low capacitance of ~8 μF cm^{-2} for PPF, compared to ~ 35 μF cm^{-2} for GC after heat treatment at 1000 ºC.[37] The low capacitance of PPF, which is probably due to its lower surface roughness,[37] results in low background current, making PPF attractive for electroanalytic sensing applications.

Recently, Gooding and coworkers investigated the variables associated with the fabrication of PPF at pyrolysis temperatures between 1000 and 1100 ºC.[42] They found that slower gas flow rates gave rougher surfaces. Furthermore, the resistivity of the PPF samples was seen to depend on their position in the furnace, with those in the middle having lower resistivity than those at the ends. This could be due to a higher heating capacity in the middle of the furnace tube, despite claims from manufacturers that the heat should be uniform within the relevant region.[42] This suggests that considerable difficulty could be experienced in the fabrication of reproducible PPF samples.

In this thesis the preparation of PPF was undertaken in a forming gas (95% N_2 + 5% H_2) atmosphere at a pyrolysis temperature of 1060 ºC. These conditions would be expected to result in low resistivity PPF with fast electron transfer kinetics and a low O/C ratio. For further details, see Section 2.3.2.

1.2 Dediazoniation of Aryldiazonium Salts

Modification of surfaces via reaction with aryldiazonium salts is generally thought to proceed via dediazoniation, which results in the formation of the highly stable molecular dinitrogen, and for which there are two common pathways; homolytic (Scheme 1.1) and heterolytic cleavage (Scheme 1.3).[43]

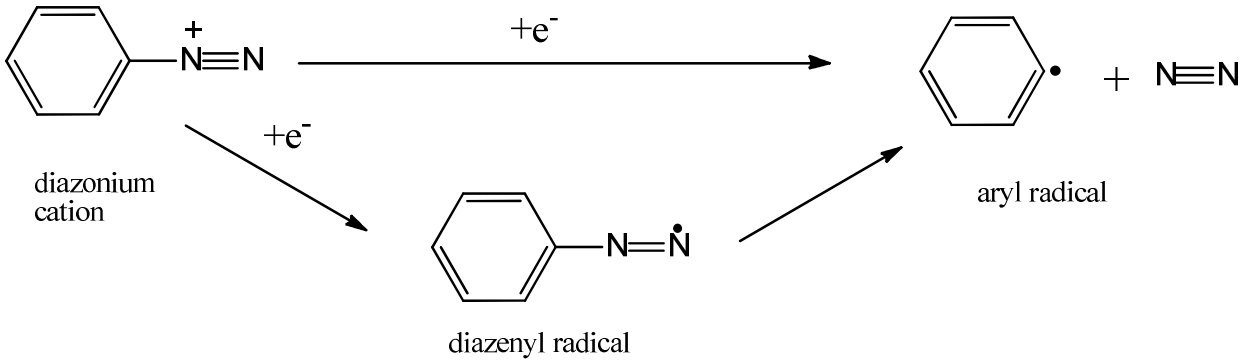

Scheme 1.1. Homolytic dediazoniation of benzenediazonium cation.

Homolytic cleavage proceeds via electron transfer from an electron donor to the diazonium cation. It can result in the formation of an unstable diazenyl radical which decomposes to give an aryl radical and dinitrogen. Alternatively, it can proceed in a concerted fashion without the formation of a diazenyl radical. Reduction can be brought about electrochemically[44], by chemical reduction[45-51] or photochemically.[43, 52] In the electrochemically induced reaction, the electron donor is the electrode. A variety of chemical reducing agents have been used to achieve homolytic dediazoniation including metal cations, [45, 49, 50]anions,[46-48, 50] and solvents[51]. Photochemical dediazoniation proceeds from the excitation of a charge-transfer complex between the diazonium cation and a counterion, with the counterion essentially acting as a reducing agent.[43, 52] It has been suggested that this can occur to a small extent in daylight.[43] For this reason all experiments involving the modification of surfaces via spontaneous reaction with aryldiazonium salts (Chapters 4 and 5) were conducted in the absence of light.

Elofson and coworkers have investigated the effect of various *para* substituents on polarographic half wave reduction potential ($E_{1/2}$) of benzene diazonium salts.[44] They found that electron donating substituents shift $E_{1/2}$ to more negative potentials and electron withdrawing substituents shift it to more positive potentials. Hence, the ease of reduction of a *para* substituted benzene diazonium salts increases as the *para* substituent becomes more electron withdrawing.[44]

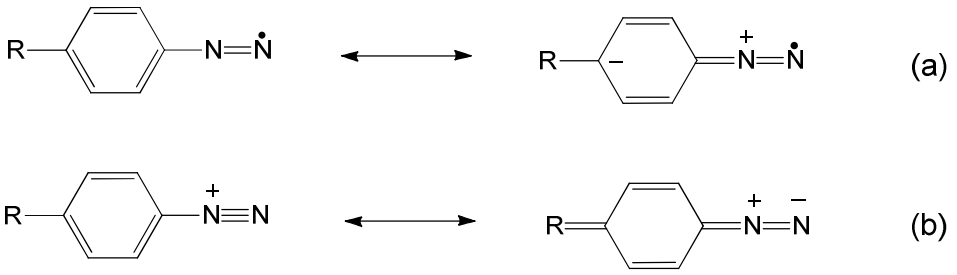

Scheme 1.2. Stabilization of diazenyl radical by *para* electron withdrawing group (a) and stabilization of diazonium cation by *para* electron donating group (b).

This has been attributed to the resonance stabilization of the diazenyl radical by election withdrawing groups (Scheme 1.2 (a)) and the stabilization of the diazonium salts by electron donating groups (Scheme 1.2 (b)).[43, 51] The stabilization of diazonium cations by electron donating *para* substituents has also been predicted by theoretical calculations.[53]

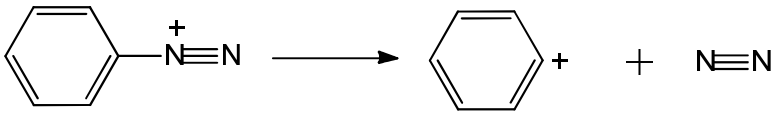

Scheme 1.3. Heterolytic dediazoniation of benzene diazonium cation.

An alternative reaction pathway for aryldiazonium salts is heterolytic dediazoniation (Scheme 1.3). Heterolytic dediazoniation proceeds via loss of dinitrogen and formation of an aryl cation. Unlike homolytic dediazoniation, the process does not take place via electron transfer from an external source to the diazonium cation; rather the reaction is a thermal decomposition.[43, 51, 54, 55]

Whether the homolytic or heterolytic dediazoniation occurs depends on the experimental conditions. In the presence of an electron source (electrode or reducing agent) the homolytic pathway is almost always preferred.[43, 55] Higher temperatures favor the heterolytic pathway.[43, 55] The solvent also has a significant effect on the reaction pathway. Solvents with a higher nucleophilicity generally favor the homolytic pathway. This can be accounted for a by a mechanism in which the solvent acts as an electron donor to the diazonium cation, leading to the production the aryl radical.[51]

1.3 Covalent Surface Modification Using Aryldiazonium Salts

Dediazoniation of aryldiazonium cations close to a surface can lead to attack of the dediazoniation product on the surface, resulting in the formation of covalently bound film at the surface. The mechanism of film formation, the characteristics of the films, and their possible applications are discussed in this section.

1.3.1 Electro-Induced Modification using Aryldiazonium Salts

In 1992, Pinson and coworkers published a paper describing the modification of GC electrodes with *p*-nitrophenyl (NP) films via electro-reduction of *p*-nitrobenzene diazonium salt (NBD).[10] Since that time there have been numerous reports of the modification of carbon,[2, 56-94] metal[92, 95-109] and semiconductor[110-116] surfaces via electro-reduction of a wide range of aryldiazonium salts.

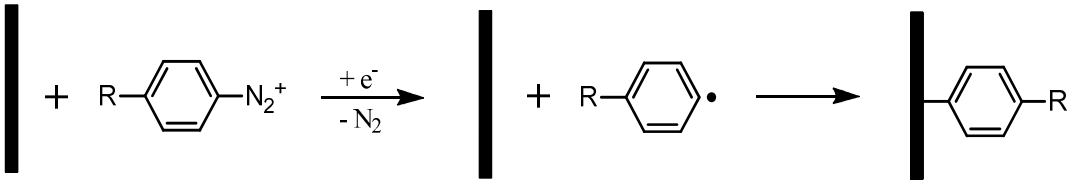

Scheme 1.4. Proposed mechanism for modification of surfaces via reduction of aryldiazonium salts

Since the modification is carried out by electro-reduction, it is generally assumed that it proceeds via homolytic dediazoniation to generate an aryl radical which subsequently attacks the surface resulting in the formation of a covalent bond (Scheme 1.4). It has been shown that under the conditions generally used for modification, homolytic cleavage occurs in a concerted fashion, without the formation of a diazenyl radical intermediate.[67]

There is considerable evidence for the existence of covalent bonds between the aryl modifiers and surfaces. Diazonium cation derived films at GC are stable to extensive sonication treatment, heating to 700 K in a vacuum,[56] and over a relatively large potential window (~ -2.0 to 1.8 V vs. Ag/AgCl) in aqueous conditions.[70] This high stability is evidence for the existence of a strong C-C bond between the surface and the modifier. The absence of the diazonium cation functionality upon modification has been observed by infrared spectroscopy[77] and XPS[94] indicating the diazonium functionality reacts during modification. Spectroscopic evidence of a covalent bond between the carbon surfaces and the aryl modifiers has also been found. Time-of-flight secondary-ion mass spectroscopy (TOF-SIMS) of diazonium cation derived films on GC has shown molecular fragments consisting of both film and electrode material, suggesting covalent bonding between the film and the GC.[74] Furthermore, polarized Raman spectroscopy of diazonium cation derived films at PPF indicates that the modifiers are predominantly orientated perpendicular to the surface, consistent with covalent attachment.[77]

Evidence of covalent binding is not restricted to carbon surfaces. XPS has shown the existence of C-Fe and C-Cu bonds after electrochemical modification of Fe and Cu, respectively, using diazonium salts.[95, 96] Infrared reflection absorption spectroscopy has demonstrated the loss of the diazonium cation moiety and the presence of NP groups orientated perpendicular to the surface, upon electrochemical reduction of NBD at gold surfaces.[99]

McCreery and coworkers observed that the modification via electro-reduction of aryldiazonium salts occurs at both the edge planes and basal planes of carbon.[57] Later McDermott and coworkers found that attachment occurs at the more reactive edge plane sites first, and at the basal plane only at longer deposition times.[60] This is not surprising considering the faster rates of heterogeneous electron transfer observed at the edge plane (see Section 1.1). Furthermore, the

findings are consistent with theoretical calculations that predict higher bond energy gains for attachment of the phenyl groups to the edge plane sites (265 and 107 kJ mol^{-1} respectively for zigzag and armchair sites) than to the basal plane sites (24 kJ mol^{-1}).[117] Attachment is not limited to carbon sites; TOF-SIMS has been used to show that modifiers also attach to surface oxygen functionalities at GC.[74]

After modification of HOPG with *p*-diethylaniline via electro-reduction of the corresponding diazonium cation, McDermott and coworkers observed nucleated clusters up to 2.5 nm in height on the surface. Since the length of *p*-diethylaniline is ~0.8 nm,[60] it was proposed that multilayer formation can occur via coupling of further aryl radicals to those already immobilized on the surface.[60] Formation of multilayers has also been shown to occur at GC, PPF, Si and metal surfaces.[11, 61, 62, 68, 69, 72, 74, 95, 113] Combellas and coworkers have proposed that multilayer formation occurs via aromatic homolytic substitution (Scheme 1.5).[11, 74] For steric reasons, attack of the radical on the *para*-substituted surface-bound aryl groups is believed to occur *ortho* to the R group (i.e. *meta* to the surface).[11]

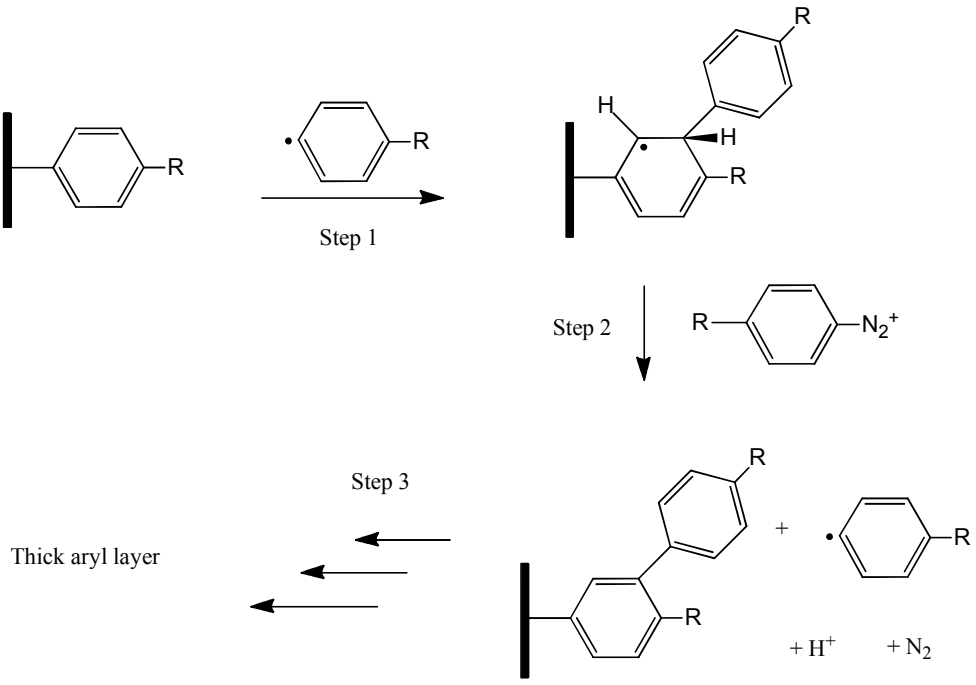

Scheme 1.5. Proposed mechanism for formation of multilayers upon modification of surfaces by reduction of aryldiazonium salts via aromatic homolytic substitution.[74]

In the proposed mechanism, an aryl radical attacks a previously bound aryl group resulting in the formation of a surface bound cyclohexadienyl radical (Scheme 1.5, step 1). A diazonium cation oxidizes the cyclohexadienyl radical and is thereby reduced (Scheme 1.5, step 2) resulting in another aryl radical and further propagation of the film. This film growth process is self sustaining and can, in principle, go on indefinitely.[74] However, significant amounts of data indicate that film growth is actually self limiting. Downard and coworkers have shown that the films self limit at thicknesses that depend on the potential applied to achieve modification.[61, 69] More negative applied potentials result in films that become self limiting at higher surface concentrations and film thicknesses. This indicates that film growth requires effective electron transfer from the substrate to diazonium cation in solution, which can occur through thicker films at more negative applied potentials.[61] Hence, it appears that multilayer formation does not occur primarily via reduction of diazonium cations by cyclohexadienyl radicals (Scheme 1.5, step 2) but rather via reduction of diazonium cations by the surface.

If step 1 of Scheme 1.5 is correct, the question arises as to the fate of the unstable cyclohexadienyl radical. The possibility of oxidation of the radical by the surface is unlikely since a negative potential is applied during modification. A more plausible reaction pathway, suggested by Combellas and coworkers, is a disproportionation reaction between two surface bound cyclohexadienyl radicals (Scheme 1.6).[74]

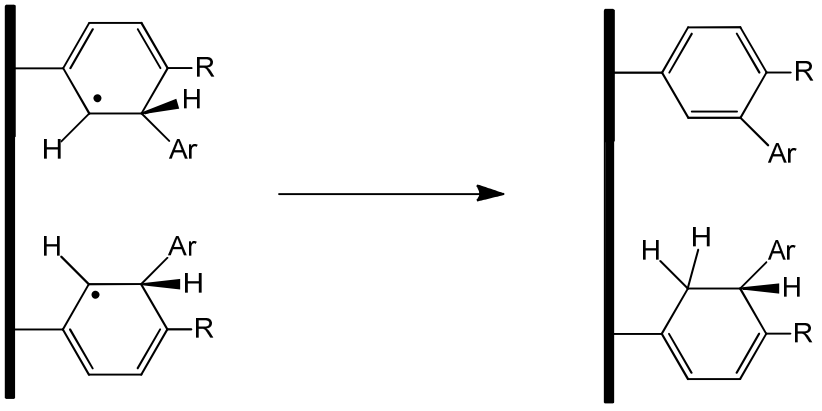

Scheme 1.6. Proposed disproportionation reaction between two surface bound cyclohexadienyl radicals.[74]

A consequence of this mechanism is that a significant amount of cyclohexadiene groups are included in the film structure; and indeed, some of the fragments detected by TOF-SIMS from NP films on GC can be interpreted as indicating the presence of cyclohexadiene groups.[74] Another possible mechanism by which the cyclohexadienyl radicals can react without reducing diazonium catons is given in Scheme 1.7. Here an aryl radical, produced by electrochemical reduction by the surface, acts in essentially the same manner as the •OH radical in the Gomberg-Bachmann reaction[118], gaining a H atom and restoring the aromaticity of the ring.

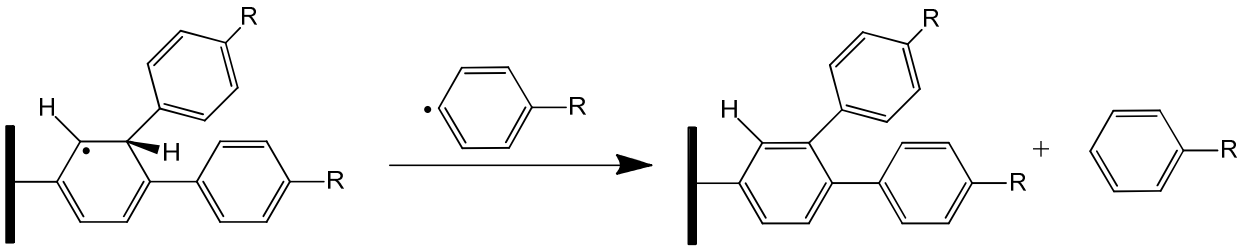

Figure 1.7. Proposed alternative reaction of cyclohexadienyl radicals via Gomberg-Bachmann type mechanism.

It is plausible that both the disproportionation reaction shown in Scheme 1.6 and the mechanism proposed in Scheme 1.7 account for the fate of the cyclohexadienyl radical.

TOF-SIMS and XPS have confirmed the presence of azo linkages in benzene diazonium cation derived films at carbon and metal surfaces.[58, 83, 93, 95, 96, 119] Bélanger and coworkers proposed that aryl groups can bind directly to carbon surfaces via azo linkages, by the mechanism shown in Scheme 1.8.[58] The mechanism is supported by TOF-SIMS data, which have shown the presence of C(OH)-C-N=N-C_6H_5 fragments at aryl modified GC.[83] Pinson and coworkers pointed out that a similar mechanism could operate on metals, if surface oxides are present.[96] However, there is also evidence that azo groups not only bind directly to the surface, but are also incorporated into the multilayer film structure by binding to aryl groups already attached to the surface. McCreery and coworkers have confirmed that this occurs at diazonium cation-derived multilayer films at oxide-free Cu surfaces.[119] The presence of a single nitrogen XPS peak assigned to the azo group indicates that the Cu-N=N-Ar moieties are unlikely, since they would be expected to give two azo nitrogen signals.[119] TOF-SIMS has confirmed the presence of Ar-N=N-Ar type fragments in

films formed at Cu and Fe.[83] Hence, there is significant evidence that azo groups are incorporated into the multilayer film structure and not exclusively bound directly to the surface.

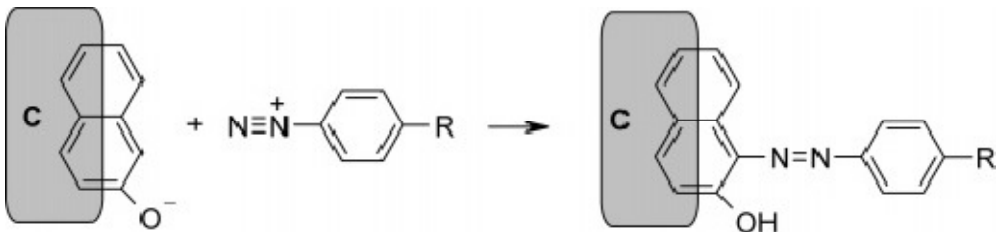

Scheme 1.8. Proposed mechanism for attachment of diazonium cations to GC leading to formation of azo linkages. Reproduced from reference 58.

McCreery and coworkers have proposed that azo linkages can be incorporated into a multilayer film structure via electrophilic aromatic substitution (EAS; Scheme 1.9). Electron donation by the surface into a surface bound phenyl group activates the carbons *ortho* and *para* to the surface-aryl bond leading to EAS at these positions and the formation of an Ar-N=N-Ar moiety in the film structure.[119]

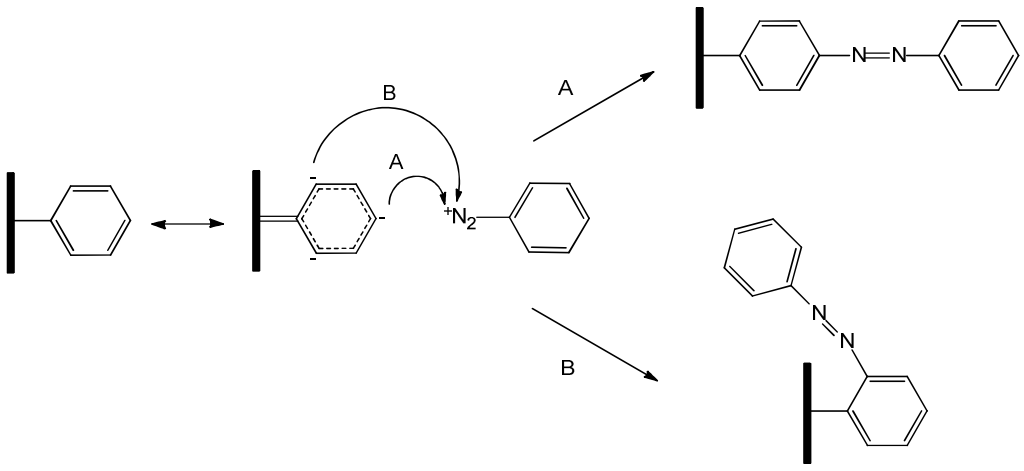

Scheme 1.9. Incorporation of azo linkages into multilayer film structure via EAS.

In support of this mechanism, films formed at oxide-free Cu have a higher azo content than those formed at Cu-O surfaces, as would be expected for the EAS mechanism since the activation should be much more effective though Cu-Ar than through Cu-O-Ar bonds.[119] However, azo bonds have been detected in films derived from *p*-nitrobenezene diazonium salt,[58, 93, 119] where EAS *para* to the surface is not possible. Furthermore loss of *p*-NO_2 does not occur during multilayer formation.[72] EAS on the *ortho* position is highly unlikely due to the unfavorable resulting steric interactions between the N=N-Ar moiety and the surface. The steric issue is resolved if azo bond formation occurs in outer layers of the film rather than at aryl groups attached directly to the surface. However, effective activation of the aryl groups is unlikely to occur further from the surface, especially since aryl groups are expected to attach (by radical attack) to the (unactivated) carbon *meta* to the bond to the surface. Hence, EAS does not satisfactorily account for the formation of azo linkages in multilayer films derived from *p*-nitrobenzene diazonium salt.

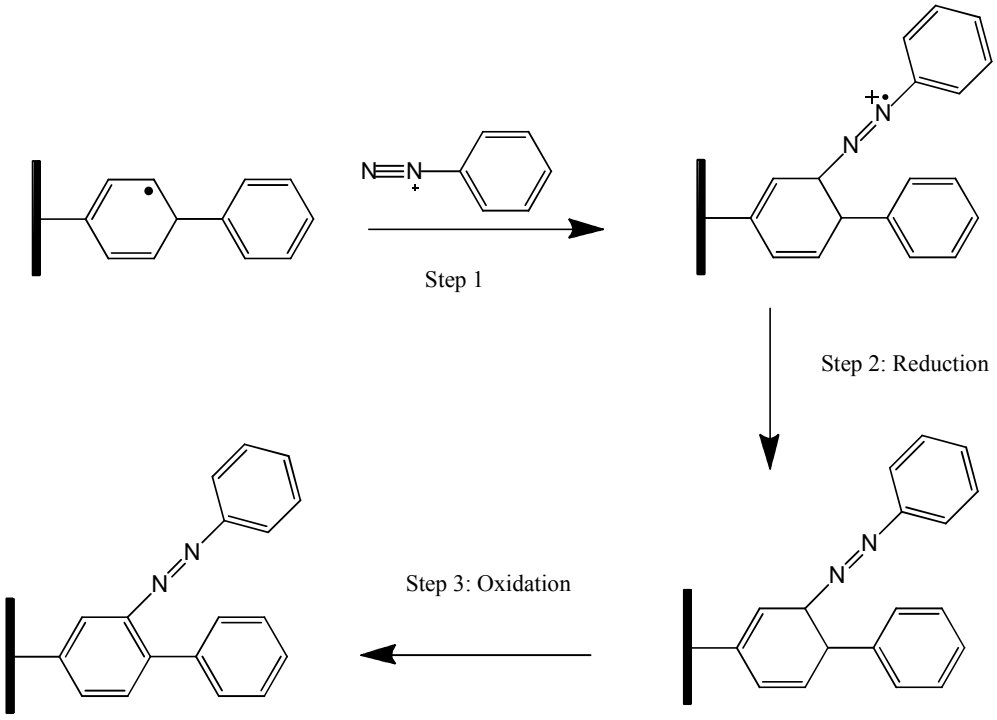

Scheme 1.10. Mechanism for incorporation of azo bonds into diazonium derived film proposed by Pinson and coworkers.[83]

Another mechanism for the incorporation of azo linkages into multilayer films, suggested by Pinson and coworkers, was expressed in terms of modification with unsubsituted benzene diazonium cations, as shown in Scheme 1.10. [83] They proposed that the diazonium cation attacks the surface-bound cyclohexadienyl radical (Scheme 1.10, step 1) that is produced from an aryl radical attacking a surface bound benzene group (see above). Subsequently, the resulting moiety is reduced (step 2) and then oxidized (step 3), resulting in the incorporation of the azo group in the film.[83] However, as discussed above, azo bonds are present in films derived from *p*-nitrobenzene diazonium salt. If the mechanism in Scheme 1.10 were to occur at a *para*-substituted film, attachment of the diazonium cation would have to occur *meta* to the *para* substituent (and *ortho* to the bond to surface). For steric reasons this is highly unlikely. However, it is possible that azo coupling occurs, in the manner shown by Scheme 1.10, but at aryl groups that are not directly bound to the surface. This is consistent with the observation that the azo content of NP films at Cu increases with film thickness.[119]

The packing density of multilayers formed by electro-reduction of diazonium cations at PPF has also been examined. NP films formed at PPF via electro-reduction of the corresponding diazonium salt are loosely packed multilayers with packing densities of ~25 % of that of ideal tight-packed systems.[69] There is also evidence of the formation of loosely packed multilayers of *p*-carboxyphenyl and *p*-methylphenyl at gold using diazonium chemistry.[109]

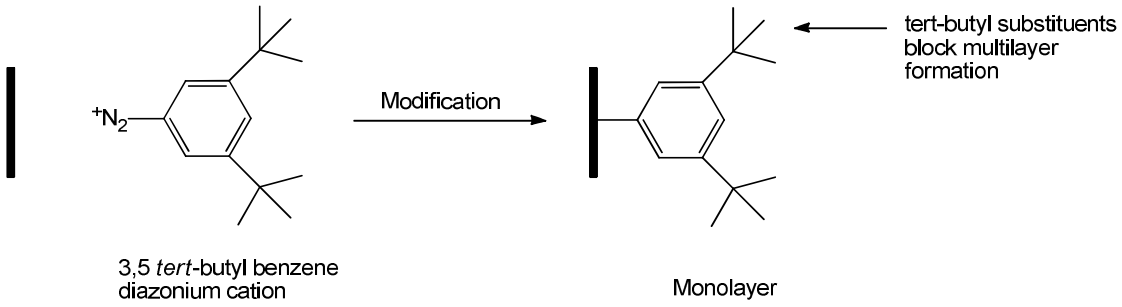

Scheme 1.11. Strategy for achieving monolayers on surfaces via reduction of 3, 5-*tert*-butyl benzene diazonium salt, reported by Pinson and coworkers.[91]

The high reactivity of aryl radicals means that multilayer formation is generally observed upon modification of surfaces using diazonium salts. However, for many applications monolayers are desirable. Pinson and coworkers have shown that monolayers are formed upon the reduction of 3,5-*tert*-butyl benzene diazonium salt (Scheme 1.11), since the *tert*-butyl substituents prevent reaction of bound aryl groups with further aryl radicals.[91] However, the 3, 5-*tert*-butyl benzene monolayers are relatively inert, and hence, not suitable films for coupling reactions.

To address this shortcoming, Daasbjerg, Pedersen and coworkers have reported the preparation of monolayers with nucleophilic[120] and electrophilic[87] substituents, which can serve as reactive layers for subsequent coupling reactions. Monolayer formation is achieved via a "formation-degradation" approach. The approach relies on using diazonium salts with pendant functional groups that both prevent attack of aryl radicals on the remainder of the molecule, and can be cleaved to expose a reactive functional group after film formation. In one report, Daasbjerg, Pederson and coworkers modified GC with diaryl disulfide films via electrochemical reduction of the corresponding *para*-substituted diazonium salt, resulting in the formation of a multilayer film.[120] Reductive cleavage of the Ar-S-S-Ar disulphide gave an electrode surface that had properties consistent with the presence of a nucleophilic thiophenolate ($Ar\text{-}S^-$) monolayer (Scheme 1.12). This approach has also been used to functionalize the sidewalls of carbon nanotubes with thiophenolate monolayers.[121]

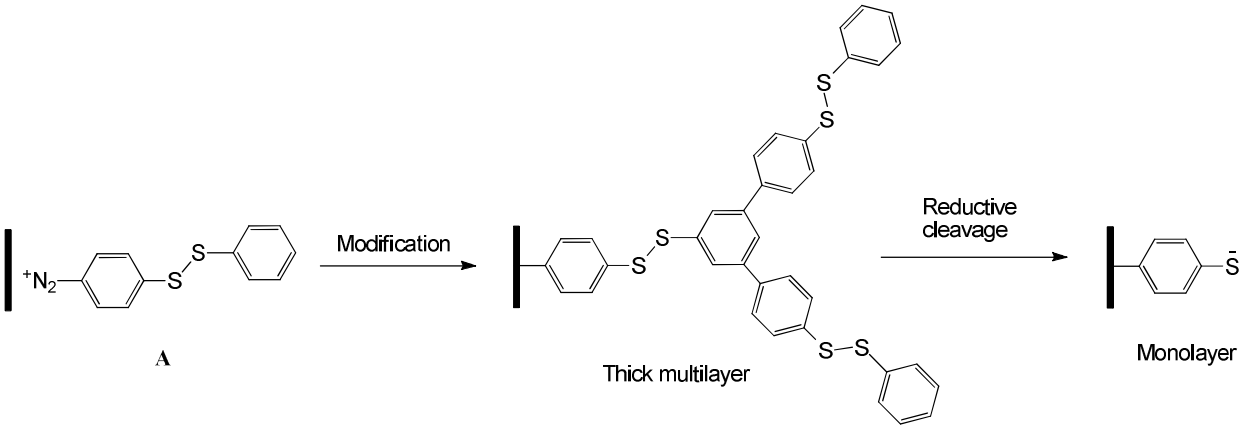

Scheme 1.12. Strategy for functionalizing surfaces with nucleophilic monolayer, reported by Daasbjerg, Pedersen and coworkers.[120]

A similar "formation-degradation" strategy has been used to prepare electrophilic monolayers, by modifying GC electrodes by electro-reduction of (E)-4-((2-(2-(trimethylammonio)-acetyl)hydrazono)methyl) benzenediazonium salt (Scheme 1.13, A).[87] The *para* subsistent protects the aryl ring of the surface bound modifier from attack by aryl radicals. The protection results from several features of the *para* substituent. Firstly, the positively charged ammonium group repels diazonium cations in solution. Secondly, the long-chain *para* substituent is expected to diminish electron transfer from the electrode to the diazonium cations in solution, inhibiting multilayer formation. Thirdly, any multilayer formation would be expected to occur on the *para* substituent, which is cleaved off after modification. As expected, after modification, hydrolysis of the hydrazone functionalities left only a monolayer (or near monolayer) of electrophilic benzaldehyde functionalities at the surface.[87]

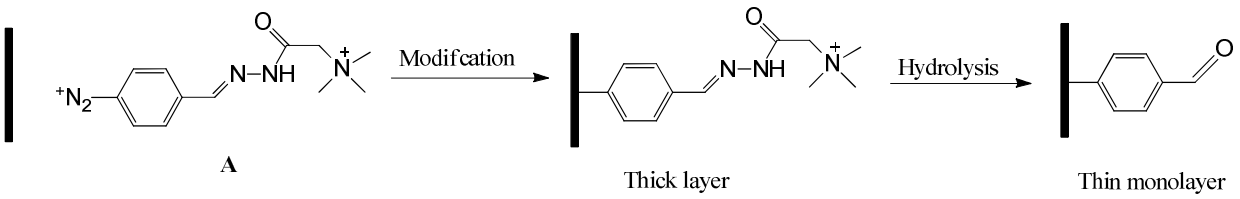

Scheme 1.13. Strategy for functionalizing surfaces with electrophilic monolayers, reported by Daasbjerg, Pedersen and coworkers.[87]

1.3.2 Spontaneous Modification using Aryldiazonium Salts

Spontaneous modification of surfaces using aryldiazonium salts is achieved by immersing a substrate in a solution of a diazonium salt in the absence of an applied potential. Hence "spontaneous modification" refers to modification which occurs *spontaneously at open circuit potential* (OCP). Spontaneous modification has been shown to proceed at carbon[74, 122-125], metal[119, 124-131] and semiconductor surfaces[132-134]. In addition, it has proved particularly useful for the modification of carbon powder and carbon nanotubes by eliminating the need for immobilization of the species on an electrode prior to modification.[135-140]

Since there is no potential applied during spontaneous modification, the mechanism by which the modification occurs is less clear than for electro-reduction of diazonium salts. One proposal is that the surface reduces the diazonium salt at OCP leading to formation of aryl radicals, which then attack the surface. There is some evidence to support this mechanism. Vautrin-Ul and coworkers investigated the reactions of several *para*-substituted benzene diazonium salts at GC and a number of metals.[125] Two important trends were found. Firstly, modification is more favorable when the *para* substituent is more electron withdrawing and the diazonium salts is consequently more easily reduced to the aryl radical. Secondly, modification becomes more favorable when the OCP of the substrate is more negative making it a better reducing agent. In a different study Thiebault and coworkers showed that modification of reduced (conducting) poly(tetrafluoroethylene) via spontaneous reaction with aryldiazonium salts occurs.[141] However modification of unreduced (non-conducting) poly(tetrafluoroethylene) was not observed, suggesting that the ability of the surface to donate electrons is a necessary condition for modification to occur.[125] In another study, Bidan and coworkers found that spontaneous modification of GC occurs only with diazonium salts with a reduction potential that is sufficiently positive.[123] Bélanger and coworkers found that the modification of copper leads to thicker layers in acetonitrile (ACN) than in aqueous conditions and suggested that this could be attributed to the lower OCP of Cu in ACN compared to aqueous conditions.[128] Several workers have also observed an increase in OCP of substrates during modification, consistent with the build-up of positive charge in the surface, resulting from the transfer of electron from the substrate to the diazonium cation.[119, 123, 140] However, these studies have not confirmed that the observed increase in OCP is caused by the presence of the diazonium functionality in solution.

Another possible mechanism for the spontaneous process involves reduction of the diazonium cation moiety by the solvent, producing an aryl radical[43] that subsequently attacks the surface. However, the solvents in which spontaneous modification has been observed (ACN and aqueous acid) have low nucleophilicity parameters[142] and are not expected to produce significant amounts of aryl radicals.[51] Rather, in these solvents, thermal heterogeneous cleavage to produce an aryl cation is expected in the absence of an electron donor.[51]

It has been shown that an increase in temperature during spontaneous modification with NP films leads to higher surface concentrations.[124] This is indicative of modification via an aryl cation intermediate resulting from thermal heterogeneous dediazoniation.[55] However, the data are also consistent with a reaction that proceeds purely via a radical intermediate at low temperatures, but via both radical and cationic intermediates at higher temperatures. Finally, it is also possible that the reaction proceeds via photochemical dediazoniation of diazonium salts (Section 1.2). In most, if not all, of the accounts of spontaneous modification light was not reported to have been excluded. In Chapters 4 and 5 of this thesis, the spontaneous modification using diazonium salts is studied in the absence of light to eliminate the possibility of photochemical dediazoniation.

As in the case of films formed by electrochemical reduction of diazonium salts, films formed by the spontaneous reaction are stable to extended sonication, providing evidence that they are covalently attached to the surface.[119, 124, 125, 128, 132] Furthermore, infrared reflection absorption spectroscopy and XPS have shown the absence of diazonium cation moieties at the surfaces after spontaneous modification, indicating that they have reacted, presumably with the surface.[124, 128, 132] Polarized infrared spectroscopy has shown that spontaneous modification of semiconductors results in the modifiers adopting an orientation perpendicular to the surface, consistent with covalent attachment.[132] At Cu, bonding to the surface was observed (by XPS) to occur both directly to the Cu surface via a Cu-C bond, and through native oxides via Cu-O-C bonds.[119] Bélanger and coworkers observed a drop in oxygen content upon modification of oxidized carbon black by spontaneous reaction with NBD. They proposed that this loss could be brought about by a displacement of carboxylic acid functionalities on the surface by attack of aryl radicals (Scheme 1.14).[139]

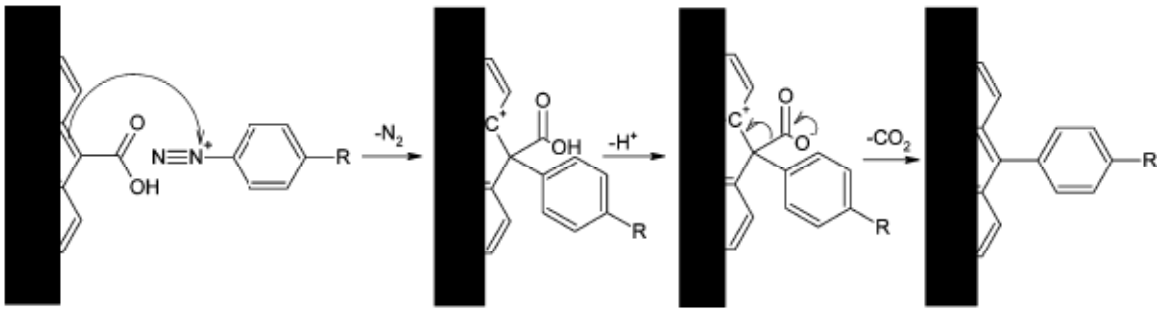

Figure 1.14. Proposed mechanism for modification of carbon via reduction of aryldiazonium salts and decarboxylation of the surface. Reproduced from reference 139.

AFM film thickness measurements have revealed the formation of multilayers upon spontaneous modification of iron with NP films.[124] XPS data have also indicated the formation of multilayers at Cu,[119, 128] while surface concentrations indicative of multilayers have also been observed at GC surfaces.[124] However, the high surface roughness of GC makes it difficult to draw strong conclusions concerning film thickness from the surface concentration data.

1.3.3 Applications of Surfaces Modified using Aryldiazonium Salts

Surfaces modified by aryldiazonium chemistry have applications in a number of areas, most notably, molecular electronics and the development of bio and chemical sensors. These will be discussed in turn.

Molecular electronics involves the integration of molecular components into electronic devices.[3, 4] One important area of molecular electronics is the development of molecular junctions, which are composed of a layer of parallel molecules between two conducting contacts.[4, 5] Since a large number of different molecules with different electronic and structural features can be integrated into molecular junctions, such junctions can be fabricated with a large number of different current/potential characteristics. Hence, molecular junctions can be "tailored" to give specific control over an applied potential and an observed current.[65] Molecular junctions have been prepared via covalent modification of carbon substrates with aryldiazonium salts followed by deposition of a metal layer on the modified surface to give a diazonium cation derived film "sandwiched" between two "contacts".[4, 5, 143-147]

McCreery and coworkers have undertaken significant work in the development of "conductance switches". Their work stemmed from the observation that the conductance of certain biphenyl diazonium cation derived films increases significantly after the application of a negative voltage.[66, 148] This "conductance switching" is believed to come about by injection of electrons into the biphenyl layer, which changes the electronic structure of the layer and facilitates tunneling through the film, giving an increase of conductance.[148] For example, in the case of a *p*-

nitroazobenzene junction, the injection of electrons was proposed to switch the film from a less conducting phenyl form to a more conducting quinoid form (Figure 1.3).[66, 143]

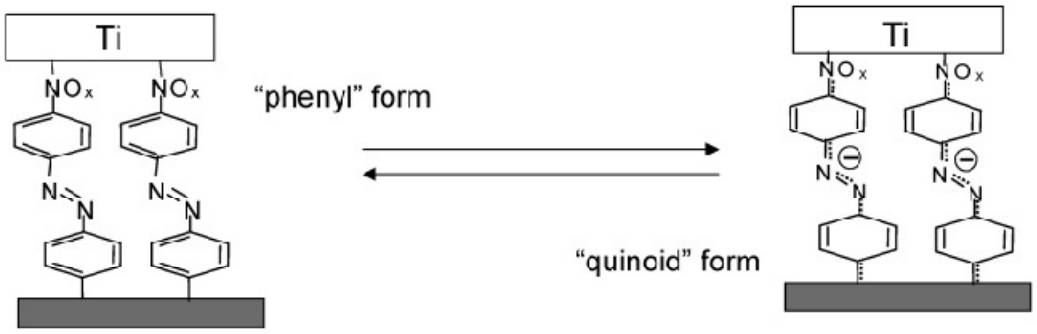

Figure 1.3. Carbon/*p*-nitroazobenene/titanium molecular junction exhibiting conductance switching between the phenyl and quinoid forms of the *p*-nitroazobezene. Reproduced from reference 143.

The "conductance switching" of the films led McCreery and coworkers to develop electronic junctions that can act as switches, [4, 5, 143, 146] which have potential to be integrated into electronic circuits and to function as molecular memory devices.

The preparation of chemical sensors and biosensors has attracted considerable attention over the past few decades. These devices are capable of detecting specific chemical functionalities without the need for sample preparation or expensive chemical characterization equipment (spectrometers etc).[2] Figure 1.4 shows a general schematic of a sensor. Typically, a recognition species is immobilized on a transducer. The recognition species is chosen on the basis of having a highly selective interaction with the target analyte. When the transducer is an electrode, selective reaction of the analyte with the bound recognition species gives an electrochemical signal, allowing for the detection of the analyte.[2]

In order to ensure long-term performance of the sensor it is important that the recognition species is effectively immobilized on the electrode surface. This is often achieved by binding the recognition species to the electrode via a SAM formed by thiol chemistry on gold. However, the thiol-gold bond is relatively weak, and hence, attachment using diazonium cation chemistry is an

attractive alternative, given that the modification method results in stable films at many surfaces. Furthermore, modification using diazonium salts has been shown to proceed on a larger range of surfaces than modification using thiols, allowing for greater flexibility in selection of the transducer/electrode.[2]

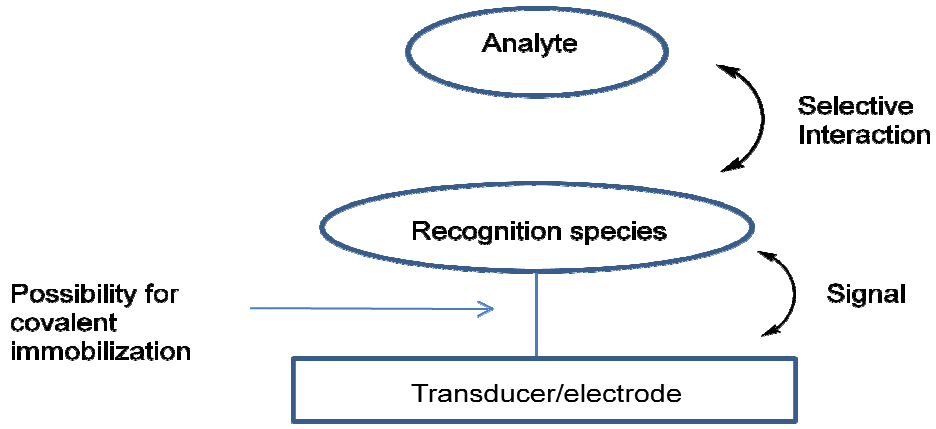

Figure 1.4. General schematic for a chemical or biosensor.

A number of chemical sensors have been fabricated by attaching recognition species to electrodes using diazonium cation chemistry. O'Sullivan and coworkers have described the preparation of a reusable amperometric hydrazine sensor via immobilization of an *o*-aminophenol film on a GC electrode via electro reduction of the corresponding diazonium salt.[78] Compton and coworkers have described the modification of carbon powder with anthraquinone groups using diazonium chemistry. The functionalized powder was subsequently immobilized on a graphite electrode, which then served as a pH probe.[149] In a related study, Hall and coworkers developed a pH sensor by functionalizing GC with hydroquinone via electro-reduction of the diazonium precursor.[150] Very recently, Xu and coworkers developed a sensitive Cd^{2+} and Pb^{2+} sensor by covalently modifying GC with *p*-carboxyphenyl groups via reduction of the corresponding diazonium salt.[151] Bio-sensors have also been developed by attachment of biomolecules to electrodes. For example, in the work of Gooding and coworkers, Gly-Gly-His was coupled to GC electrodes which had been modified with *p*-carboxyphenyl functionalities via electro-reduction of the corresponding diazonium salt. The peptide-modified electrode was shown to serve as sensor for the detection of Cu^{2+} ions.[152] Limoges and coworkers have

developed an electrode capable of detecting histidine-tagged proteins.[75] Initially, a GC electrode was modified with nitrilotriacetic moiety via reduction of the corresponding diazonium salt. The modified electrode was capable of chelating Cu^{2+} and Ni^{2+} ions. Subsequently, the surface was seen to specifically bind histidine-tagged proteins.[75]

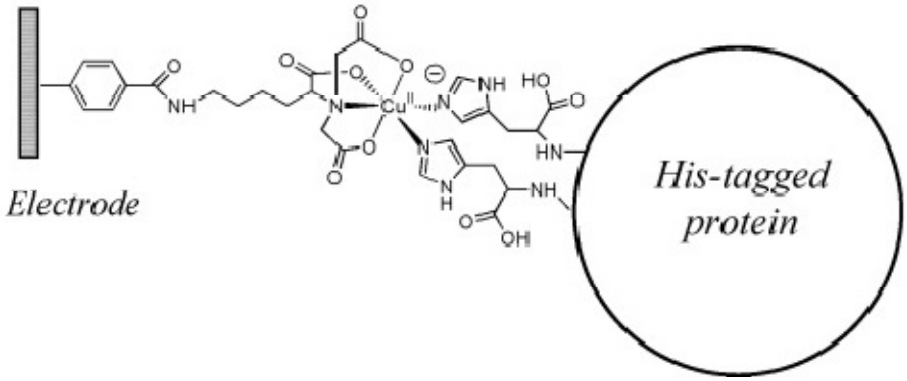

Figure 1.5. Schematic for sensor developed by Limoges and coworkers. Reproduced from reference 75.

Sensors can also be developed by immobilizing enzymes on electrode surfaces to serve as recognition species. Considerable work has been undertaken immobilizing glucose oxidase (GOx) on diazonium cation derived films, due to the potential of the resulting electrodes in glucose sensing applications.[2, 153-156] The first report came as early as 1992 where Pinson and coworkers coupled GOx to *p*-phenylacetic groups immobilized on a GC electrode using diazonium cation chemistry. Electron transfer from the enzyme to the electrode was achieved using ferrocene methanol as a redox mediator in solution.[154] Recently, Gooding and coworkers demonstrated direct electron transfer between GOx immobilized on a GC electrode and the electrode surface.[155] Initially the electrode was modified with a mixed layer of *p*-carboxyphenyl and a 2 nm long molecular wire using diazonium cation chemistry. This was followed by covalent coupling of GOx to the *p*-carboxyphenyl groups leading to immobilization of GOx on the surface. The molecular wire protruding into the enzyme allowed for direct electron transfer between the surface and the GOx (Figure 1.6).[155]

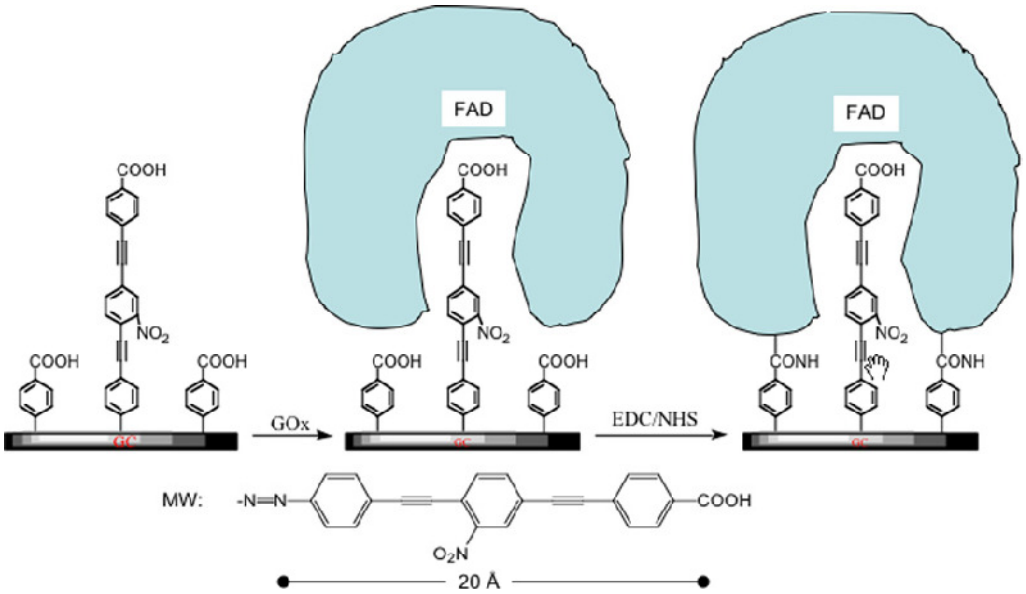

Figure 1.6. Method for immobilization and achieving direct electron transfer from GOx to an electrode by use of a 2 nm molecular wire. Reproduced from reference 155.

Immobilization of enzymes using diazonium cation chemistry has not been limited to GOx. For example, Brozik and coworkers have attached diazonium cation functionalized horseradish peroxidase to GC electrodes and demonstrated direct electron transfer between the enzyme and the electrode. The system has potential applications in hydrogen peroxide sensing. [157] In another study, acetylcholinesterase was immobilized on a modified carbon electrode, allowing for the detection of pesticides.[158] In a further example, diazonium cation chemistry was used to immobilize tyrosinase on a boron-doped diamond electrode resulting in an amperometric sensor for phenolic compounds.[159]

Biological molecules other than enzymes have also been bound to surfaces (using diazonium chemistry) for sensing applications. Marquette and coworkers were able to immobilize rabbit and human immunoglobulins on screen-printed graphite electrode microarrays.[160] The resulting biochip allowed for the specific detection of anti-rabbit immunoglobulin antibodies.[160] A similar method has been used to fabricate a sensor array capable of simultaneous detection of a DNA sequence related to the breast cancer BRCA1 gene and the human cytokine protein interleukin-12.[161] This was undertaken by immobilizing a DNA sequence related to the BRCA1 gene onto five of nine individually addressable gold microelectrodes. The remainder of the electrodes were

modified with an antibody for selectively sensing human cytokine protein interleukin-12. The strategy allows for the development of biochips suitable for simultaneous testing for a large number of specific medical conditions and predispositions.[161, 162]

Immobilization of biomolecules using diazonium cation chemistry has also been applied to the optimization of bio-fuel cells. In the work of Barrière, Leech and coworkers, enzymatic hydrogels were covalently immobilized on modified electrode surfaces via binding to diazonium cation derived films to improve the stability of an enzymatic bio-fuel cell.[163, 164] The improvement of the stability of bio-fuel cells by covalent immobilization of enzymatic hydrogels to the surface via binding to diazonium cation derived films is further discussed and investigated in Chapter 7 of this thesis.

1.4 Aims

The overall aims of the current thesis are to gain a better understanding of mechanisms of formation and properties of diazonium cation derived films. Of particular interest are films formed via spontaneous modification. The specific aims are given below:

- To investigate various electrochemically active surface modifiers and compare their suitabilities as model modifiers for studying diazonium derived films.

- To investigate the surface concentrations, thicknesses and densities of films formed at carbon and gold substrates via spontaneous reaction with aryldiazonium salts.

- To gain further insight into the mechanisms of formation of films prepared at carbon and gold substrates via spontaneous reaction with aryldiazonium salts.

- To investigate the applications of spontaneous modification in the patterning of surfaces by microcontact printing of aryldiazonium salts.

- To investigate the possibility of enhancing the stability of enzymatic hydrogels by covalent attachment of the hydrogel to electrode surfaces using electrodes modified by diazonium cation chemistry.

1.5 References

1. Love, J. C.; Estroff, L. A.; Kriebel, J. K.; Nuzzo, R. G.; Whitesides, G. M., Self-assembled monolayers of thiolates on metals as a form of nanotechnology. *Chem. Rev.* **2005,** 105, 1103-1169.

2. Gooding, J. J., Advances in interfacial design sensors: Aryl diazonium salts for electrochemical biosensors and for modifying carbon and metal electrodes. *Electroanalysis* **2008,** 20, 573-582.

3. McCreery, R. L., Analytical challenges in molecular electronics. *Anal. Chem.* **2006,** 78, 3490-3497.

4. McCreery, R. L.; Bergren, A. J., Progress with Molecular Electronic Junctions: Meeting Experimental Challenges in Design and Fabrication. *Adv. Mater.* **2009,** 21, 4303-4322.

5. McCreery, R. L., Molecular electronic junctions. *Chem. Mater.* **2004,** 16, 4477-4496.

6. Nuzzo, R. G.; Allara, D. L., Adsorption of Bifunctional Organic Disulfides on Gold Surfaces. *J. Am. Chem. Soc.* **1983,** 105, 4481-4483.

7. Schreiber, F., Structure and growth of self-assembling monolayers. *Prog. Surf. Sci.* **2000,** 65, 151-256.

8. Sagiv, J., Organized Monolayers by Adsorption .1. Formation and Structure of Oleophobic Mixed Monolayers on Solid-Surfaces. *J. Am. Chem. Soc.* **1980,** 102, 92-98.

9. Depalma, V.; Tillman, N., Friction and Wear of Self-Assembled Trichlorosilane Monolayer Films on Silicon. *Langmuir* **1989,** 5, 868-872.

10. Delamar, M.; Hitmi, R.; Pinson, J.; Saveant, J. M., Covalent Modification of Carbon Surfaces by Grafting of Functionalized Aryl Radicals Produced from Electrochemical Reduction of Diazonium Salts. *J. Am. Chem. Soc.* **1992,** 114, 5883-5884.

11. Pinson, J.; Podvorica, F., Attachment of organic layers to conductive or semiconductive surfaces by reduction of diazonium salts. *Chem. Soc. Rev.* **2005,** 34, 429-439.

12. Downard, A. J., Electrochemically assisted covalent modification of carbon electrodes. *Electroanalysis* **2000,** 12, 1085-1096.

13. Jenkins, G. M.; Kawamura, K., Structure of Glassy Carbon. *Nature* **1971,** 231, 175-176.

14. Pesin, L. A., Structure and properties of glass-like carbon. *J. Mater. Sci.* **2002,** 37, 1-28.

15. Harris, P. J. F., Fullerene-related structure of commercial glassy carbons. *Philos. Mag.* **2004,** 84, 3159-3167.

16. Oberlin, A., High-Resolution TEM studies of carbonization and graphitization. In *Chem. Phys. Carbon*, Thrower, P. A., Ed. Marcel Dekker: 1989; Vol. 22, pp 1-143.

17. Heiduschka, P.; Munz, A. W.; Gopel, W., Impedance Spectroscopy and Scanning-Tunneling-Microscopy of Polished and Electrochemically Pretreated Glassy-Carbon. *Electrochim. Acta* **1994,** 39, 2207-2223.

18. Collier, W. G.; Tougas, T. P., Determination of Surface Hydroxyl-Groups on Glassy-Carbon with X-Ray Photoelectron-Spectroscopy Preceded by Chemical Derivatization. *Anal. Chem.* **1987,** 59, 396-399.

19. Tougas, T. P.; Collier, W. G., Determination of Surface Carbonyl Groups on Glassy-Carbon with X-Ray Photoelectron-Spectroscopy Preceded by Derivatization with Pentafluorophenylhydrazine. *Anal. Chem.* **1987,** 59, 2269-2272.

20. Hoekstra, K. J.; Bein, T., Adsorption of zirconium-phosphonate multilayers onto phosphate-derivatized glassy carbon substrates. *Chem. Mater.* **1996,** 8, 1865-1870.

21. Menendez, J. A.; Phillips, J.; Xia, B.; Radovic, L. R., On the modification and characterization of chemical surface properties of activated carbon: In the search of carbons with stable basic properties. *Langmuir* **1996,** 12, 4404-4410.

22. Menendez, J. A.; Xia, B.; Phillips, J.; Radovic, L. R., On the modification and characterization of chemical surface properties of activated carbon: Microcalorimetric, electrochemical, and thermal desorption probes. *Langmuir* **1997,** 13, 3414-3421.

23. Radovic, L. R.; Bockrath, B., On the chemical nature of graphene edges: Origin of stability and potential for magnetism in carbon materials. *J. Am. Chem. Soc.* **2005,** 127, 5917-5927.

24. Lee, H.; Son, Y. W.; Park, N.; Han, S. W.; Yu, J. J., Magnetic ordering at the edges of graphitic fragments: Magnetic tail interactions between the edge-localized states. *Phys. Rev. B* **2005,** 72.

25. Jiang, D. E.; Sumpter, B. G.; Dai, S., Unique chemical reactivity of a graphene nanoribbon's zigzag edge. *J. Chem. Phys.* **2007,** 126.

26. Bowling, R. J.; Packard, R. T.; McCreery, R. L., Activation of Highly Ordered Pyrolytic-Graphite for Heterogeneous Electron-Transfer - Relationship between Electrochemical Performance and Carbon Microstructure. *J. Am. Chem. Soc.* **1989,** 111, 1217-1223.

27. Bowling, R.; Packard, R. T.; McCreery, R. L., Mechanism of Electrochemical Activation of Carbon Electrodes - Role of Graphite Lattice-Defects. *Langmuir* **1989,** 5, 683-688.

28. Williams, C. G.; Edwards, M. A.; Colley, A. L.; Macpherson, J. V.; Unwin, P. R., Scanning Micropipet Contact Method for High-Resolution Imaging of Electrode Surface Redox Activity. *Anal. Chem.* **2009,** 81, 2486-2495.

29. Engstrom, R. C., Electrochemical Pretreatment of Glassy-Carbon Electrodes. *Anal. Chem.* **1982,** 54, 2310-2314.

30. Kepley, L. J.; Bard, A. J., Ellipsometric, Electrochemical, and Elemental Characterization of the Surface Phase Produced on Glassy-Carbon Electrodes by Electrochemical Activation. *Anal. Chem.* **1988,** 60, 1459-1467.

31. Zhao, Q. L.; Zhang, Z. L.; Bao, L.; Pang, D. W., Surface structure-related electrochemical behaviors of glassy carbon electrodes. *Electrochem. Commun.* **2008,** 10, 181-185.

32. Weisshaar, D. E.; Kuwana, T., Considerations for Polishing Glassy-Carbon to a Scratch-Free Finish. *Anal. Chem.* **1985,** 57, 378-379.

33. Kiema, G. K.; Aktay, M.; McDermott, M. T., Preparation of reproducible glassy carbon electrodes by removal of polishing impurities. *J. Electroanal. Chem.* **2003,** 540, 7-15.

34. McDermott, M. T.; McDermott, C. A.; McCreery, R. L., Scanning Tunneling Microscopy of Carbon Surfaces - Relationships between Electrode-Kinetics, Capacitance, and Morphology for Glassy-Carbon Electrodes. *Anal. Chem.* **1993,** 65, 937-944.

35. Chen, Q. Y.; Swain, G. M., Structural characterization, electrochemical reactivity, and response stability of hydrogenated glassy carbon electrodes. *Langmuir* **1998,** 14, 7017-7026.

36. Kim, J.; Song, X.; Kinoshita, K.; Madou, M.; White, B., Electrochemical studies of carbon films from pyrolyzed photoresist. *J. Electrochem. Soc.* **1998,** 145, 2314-2319.

37. Ranganathan, S.; McCreery, R.; Majji, S. M.; Madou, M., Photoresist-derived carbon for microelectromechanical systems and electrochemical applications. *J. Electrochem. Soc.* **2000,** 147, 277-282.

38. Kostecki, R.; Schnyder, B.; Alliata, D.; Song, X.; Kinoshita, K.; Kotz, R., Surface studies of carbon films from pyrolyzed photoresist. *Thin Solid Films* **2001,** 396, 36-43.

39. Ranganathan, S.; McCreery, R. L., Electroanalytical performance of carbon films with near-atomic flatness. *Anal. Chem.* **2001,** 73, 893-900.

40. Ray, K.; McCreery, R. L., Spatially resolved Raman spectroscopy of carbon electrode surfaces: Observations of structural and chemical heterogeneity. *Anal. Chem.* **1997,** 69, 4680-4687.

41. Chen, P. H.; McCreery, R. L., Control of electron transfer kinetics at glassy carbon electrodes by specific surface modification. *Anal. Chem.* **1996,** 68, 3958-3965.

42. Fairman, C.; Yu, S. S. C.; Liu, G. Z.; Downard, A. J.; Hibbert, D. B.; Gooding, J. J., Exploration of variables in the fabrication of pyrolysed photoresist. *J. Solid State Electrochem.* **2008,** 12, 1357-1365.

43. Galli, C., Radical Reactions of Arenediazonium Ions - an Easy Entry into the Chemistry of the Aryl Radical. *Chem. Rev.* **1988,** 88, 765-792.

44. Elofson, R. M.; Gadallah, F. F., Substituent Effects in Polarography of Aromatic Diazonium Salts. *J. Org. Chem.* **1969,** 34, 854-&.

45. Waters, W. A., Decomposition reactions of the aromatic diazo-compounds Part X Mechanism of the sandmeyer reaction. *J. Chem. Soc* **1942**, 266-270.

46. Kornblum, N.; Cooper, G. D.; Taylor, J. E., The Chemistry of Diazo Compounds .2. Evidence for a Free Radical Chain Mechanism in the Reduction of Diazonium Salts by Hypophosphorous Acid. *J. Am. Chem. Soc.* **1950,** 72, 3013-3020.

47. Kornblum, N.; Kelley, A. E.; Cooper, G. D., The Chemistry of Diazo Compounds .3. the Reduction of Diazonium Salts by Phosphorous Acid. *J. Am. Chem. Soc.* **1952,** 74, 3074-3076.

48. Friedman, L.; Chlebows.Jf, Aprotic Diazotization of Aniline in Presence of Iodine. *J. Org. Chem.* **1968,** 33, 1636-1638.

49. Citterio, A.; Minisci, F.; Albinati, A.; Bruckner, S., Steric and Polar Effects in Free-Radical Reactions - an Unusual Type of Azocoupling by Free-Radical Decomposition of Diazonium Salts. *Tetrahedron Lett.* **1980,** 21, 2909-2910.

50. Galli, C., An Investigation of the 2-Step Nature of the Sandmeyer Reaction. *J. Chem. Soc., Perkin Trans. 2* **1981**, 1459-1461.

51. Zollinger, H., *Diazo chemistry I: aromaric and heteroaromatic compounds*. VHC Publishers: New York, 1994.

52. Ando, W., Photochemistry of the diazonium and diazo groups. In *Chemisrty of the diazonium and diazo groups*, Patai, S., Ed. John Wiley and Sons, Ltd.: Bristol, 1978; Vol. 1, pp 341-488.

53. Moffat, J. B., General theoretical aspects of the diazonium and diazo groups. In *The chemistry of diazonium and diazo groups*, Patai, S., Ed. John Wiley and Sons, Ltd.: Bristol, 1978; Vol. 1, pp 1-77.

54. Detar, D. F.; Ballentine, A. R., The Mechanisms of Diazonium Salt Reactions .2. a Redetermination of the Rates of the Thermal Decomposition of 6-Diazonium Salts in Aqueous Solution. *J. Am. Chem. Soc.* **1956,** 78, 3916-3920.

55. Lewin, A. H.; Cohen, T., Mechanism of Copper-Induced Pschorr Cyclization . a New Phenol Synthesis Involving Hydroxylation of Intermediate Radical by Cupric Ion. *J. Org. Chem.* **1967,** 32, 3844-3850.

56. Allongue, P.; Delamar, M.; Desbat, B.; Fagebaume, O.; Hitmi, R.; Pinson, J.; Saveant, J. M., Covalent modification of carbon surfaces by aryl radicals generated from the electrochemical reduction of diazonium salts. *J. Am. Chem. Soc.* **1997,** 119, 201-207.

57. Liu, Y. C.; McCreery, R. L., Reactions of Organic Monolayers on Carbon Surfaces Observed with Unenhanced Raman-Spectroscopy. *J. Am. Chem. Soc.* **1995,** 117, 11254-11259.

58. Saby, C.; Ortiz, B.; Champagne, G. Y.; Bélanger, D., Electrochemical modification of glassy carbon electrode using aromatic diazonium salts .1. Blocking effect of 4-nitrophenyl and 4-carboxyphenyl groups. *Langmuir* **1997,** 13, 6805-6813.

59. Ortiz, B.; Saby, C.; Champagne, G. Y.; Bélanger, D., Electrochemical modification of a carbon electrode using aromatic diazonium salts. 2. Electrochemistry of 4-nitrophenyl modified glassy carbon electrodes in aqueous media. *J. Electroanal. Chem.* **1998,** 455, 75-81.

60. Kariuki, J. K.; McDermott, M. T., Nucleation and growth of functionalized aryl films on graphite electrodes. *Langmuir* **1999,** 15, 6534-6540.

61. Downard, A. J., Potential-dependence of self-limited films formed by reduction of aryldiazonium salts at glassy carbon electrodes. *Langmuir* **2000,** 16, 9680-9682.

62. Kariuki, J. K.; McDermott, M. T., Formation of multilayers on glassy carbon electrodes via the reduction of diazonium salts. *Langmuir* **2001,** 17, 5947-5951.

63. Downard, A. J.; Prince, M. J., Barrier properties of organic monolayers on glassy carbon electrodes. *Langmuir* **2001,** 17, 5581-5586.

64. Tammeveski, K.; Kontturi, K.; Nichols, R. J.; Potter, R. J.; Schiffrin, D. J., Surface redox catalysis for O_2 reduction on quinone-modified glassy carbon electrodes. *J. Electroanal. Chem.* **2001**, 101-112.

65. Anariba, F.; McCreery, R. L., Electronic conductance behavior of carbon-based molecular junctions with conjugated structures. *J. Phys. Chem. B* **2002,** 106, 10355-10362.

66. Itoh, T.; McCreery, R. L., In situ Raman spectroelectrochemistry of electron transfer between glassy carbon and a chemisorbed nitroazobenzene monolayer. *J. Am. Chem. Soc.* **2002,** 124, 10894-10902.

67. Andrieux, C. P.; Pinson, J., The standard redox potential of the phenyl radical/anion couple. *J. Am. Chem. Soc.* **2003,** 125, 14801-14806.

68. Anariba, F.; DuVall, S. H.; McCreery, R. L., Mono- and multilayer formation by diazonium reduction on carbon surfaces monitored with atomic force microscopy "scratching". *Anal. Chem.* **2003,** 75, 3837-3844.

69. Brooksby, P. A.; Downard, A. J., Electrochemical and atomic force microscopy study of carbon surface modification via diazonium reduction in aqueous and acetonitrile solutions. *Langmuir* **2004,** 20, 5038-5045.

70. D'Amours, M.; Bélanger, D., Stability of substituted phenyl groups electrochemically grafted at carbon electrode surface. *J. Phys. Chem. B* **2003,** 107, 4811-4817.

71. Baranton, S.; Bélanger, D., Electrochemical derivatization of carbon surface by reduction of in situ generated diazonium cations. *J. Phys. Chem. B* **2005,** 109, 24401-24410.

72. Brooksby, P. A.; Downard, A. J., Multilayer nitroazobenzene films covalently attached to carbon. An AFM and electrochemical study. *J. Phys. Chem. B* **2005,** 109, 8791-8798.

73. Brooksby, P. A.; Downard, A. J., Nanoscale patterning of flat carbon surfaces by scanning probe lithography and electrochemistry. *Langmuir* **2005,** 21, 1672-1675.

74. Combellas, C.; Kanoufi, F.; Pinson, J.; Podvorica, F. I., Time-of-flight secondary ion mass spectroscopy characterization of the covalent bonding between a carbon surface and aryl groups. *Langmuir* **2005,** 21, 280-286.

75. Blankespoor, R.; Limoges, B.; Schollhorn, B.; Syssa-Magale, J. L.; Yazidi, D., Dense monolayers of metal-chelating ligands covalently attached to carbon electrodes electrochemically and their useful application in affinity binding of histidine-tagged proteins. *Langmuir* **2005,** 21, 3362-3375.

76. Downard, A. J.; Garrett, D. J.; Tan, E. S. Q., Microscale patterning of organic films on carbon surfaces using electrochemistry and soft lithography. *Langmuir* **2006,** 22, 10739-10746.

77. Anariba, F.; Viswanathan, U.; Bocian, D. F.; McCreery, R. L., Determination of the structure and orientation of organic molecules tethered to flat graphitic carbon by ATR-FT-IR and Raman spectroscopy. *Anal. Chem.* **2006,** 78, 3104-3112.

78. Nassef, H. M.; Radi, A. E.; O'Sullivan, C. K., Electrocatalytic oxidation of hydrazine at o-aminophenol grafted modified glassy carbon electrode: Reusable hydrazine amperometric sensor. *J. Electroanal. Chem.* **2006,** 592, 139-146.

79. Radi, A. E.; Montornes, J. M.; O'Sullivan, C. K., Reagentless detection of alkaline phosphatase using electrochemically grafted films of aromatic diazonium salts. *J. Electroanal. Chem.* **2006,** 587, 140-147.

80. Yu, B. C.; Shirai, Y.; Tour, J. M., Syntheses of new functionalized azobenzenes for potential molecular electronic devices. *Tetrahedron* **2006,** 62, 10303-10310.

81. Vila, N.; Van Brussel, M.; D'Amours, M.; Marwan, J.; Buess-Herman, C.; Bélanger, D., Metallic and bimetallic Cu/Pt species supported on carbon surfaces by means of substituted phenyl groups. *J. Electroanal. Chem.* **2007,** 609, 85-93.

82. Grivea, S.; Mercier, D.; Vautrin-Ul, C.; Chausse, A., Electrochemical grafting by reduction of 4-aminoethylbenzenediazonium salt: Application to the immobilization of (bio)molecules. *Electrochem. Commun.* **2007,** 9, 2768-2773.

83. Doppelt, P.; Hallais, G.; Pinson, J.; Podvorica, F.; Verneyre, S., Surface modification of conducting substrates. Existence of azo bonds in the structure of organic layers obtained from diazonium salts. *Chem. Mater.* **2007,** 19, 4570-4575.

84. Louault, C.; D'Amours, M.; Bélanger, D., The electrochemical grafting of a mixture of substituted phenyl groups at a glassy carbon electrode surface. *ChemPhysChem* **2008,** 9, 1164-1170.

85. Breton, T.; Bélanger, D., Modification of carbon electrode with aryl groups having an aliphatic amine by electrochemical reduction of in situ generated diazonium cations. *Langmuir* **2008,** 24, 8711-8718.

86. Baranton, S.; Bélanger, D., In situ generation of diazonium cations in organic electrolyte for electrochemical modification of electrode surface. *Electrochim. Acta* **2008,** 53, 6961-6967.

87. Malmos, K.; Dong, M. D.; Pillai, S.; Kingshott, P.; Besenbacher, F.; Pedersen, S. U.; Daasbjerg, K., Using a Hydrazone-Protected Benzenediazonium Salt to Introduce a Near-Monolayer of Benzaldehyde on Glassy Carbon Surfaces. *J. Am. Chem. Soc.* **2009,** 131, 4928-4936.

88. Schauff, S.; Ciorca, M.; Laforgue, A.; Bélanger, D., Electron Transfer Processes at Aryl-Modified Glassy Carbon Electrode. *Electroanalysis* **2009,** 12, 1499-1504.

89. Nguyen, N. H.; Esnault, C.; Gohier, F.; Bélanger, D.; Cougnon, C., Electrochemistry and Reactivity of Surface-Confined Catechol Groups Derived from Diazonium Reduction. Bias-Assisted Michael Addition at the Solid/Liquid Interface. *Langmuir* **2009,** 25, 3504-3508.

90. Cougnon, C.; Gohier, F.; Bélanger, D.; Mauzeroll, J., In Situ Formation of Diazonium Salts from Nitro Precursors for Scanning Electrochemical Microscopy Patterning of Surfaces. *Angew. Chem., Int. Ed. Engl.* **2009,** 48, 4006-4008.

91. Combellas, C.; Jiang, D. E.; Kanoufi, F.; Pinson, J.; Podvorica, F. I., Steric Effects in the Reaction of Aryl Radicals on Surfaces. *Langmuir* **2009,** 25, 286-293.

92. Liu, G. Z.; Liu, J. Q.; Bocking, T.; Eggers, P. K.; Gooding, J. J., The modification of glassy carbon and gold electrodes with aryl diazonium salt: The impact of the electrode materials on the rate of heterogeneous electron transfer. *Chem. Phys.* **2005,** 319, 136-146.

93. Yu, S. S. C.; Tan, E. S. Q.; Jane, R. T.; Downard, A. J., An electrochemical and XPS study of reduction of nitrophenyl films covalently grafted to planar carbon surfaces. *Langmuir* **2007,** 23, 11074-11082.

94. Liu, Y. C.; McCreery, R. L., Raman spectroscopic determination of the structure and orientation of organic monolayers chemisorbed on carbon electrode surfaces. *Anal. Chem.* **1997,** 69, 2091-2097.

95. Bernard, M. C.; Chausse, A.; Cabet-Deliry, E.; Chehimi, M. M.; Pinson, J.; Podvorica, F.; Vautrin-Ul, C., Organic layers bonded to industrial, coinage, and noble metals through electrochemical reduction of aryldiazonium salts. *Chem. Mater.* **2003,** 15, 3450-3462.

96. Boukerma, K.; Chehimi, M. M.; Pinson, J.; Blomfield, C., X-ray photoelectron spectroscopy evidence for the covalent bond between an iron surface and aryl groups attached by the electrochemical reduction of diazonium salts. *Langmuir* **2003,** 19, 6333-6335.

97. Maldonado, S.; Smith, T. J.; Williams, R. D.; Morin, S.; Barton, E.; Stevenson, K. J., Surface modification of indium tin oxide via electrochemical reduction of aryldiazonium cations. *Langmuir* **2006,** 22, 2884-2891.

98. Laforgue, A.; Addou, T.; Bélanger, D., Characterization of the deposition of organic molecules at the surface of gold by the electrochemical reduction of aryldiazonium cations. *Langmuir* **2005,** 21, 6855-6865.

99. Ricci, A.; Bonazzola, C.; Calvo, E. J., An FT-IRRAS study of nitrophenyl mono- and multilayers electro-deposited on gold by reduction of the diazonium salt. *Phys. Chem. Chem. Phys.* **2006,** 8, 4297-4299.

100. Lyskawa, J.; Bélanger, D., Direct modification of a gold electrode with aminophenyl groups by electrochemical reduction of in situ generated aminophenyl monodiazonium cations. *Chem. Mater.* **2006,** 18, 4755-4763.

101. Harper, J. C.; Polsky, R.; Dirk, S. M.; Wheeler, D. R.; Brozik, S. M., Electroaddressable selective functionalization of electrode arrays: Catalytic NADH detection using aryl diazonium modified gold electrodes. *Electroanalysis* **2007,** 19, 1268-1274.

102. Liu, G. Z.; Bocking, T.; Gooding, J. J., Diazonium salts: Stable monolayers on gold electrodes for sensing applications. *J. Electroanal. Chem.* **2007,** 600, 335-344.

103. Radi, A. E.; Munoz-Berbel, X.; Cortina-Ping, M.; Marty, J. L., Novel Protocol for Covalent Immobilization of Horseradish Peroxidase on Gold Electrode Surface. *Electroanalysis* **2009,** 21, 696-700.

104. Haccoun, J.; Vautrin-Ul, C.; Chausse, A.; Adenier, A., Electrochemical grafting of organic coating onto gold surfaces: Influence of the electrochemical conditions on the grafting of nitrobenzene diazonium salt. *Prog. Org. Coat.* **2008,** 63, 18-24.

105. Benedetto, A.; Balog, M.; Viel, P.; Le Derf, F.; Salle, M.; Palacin, S., Electro-reduction of diazonium salts on gold: Why do we observe multi-peaks? *Electrochim. Acta* **2008,** 53, 7117-7122.

106. Kullapere, M.; Marandi, M.; Sammelselg, V.; Menezes, H. A.; Maia, G.; Tammeveski, K., Surface modification of gold electrodes with anthraquinone diazonium cations. *Electrochem. Commun.* **2009,** 11, 405-408.

107. Shewchuk, D. M.; McDermott, M. T., Comparison of Diazonium Salt Derived and Thiol Derived Nitrobenzene Layers on Gold. *Langmuir* **2009,** 25, 4556-4563.

108. Harper, J. C.; Polsky, R.; Wheeler, D. R.; Lopez, D. M.; Arango, D. C.; Brozik, S. M., A Multifunctional Thin Film Au Electrode Surface Formed by Consecutive Electrochemical Reduction of Aryl Diazonium Salts. *Langmuir* **2009,** 25, 3282-3288.

109. Paulik, M. G.; Brooksby, P. A.; Abell, A. D.; Downard, A. J., Grafting aryl diazonium cations to polycrystalline gold: Insights into film structure using gold oxide reduction, redox probe electrochemistry, and contact angle behavior. *J. Phys. Chem. C* **2007,** 111, 7808-7815.

110. Allongue, P.; de Villeneuve, C. H.; Pinson, J.; Ozanam, F.; Chazalviel, J. N.; Wallart, X., Organic monolayers on Si(111) by electrochemical method. *Electrochim. Acta* **1998,** 43, 2791-2798.

111. Allongue, P.; de Villeneuve, C. H.; Pinson, J., Structural characterization of organic monolayers on Si < 111 > from capacitance measurements. *Electrochim. Acta* **2000,** 45, 3241-3248.

112. Hartig, P.; Dittrich, T.; Rappich, J., Surface dipole formation and non-radiative recombination at p-Si(111) surfaces during electrochemical deposition of organic layers. *J. Electroanal. Chem.* **2002,** 524, 120-126.

113. Allongue, P.; de Villeneuve, C. H.; Cherouvrier, G.; Cortes, R.; Bernard, M. C., Phenyl layers on H-Si(111) by electrochemical reduction of diazonium salts: monolayer versus multilayer formation. *J. Electroanal. Chem.* **2003,** 550, 161-174.

114. Rappich, J.; Merson, A.; Roodenko, K.; Dittrich, T.; Gensch, M.; Hinrichs, K.; Shapira, Y., Electronic properties of Si surfaces and side reactions during electrochemical grafting of phenyl layers. *J. Phys. Chem. B* **2006,** 110, 1332-1337.

115. Charlier, J.; Palacin, S.; Leroy, J.; Del Frari, D.; Zagonel, L.; Barrett, N.; Renault, O.; Bailly, A.; Mariolle, D., Local silicon doping as a promoter of patterned electrografting of diazonium for directed surface functionalization. *J. Mater. Chem.* **2008,** 18, 3136-3142.

116. Charlier, J.; Golus, E.; Bureau, C.; Palacin, S., Selectivity of organic grafting as a function of the nature of semiconducting substrates. *J. Electroanal. Chem.* **2009,** 625, 97-100.

117. Jiang, D. E.; Sumpter, B. G.; Dai, S., How do aryl groups attach to a graphene sheet? *J. Phys. Chem. B* **2006,** 110, 23628-23632.

118. Zollinger, H., Reactivity and Stability of Arenediazonium Ions. *Acc. Chem. Res.* **1973,** 6, 335-341.

119. Hurley, B. L.; McCreery, R. L., Covalent bonding of organic molecules to Cu and Al alloy 2024 T3 surfaces via diazonium ion reduction. *J. Electrochem. Soc.* **2004,** 151, B252-B259.

120. Nielsen, L. T.; Vase, K. H.; Dong, M. D.; Besenbacher, F.; Pedersen, S. U.; Daasbjerg, K., Electrochemical approach for constructing a monolayer of thiophenolates from grafted multilayers of diaryl disulfides. *J. Am. Chem. Soc.* **2007,** 129, 1888-1889.

121. Peng, Z. Q.; Holm, A. H.; Nielsen, L. T.; Pedersen, S. U.; Daasbjerg, K., Covalent Sidewall Functionalization of Carbon Nanotubes by a "Formation-Degradation" Approach. *Chem. Mater.* **2008,** 20, 6068-6075.

122. Seinberg, J. M.; Kullapere, M.; Maeorg, U.; Maschion, F. C.; Maia, G.; Schiffrin, D. J.; Tammeveski, K., Spontaneous modification of glassy carbon surface with anthraquinone from the solutions of its diazonium derivative: An oxygen reduction study. *J. Electroanal. Chem.* **2008,** 624, 151-160.

123. Le Floch, F.; Simonato, J. P.; Bidan, G., Electrochemical signature of the grafting of diazonium salts: A probing parameter for monitoring the electro-addressed functionalization of devices. *Electrochim. Acta* **2009,** 54, 3078-3085.

124. Adenier, A.; Cabet-Deliry, E.; Chausse, A.; Griveau, S.; Mercier, F.; Pinson, J.; Vautrin-Ul, C., Grafting of nitrophenyl groups on carbon and metallic surfaces without electrochemical induction. *Chem. Mater.* **2005,** 17, 491-501.

125. Adenier, A.; Barre, N.; Cabet-Deliry, E.; Chausse, A.; Griveau, S.; Mercier, F.; Pinson, J.; Vautrin-Ul, C., Study of the spontaneous formation of organic layers on carbon and metal surfaces from diazonium salts. *Surf. Sci.* **2006,** 600, 4801-4812.

126. Fan, F. R. F.; Yang, J. P.; Dirk, S. M.; Price, D. W.; Kosynkin, D.; Tour, J. M.; Bard, A. J., Determination of the molecular electrical properties of self-assembled monolayers of compounds of interest in molecular electronics. *J. Am. Chem. Soc.* **2001,** 123, 2454-2455.

127. Combellas, C.; Delamar, M.; Kanoufi, F.; Pinson, J.; Podvorica, F. I., Spontaneous grafting of iron surfaces by reduction of aryldiazonium salts in acidic or neutral aqueous solution. Application to the protection of iron against corrosion. *Chem. Mater.* **2005,** 17, 3968-3975.

128. Chamoulaud, G.; Bélanger, D., Spontaneous derivatization of a copper electrode with in situ generated diazonium cations in aprotic and aqueous media. *J. Phys. Chem. C* **2007,** 111, 7501-7507.

129. Liang, H. H.; Tian, H.; McCreery, R. L., Normal and surface-enhanced Raman spectroscopy of nitroazobenzene submonolayers and multilayers on carbon and silver surfaces. *Appl. Spectrosc.* **2007,** 61, 613-620.

130. Podvorica, F. I.; Kanoufi, F.; Pinson, J.; Cornbellas, C., Spontaneous grafting of diazoates on metals. *Electrochim. Acta* **2009,** 54, 2164-2170.

131. Fan, F. R. F.; Yang, J. P.; Cai, L. T.; Price, D. W.; Dirk, S. M.; Kosynkin, D. V.; Yao, Y. X.; Rawlett, A. M.; Tour, J. M.; Bard, A. J., Charge transport through self-assembled monolayers of compounds of interest in molecular electronics. *J. Am. Chem. Soc.* **2002,** 124, 5550-5560.

132. Stewart, M. P.; Maya, F.; Kosynkin, D. V.; Dirk, S. M.; Stapleton, J. J.; McGuiness, C. L.; Allara, D. L.; Tour, J. M., Direct covalent grafting of conjugated molecules onto Si, GaAs, and Pd surfaces from aryidiazonium salts. *J. Am. Chem. Soc.* **2004,** 126, 370-378.

133. Chen, B.; Lu, M.; Flatt, A. K.; Maya, F.; Tour, J. M., Chemical reactions in monolayer aromatic films on silicon surfaces. *Chem. Mater.* **2008,** 20, 61-64.

134. Lu, M.; Nolte, W. A.; He, T.; Corley, D. A.; Tour, J. M., Direct Covalent Grafting of Polyoxometalates onto Si Surfaces. *Chem. Mater.* **2009,** 21, 442-446.

135. Bahr, J. L.; Tour, J. M., Highly functionalized carbon nanotubes using in situ generated diazonium compounds. *Chem. Mater.* **2001,** 13, 3823-+.

136. Dyke, C. A.; Tour, J. M., Unbundled and highly functionalized carbon nanotubes from aqueous reactions. *Nano Lett.* **2003,** 3, 1215-1218.

137. Strano, M. S.; Dyke, C. A.; Usrey, M. L.; Barone, P. W.; Allen, M. J.; Shan, H. W.; Kittrell, C.; Hauge, R. H.; Tour, J. M.; Smalley, R. E., Electronic structure control of single-walled carbon nanotube functionalization. *Science* **2003,** 301, 1519-1522.

138. Abiman, P.; Wildgoose, G. G.; Compton, R. G., Investigating the mechanism for the covalent chemical modification of multiwalled carbon nanotubes using aryl diazonium salts. *Int. J. Electrochem. Sci.* **2008,** 3, 104-117.

139. Toupin, M.; Bélanger, D., Spontaneous functionalization of carbon black by reaction with 4-nitrophenyldiazonium cations. *Langmuir* **2008,** 24, 1910-1917.

140. Smith, R. D. L.; Pickup, P. G., Voltammetric quantification of the spontaneous chemical modification of carbon black by diazonium coupling. *Electrochim. Acta* **2009,** 54, 2305-2311.

141. Combellas, C.; Kanoufi, F.; Mazouzi, D.; Thiebault, A.; Bertrand, P.; Medard, N., Surface modification of halogenated polymers. 4. Functionalisation of poly(tetrafluoroethylene) surfaces by diazonium salts. *Polymer* **2003,** 44, 19-24.

142. Kamlet, M. J.; Abboud, J. L. M.; Abraham, M. H.; Taft, R. W., Linear Solvation Energy Relationships .23. a Comprehensive Collection of the Solvatochromic Parameters, Pi-Star, Alpha and Beta, and Some Methods for Simplifying the Generalized Solvatochromic Equation. *J. Org. Chem.* **1983,** 48, 2877-2887.

143. McCreery, R.; Dieringer, J.; Solak, A. O.; Snyder, B.; Nowak, A. M.; McGovern, W. R.; DuVall, S., Molecular rectification and conductance switching in carbon-based molecular junctions by structural rearrangement accompanying electron injection. *J. Am. Chem. Soc.* **2003,** 125, 10748-10758.

144. Kalakodimi, R. P.; Nowak, A. M.; McCreery, R. L., Carbon/molecule/metal and carbon/molecule/metal oxide molecular electronic junctions. *Chem. Mater.* **2005,** 17, 4939-4948.

145. McCreery, R. L.; Viswanathan, U.; Kalakodimi, R. P.; Nowak, A. M., Carbon/molecule/metal molecular electronic junctions: the importance of "contacts". *Faraday Discuss.* **2006,** 131, 33-43.

146. Ssenyange, S.; Yan, H. J.; McCreery, R. L., Redox-driven conductance switching via filament formation and dissolution in carbon/molecule/TiO2/Ag molecular electronic junctions. *Langmuir* **2006,** 22, 10689-10696.

147. Bergren, A. J.; Harris, K. D.; Deng, F. J.; McCreery, R. L., Molecular electronics using diazonium-derived adlayers on carbon with Cu top contacts: critical analysis of metal oxides and filaments. *J. Phys.: Condens. Matter* **2008,** 20.

148. Solak, A. O.; Eichorst, L. R.; Clark, W. J.; McCreery, R. L., Modified carbon surfaces as "organic electrodes" that exhibit conductance switching. *Anal. Chem.* **2003,** 75, 296-305.

149. Wildgoose, G. G.; Pandurangappa, M.; Lawrence, N. S.; Jiang, L.; Jones, T. G. J.; Compton, R. G., Anthraquinone-derivatised carbon powder: reagentless voltammetric pH electrodes. *Talanta* **2003,** 60, 887-893.

150. Yang, X. H.; Hall, S. B.; Burrell, A. K.; Officer, D. L., A pH-responsive hydroquinone-functionalised glassy carbon electrode. *Chem. Commun. (Cambridge, U. K.)* **2001**, 2628-2629.

151. Fan, L. S.; Chen, J.; Zhu, S. Y.; Wang, M.; Xu, G. B., Determination of Cd2+ and Pb2+ on glassy carbon electrode modified by electrochemical reduction of aromatic diazonium salts. *Electrochem. Commun.* **2009,** 11, 1823-1825.

152. Liu, G. Z.; Nguyen, Q. T.; Chow, E.; Bocking, T.; Hibbert, D. B.; Gooding, J. J., Study of factors affecting the performance of voltammetric copper sensors based on Gly-Gly-His modified glassy carbon and gold electrodes. *Electroanalysis* **2006,** 18, 1141-1151.

153. Wang, J.; Carlisle, J. A., Covalent immobilization of glucose oxidase on conducting ultrananocrystalline diamond thin films. *Diamond Relat. Mater.* **2006,** 15, 279-284.

154. Bourdillon, C.; Delamar, M.; Demaille, C.; Hitmi, R.; Moiroux, J.; Pinson, J., Immobilization of Glucose-Oxidase on a Carbon Surface Derivatized by Electrochemical Reduction of Diazonium Salts. *J. Electroanal. Chem.* **1992,** 336, 113-123.

155. Liu, G. Z.; Paddon-Row, M. N.; Gooding, J. J., A molecular wire modified glassy carbon electrode for achieving direct electron transfer to native glucose oxidase. *Electrochem. Commun.* **2007,** 9, 2218-2223.

156. Yang, X. H.; Hall, S. B.; Tan, S. N., Electrochemical reduction of a conjugated cinnamic acid diazonium salt as an immobilization matrix for glucose biosensor. *Electroanalysis* **2003,** 15, 885-891.

157. Polsky, R.; Harper, J. C.; Dirk, S. M.; Arango, D. C.; Wheeler, D. R.; Brozik, S. M., Diazonium-functionalized horseradish peroxidase immobilized via addressable electrodeposition: Direct electron transfer and electrochemical detection. *Langmuir* **2007,** 23, 364-366.

158. Vakurov, A.; Simpson, C. E.; Daly, C. L.; Gibson, T. D.; Millner, P. A., Acetylcholinesterase-based biosensor electrodes for organophosphate pesticide detection I. Modification of carbon surface for immobilization of acetylcholinesterase. *Biosens. Bioelectron.* **2004,** 20, 1118-1125.

159. Zhou, Y. L.; Zhi, J. F., Development of an amperometric biosensor based on covalent immobilization of tyrosinase on a boron-doped diamond electrode. *Electrochem. Commun.* **2006,** 8, 1811-1816.

160. Corgier, B. P.; Marquette, C. A.; Blum, L. J., Diazonium-protein adducts for graphite electrode microarrays modification: Direct and addressed electrochemical immobilization. *J. Am. Chem. Soc.* **2005,** 127, 18328-18332.

161. Harper, J. C.; Polsky, R.; Wheeler, D. R.; Dirk, S. M.; Brozik, S. M., Selective immobilization of DNA and antibody probes on electrode arrays: Simultaneous electrochemical detection of DNA and protein on a single platform. *Langmuir* **2007,** 23, 8285-8287.

162. Polsky, R.; Harper, J. C.; Wheeler, D. R.; Dirk, S. M.; Arango, D. C.; Brozik, S. M., Electrically addressable diazonium-functionalized antibodies for multianalyte electrochemical sensor applications. *Biosens. Bioelectron.* **2008,** 23, 757-764.

163. Pellissier, M.; Barriere, F.; Downard, A. J.; Leech, D., Improved stability of redox enzyme layers on glassy carbon electrodes via covalent grafting. *Electrochem. Commun.* **2008,** 10, 835-838.

164. Boland, S.; Jenkins, P.; Kavanagh, P.; Leech, D., Biocatalytic fuel cells: A comparison of surface pre-treatments for anchoring biocatalytic redox films on electrode surfaces. *J. Electroanal. Chem.* **2009,** 626, 111-115.

Chapter 2. General Experimental Methods

2.1 Introduction

This chapter describes materials, equipment, and general experimental procedures used throughout this thesis. Experimental information pertaining only to a specific chapter can be found in the experimental section of the relevant chapter.

2.2 Chemicals and Preparative Methods

2.2.1 Solutions

All aqueous solutions were prepared using Milli Q (MQ) water, > 18 MΩ cm. 0.1 M phosphate buffer (PB), pH 7.4, was prepared by dissolving 3.12 g of NaH_2PO_4 and 11.36 g of Na_2HPO_4 in 1 L of MQ water. Acetonitrile (ACN, HPLC grade) used for electrochemistry and in surface modification, was dried over CaH_2 for at least two days, and then refluxed under an N_2 atmosphere for two hours prior to distilling in an N_2 atmosphere.

2.2.2 Preparation of Tetrabutylammonium Tetraflouroborate Electrolyte

Tetrabutylammonium tetraflouroborate ($[Bu_4N]BF_4$) was prepared by mixing tetraammonium hydroxide (TBAOH, 40%, Acros Organics) with fluoroboric acid (HBF_4, 50%, Acros Organics). 5 mL of HBF_4 was diluted to 25 mL with MQ water. 20 mL of TBAOH was diluted to 100 mL using MQ water. Upon adding the diluted HBF_4 to the diluted TBAOH a white precipitate ($[Bu_4N]BF_4$) formed. The precipitate was filtered, washed with MQ water, and suction dried under vacuum for several hours. Subsequently, the electrolyte was dried in an oven at 60 °C for at least five days, and then under vacuum at 80 °C for a further day. The dry electrolyte was stored under vacuum.

2.2.3 Synthesis of Aryldiazonium Salts

Aryldiazonium tetrafluoroborate salts were synthesized using standard chemistry.[1] Initially, 5 mmol of the appropriate arylamine was added to 2 mL of 50 % HBF_4 diluted to 4 mL with MQ water. The solution was placed in an ice bath. 5 mmol of sodium nitrite was dissolved in a minimum of MQ water (~ 1 mL) and cooled in an ice bath. The sodium nitrite solution was added drop-wise to the aryl amine solution, with constant stirring, resulting in the formation of a precipitate (the aryldiazonium tetrafluoroborate salt). The precipitate was then collected using a vacuum filter. The product was re-precipitated from ACN, washed with cold ether, and then dried under vacuum suction for two hours. All aryldiazonium tetrafluorobortate salts were stored under vacuum in the dark. Anthraquinone-1-diazonium chloride (Fast Red AL Salt) was purchased from Aldrich.

2.2.4 Synthesis of Citrate-Capped Gold Nanoparticles

Citrate-capped gold nanoparticles were synthesized using literature methods.[2] 500 mL of a 1 mM solution of tetrachloroaurate ($HAuCl_4$, Alfa Aesar) in MQ water was refluxed with stirring. 50 mL of 38.8 mM sodium citrate in MQ water was added to the $HAuCl_4$ solution. The solution was seen to turn from a pale yellow to a burgundy color. After the color change, boiling was continued for ten minutes, and stirring was continued for an additional fifteen minutes after boiling ceased. Once cooled, the solution was filtered through a membrane filter (Millipore, 0.22 μm). The gold nanoparticle solutions were stored in the dark.

2.3 Surface Preparation

2.3.1 Glassy Carbon

Glassy carbon (GC) plates (~15 mm × 15 mm × 3 mm) and GC disk electrodes (diameter 3 mm) (Tokai Carbon Co. Ltd) were used in this work. The GC disk electrodes were produced in-house by sealing a glassy carbon rod in a Teflon tube in a manner so that only the end of the rod was

exposed. Prior to use, the GC surfaces were polished with a slurry of 1 μm alumina on a Leco polishing cloth and subsequently sonicated in acetone or methanol for five minutes and then rinsed with MQ water. Surfaces were dried with a stream of N_2 gas.

2.3.2 Pyrolyzed Photoresist Film

The procedure for fabricating pyrolyzed photoresist film (PPF) used in this work (and described below) is similar to methods previously described by other workers.[3-5] Initially, a protective coating of AZ1518 photoresist (Clariant) was spin coated onto Si (100) silicon wafers (Silicon Quest and Micro Materials) at 2000 rpm. The protective layer of photoresist was soft baked onto the silicon by placing the wafers on a hotplate at 90 °C for two minutes. Subsequently, the wafers were cut into pieces (~ 1.4 cm × 1.4 cm) using a diamond scribe. The protective layer was removed from the silicon squares by successive sonications in acetone (HPLC grade, Mallinckrodt) and isopropyl alcohol for five minutes each. The silicon pieces were then dried with a stream of N_2 gas. Photoresist AZ4620 (Clariant) was spin coated on the pre-cut silicon pieces at 3000 rpm for 30 seconds. The spin coated samples were soft baked in an oven at 60 °C overnight. Pyrolysis was achieved by heating the samples in a Radatherm tube furnace (Model 2216e) under a forming gas (95 % N_2 + 5 % H_2) atmosphere. The temperature was held at 500 °C for 30 minutes, 750 °C for 30 minutes, and 1060 °C for one hour. The furnace was then allowed to cool to room temperature (still under forming gas) before the samples were removed. The resistance of every PPF sample was tested prior to use. Only samples with resistances < 30 Ω square^{-1} were used. All PPF samples were sonicated in IPA for 10 seconds, and then dried with a steam of N_2, before use.

2.3.3 Gold Surfaces

Two types of gold substrates, Au/NiCr/Si and Au/mica, were fabricated and used in the work described in this thesis. All gold substrates were fabricated by thermal evaporation using a Balzer's Evaporator. Au/NiCr/Si substrates were prepared by thermally depositing 30 nm of

nichrome, followed by 250 nm of gold, on to pre cut (1.0 cm × 1.0 cm) Si (100) wafer (Silicon Quest and Micro Materials). Deposition occurred through a mask, giving a gold area of 0.785 cm^2 on each sample. The thicknesses of the layers were monitored and controlled using an integrated quartz crystal thickness monitor (SMQ 160, Sigma Instruments). The Si (100) wafer was protected with photoresist prior to cutting, in the same manner as described in Section 2.3.2.

Au/mica substrates were prepared by depositing 250 nm of gold onto mica by thermal evaporation. After deposition, metal disks were bound onto the exposed gold face using Epoxi-Patch (Dexter) cement. The samples were then cured at 60 °C for 24 hours. Subsequently the mica was cleaved off the gold substrates by immersion in liquid N_2 exposing the smooth gold surfaces.

2.4 Electrochemistry

2.4.1 Instrumentation

All cyclic voltammetry and electrochemical depositions were carried out using a Ecochemie Autolab PGSTAT 302 Potentiostat, computer-controlled EG & G PAR 273A Potentiostat, or a EG&G PAR 173 Potentiostat coupled to a Powerlab 4SP (AD Instruments). All open circuit potential (OCP) measurements were made using a Digitech QM1320 multimeter.

2.4.2 Electrochemical Cells and Electrodes

Electrochemical cells were stored in a 10 % HNO_3 acid bath. Prior to use the cells were thoroughly rinsed with acetone and dried at 60 °C. A Pt wire auxiliary electrode was used in all cyclic voltammetry and electro-deposition experiments. A saturated calomel electrode (SCE) reference electrode was used in all aqueous electrochemistry. In non-aqueous conditions a Ag wire pseudo-reference electrode was used, except in open circuit potential measurements, and associated cyclic voltammograms, in Chapter 4, for which a silver-silver nitrate (Ag/Ag+)

reference electrode was used. A pear-shaped glass cell was used in all experiments where the working electrode was a GC disk electrode. The GC disk electrodes used have a geometric surface area of 0.071 cm^2.

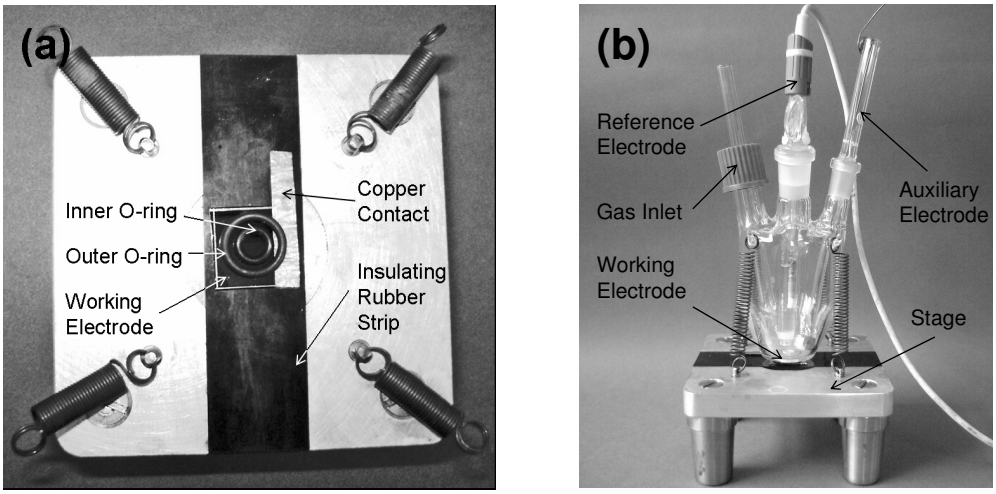

Figure 2.1. (a) Top down view of stage with working electrode, O-rings, and copper contact in place. (b) Assembled cell on stage with gas inlet and electrodes inserted.

Electrochemistry on GC plates, PPF, and gold samples required a different setup. The sample (the working electrode) was placed on an insulated region on a metal stage. A Viton O-ring was placed on the sample to define the area of the working electrode. A copper strip or gold wire was then placed on the electrode surface, outside the O-ring, to achieve electrical contact to the working electrode. A second larger O-ring was placed over the copper strip, outside the inner O-ring, to hold the copper in place (Figure 2.1 a). A pear shaped glass cell with a hole in the base was then placed on the metal stage so that the centre of the hole aligned with the center of the inner O-ring. Four springs attached to the stage were then attached to four positions of the cell in order to hold the cell in place and assure a tight seal between the cell and the O-ring, and the electrode and the O-ring (Figure 2.1 b). Unless stated otherwise, a 008 Viton O-ring was used as the inner O-ring, giving a geometric working electrode area of 0.18 cm^2. The area was calculated using the internal diameter of the O-ring, given by the manufacturer.

2.5 Atomic Force Microscopy

2.5.1 Instrumentation

Atomic force microscopy (AFM) was carried out using a Nanoscope Dimension TM 3100 controller (Digital Instruments) integrated with a Nanoscope IIIa scanning probe microscope controller (Digital Instruments).

2.5.2 Imaging

Topographical imaging was performed in non-contact mode using a silicon cantilever with Al backside (model NSC 15, Ultrasharp). Images were recorded at scan rates of ≤ 1 Hz with a resolution of 512 samples per line.

2.5.3 Film Thickness Measurements

AFM film thickness measurements were conducted using methods similar to those described previously by other workers[3] and are outlined below. The measurements were conducted in non-contact mode using silicon cantilevers (models NSC 12, CSC 12, and CSC 38, Ultrasharp). The cantilever configurations consisted of three cantilever tips of different lengths situated on a single silicon chip (Figure 2.2).

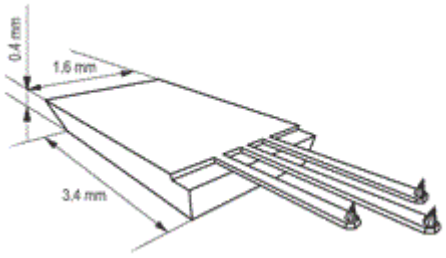

Figure 2.2. Schematic drawing of a three cantilever CSC 38 AFM probe.

In order to remove a section of the film from the surface, one of the two shorter tips was aligned in the usual manner for non-contact mode. When the chosen shorter AFM tip had approached the surface to begin a tapping mode scan, the longer tip imbedded into the surface and, upon scanning, removed a 10 μm × 1.25 μm section of film (Figure 2.3).

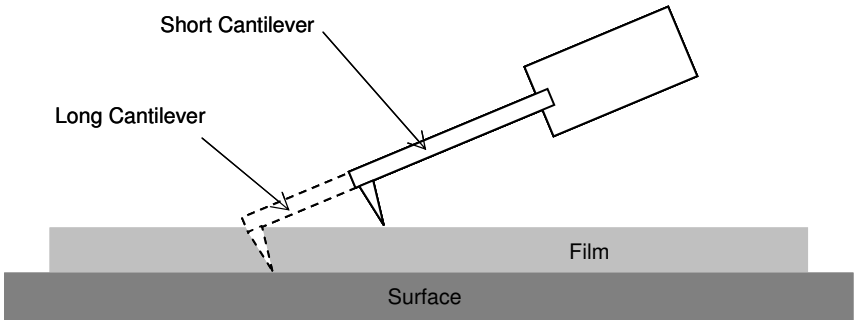

Figure 2.3. Schematic of a cross sectional view of an AFM film thickness experiment.

Four to six scans (depending on substrate, four on Au/mica, six on PPF) were carried out to remove the section of film, resulting in a 'scratch' in the film. After 'scratching' the tips were withdrawn from the surface and the short tip (in resonance) was positioned over the scratch to capture an image. Alternatively, the longer central tip was left positioned over the scratch and the AFM alignment was refocused (and re-tuned) over the longer tip. An image was then captured using the longer tip. In some cases, scratching of the bare surface also resulted in removal of a small amount (< 0.3 nm) of the surface. In those cases the data was adjusted by subtracting the depth of the scratch on the bare surface from the measured film thickness of the samples. This varied according to substrate, and the particular batch of the substrate. To ensure the measured thicknesses relate to the *p*-nitrophenyl (NP) films, rather than the reduced NP films, film measurements of NP films were undertaken on sections outside of the areas that were subject to electro-reduction.

For each sample, two scratches were made and imaged. In order to avoid interference from debris and surface defects, three areas of each scratch were selected for analysis. An average cross section was obtained for each of the selected areas of a scratch. Two film thicknesses were then determined from each average cross section, one from the step on the right side of the

section and the other from the left. Hence, unless stated otherwise, the film thickness for a sample was an average of twelve values (two scratches, three average cross sections per scratch, two values obtained from each cross section). The analysis was carried out using Nanoscope (Version 5.31R1) software. The uncertainty was determined by taking two standard deviations of the mean of the twelve thickness values.

2.5.4 Determination of Surface Roughness

Surface roughness was determined by imaging (see section 2.5.2) 1.5 μm × 1.5 μm sections of the sample. Three sections were imaged on each sample. Five areas were selected for analysis from each section, giving fifteen surface roughness values (Ra) for each sample. The reported surface roughness for a sample is the average of the fifteen roughness values obtained for the sample. Roughness analysis was carried out using Nanoscope (Version 5.31R1) software. The uncertainty for each sample was determined by taking two standard deviations of the average of the fifteen roughness values obtained for the sample.

2.6 Scanning Electron Microscopy

Scanning electron microscopy (SEM) was carried out using a JEOL 7000 high-resolution scanning electron microscope. An accelerating voltage of 15 kV was used.

2.7 Optical Microscopy

Optical microscopy was undertaken using an Olympus BX60 (inverted light) microscope connected to a LEICA DFC320 camera. A polarizer was fitted to the microscope allowing for differential interference contrasting settings. Magnifications of 50, 100, 200, 500 and 1000 × were possible. Images were processed using LEICA Application Suite V 2.3.1 R1 software for Windows XP.

2.8 Water Contact Angle Measurements

To obtain static water contact angles, a sample was placed on a horizontal stage and a 1 μL drop of MQ water was deposited onto the surface from a microsyringe. Immediately after depositing the drop an image was captured using an Edmund Scientific video camera and Matrox Intellicam Software for Windows XP software. Contact angles were determined using the Drop Analysis plugin for ImageJ.

2.9 X-Ray Photoelectron Spectroscopy

X-ray photoelectron spectroscopy (XPS) and the corresponding peak fitting, was carried out by Dr Byrony James, Department of Chemical and Materials Engineering at the University of Auckland. XPS data was obtained using a Kratos Axis Ultra DLD spectrometer equipped with a monochromatic Al Kα source (1486.6 eV), operated at 150 W. Narrow scans were recorded with a step size of 0.1 eV and a pass energy of 20 eV. Peak positions were referenced to aromatic carbon at 284.7 eV.

2.10 Atomic Absorption Spectroscopy

Atomic absorption spectroscopy was carried out using a Varian Spectra AA 220FS at a wavelength of 242.8 nm. A spectroscopic slit width of 1 nm, and lamp current 4 mA, was used. Gold calibration standards (100, 200, 400, and 600 pbb) were prepared using hydrogen tetrachloroaurate in 0.1 M H_2SO_4.

2.11 General Surface Modification Procedures

All solutions used to achieve surface modification were degassed with N_2 for ≥ 5 minutes prior to modification. A constant stream of N_2 was maintained over the solution during modification (except in the case of Microcontact printing, Chapter 6). In cases where isolation of the required aryldiazonium salt was not possible, modification was achieved by using the in situ generated aryldiazonium cation. Modification utilizing in situ generated aryldiazonium cations was achieved using a method developed by Bélanger and coworkers.[6] Initially a specific quantity of the relevant arylamine was dissolved in 0.5 M HCl. Subsequently, an equimolar quantity of sodium nitrite, dissolved in a minimum of 0.5 M HCl, was added to the arylamine solution. The solution was stirred by degassing with N_2 for five minutes prior to modification. After modification, all surfaces were sonicated for five minutes in MQ water and dried with a stream of N_2.

2.11.1 Electrochemical Modification of Surfaces

Unless stated otherwise, electrochemical modification via electro-reduction of isolated aryldiazonium salts was conducted in 1 mM solutions of the selected aryldiazonium salt. Modification via an in situ generated aryldiazonium cation utilized a 5 mM solution of the relevant aryl amine. Electro-modification was achieved either by carrying out cyclic voltammetric scans in the potential region for the reduction of the aryldiazonium salt, or by holding at a potential more negative than the observed peak assigned to reduction of the aryldiazonium salt.

2.11.2 Spontaneous Modification of Surfaces

All spontaneous modification was carried out in the absence of light in a temperature controlled room at (25 ± 2) ºC. Unless stated otherwise, spontaneous modification using an isolated

aryldiazonium salt was conducted in a 10 mM solution of the selected aryldiazonium salt. Modification via an in situ generated aryldiazonium cation was undertaken using a 10 mM solution of the relevant aryl amine.

2.12 Data Analysis and Software

2.12.1 Determination of Charge and Electrochemical Surface Concentration

The charge (Q) transferred during an electrochemical process was determined from the relevant voltametmetic peak area, in accordance with Equation 2.1.

$$Q = \frac{\int I \, \mathrm{d}V}{\dot{V}} \qquad (2.1)$$

Where I is the current (in amps), V is the potential (in volts) and $\dot{V}$ is the (constant) potential scan rate (in volts per second). Since $(V \times A)/(V\ s^{-1}) = A\ s = C$, this gives the total transferred charge (in coulombs).

Integration was performed using Linkfit curve fitting software.[7] Voigt curves were fitted to the voltammetric peaks via the Levenberg-Marquardt algorithm.[8] Third order polynomial baselines were determined using the nonlinear least squares iteration and were subtracted from the voltammogram prior to the curve fit. Previous work within the research group has estimated the error associated with the integration to be ~ 20 %.[9]

Electrochemical surface concentrations were calculated from corresponding charges using Equation (2.2).[10]

$$\Gamma = \frac{Q}{nFA} \qquad (2.2)$$

where Γ is the electrochemical surface concentration (in mol cm^{-2}), Q is the charge associated with the observed redox process (in coulombs), F is Faradays constant (96485 C mol^{-1}), n is the number of moles of electrons transferred for each mole of the redox process, and A is the area of the working electrode (in cm^2).

2.12.2 Software

All graphing and curve fitting (other than that described in Section 2.12.1) was carried out using Sigmaplot 9.0 software. Calculations were performed in Microsoft Excel 2002.

2.13 References

1. Saunders, K. H.; Allen, R. L. M., *Aromatic Diazo Compounds*. 3rd ed.; Edward Arnold: London, 1985.

2. Bright, R. M.; Musick, M. D.; Natan, M. J., Preparation and characterization of Ag colloid monolayers. *Langmuir* **1998,** 14, 5695-5701.

3. Brooksby, P. A.; Downard, A. J., Electrochemical and atomic force microscopy study of carbon surface modification via diazonium reduction in aqueous and acetonitrile solutions. *Langmuir* **2004,** 20, 5038-5045.

4. Kim, J.; Song, X.; Kinoshita, K.; Madou, M.; White, B., Electrochemical studies of carbon films from pyrolyzed photoresist. *J. Electrochem. Soc.* **1998,** 145, 2314-2319.

5. Ranganathan, S.; McCreery, R. L., Electroanalytical performance of carbon films with near-atomic flatness. *Anal. Chem.* **2001,** 73, 893-900.

6. Baranton, S.; Belanger, D., Electrochemical derivatization of carbon surface by reduction of in situ generated diazonium cations. *J. Phys. Chem. B* **2005,** 109, 24401-24410.

7. Loring, J. S., *Linkfit*. 2004.

8. Levenberg, K., A method for the solution of certain non-linear problems in least squares. *The Quarterly of Applied Mathematics* **1944,** 2, 164-168.

9. Yu, S. C., *PhD thesis: covalent attachment of nanoscale organic films to carbon electrodes*. University of Canterbury: 2008.

10. Bard, A. J.; Faulkner, L. R., *Electrochemical Methods: Fundamentals and Applications*. 2nd ed.; John Wiley & Sons, Inc: Danvers, 2001.

Chapter 3. Modification of Glassy Carbon with Electro-Active Films by Electro-Reduction of Aryldiazonium Salts

3.1 Introduction

Covalent modification of carbon surfaces by electrochemical reduction of aryldiazonium salts has been reviewed in Section 1.3.1 of this thesis. To briefly recap, Scheme 3.1 shows the radical coupling reaction by which electrochemical modification of surfaces using aryldiazonium salts has been proposed to proceed.[1] The electrochemically induced one-electron reduction of the aryldiazonium cation leads to the formation of an aryl radical which reacts with the surface resulting in the formation of a surface-C bond (in the case of a carbon surface a C-C bond). It has been shown by a number of workers that electro-reduction of diazonium salts at carbon surfaces can result in the formation of multilayers[2-6] via a process in which aryl radicals react with other aryl groups already bound to the surface.

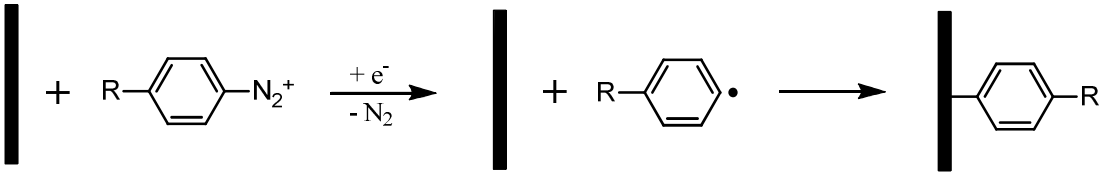

Scheme 3.1. Electrochemical reduction of a aryldiazonium cation leading to covalent attachment of an aryl group on a surface.[1]

Characterization of films formed using aryldiazonium salts presents considerable challenges. One method is to modify the surface with electro-active functionalities[1, 5, 7-12] that can be detected using cyclic voltammetry; the surface concentration of electro-active groups can then be calculated from the charge associated with the film redox reactions (in the manner described in Section 2.12.1).

The aim of this chapter is to examine the utility of various electro-active films in terms of their suitability for film characterization. To date only a limited number of electro-active diazonium cation modifiers have been reported. The most commonly used is *p*-nitrophenyl (NP), and NP films have become the benchmark for electrochemical film characterization studies. NP films exhibit a chemically reversible redox couple in aprotic conditions; in protic conditions the redox system is irreversible. However, in both situations the NP redox responses have drawbacks and limitations. The reversible NP redox couple requires very dry conditions making it experimentally difficult to observe. Furthermore, the system exhibits poor stability upon repeat cycling. The NP reduction observed in protic conditions can be observed only on the first scan, due its irreversible nature, and hence only allows for "one-shot" determination of surface concentration. In this work, anthraquinone and *o*-nitrophenol diazonium cation derivatives were chosen to be investigated as possible alternative modifiers to NP since they have both been reported to exhibit reversible redox systems in aqueous conditions.[9, 11] Furthermore, the diazonium salts of both are either commercially available, or can be easily synthesized from a commercially available precursor.

3.2 Experimental

Potassium ferricyanide ($K_3Fe(CN)_6$) redox-probe voltammetry was carried out using 1 mM of $K_3Fe(CN)_6$ in 0.1 M phosphate buffer, pH 7.4. The electrochemistry of anthraquinone modified glassy carbon surfaces was investigated in 0.1 M KOH. The electrochemistry of *p*-nitrophenyl (NP) and *o*-nitrophenol (NPOH) films was studied in 0.14 M H_2SO_4. All modification was conducted using a 1 mM solution of the relevant aryldiazonium salt. Cyclic voltammograms were recorded at a scan rate of 100 mV s^{-1}, unless specified otherwise. Glassy carbon (GC) disk electrodes (area = 0.071 cm^2) were used as working electrodes for all the work described in this chapter.

3.3 Modification of GC with NP Films

3.3.1 Electro-Reduction of NBD at GC

The electrochemically induced modification of GC with *p*-nitrophenyl (NP) functionalities via the electro-reduction of *p*-nitrobenzene diazonium tetrafluoroborate salt (NBD) was investigated in 0.14 M H_2SO_4 and in acetonitrile (ACN) containing 0.1 M tetrabutylammonium tetrafluoroborate ($[Bu_4N]BF_4$) electrolyte. Modification was conducted in both media by recording cyclic voltammetric scans (initial potential ~0.5 V) in the presence of 1 mM NBD. Figure 3.1 shows the irreversible reduction peaks assigned to the one-electron reduction of NBD in ACN (a) and in 0.14 M H_2SO_4 (b).

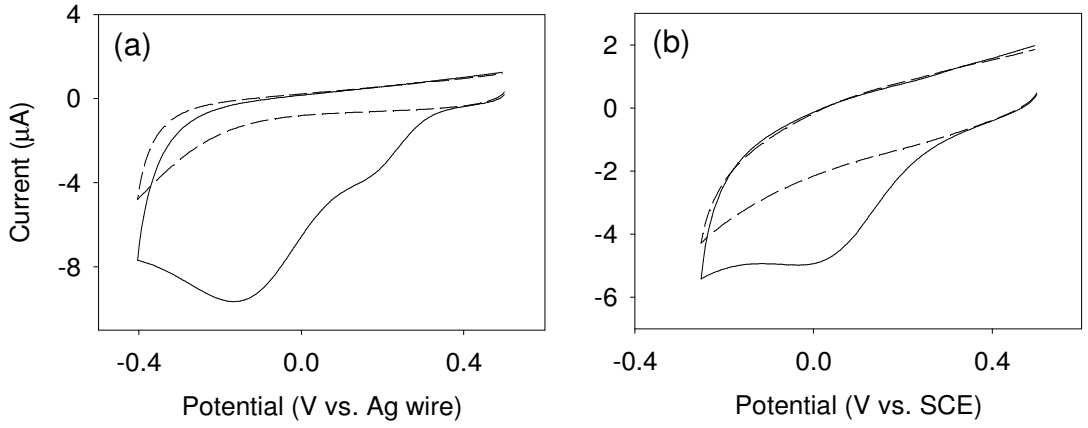

Figure 3.1. Electrochemical reduction of NBD at a GC disk working electrode in 0.1 M $[Bu_4N]BF_4$/ACN (a) and 0.14 M H_2SO_4 (b): (—) first scan; (---) second scan with one minute of stirring by bubbling with N_2 gas between the scans. Scan rate = 100 mV s^{-1}.

In both cases the solution was stirred (by bubbling with N_2 gas) for one minute between the first (—) and the second (---) scans. The disappearance of the reduction peak on the second scan is consistent with the formation of a passivating film, which blocks the reduction of NBD by inhibiting electron transfer from the electrode surface to NBD in solution. This passivating effect of diazonium cation derived films has been previously reported by other workers.[1, 5, 9, 10] The accepted mechanism for film formation is shown in Scheme 3.1, with R = NO_2. For convenience,

NP films on GC, generated in ACN and 0.14 M H_2SO_4, will be referred to as $NP_{GC\text{-}ACN}$ and $NP_{GC\text{-}Aq}$, respectively.

3.3.2 Effect of NP Modification on Redox Probe Voltammetry of $Fe(CN)_6^{3-}$

Comparison of the cyclic voltammetric response of solution redox probes at modified and unmodified electrodes is a useful method for verifying surface modification. Ferricyanide ($Fe(CN)_6^{3-}$) is a surface-sensitive inner-sphere redox probe,[13] which is commonly used for this purpose.[14-16] After the standard post-modification sonication procedure, the redox response of the $NP_{GC\text{-}ACN}$ and $NP_{GC\text{-}Aq}$ modified electrodes, prepared as described above, was examined. Figure 3.2 shows cyclic voltammograms recorded in the presence of ($Fe(CN)_6^{3-}$) at bare, freshly polished GC (—), and $NP_{GC\text{-}ACN}$ (a) and $NP_{GC\text{-}Aq}$ (b) modified GC (---).

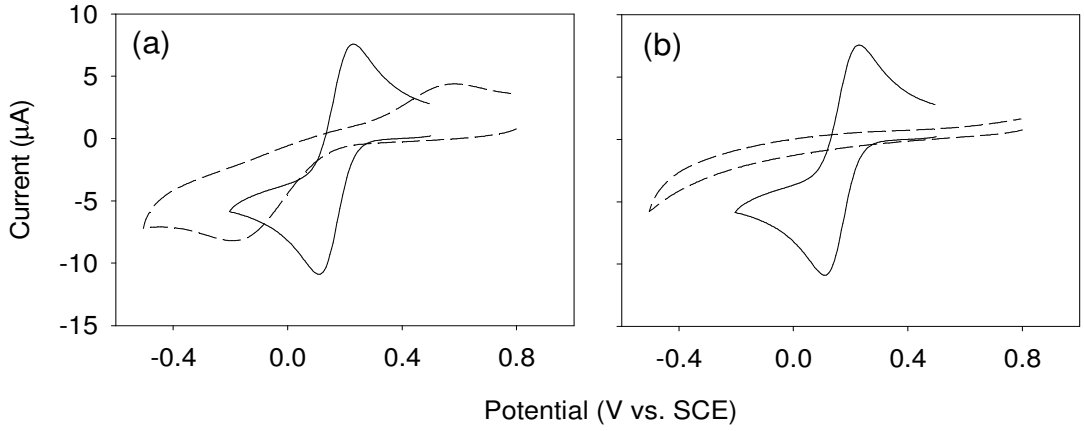

Figure 3.2. Cyclic voltammograms recorded in the presence of ($Fe(CN)_6^{3-}$) at bare freshly polished GC (—), and $NP_{GC\text{-}ACN}$ (a) and $NP_{GC\text{-}Aq}$ (b) modified GC (---). Initial potential > 0.4 V vs. SCE. Scan rate = 100 mV s^{-1}.

The cyclic voltammogram recorded at the bare GC electrode shows the quasi-reversible $Fe(CN)_6^{3-/4-}$ redox couple at $E_{1/2} \approx 0.15$ V vs. SCE with a peak separation $\Delta E_p = 0.14$ V. Upon modification with a $NP_{GC\text{-}ACN}$ film, the peak separation increases to $\Delta E_p = 0.81$ V, indicating a decrease in the rate of electron transfer to and from $Fe(CN)_6^{3-/4-}$. This suppressed $Fe(CN)_6^{3-/4-}$ response is evidence for the presence of an insulting film at the electrode surface and has been

observed by other workers for diazonium cation derived films.[14, 16] Upon modification of GC with a NP_{GC-Aq} film, the $Fe(CN)_6^{3-/4-}$ redox couple is seen to disappear completely, indicating the NP film formed in aqueous conditions inhibits electron transfer more strongly than that formed in ACN. These voltammograms demonstrate that redox probe voltammetry is a useful technique for confirming the presence of a blocking film on the electrode surface.

3.3.3 Electrochemistry of NP Modified GC

Electrode modification via electro-reduction of NBD leads to the formation of an electro-active NP film on the surface. The resulting film can be directly detected in both protic and aprotic conditions using cyclic voltammetry. In strictly dry aprotic conditions the NP groups exhibit a one electron chemically reversible reduction (Scheme 3.2).[17]

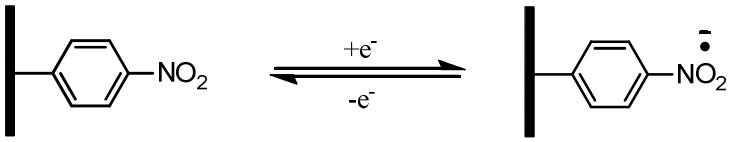

Scheme 3.2. Chemically reversible one electron reduction of surface bound NP group in aprotic conditions.

There are several difficulties associated with detecting and quantifying NP in aprotic medium. Firstly, since the redox process involves only one electron, small voltammetric peaks are observed. Secondly, the requirement for very dry conditions, to avoid decomposition of the radical anion, presents experimental challenges.[18] For these reasons, in this work reduction in protic conditions (described below) was used to detect and characterize NP films.

In protic conditions NP films can be detected and characterized by observing the irreversible multi-electron reduction of the bound NP groups (Scheme 3.3).

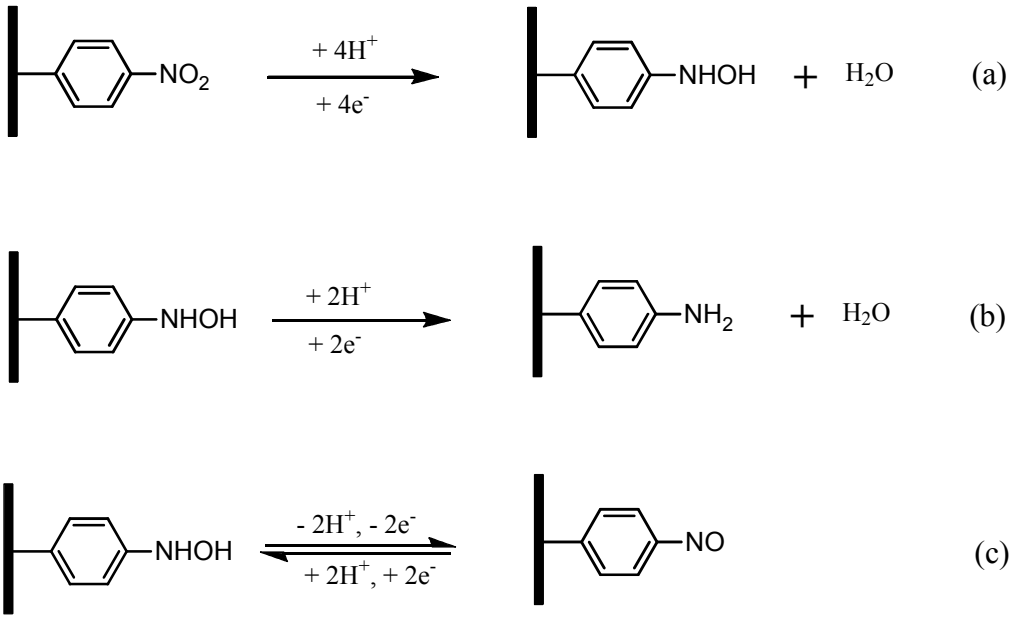

Scheme 3.3. (a) Irreversible four-electron reduction of bound NP to bound hydroxyaminophenyl. (b) Irreversible two electron reduction of bound hydroxyaminophenyl to bound aminophenyl. (c) Chemically reversible hydroxyaminophenyl/nitrosophenyl redox couple.[12]

Figure 3.3 shows consecutive cyclic voltammograms of $NP_{GC\text{-}ACN}$ (a) and $NP_{GC\text{-}Aq}$ (b) films at GC in 0.14 M H_2SO_4, prepared as described in Section 3.3.1. Scanning in the negative direction from an initial potential of 0.8 V shows a reduction peak at $E_{p,c} \approx$ -0.6 V during the first scan (—). This peak is not seen in the second scan (---) indicating that it is associated with a chemically irreversible process (or processes). The peak has been assigned to the six-electron reduction of NP groups to aminophenyl (AP) groups (Scheme 3.3 (a) and (b)) and the four-electron reduction of NP groups to hydroxyaminophenyl (APOH) groups (Scheme 3.3 (a)).[12] After reduction of the NP groups, a reversible redox couple is observed at $E_{1/2} \approx$ 0.3 V. This reversible redox couple is assigned to the APOH/nitrosophenyl redox couple (Scheme 3.3 (c)) and arises due to the incomplete reduction of APOH to AP. [12] These peaks were originally assigned by Bélanger and coworkers.[12] Note that the small oxidation peak observed at $E_{p,a} \approx$ 0.1 V in Figure 3.3 (b) was seen intermittently and is probably a solvent effect not associated with the bound NP film.

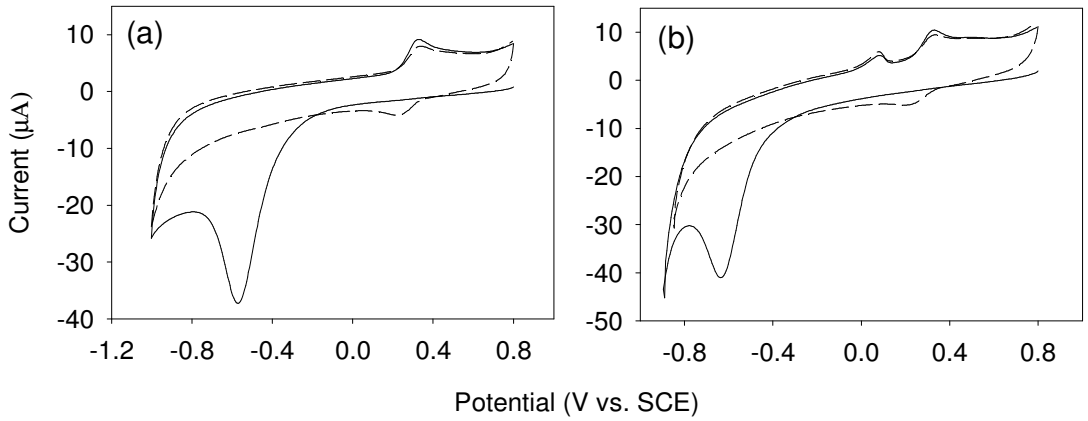

Figure 3.3. Consecutive cyclic voltammograms of $NP_{GC\text{-}ACN}$ (a) and $NP_{GC\text{-}Aq}$ (b) films at GC (prepared as described in Section 3.3.1) in 0.14 M H_2SO_4; (—) first scan and (---) second scan. Scan rate = 100 mV s^{-1}.

Determination of the peak areas, and hence the charge-transfers associated with the peaks, allows estimation of the surface concentration of electro-active NP groups, Γ_{NP}. Initially, the surface concentration of APOH groups, Γ_{APOH}, produced by four-electron reduction of the NP groups is calculated from the charge transfer, Q_{ox}, associated with the two-electron APOH oxidation (step (c) of Scheme 3.3) observed during the first scan at $E_{p,a} \approx 0.4$ V, using Equation 3.1.

$$\Gamma_{\mathrm{APOH}} = \frac{Q_{\mathrm{ox}}}{2FA} \qquad (3.1)$$

Similarly the surface concentration of AP groups produced by electro-reduction of NP groups, Γ_{AP}, can be calculated using Equation 3.2,

$$\Gamma_{\mathrm{AP}} = \frac{Q_{red} - 2Q_{ox}}{6FA} \qquad (3.2)$$

where Q_{red} is the charge associated with the irreversible reduction peak observed at $E_{p,c} \approx -0.6$ V. Finally, the surface concentration of electro-active NP groups, Γ_{NP}, prior to electro-reduction is calculated using Equation 3.3.[19]

$$\Gamma_{NP} = \Gamma_{AP} + \Gamma_{APOH} = \frac{Q_{ox} + Q_{red}}{6FA} \quad (3.3)$$

Table 3.1 shows the calculated values of Γ_{APOH}, Γ_{AP}, and Γ_{NP}, for the $NP_{GC\text{-}ACN}$ and $NP_{GC\text{-}Aq}$ films prepared as described in Section 3.3.1. The surface concentrations of NP groups prior to electro-reduction, Γ_{NP}, were determined to be 15.3×10^{-10} mol cm^{-2} and 9.6×10^{-10} mol cm^{-2} for $NP_{GC\text{-}ACN}$ and $NP_{GC\text{-}Aq}$ films, respectively. These are similar to the theoretical value for a close-packed monolayer of NP groups on a perfectly flat surface (12×10^{-10} mol cm^{-2}).[20] However, polished GC has been shown to have a typical surface roughness factor (actual area/geometric area) between 1.5 and 2.5.[21] Hence, based on the active, rather than geometric, surface area of the GC, Γ_{NP} for $NP_{GC\text{-}ACN}$ and $NP_{GC\text{-}Aq}$ films are estimated to be in the range of $6.1 - 10.2 \times 10^{-10}$ mol cm^{-2} and $3.8 - 6.4 \times 10^{-10}$ mol cm^{-2}, respectively. Assuming close-packed layer structures, these values suggest that sub-monolayer films are formed. However, Brooksby et al. determined that the packing density of NP films formed by electro-reduction NBD at pyrolyzed photoresist films (PPF, ultra-flat carbon) is $(2.5 \pm 0.5) \times 10^{-10}$ mol cm^{-2} per monolayer thickness.[5] Assuming a similar packing density at GC, it can be concluded that the $NP_{GC\text{-}ACN}$ and $NP_{GC\text{-}Aq}$ films formed here are loosely packed multilayers approximately 2 to 4 and 1 to 3 layers thick, respectively.

Table 3.1. Surface concentrations of AP groups, Γ_{AP}, and APOH groups, Γ_{APOH}, produced during the electro-reduction of NP films and surface concentrations electro-active NP groups, Γ_{NP}, prior to electro-reduction, at $NP_{GC\text{-}ACN}$ and $NP_{GC\text{-}Aq}$ modified GC.

Film	Surface Concentration (10^{-10} mol cm^{-2})		
Type	Γ_{AP}	Γ_{APOH}	Γ_{NP}
$NP_{GC\text{-}ACN}$	9.0	6.3	15.3
$NP_{GC\text{-}Aq}$	6.7	2.9	9.6

Although films formed in aqueous conditions have a lower surface concentration of electro-active NP groups than the corresponding films formed in ACN, they appeared more blocking to the $Fe(CN)_6^{3-/4-}$ redox response (see Section 3.3.2). This finding is consistent with the work of Brooksby et al. who found that modification of PPF with NP films in aqueous conditions led to

lower surface concentrations, but a more effectively blocked $Fe(CN)_6^{3-/4-}$ redox response, than for the corresponding films formed in ACN.[5] On the basis of these findings it was suggested by the same workers that, during preparation in aqueous conditions, denser NP films are formed which become blocking more quickly than the films formed in ACN. Inhibition of electron transfer from the electrode to NBD in solution prevents electro-reduction of the NBD cation, and hence prevents film growth, leading to lower surface concentrations for the films formed in aqueous conditions than for those formed in ACN.[5] Further evidence supporting these findings is obtained by considering the potential at which the reduction of the $NP_{GC\text{-}ACN}$ and the $NP_{GC\text{-}Aq}$ films occurs (Figure 3.3). The more negative peak potential for the reduction of the $NP_{GC\text{-}Aq}$ film ($E_{p,c}$ = -0.65 V) than for the $NP_{GC\text{-}ACN}$ film ($E_{p,c}$ = -0.58 V) is indicative of slower electron transfer to NP groups within the $NP_{GC\text{-}Aq}$ film. The deceased rate of electron transfer may arise from slower diffusion of solvent into the film. This supports the hypothesis that NP films formed in aqueous conditions are denser than those formed in ACN.

The ease of electrochemical detection and quantification of bound NP groups has made NBD a popular aryldiazonium salt for studying the reaction of aryldiazonium salts with surfaces, and for characterizing the resulting films.[1, 5, 7, 8, 12, 14, 19] However, there are a number of unresolved issues surrounding the calculation of surface concentration on the basis of the NP reduction. Although the same criteria for determining peak areas have been used throughout this thesis, the absolute values have considerable associated uncertainties (approximately 20 %, see section 2.12). For cyclic voltammograms such as those in Figure 3.3 it is unclear where the baseline for the irreversible reduction peak (at $E_{p,c} \approx$ -0.6 V) should be positioned. The problem arises in part because the reduction peak is situated close to the solvent limit, making it unclear how much of the observed charge is associated with NP reduction and how much is associated with solvent reduction. The problem is compounded by the fact that during the recording of cyclic voltammograms the film, and hence the baseline for the peak, is constantly changing. Consequently the second scan cannot serve as an accurate baseline.[22] The two types of electro-active films investigated below were chosen in part to minimize these problems. Both exhibit electrochemical systems that are less convoluted with the solvent limit.

3.4 Modification of GC with NPOH Films

O'Sullivan and coworkers have reported the modification of GC electrodes with *o*-nitrophenol (NPOH) films via electro-reduction of 4-hydroxy-3-nitrobenzenediazonium salt (HNBD).[11] After reduction of the NPOH films, the resulting *o*-aminophenol films exhibited a chemically reversible two-electron redox couple in aqueous conditions at a mild potential.[11] In this section, the feasibility of the system for film characterization studies was investigated.

3.4.1 Electro-Reduction of HNBD at GC

The electrochemically induced modification of GC with NPOH films via reduction of HNBD was investigated by cyclic voltammetry in 0.1 M $[Bu_4N]BF_4$/ACN and 0.14 M H_2SO_4. However, scanning in the negative direction between 0.5 and -0.5 V revealed no peaks in either medium, despite reports of the reduction of HNBD in this potential range.[11]

Further experiments were undertaken to determine whether modification was successful and, if so, the potential at which modification occurs. These were carried out by holding a GC electrode at a fixed potential for ten seconds in the presence of HNBD in 0.14 M H_2SO_4. After the standard post modification sonication procedure, the electrode was transferred to a cell containing 0.14 M H_2SO_4 and cyclic voltammograms were recorded between 0.8 and -0.8 by scanning in the negative direction from an initial potential of -0.1 V. The procedure was repeated, applying various selected potentials for ten seconds, in the presence of HNBD, between +1.0 and -0.2 V vs. SCE. The electrode was polished before each deposition to remove any previous film material. Figure 3.4 shows a cyclic voltammogram of a GC electrode in 0.14 M H_2SO_4 after modification with NPOH by application a fixed potential (-0.2 V vs. SCE). The irreversible reduction at $E_{p,c} \approx$ -0.4 V is assigned to the NPOH reduction (Scheme 3.4 (a) and (b)). Subsequently, two reversible redox couples were observed at $E_{1/2} \approx$ 0.1 and 0.25 V. These couples are assigned to the hydroxyaminophenol/nitrosophenol couple (Scheme 3.4 (c)), which appears to proceed via two consecutive one-electron processes. The reversible couple observed at $E_{1/2} \approx$ 0.5 V is assigned to the *o*-aminophenol/*o*-quinoneimine couple (Scheme 3.4 (d)).[11, 23]

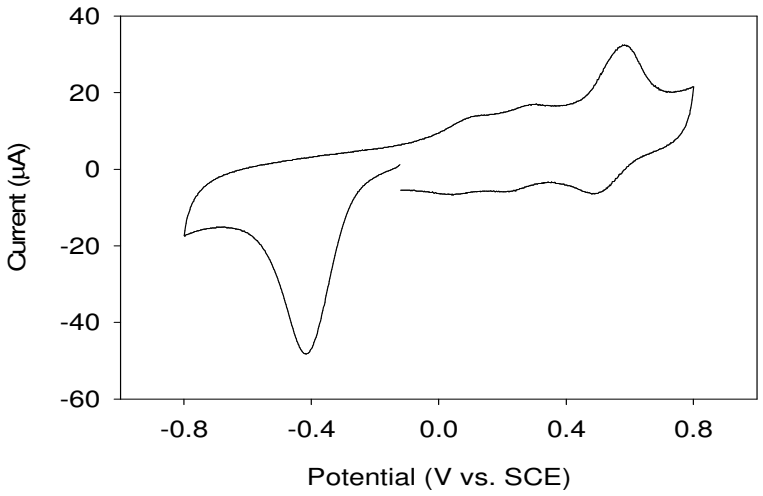

Figure 3.4. Cyclic voltammogram of the electrochemistry of NPOH modified GC. Modification was achieved by applying a potential of -0.2 V vs. SCE in 1 mM solution of HNBD in 0.14 M H_2SO_4 for ten seconds.

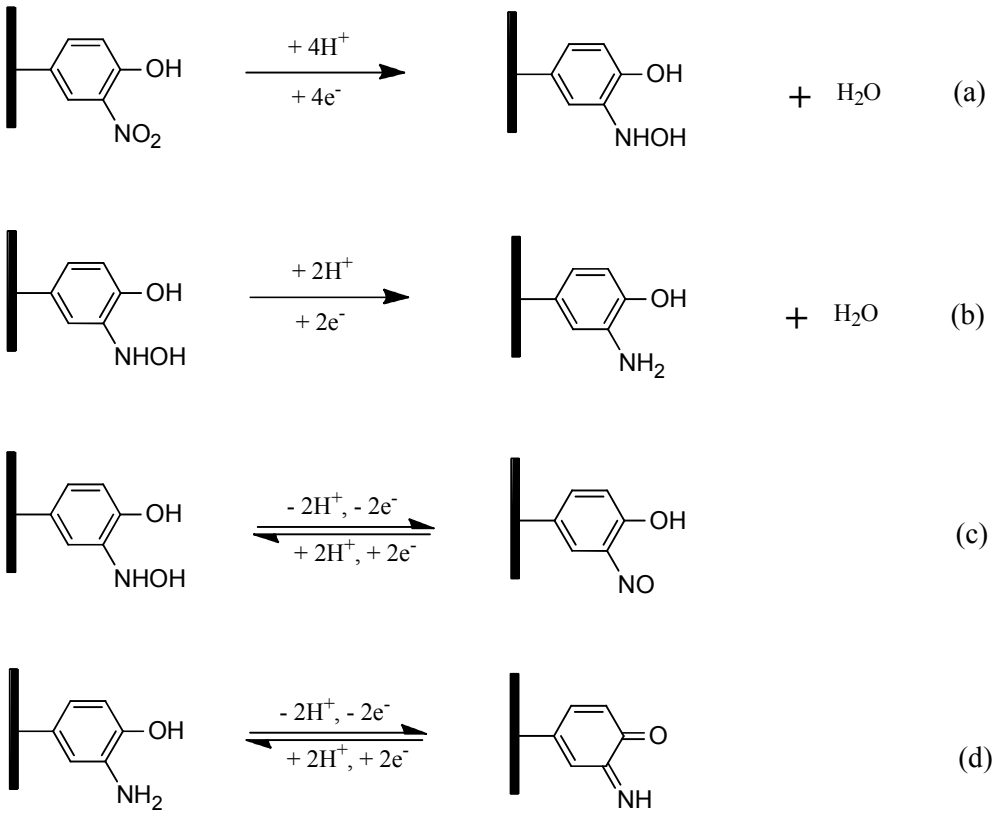

Scheme 3.4. (a) Irreversible four-electron reduction of a bound NPOH to bound hydroxyaminophenol. (b) Irreversible two-electron reduction of bound hydroxyaminophenol to bound aminophenol. (c) Chemically reversible hydroxyaminophenol/nitrosophenol redox couple. (d) Chemically reversible *o*-aminophenol/*o*-quinoeimine couple.

The cyclic voltammetric peaks, assigned to the *o*-nitrophenol redox systems were observed for electrodes modified at all the applied potentials between -0.2 and 1.0 V, indicating modification had occurred in all instances. The surface concentration of NPOH groups was calculated from the nitrophenol reduction (steps (a) and (b)) and the hydroxyaminophenol/nitrosophenol redox couple (step (c)) a described for $\Gamma_{NPOH}(1)$ in Section 3.4.2. Figure 3.5 shows a plot $\Gamma_{NPOH}(1)$ vs. the potential applied to achieve modification.

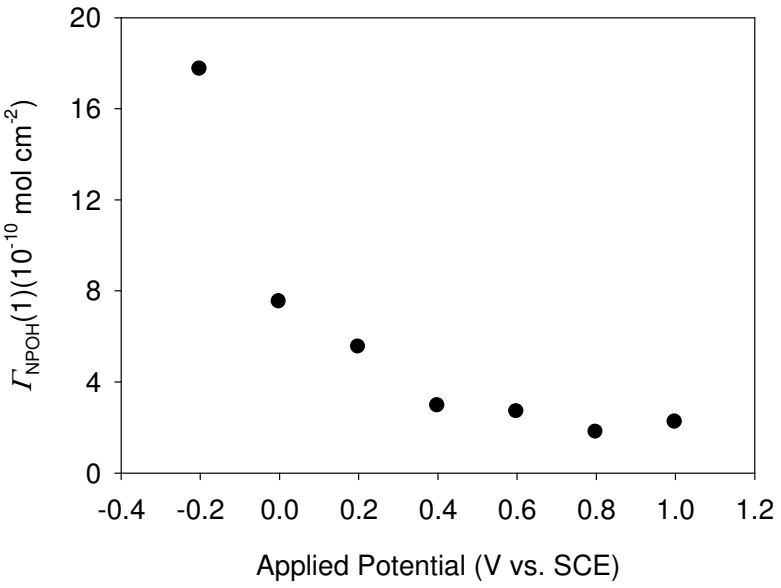

Figure 3.5. Surface concentration of electro-active *o*-nitrophenol groups at the surface vs. potential applied to achieve modification.

Low surface concentrations (~ 3×10^{-10} mol cm^{-2}) of nitrophenol groups are obtained at applied potentials $\geq$ 0.4 V vs. SCE. The presence of the small amounts of nitrophenol groups present after application of these relatively high potentials could be due to rapid spontaneous reaction (see Section 1.3.2) of HNBD with the surface after immersion of the electrode in the HNBD solution but prior to the application of a potential. At potentials < 0.4 V vs. SCE there is an increase in $\Gamma_{NPOH}(1)$ with a decrease in the applied potential, indicating that the reduction of HNBD, and electro-induced modification of the GC, occurs at potentials < 0.4 V vs. SCE. In the work of O'Sullivan and coworkers, the reduction of HNBD was observed at 0.353 V vs.

Ag/AgCl using cyclic voltammetry under similar conditions.[11] The reason why the HNBD reduction peak was observed in that investigation, but not in the present work, remains unclear. However, the potential of the HNBD reduction peak observed by O'Sullivan and coworkers is consistent with the potential for the reduction of HNBD determined in the present work.

3.4.2 Electrochemistry of NPOH Modified GC

The feasibility of the *o*-aminophenol/*o*-quinoeimine couple (Scheme 3.4, step (d)) for film characterization studies was further investigated. The surface concentration of electro-active nitrophenol groups, Γ_{NPOH}, can be calculated in two manners from cyclic voltammograms like that shown in Figure 3.4. Firstly it can be calculated from the irreversible nitrophenol reduction (Q_{red} for steps (a) and (b) in Scheme 3.4 obtained from the peak near -0.4 V vs. SCE) and the hydroxyaminophenol oxidation ($Q_{ox(c)}$ for step (c) from the oxidation peaks in the range 0.0 – 0.4 V) using Equation 3.4. The values calculated by this method will be referred to as $\Gamma_{NPOH}(1)$.

$$\Gamma_{NPOH}(1) = \frac{Q_{ox(c)} + Q_{red}}{6FA} \qquad (3.4)$$

Secondly, Γ_{NPOH} can be calculated by using the *o*-aminophenol oxidation ($Q_{ox(d)}$ for step (d), peak at ~0.50 V) to determine the concentration of aminophenol groups produced by electro-reduction of the nitrophenol functionalities and then adding this to the concentration of the hydroxyaminophenol groups ($Q_{ox(c)}$ from step (c)). The values calculated by this method, using Equation 3.5, will be referred to as $\Gamma_{NPOH}(2)$.

$$\Gamma_{NPOH}(2) = \frac{Q_{ox(c)} + Q_{ox(d)}}{2FA} \qquad (3.5)$$

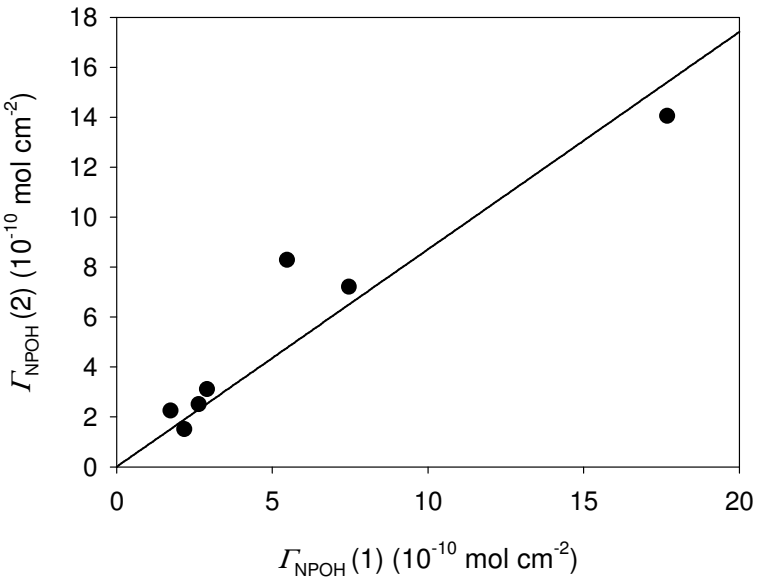

Figure 3.6. Γ_{NPOH} (2) vs. Γ_{NPOH} (1). Linear regression line forced through origin with slope = 0.87 (± 0.15), R^2= 0.88.

Figure 3.6 shows a plot of Γ_{NPOH} (2) vs. Γ_{NPOH} (1). The slope of 0.88 (± 0.16) shows that the values for Γ_{NPOH} (2) are the same as those for Γ_{NPOH} (1), at the 95% confidence. This gives additional confidence in the accuracy of the surface concentrations determined by both methods.

3.5 Modification of GC with AQ Films

Pinson and coworkers were the first to report the modification of GC electrodes with anthraquinone (AQ) films via electro-reduction of anthraquinone-1-diazonium chloride.[7] The AQ films have been shown to exhibit a reversible two-electron redox couple in aqueous conditions,[9] and have been used to modify a number of surfaces.[24-27] In this section, the feasibility of the AQ system for film characterization studies was investigated.

3.5.1 Electro-Reduction of Anthraquinone Diazonium Cation at GC

Modification of GC electrodes via the electro-reduction of anthraquinone-1-diazonium cation was investigated in 0.1 M $[Bu_4N]BF_4$/ACN and 0.14 M H_2SO_4. Modification was carried out by scanning in the negative direction between +0.8 and 0.0 V. Figure 3.7 shows voltammetric scans in the presence of 1 mM anthraquinone-1-diazonium chloride in ACN (a) and 0.14 M H_2SO_4 (b). In the first scan (—) an irreversible reduction peak was observed at $E_{p,c} \approx 0.3$ V in both media.

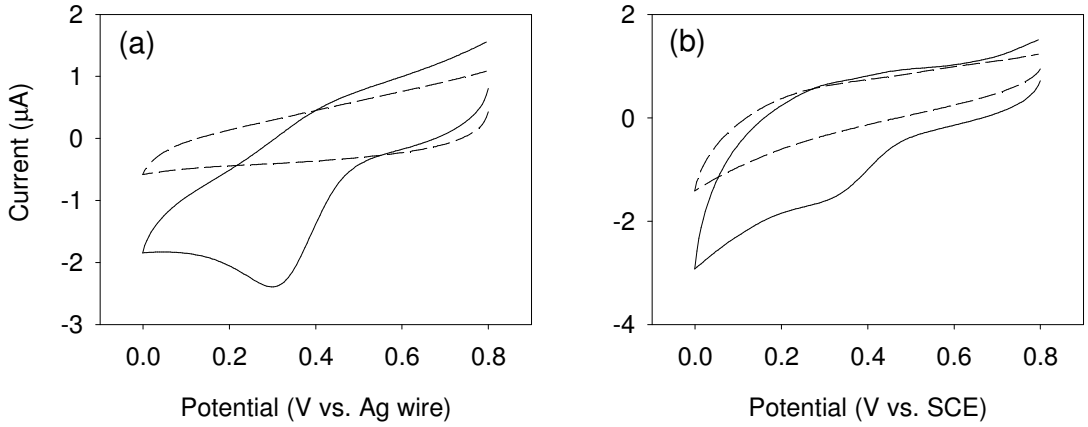

Figure 3.7. Cyclic voltammograms in the presence of 1 mM anthraquinone-1-diazonium chloride at GC in 0.1 M $[Bu_4N]BF_4$/ACN (a) and 0.14 M H_2SO_4 (b); first scan(—) and second scan (---) after holding at 0.0 V for 300 seconds followed by one minute of stirring by bubbling with N_2. Scan rate = 100 mV s^{-1}.

The peak observed at 0.3 V in ACN has been previously assigned the reduction of the anthraquinone-1-diazonium cation.[9] After the first scan, the potential was held at 0 V for 300 seconds. Subsequently the solutions were stirred, by bubbling with N_2 for one minute, before the second scan (---) was recorded over the same range as the first. The second scans revealed no reduction peak, suggesting that a passivating layer had formed on the GC electrode surfaces. The GC electrodes modified with AQ in ACN and 0.14 M H_2SO_4 will, for convenience, be referred to as $AQ_{GC\text{-}ACN}$ and $AQ_{GC\text{-}Aq}$, respectively.

3.5.2 Electrochemistry of AQ Modified GC

After the standard post-modification sonication procedure, the electrochemistry of the $AQ_{GC\text{-}ACN}$ and $AQ_{GC\text{-}Aq}$ films, prepared as described in Section 3.5.1, was investigated in 0.1 M KOH. This medium was chosen since it has been used previously for investigating the electrochemistry of AQ films.[9] Figure 3.8 shows cyclic voltammograms recorded between 0.0 and -1.3 V vs. SCE (initial potential = 0.0 V). A chemically reversible redox couple is observed at $E_{1/2} \approx$ -0.85 V, for both the $AQ_{GC\text{-}ACN}$ film (—) and the $AQ_{GC\text{-}Aq}$ film (---).

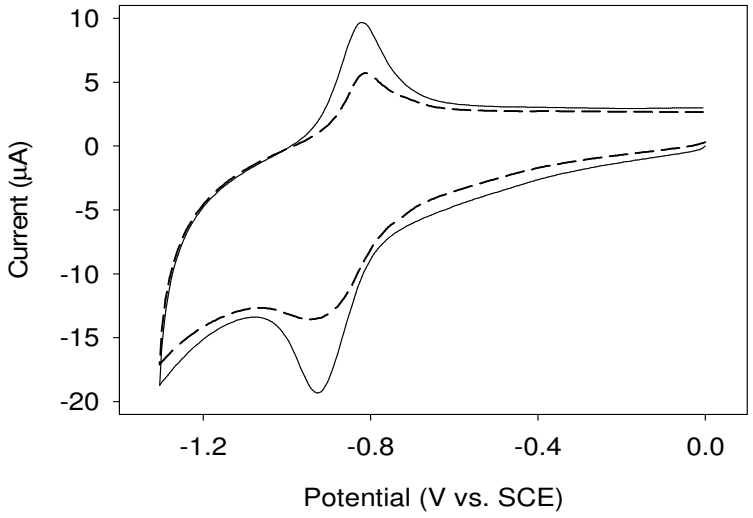

Figure 3.8. Cyclic voltammograms of $AQ_{GC\text{-}ACN}$ (—) and $AQ_{GC\text{-}Aq}$ (---) films at GC in 0.1 M KOH. Scan rate = 100 mV s^{-1}.

The observed redox couple has been previously assigned to the reversible two-electron AQ redox system (Scheme 3.5).[9]

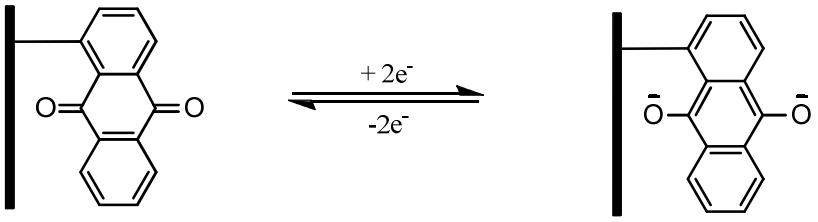

Scheme 3.5. Surface bound AQ exhibiting a chemically reversible two-electron redox couple.

Further experiments were undertaken to confirm that the redox couple assigned to the AQ moiety is associated with a surface-bound species. Figure 3.9 shows cyclic voltammetric scans carried out in aqueous KOH solution in the potential region of the AQ redox couple at scan rates of 50, 100, 200, 300, and 400 mV s^{-1} for both $AQ_{GC\text{-}ACN}$ (a) and $AQ_{GC\text{-}Aq}$ (b) films.

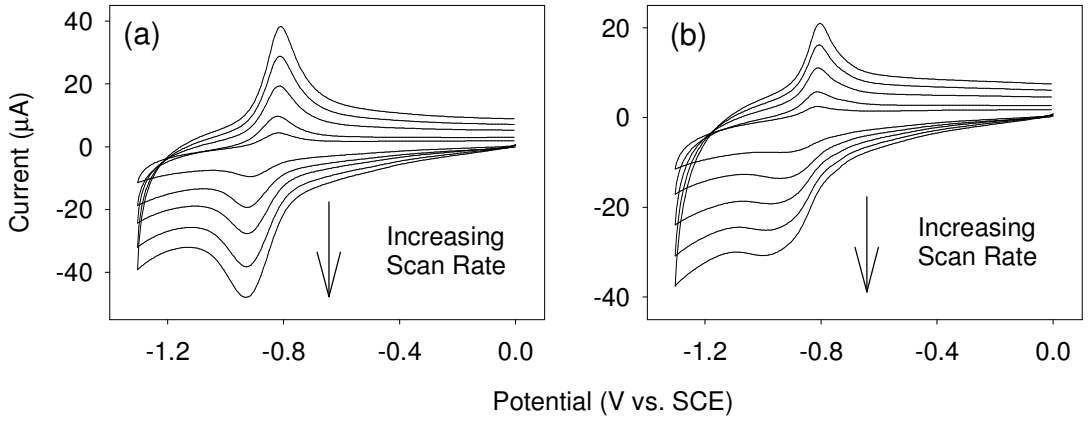

Figure 3.9. Cyclic voltammograms of $AQ_{GC\text{-}ACN}$ (a) and $AQ_{GC\text{-}Aq}$ (b) films at GC in 0.1 M KOH at 50, 100, 200, 300, and 400 mV s^{-1}.

Figure 3.10 shows plots of cathodic (●) and anodic (○) peak currents of the AQ redox couple for $AQ_{GC\text{-}ACN}$ (a) and $AQ_{GC\text{-}Aq}$ (b) films vs. scan rate. The linear relationships between the peak currents and the scan rates indicates the AQ moieties are surface bound.[28]

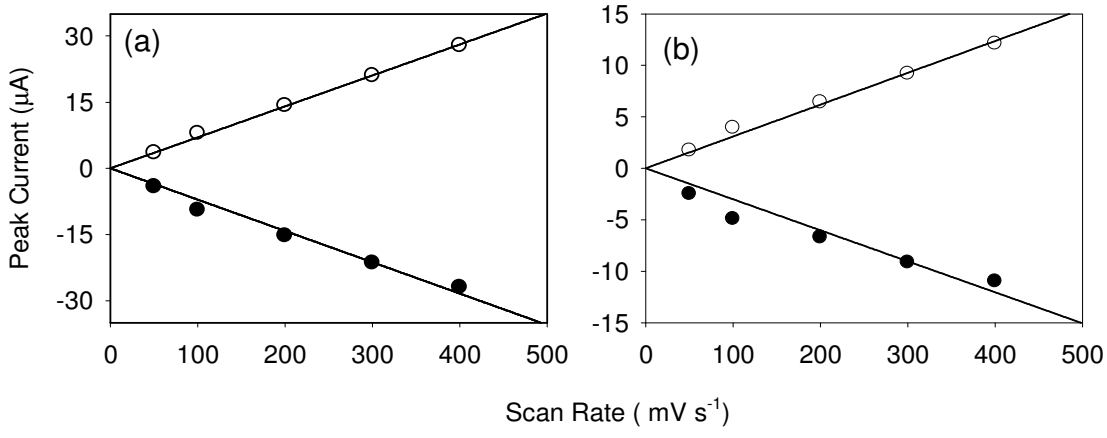

Figure 3.10. Plots of cathodic (●) and anodic (○) peak currents of the of the AQ redox couple at $AQ_{GC\text{-}ACN}$ (a) and $AQ_{GC\text{-}Aq}$ (b) modified GC vs. scan rate. All $R^2 \geq 0.93$

The surface concentrations of electro-active AQ functionalities, Γ_{AQ}, of the $AQ_{GC\text{-}ACN}$ and $AQ_{GC\text{-}Aq}$ films were calculated from the areas of both the reduction peaks and oxidation peaks in Figure 3.8 (scan rate = 100 mV s^{-1}), using Equation 2.2. The results are given in Table 3.2.

Table 3.2. Γ_{AQ} in $AQ_{GC\text{-}ACN}$ and $AQ_{GC\text{-}Aq}$ films, calculated from both the AQ reduction and the AQ oxidation. Scan rate = 100 mV s^{-1}.

Film Type	Γ_{AQ} (10^{-10} mol cm^{-2})	
	Reduction	Oxidation
$AQ_{GC\text{-}ACN}$	9.9	8.3
$AQ_{GC\text{-}Aq}$	7.1	4.1

Higher Γ_{AQ} was found, for both $AQ_{GC\text{-}ACN}$ and $AQ_{GC\text{-}Aq}$ films, when the voltammeteric peaks assigned to the AQ reduction, rather than those assigned to the oxidation, were used to calculate the surface concentration. This observation has several possible explanations. Firstly, AQ is known to catalyze oxygen reduction, which increases the peak current (and area) for the reduction process.[9] Although the AQ electrochemistry was investigated in N_2-purged solutions, it is not possible to unequivocally rule out the presence of trace oxygen. If trace oxygen is present, the reduction peaks would give erroneously high Γ_{AQ} values. Secondly, it is possible that some AQ^- or AQ^{2-} is re-oxidized slowly and that the charge for this process is not included in the determination of the oxidation peak area. If this is the case, the oxidation peaks would give erroneously low Γ_{AQ} values. These complications render surface concentrations calculated from AQ electrochemistry uncertain, and reduce the usefulness of AQ films in film characterization studies.

The $AQ_{GC\text{-}ACN}$ film gave higher Γ_{AQ} values than the $AQ_{GC\text{-}Aq}$ film (Table 3.2). Inspection of the cyclic voltammograms in Figure 3.8 shows further differences between the films. The $AQ_{GC\text{-}Aq}$ modified surface has a larger peak separation (ΔE_p = 0.15 V) than the $AQ_{GC\text{-}ACN}$ surface (ΔE_p = 0.13 V), indicative of slower electron transfer in the $AQ_{GC\text{-}Aq}$ film. The $AQ_{GC\text{-}Aq}$ film also shows a broader reduction peak than the $AQ_{GC\text{-}ACN}$ film, providing further evidence of slower electron transfer for the film prepared in aqueous conditions than that prepared in ACN. Slower electron

transfer could be due to a slower rate of diffusion of solvent and ions in $AQ_{GC\text{-}Aq}$ than in $AQ_{GC\text{-}ACN}$ films, indicating a denser structure for the film formed in aqueous conditions. These results are consistent with the differences observed between NP films formed in aqueous acid and ACN in Section 3.3.3 and previously reported by other workers.[5] It appears that diazonium cation derived AQ and NP films formed in aqueous conditions are denser than those prepared in ACN, making them more effective at blocking electron transfer, and less permeable to solvent and ion penetration. Slower rates of electron transfer across the denser films formed in aqueous conditions prevents production of further radicals during film growth leading to lower surface concentrations.

3.5.3 Stability of Redox Electrochemistry of AQ Modified GC

The stability of the AQ redox couple at the $AQ_{GC\text{-}ACN}$ and $AQ_{GC\text{-}Aq}$ surfaces to potential cycling was investigated. 100 cyclic voltammetric scans of the surfaces were carried out in 0.1 M KOH between 0.0 and -1.3 V vs. SCE (initial potential = 0.0 V). Every 10^{th} scan was recorded and Γ_{AQ} values were calculated from both the reduction and the oxidation peak for each recorded scan. The Γ_{AQ} values were plotted as a function of the number of cyclic voltammeteric scans carried out (Figure 3.11).

The surface concentration of electro-active AQ groups, $\Gamma_{AQ,}$ calculated from both the reduction (●) and oxidation (○) peaks is seen to decrease upon repetitive cycling for both $AQ_{GC\text{-}ACN}$ (a) and $AQ_{GC\text{-}Aq}$ (b) films. The cause of the decrease could be either loss of physically entrapped, but not covalently bound, film material, or loss of electro-activity of strongly bound AQ functionalities. It is worth noting that the Γ_{AQ} values calculated at the beginning of the cycling (number of cycles = 1) in Figure 3.11 are lower than those determined immediately after modification, given in Table 3.2. This can be accounted for by loss of electrochemically active AQ functionalities during prior experiments described in Section 3.5.2.

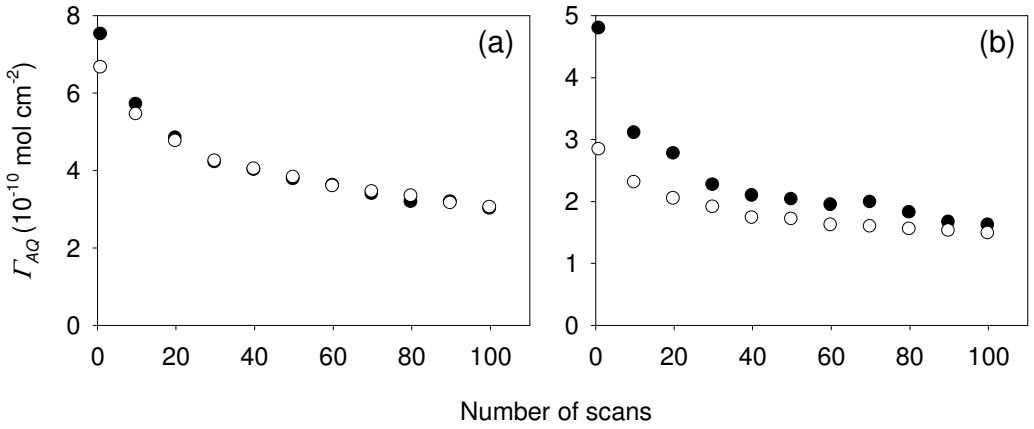

Figure 3.11. Γ_{AQ} calculated from both the reduction (●) and the oxidation (○) signal, for $AQ_{GC\text{-}ACN}$ (a) and $AQ_{GC\text{-}AQ}$ (b) modified GC vs. the number of consecutive cyclic voltammetric scans carried out in 0.1 M KOH. Scan rate = 100 mV s^{-1}.

3.6 Conclusion

The suitability of three electro-active modifiers, NP, NPOH, and AQ, for film characterization studies was investigated. All three exhibited both advantages and disadvantages.

NP reduction in protic conditions is irreversible, making repeat measurements impossible and allowing for only "one shot" at the determination of the surface concentration of a film. Furthermore, the determination of surface concentrations from the irreversible reduction of NP films has an undesirable element of uncertainty due to the ambiguities involved in determining peak area. However, NP films also have a number of advantages over NPOH and AQ films. Firstly, the most useful diazonium cation derived films, in terms of subsequent coupling reactions, and hence many applications, are the *p*-aminophenyl and *p*-carboxyphenyl films. The NP moiety is structurally analogous these, whereas the NPOH and AQ moieties are not. Hence morphological data concerning NP films is of more interest than the corresponding data for the other films. Secondly, the majority of previous film characterization work has been carried out on NP films, making fuller interpretation of further data possible. Finally, the reduction NP films gives aminophenyl groups at the surface, which are useful moieties for subsequent coupling reactions.

o-Aminophenol films, derived from NPOH films, exhibit a reversible redox couple at a mild potential. Electrochemical measurements indicated the surface concentrations obtained from the *o*-aminophenol redox couple are similar to those obtained from the NPOH reduction, giving additional confidence in their accuracy. However, cyclic voltammetry showed no peak that could be assigned to the reduction of HNBD during the film formation process. This is not ideal for film characterization studies where the absence of a peak associated with the reduction of the diazonium salt is used as evidence to show that the diazonium moiety has reacted during spontaneous modification (Chapters 4, 5, and 6).

AQ films exhibit a reversible, two-electron redox couple. However, the couple exhibited poor stability, indicating it is unsuitable for repeat measurements. Furthermore, surface concentrations calculated from the AQ reduction were consistently higher than those calculated from the oxidation. It is unclear which of these peaks (if any) gives an accurate surface concentration, thus making the AQ unsuitable for film characterization studies.

Although NPOH and AQ films have certain advantages over NP films in terms of their suitability for film characterization work, these did not outweigh their disadvantages. Therefore, NP films were used for the majority of film characterization studies in the remainder of this thesis.

3.7 References

1. Delamar, M.; Hitmi, R.; Pinson, J.; Savéant, J. M., Covalent Modification of Carbon Surfaces by Grafting of Functionalized Aryl Radicals Produced from Electrochemical Reduction of Diazonium Salts. *J. Am. Chem. Soc.* **1992,** 114, 5883-5884.

2. Kariuki, J. K.; McDermott, M. T., Nucleation and growth of functionalized aryl films on graphite electrodes. *Langmuir* **1999,** 15, 6534-6540.

3. Kariuki, J. K.; McDermott, M. T., Formation of multilayers on glassy carbon electrodes via the reduction of diazonium salts. *Langmuir* **2001,** 17, 5947-5951.

4. Anariba, F.; DuVall, S. H.; McCreery, R. L., Mono- and multilayer formation by diazonium reduction on carbon surfaces monitored with atomic force microscopy "scratching". *Anal. Chem.* **2003,** 75, 3837-3844.

5. Brooksby, P. A.; Downard, A. J., Electrochemical and atomic force microscopy study of carbon surface modification via diazonium reduction in aqueous and acetonitrile solutions. *Langmuir* **2004,** 20, 5038-5045.

6. Combellas, C.; Kanoufi, F.; Pinson, J.; Podvorica, F. I., Time-of-flight secondary ion mass spectroscopy characterization of the covalent bonding between a carbon surface and aryl groups. *Langmuir* **2005,** 21, 280-286.

7. Allongue, P.; Delamar, M.; Desbat, B.; Fagebaume, O.; Hitmi, R.; Pinson, J.; Savéant, J. M., Covalent modification of carbon surfaces by aryl radicals generated from the electrochemical reduction of diazonium salts. *J. Am. Chem. Soc.* **1997,** 119, 201-207.

8. Downard, A. J., Potential-dependence of self-limited films formed by reduction of aryldiazonium salts at glassy carbon electrodes. *Langmuir* **2000,** 16, 9680-9682.

9. Tammeveski, K.; Kontturi, K.; Nichols, R. J.; Potter, R. J.; Schiffrin, D. J., Surface redox catalysis for O_2 reduction on quinone-modified glassy carbon electrodes. *J. Electroanal. Chem.* **2001**, 101-112.

10. Brooksby, P. A.; Downard, A. J., Multilayer nitroazobenzene films covalently attached to carbon. An AFM and electrochemical study. *J. Phys. Chem. B* **2005,** 109, 8791-8798.

11. Radi, A. E.; Montornes, J. M.; O'Sullivan, C. K., Reagentless detection of alkaline phosphatase using electrochemically grafted films of aromatic diazonium salts. *J. Electroanal. Chem.* **2006,** 587, 140-147.

12. Ortiz, B.; Saby, C.; Champagne, G. Y.; Bélanger, D., Electrochemical modification of a carbon electrode using aromatic diazonium salts. 2. Electrochemistry of 4-nitrophenyl modified glassy carbon electrodes in aqueous media. *J. Electroanal. Chem.* **1998,** 455, 75-81.

13. Chen, P. H.; McCreery, R. L., Control of electron transfer kinetics at glassy carbon electrodes by specific surface modification. *Anal. Chem.* **1996,** 68, 3958-3965.

14. Saby, C.; Ortiz, B.; Champagne, G. Y.; Bélanger, D., Electrochemical modification of glassy carbon electrode using aromatic diazonium salts .1. Blocking effect of 4-nitrophenyl and 4-carboxyphenyl groups. *Langmuir* **1997,** 13, 6805-6813.

15. Brooksby, P. A.; Downard, A. J.; Yu, S. S. C., Effect of applied potential on arylmethyl films oxidatively grafted to carbon surfaces. *Langmuir* **2005,** 21, 11304-11311.

16. Baranton, S.; Bélanger, D., Electrochemical derivatization of carbon surface by reduction of in situ generated diazonium cations. *J. Phys. Chem. B* **2005,** 109, 24401-24410.

17. Bard, A.; Lund, H., *Encyclopedia of electrochemistry of the elements (organic section)*. Dekker: 1973; Vol. XIII.

18. Baizer, M. M., *Organic electrochemistry : an introduction and a guide*. M. Dekker: New York 1973.

19. Yu, S. S. C.; Tan, E. S. Q.; Jane, R. T.; Downard, A. J., An electrochemical and XPS study of reduction of nitrophenyl films covalently grafted to planar carbon surfaces *Langmuir* **2008,** 24, 7038-7038.

20. Liu, Y. C.; McCreery, R. L., Reactions of Organic Monolayers on Carbon Surfaces Observed with Unenhanced Raman-Spectroscopy. *J. Am. Chem. Soc.* **1995,** 117, 11254-11259.

21. Pontikos, N. M.; McCreery, R. L., Microstructural and Morphological-Changes Induced in Glassy-Carbon Electrodes by Laser Irradiation. *J. Electroanal. Chem.* **1992,** 324, 229-242.

22. Downard, A. J., Nanoscale films covalently attached to conducting substrates: structure and dynamic behaviour of the layers. *International Journal of Nanotechnology* **2009,** 6, 233-244.

23. Nassef, H. M.; Radi, A. E.; O'Sullivan, C. K., Electrocatalytic oxidation of hydrazine at o-aminophenol grafted modified glassy carbon electrode: Reusable hydrazine amperometric sensor. *J. Electroanal. Chem.* **2006,** 592, 139-146.

24. Pandurangappa, M.; Lawrence, N. S.; Compton, R. G., Homogeneous chemical derivatisation of carbon particles: a novel method for funtionalising carbon surfaces. *Analyst* **2002,** 127, 1568-1571.

25. Seinberg, J. M.; Kullapere, M.; Maeorg, U.; Maschion, F. C.; Maia, G.; Schiffrin, D. J.; Tammeveski, K., Spontaneous modification of glassy carbon surface with anthraquinone from the solutions of its diazonium derivative: An oxygen reduction study. *J. Electroanal. Chem.* **2008,** 624, 151-160.

26. Kullapere, M.; Marandi, M.; Sammelselg, V.; Menezes, H. A.; Maia, G.; Tammeveski, K., Surface modification of gold electrodes with anthraquinone diazonium cations. *Electrochem. Commun.* **2009,** 11, 405-408.

27. Smith, R. D. L.; Pickup, P. G., Voltammetric quantification of the spontaneous chemical modification of carbon black by diazonium coupling. *Electrochim. Acta* **2009,** 54, 2305-2311.

28. Bard, A. J.; Faulkner, L. R., *Electrochemical Methods: Fundamentals and Applications*. 2nd ed.; John Wiley & Sons, Inc: Danvers, 2001.

Chapter 4. Modification of Carbon Surfaces by Spontaneous Reaction of Aryldiazonium Salts

4.1 Introduction

The modification of surfaces via spontaneous reaction with aryldiazonium salts has been reviewed in Section 1.3.2 of this thesis. To briefly recap, spontaneous modification is achieved by immersing a surface in a solution of aryldiazonium salt in the absence of an applied potential.[1-14] Hence, the term "spontaneous modification" refers to modification which proceeds *spontaneously at open circuit potential* (OCP). Spontaneous modification has a number of advantages over electrochemically induced modification. Firstly, since there is no need to apply a potential to achieve modification, no potentiostat is required. Secondly, the modification of particles in solution, such as nanotubes and nanoparticles, is straightforward using the spontaneous reaction, with no requirement that the particles are immobilized on an electrode prior to modification.[15-20] Finally, as described in Chapter 6 of this thesis, the spontaneous reaction has been applied to the patterning of surfaces by microcontact printing of aryldiazonium salts. The spontaneous modification of surfaces using aryldiazonium salts has been shown to proceed at metals,[1, 2, 4-8, 11] semiconductors[3, 12, 13] and carbon surfaces.[4, 6, 9, 10, 14]

The spontaneous modification of carbon has attracted considerable attention due to the strength of the C-C bond formed between the carbon surface and the bound film, the low cost of carbon electrodes and the biocompatibility of the carbon substrate. These attributes make modified carbon electrodes attractive for many applications. Although considerable work has been undertaken on the spontaneous modification of carbon using aryldiazonium salts, the characteristics of the films and the mechanism by which they form are not yet fully understood.

The aims of the current chapter are twofold. One is to study the concentrations, thicknesses and densities of films formed via the spontaneous reaction of aryldiazonium salts at carbon surfaces. The other is to gain insight into the mechanism by which the spontaneous modification proceeds.

4.2 Experimental

Conditions used for the spontaneous modification of surfaces at OCP are described in Section 2.11.2. Briefly, spontaneous modification was carried out in an O_2 free solution of 10 mM diazonium salt in the absence of light at (25 ±2) ºC. Modification in aqueous conditions was undertaken in 0.14 M H_2SO_4; and in ACN in 0.1 M $[Bu_4N]BF_4$/ACN. After modification, the surfaces were subjected to five minutes of sonication in Milli Q water.

All experiments at glassy carbon (GC) were conducted using GC disk electrodes (for specifications see Section 2.3.1 and 2.4.2). All *p*-nitrophenyl (NP) electro-reduction was carried out by recording either a single, or two consecutive, cyclic voltammetric scans between ~ 0.8 and -1.2 V vs. SCE in 0.14 M H_2SO_4. Potassium ferricyanide ($K_3Fe(CN)_6$) redox probe voltammetry was carried out using 5 mM of $K_3Fe(CN)_6$ in 0.1 M phosphate buffer pH 7.4. All cyclic voltammograms were carried out at a scan rate of 100 mV s^{-1}.

Water contact angle measurements of *p*-carboxyphenyl (CP) modified pyrolyzed photoresist films (PPF) were conducted by placing three drops of water on each sample and determining the contact angle of each as described in Section 2.8. Four samples were prepared and the value given is the arithmetic mean of the total 12 measurements performed; the error was calculated as two standard deviations of the mean. Water contact angle measurements of NP modified PPF were conducted in the analogous manner, but by placing just two drops on each sample. Each value is the arithmetic mean of the two measurements performed for each sample.

4.3 Spontaneous Modification of GC with NP Films

Initial experiments focused on the spontaneous formation of NP films at GC by immersion of GC in *p*-Nitrobenzene diazonium tetrafluoroborate salt (NBD). The effects of immersion time and the medium (0.1 M $[Bu_4N]BF_4$ /ACN or 0.14 M H_2SO_4) in which modification was undertaken were investigated. Subsequently, open circuit potential (OCP) measurements were undertaken in order to gain insight into the role of the surface in the film formation process.

4.3.1 Electro-Reduction of NP Films Spontaneously Attached to GC

GC disk electrodes were immersed for 60 minutes in 10 mM NBD/0.14 M H_2SO_4 and 10 mM NBD/0.1 M $[Bu_4N]BF_4$-ACN solutions. Figure 4.1 shows cyclic voltammograms (initial potential 0.7 V vs. SCE) of the modified GC electrodes in 0.14 M H_2SO_4.

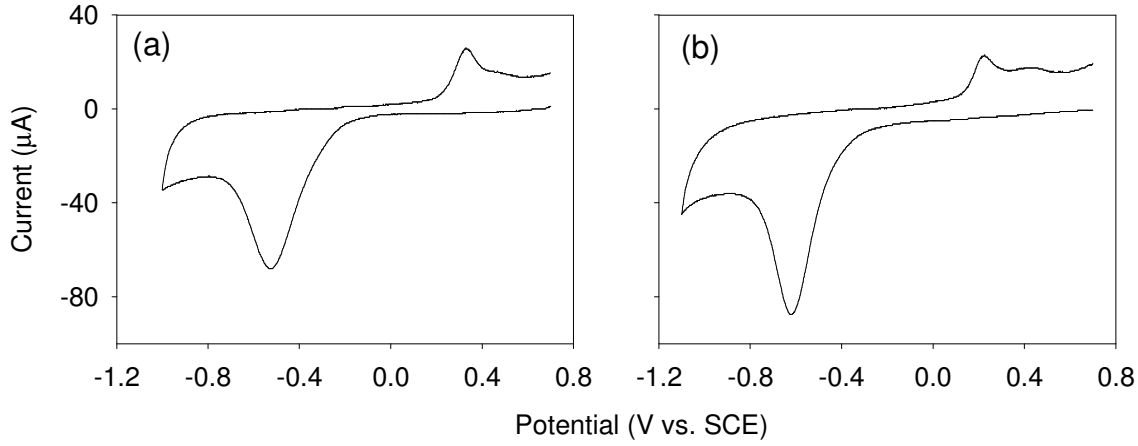

Figure 4.1. Cyclic voltammograms of GC electrodes in 0.14 M H_2SO_4 after immersion for 60 minutes in 10 mM NBD/0.1 M $[Bu_4N]BF_4$-ACN (a) and 10 mM NBD/0.14 M H_2SO_4 (b). Scan rate = 100 mV s^{-1}.

The characteristic, irreversible NP reduction ($E_{p,c}$ ≈ -0.5 V) and the hydroxyaminophenyl (APOH) oxidation ($E_{p,a}$ ≈ 0.3 V) were observed for both samples, indicating that the modification proceeds in both media. These results are consistent with those of other workers who have observed the spontaneous modification of GC using aryldiazonium salts in both ACN[4,

[6, 9, 10, 14] and aqueous conditions[9]. For brevity, NP films formed spontaneously at GC in ACN and 0.14 M H_2SO_4 will be referred to as NP-SPN_{GC-ACN} and NP-SPN_{GC-Aq}, respectively.

The cyclic voltammograms in Figure 4.1 show no peak at 0.0 V vs. SCE, the potential region where the reduction of the diazonium moiety would have been expected (see Figure 4.4 (a)). This indicates that, during modification in both ACN and aqueous conditions, the diazonium cation moiety has reacted. While this is not conclusive evidence for covalent attachment to the surface, reaction of the diazonium cation is a necessary condition for covalent attachment. However, formation of a physisorbed (rather than covalently bound) film of NP dimers and oligomers is also consistent with the data.

Further experiments were undertaken to determine the effect of immersion time in NBD solution on the surface concentration of electro-active NP groups, Γ_{NP}. GC disks were modified by immersion in 10 mM NBD/0.1 M $[Bu_4N]BF_4$-ACN and 10 mM NBD/0.14 M H_2SO_4. Samples were prepared at immersion times of 10, 30, 60 and 120 minutes. Subsequently, cyclic voltammograms of the surfaces were recorded between ~0.7 and -1.1 V in 0.14 M H_2SO_4 with an initial potential of 0.7 V. From the resulting voltammograms, Γ_{NP} was calculated for each sample, as described in Section 3.3.3. Figure 4.2 shows a plot of Γ_{NP} vs. immersion time for the GC electrodes modified using NBD in 0.1 M $[Bu_4N]BF_4$/ACN (○) and 0.14 M H_2SO_4 (●).

Γ_{NP} was found to follow the same trend with immersion time for both NP-SPN_{GC-ACN} and NP-SPN_{GC-Aq} films. In both media, the surface concentrations are seen to increase over ~30 minutes immersion time to a maximum of ~38 × 10^{-10} mol cm^{-2}. This increase can be attributed to the film growth process.

A similar increase in surface concentration with immersion time was observed by Vautrin-Ul and coworkers who monitored the growth NP films on GC spontaneously prepared by immersion in 10 mM NBD/ACN. The surface concentration, determined from the reversible NP redox system observed in aprotic conditions (see Section 3.3.3) was seen to increase with immersion time up to 58 × 10^{-10} mol cm^{-2} after 60 minutes.[4] The lower value of the peak surface concentration observed in the present work could be due to use of less rough GC surfaces, differences in

reaction conditions (Vautrin-Ul and coworkers did not report the temperature or elimination of light during immersion), and/or differences in the electrochemical redox processes used to determine the surface concentration. Tammeveski and coworkers also observed an increase in surface concentration of anthraquinone groups with reaction time upon immersion of GC electrodes in anthraquinone-1-diazonium cation (in both ACN and aqueous conditions).[9]

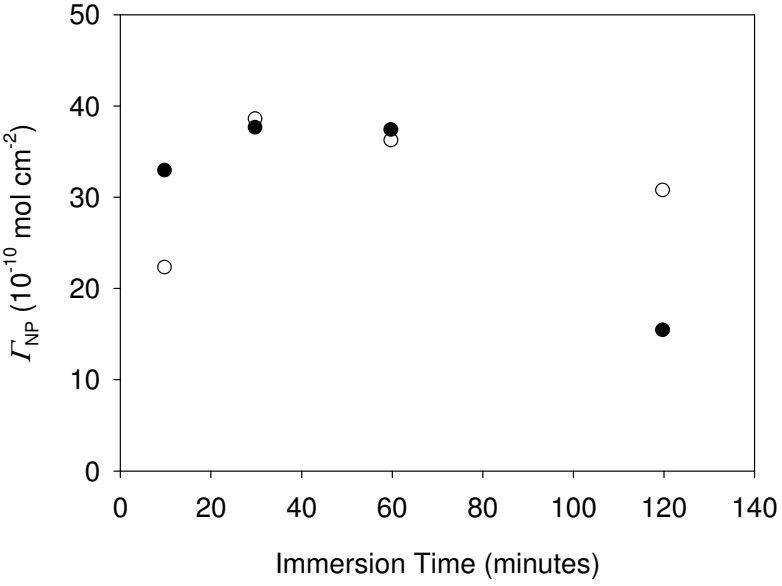

Figure 4.2. Plots of Γ_{NP}, vs. immersion time for NP films spontaneously prepared at GC using 10 mM NBD in 0.1 M $[Bu_4N]BF_4$/ACN (○) and 0.14 M H_2SO_4 (●).

In the present work, after reaching a maximum surface concentration of electro-active NP groups over 30 to 60 minutes immersion time, the surface concentrations are seen to decrease when the immersion time is extended to 120 minutes (Figure 4.2). The cause of this decrease is not clear. One possible explanation is that NP groups are lost from the film at longer immersion times. However, this seems unlikely since the films have been shown to be stable to sonication, both in the present work and by other workers.[4, 6, 9, 10] Hence, mere longer immersion in the modification solution is unlikely to cause loss of film material. A more plausible explanation for the decrease in surface concentration beyond 60 minutes immersion time is that thicker films are produced and that these are self-passivating, blocking the electro-reduction of the some NP groups in the film. This could be brought about by several factors. It is likely that electron transfer is slower to

NP groups located further from the surface in a multilayer film, due to the large electron tunneling distance and the blocking effect of groups closer to the surface. This could prevent reduction of some of the NP groups in the outer layer(s) of the film. However, this explanation only accounts for the observation that the surface concentration does not *increase* after 60 minutes, not for the observed *decrease*. The decrease can be explained by poor penetration of solvents and ions through the film to NP groups close to the surface, due to a blocking effect from NP groups located further from the surface (which would be expected to be present in thicker films formed at longer immersion times). This could prevent electro-reduction of the NP groups close to the surface, and lead to a drop in the electrochemically determined surface concentration. It is also worth noting that the initial increase in surface concentration, as well as the later decrease, occurs more quickly in aqueous conditions than in ACN. This suggests the film formation occurs more quickly in aqueous conditions.

Further evidence for the effects of film growth on the electro-activity of NP groups is obtained by investigating the effect of immersion time on the potential of the irreversible NP reduction peak, $E_{p,c}$. Figure 4.3 shows a plot of $E_{p,c}$ vs. immersion time for NP-SPN$_{GC\text{-}ACN}$ (○) and NP-SPN$_{GC\text{-}Aq}$ (●) films.

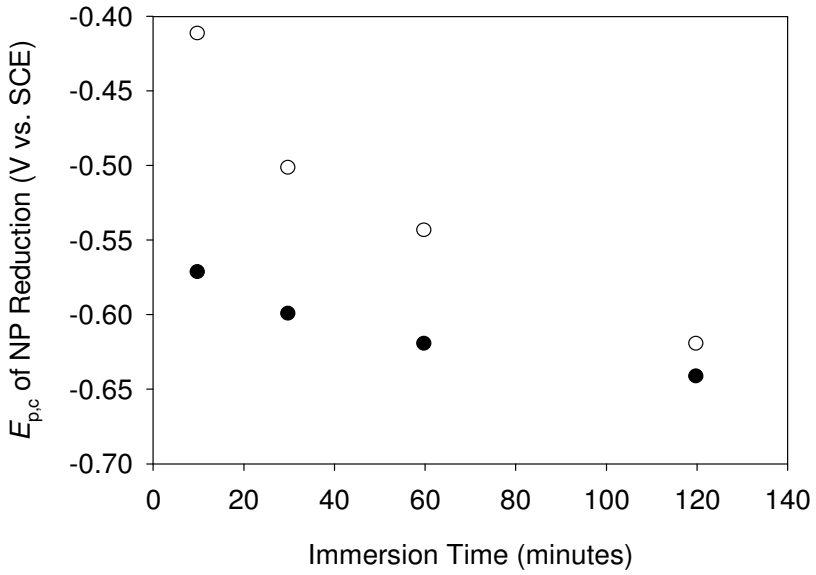

Figure 4.3. Plot of $E_{p,c}$ for NP reduction peak in 0.14 M H_2SO_4 vs. immersion time in NBD for NP-SPN$_{GC\text{-}ACN}$ (○) and NP-SPN$_{GC\text{-}Aq}$ (●) films.

Both NP-SPN$_{GC-ACN}$ and NP-SPN$_{GC-Aq}$ films showed a decrease in the peak potential for the irreversible NP reduction with an increase in immersion time, indicative of slower electron transfer to NP groups within films formed at longer immersion times. The slower electron transfer may arise from the formation of thicker, multilayer films. Electron transfer would be slower to groups located further from the surface due to an increase in tunneling distance between the NP groups and the electrode surface, across the blocking film. Furthermore, it has been shown by Brooksby et al. that depositing a *p*-methylbenzene layer on a *p*-nitroazobenene layer shifts the reduction peak for the *p*-nitroazobenene moiety to a more negative potential. It was suggested that this effect may arise from the diffusion of solvent and ions to the nitroazobenezene groups being inhibited by the outer *p*-methylbenezene layer.[21] A similar effect may be occurring with NP films, with the outer NP layer blocking the diffusion of solvent and ions to the NP groups closer to the surface and thereby shifting the NP reduction peak in the negative direction.

If this interpretation of the results is correct, and the decrease in the potential of the NP reduction is due to the formation of thicker films, then it follows that the NP-SPN$_{GC-ACN}$ films are still growing between 60 and 120 minutes immersion time, despite the observed drop in Γ_{NP} (Figure 4.2 (○)).

Figures 4.2 and 4.3 show that, at comparable immersion times and surface concentrations, $E_{p,c}$ of the NP reduction is more negative for NP-SPN$_{GC-Aq}$ than for NP-SPN$_{GC-ACN}$ films. This is similar to the finding for NP films formed by electrochemical reduction of NBD at GC (Section 3.3.3) where the NP reduction peak was more negative for a film formed in aqueous conditions, despite a higher surface concentration for the film formed in ACN. On the basis of these results, and those of previous workers[22], it was proposed (in Section 3.3.3 and by previous workers[22]) that the lower potential for the NP reduction for the film formed in aqueous conditions arises from slower diffusion of solvents and ions into the film. This suggests that the films formed in aqueous conditions are denser than those formed in ACN. The lower potential of NP reduction observed for NP-SPN$_{GC-Aq}$ films suggests that the same effect occurs when the reaction is spontaneous; that is, NP films formed spontaneously at GC in aqueous conditions are denser than the corresponding films prepared in ACN

4.3.2 OCP Behavior of GC during Modification with NP Films

As discussed in Section 1.3.2, a number of workers have suggested that the spontaneous modification of carbon surfaces via reaction with aryldiazonium salts proceeds via electron transfer from the carbon surface to the diazonium cation in solution. The aryl radicals produced by this spontaneous reduction are subsequently believed to attack the surface resulting in the formation of covalently attached films.[9, 10, 15] However, little direct evidence exists to support this proposed mechanism.

To assess whether the GC would be expected to reduce NBD at OCP, cyclic voltammograms were recorded at GC electrodes by scanning in the negative direction in 1 mM solutions of NBD in both 0.14 M H_2SO_4 and 0.1 M $[Bu_4N]BF_4$/ACN; these are shown in Figures 4.4 (a) and (b) respectively. The shaded vertical bands represent the range of OCP values for GC in 0.14 M H_2SO_4 and 0.1 M $[Bu_4N]BF_4$/ACN, obtained after 60 minutes equilibration period (see Figure 4.5 below).

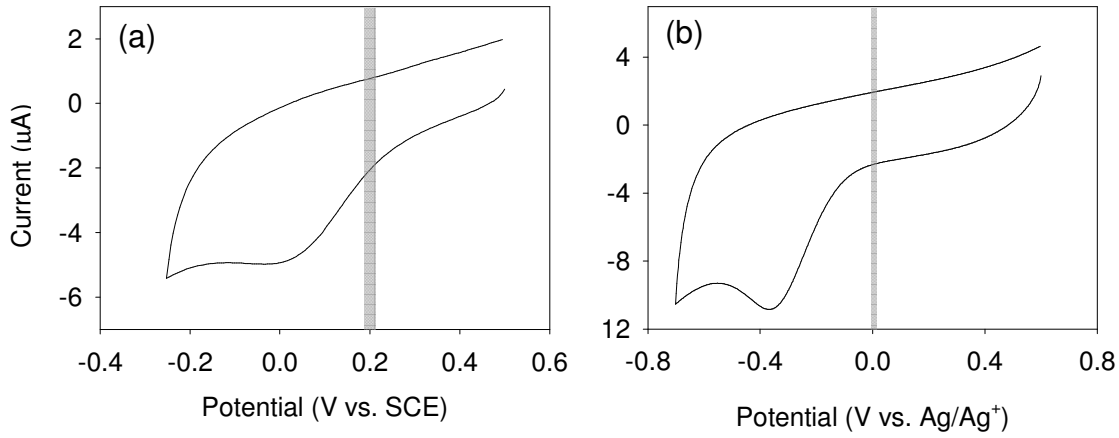

Figure 4.4. Cyclic voltammograms of GC working electrodes in 1 mM NBD in 0.14 M H_2SO_4 (a) and 0.1 M $[Bu_4N]BF_4$/ACN (b); scan rate = 100 mV s^{-1}. The range of OCP values of GC after 60 minutes equilibration (for each medium) are shown by shaded vertical bands (see Figure 4.5). Figure (a) reproduced from Figure 3.1 (b).

In 0.14 M H_2SO_4, the OCP of ~0.2 V (vs. SCE) for the GC (shaded vertical band of Figure 4.4(a)) is more negative than the high-potential edge of the peak assigned to the reduction of NBD,

which extends to ~0.3 V. Hence, under the conditions used, the GC surface at OCP would be expected to reduce NBD, thereby leading to spontaneous film formation. The OCP of ~0 V vs. Ag/Ag^+ for the GC in 0.1 M $[Bu_4N]BF_4$/ACN is seen to coincide almost exactly with of the high-potential edge of the NBD reduction peak (Figure 4.5(b)). In this case no firm conclusions can be reached as to whether NBD would be expected to be reduced, but given the higher OCP in relation to the start of the NBD reduction peak, slower spontaneous film formation might be anticipated in ACN than in aqueous conditions.

It should be noted that the cyclic voltammograms in Figure 4.4 cannot give precise information about the reduction potential, E^0, of NBD, because the process is chemically irreversible. However, E^0 is expected to be more positive than $E_{p,c}$, and the reduction of the NBD will occur at potentials positive of E^0. Hence, if the OCP is more negative than the start of the NBD reduction peak, it is reasonable to assume that reduction of NBD by the substrate can proceed at OCP. If, on the other hand, the OCP is on the positive side of the start of the reduction peak, it is not possible to deduce whether reduction will proceed at OCP. Hence, comparisons between a diazonium cation reduction peak and the OCP of an electrode selected for modification can be used only as a "rough guide" in determining if the reduction of the diazonium cation by the substrate will proceed at OCP.

Monitoring the change of OCP of a substrate during spontaneous modification can provide evidence for whether a substrate is acting as an electron donor or electron acceptor during the process. Intuitively, a drop in OCP is associated with gain of electrons, while an increase in OCP is associated with a loss of electrons from the substrate.[23] Bidan and coworkers monitored the effect of addition of NBD on the OCP of GC in 0.1 M Bu_4NPF_6/ACN. An increase in OCP was observed upon addition of NBD, consistent with electron donation from the surface to NBD in solution. However, the OCP was monitored for only a short time period (< 100 seconds) after the addition of the NBD.[10] In the present section, the experiments conducted by Bidan and coworkers are replicated and expanded by measuring the effect of NBD on the OCP of GC in both ACN and aqueous conditions over a longer timescale. Controls were also carried out to determine whether the diazonium cation substituent is responsible for any observed changes on the OCP upon addition of NBD.

GC disk electrodes were immersed in 10 mL solutions 0.14 M H_2SO_4 and 0.1 M $[Bu_4N]BF_4$/ACN. The OCP of the electrodes in blank electrolytes was monitored over a 60 minute "equilibration" period to allow a relatively stable OCP to be reached before addition of NBD. 10 mL of 20 mM of NBD/0.14 H_2SO_4 was then added, resulting in a 10 mM NBD/0.14 M H_2SO_4 solution. Similarly, 10 mL of 20 mM of NBD 0.1 M $[Bu_4N]BF_4$/ACN was added to the 10 mL solution of 0.1 M $[Bu_4N]BF_4$/ACN. After addition of the NBD solutions, the OCP of the electrodes was monitored for 120 minutes.

Control experiments were carried out separately. One control consisted of adding 10 mL of blank electrolyte (no NBD) after the 60 minute equilibration period. The other consisted of adding 10 mL of 20 mM *p*-nitroanaline to the blank electrolyte after equilibration. *p*-Nitroanaline was used to test the effect on the OCP of a molecule that is structurally similar to NBD but lacks a diazonium cation functionality. Both sorts of control experiments were conducted in both 0.1 M $[Bu_4N]BF_4$/ACN and 0.14 M H_2SO_4.

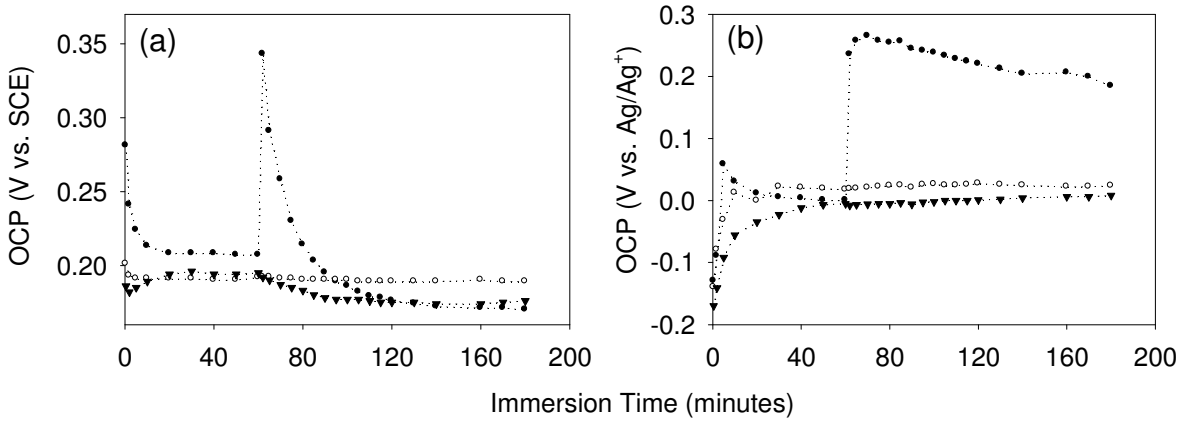

Figure 4.5. Plot of OCP vs. immersion time in 0.14 M H_2SO_4 (a) and 0.1 M $[Bu_4N]BF_4$/ACN (b) for GC disk electrodes. After an equilibration period of 60 minutes, 10 mL solutions of 20 mM NBD/electrolyte (●), 20 mM p-nitroanaline/electrolyte (▼), or 10 mL electrolyte (○) were added to the solutions.

Figure 4.5 shows the effect of adding NBD (●), *p*-nitroanaline (▼) and blank electrolyte (○) on the OCP of GC in 0.1 M $[Bu_4N]BF_4$/ACN (a) and 0.14 M H_2SO_4 (b). In both media the OCP was seen to increase immediately and significantly upon the addition of NBD. No significant changes in OCP were seen upon the addition of either blank electrolyte or *p*-nitroanaline, indicating that

the diazonium cation is responsible for the increase in OCP observed when NBD is added. The results in Figure 4.5 (b) are consistent with those of Bidan and coworkers, who monitored the OCP of GC upon addition of NBD in 0.1 M Bu_4NPF_6/ACN. In that study, an increase from ~0.0 V to 0.3 V vs. Ag/Ag^+ was also observed upon addition of NBD.[10] As mentioned above, an increase in OCP is indicative of the build-up of positive charge on the electrode surface, which would be expected if the diazonium cation is reduced by the surface. Hence, these results provide direct evidence that the spontaneous reaction of NBD with GC proceeds via the reduction of NBD by the substrate in both media. It is worth noting that the absolute potentials of the surfaces were seen to vary from sample to sample in both media. This variation is to be expected; in the absence of a redox couple controlling the potential of the electrode, the OCP will be highly sensitive to cleanliness, surface structure and residual solution O_2 concentration.[24]

In aqueous conditions, after the initial increase upon addition of NBD, the OCP is seen to decrease rapidly, returning to near its "equilibrium" value (prior to NBD addition) within ~30 minutes (Figure 4.5 (a)). In 0.1 M $[Bu_4N]BF_4$/ACN, the decrease is much slower and less pronounced, with the OCP remaining well above its initial value even 120 minutes after the addition of the NBD. The decrease can be assigned to a discharge process, through which the substrate loses positive charge by accepting electrons from some other species. The nature of the electron donor is unclear, but one possibility is solution impurities. Hence the discharge process may be slower in ACN than aqueous conditions, due to the lower concentrations of these impurities in ACN. Another possible cause of the discharge process is the formation of surface oxides, which could offset the positive charge of the carbon surface via an oxidation process of the type shown in Equation 4.1, where '(sur)' refers to surface species.

$$[xC_{(sur)}]^{2+} + H_2O \rightarrow [(x\text{-}1)C\text{-}C_{(sur)}{=}O] + 2H^+ \qquad (4.1)$$

The formation of surface oxides is known to occur at GC upon anodization in aqueous conditions,[25-28] but is not expected to occur in ACN. While this would account for the lack of a rapid discharge process in ACN, considering that anodic oxidation in aqueous media is generally carried out at a potential of ~1.8 V vs. SCE, it seems unlikely that the potential of the GC substrate, after addition of NBD, (~ 0.35 V vs. SCE) is sufficiently positive to bring about

formation of surface oxides. Hence it is tentatively proposed that the discharge process, in both media, is due to oxidation of solution impurities.

Although the charging and discharging processes observed in aqueous conditions (Figure 4.5) are complete within ~30 minutes, film growth continues for up to 120 minutes immersion time (see Section 4.3.2). This film growth is expected to transfer positive charge to the surface. Hence it appears that rapid film growth shortly after immersion of the substrate in NBD leads to a sudden increase in OCP and thereafter the film growth process slows and the rate of discharge is faster than charge accumulation, leading to a drop in the OCP to its initial value. The film continues to grow after the OCP has returned to its initial value, with discharge occurring at the same rate as the accumulation of charge, leading to no further changes in the OCP.

4.4 Spontaneous Modification of PPF with NP Films

The formation of NP films at carbon via spontaneous reaction with NBD was further investigated using pyrolyzed photoresist films (PPF) as substrates. The properties of PPF have been discussed in Section 1.1.2. Most importantly, PPF is a very smooth, GC-like substrate. The low surface roughness of PPF makes it a particularly suitable substrate for use in film thickness studies.

4.4.1 Electro-Reduction of NP Films Spontaneously Attached to PPF

The spontaneous reaction of NBD with PPF was investigated by immersing PPF samples for 60 minutes in 10 mM solutions of NBD. Modification was investigated in both 0.14 M H_2SO_4 and 0.1 M $[Bu_4N]BF_4$/ACN. After immersion, cyclic voltammograms of the surfaces were recorded between ~ 0.7 and -1.2 V vs. SCE in 0.14 M H_2SO_4 to test for the presence of the NP functionalities at the surfaces. Relatively small NP reduction peaks were observed for the samples that had been immersed in NBD/ACN, with calculated surface concentrations of 0 and 0.9×10^{-10} mol cm^{-2} for two samples. In comparison, the PPF samples modified in aqueous conditions showed much larger NP reduction peaks. However, the peak shapes, potentials and

currents varied significantly between samples, despite the fact that they were prepared under identical conditions (compare Figures 4.6 (a) and (b)). Surface concentrations determined from the voltammograms were found to range between 8.3 and 12.2 $\times 10^{-10}$ mol cm^{-2} (four samples prepared).

In the first scans, the cyclic voltammograms in Figure 4.6 show no peaks at ~0.0 V vs. SCE, the potential region where the reduction of the diazonium cation moiety would have been expected (see Figure 4.13 (a)). This indicates that the diazonium cation moiety reacts during modification, consistent with covalent attachment of the NP groups to the PPF surface.

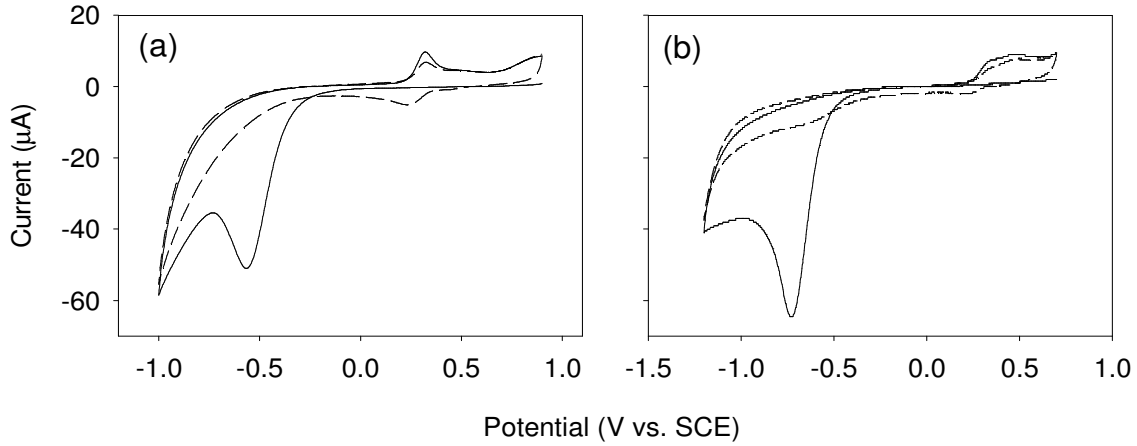

Figure 4.6. Consecutive cyclic voltammograms of PPF electrodes in 0.14 M H_2SO_4 after immersion in 10 NBD /0.14 M H_2SO_4 for 60 minutes; first scan(—) and second scan (---). Scan rate = 100 mV s^{-1}. (a) and (b) show the results of repeat experiments undertaken under identical conditions.

There are a number of possible explanations as to why the spontaneous reaction of NBD with PPF proceeds to a significant extent in aqueous conditions but not in ACN. As discussed in Section 1.3.2 (and above) the spontaneous reaction of aryldiazonium salts with surfaces has been proposed to proceed via the reduction of the aryldiazonium cations by the surface at OCP. If this mechanism is correct, the reaction would take place only if the OCP of the substrate is sufficiently low to reduce the aryldiazonium cation. Hence, one possible explanation for the lack of significant reaction of NBD with PPF in ACN is that the OCP is not sufficiently negative. This is further explored in Section 4.4.7.

The sensitivity of the reaction to the medium could also be due to a requirement for a physisorption step during the spontaneous modification process at carbon. Strano and coworkers have found evidence that the modification of single-walled carbon nanotubes (CNTs) using the 4-chlorobenzene diazonium cation proceeds via the physisorption of the cation to the CNT prior to formation of the covalent bond between the modifier and the nanotube.[29] In a recent theoretical study, Xu and coworkers performed calculations which indicated that modification of carbon nanotubes by reaction with 4-chlorobenzene diazonium salt should occur via a two-step mechanism consisting of an initial adsorption step followed by covalent modification.[30] Hence, it is possible that physisorption of NBD is required for spontaneous reaction of NBD with PPF. The assumption that physisorption of NBD to PPF occurs in aqueous conditions, but not in ACN, would explain the sensitivity of the reaction to the solvent. This suggestion is also consistent with the observation that the spontaneous reaction of NBD proceeds in ACN at GC, but not at PPF. The physisorption of methylene blue and anthraquinone-2,6-disulfonate has been shown to be much weaker at PPF than GC,[31] and it is reasonable to propose that the same is true of NBD. It is also worth noting that diazonium salts are more soluble in ACN than in aqueous conditions. The weakness of the physisorption of NBD to PPF, in conjunction with the high solubility of NBD in ACN, might prevent a physisorption step that is a prerequisite for modification.

The cyclic voltammograms of PPF modified in 0.14 M H_2SO_4 showed considerable sample-to-sample variation in the peak potentials, shapes and currents of the irreversible NP reduction and APOH/nitrosophenyl couples, even when they were prepared using identical conditions and immersion times (compare Figures 4.6 (a) and (b)). Some samples showed a well defined APOH/nitrosophenyl couple at $E_{1/2} \approx 0.3$ V, as shown in Figure 4.6 (a). These voltammograms are similar to those previously observed for NP-modified GC (see Sections 3.3 and 4.3). Other samples exhibited a poorly defined and broader APOH/nitrosophenyl couple, as shown in Figure 4.6 (b). This makes the determination of the peak area of the APOH oxidation less reliable, and hence, increases the uncertainty associated with the determination of the surface concentrations of electro-active NP groups in the corresponding films.

Compton and coworkers have investigated the spontaneous modification of carbon nanotubes (CNTs) with NP groups using NBD in the presence and absence of hypophosphorous acid (a mild

reducing agent).[20] Cyclic voltammograms of CNTs modified in the presence of hypophosphorous acid exhibited a single well-defined APOH/nitrosophenyl couple. In contrast, when modification was carried out in the absence of hypophosphorous acid, the APOH/nitrosophenyl couple was seen as two closely spaced oxidation and reduction peaks. Furthermore, the irreversible NP reduction was observed at a more negative potential for CNTs modified in the absence of hypophosphorous acid than for those modified in its presence. On the basis of these findings it was proposed that, in the presence of hypophosphorous acid, the modification of CNTs with NP groups proceeds via a radical intermediate, whereas, in the absence of hypophosphorous acid, the reaction proceeds via an aryl cation intermediate. The cationic intermediate can not only react with sp^2 carbon atoms on the CNT via the electrophilic addition, but can also form ester linkages via reaction with surface carboxylic acid groups, which are known to exist at the edges of CNTs (and on PPF). This gives rise to two types of bound NP groups (those with ester linkages and those without) and hence results in two APOH/nitrosophenyl processes observed at different potentials. In the case of the radical intermediate, reaction only occurs at the sp^2 hybridized CNT carbon atoms, and not at the carboxylic acid groups, giving rise to only one type of bonding to the CNTs, and hence, only one APOH/nitrosophenyl peak. Furthermore, in the case where the reaction is carried out in the absence of hypophosphorous acid, it was suggested that the contribution of the ester-NP groups shifts the irreversible NP reduction to a more negative potential, and the reaction is proposed to proceed via an aryl cation intermediate.[20] While these mechanistic suggestions are largely speculative, they could explain the variation in NP reduction and APOH/nitrosophenyl couple signals observed in the present work. Considering the cyclic voltammograms in Figure 4.6, such an interpretation would have the reduction in Figure 4.6 (a) assigned to that of NP groups bound directly to carbon, and those in Figure 4.6 (b) to NP groups bound both directly to the carbon surface and via ester linkages. Hence, assuming the reaction takes place via a cationic intermediate, sample-to-sample variations in the prevalence of carboxylic acid groups on the PPF surface could account for the variability in the cyclic voltammograms. On the other hand, this interpretation is not consistent with the results obtained for spontaneously prepared films at GC. Figure 4.1 (b) shows that the film formed at GC has a less negative reduction peak than that formed at PPF (Figure 4.6 (b)), despite GC having a significantly higher surface oxygen concentration (see Section 1.1.2). A simpler explanation is

that differences in the cyclic voltammograms of NP films spontaneously formed at PPF may be due to differences in film thickness, which shifts the reduction peak potential (see above).

To investigate the effect of the immersion time on the surface concentration of NP groups in spontaneously prepared NP films, PPF samples were immersed for times of 5, 10, 30, 60 and 120 minutes in 10 mM NBD/0.14 M H_2SO_4 solution. After standard post modification sonication the samples were transferred to a cell containing 0.14 M H_2SO_4 and reduction of the bound NP groups was carried by recording cyclic voltammograms between ~ 0.7 and -1.2 V (initial potential ~0.7 V). Subsequently, the surface concentration of electro-active NP groups, Γ_{NP}, was calculated using the method outlined in Section 3.3.3.

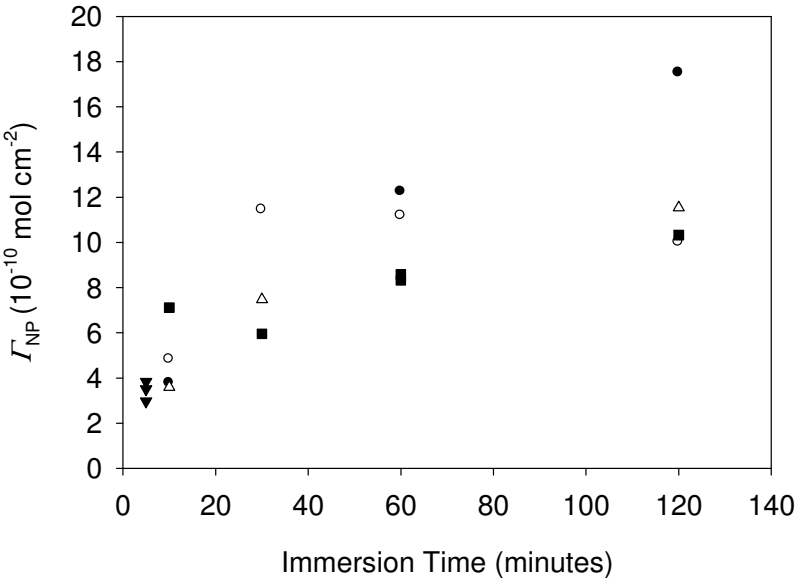

Figure 4.7. Plot of Γ_{NP} vs. immersion time in for PPF samples after immersion in 10 mM NBD/0.14 M H_2SO_4.

Figure 4.7 shows a plot of Γ_{NP} vs. immersion time for NP films spontaneously prepared at PPF in 10 mM NBD/0.14 M H_2SO_4. The different symbols (Δ,▼,●,○,■) represent experiments carried out on different days, with a fresh solution of NBD made on each day. Lower Γ_{NP} values were found for the NP films spontaneously prepared at PPF than for those prepared at GC (Figure 4.2) under the same conditions. This is not surprising considering the lower surface roughness of PPF than GC. Figure 4.7 shows Γ_{NP} increasing with immersion time up to 30 minutes. However, due

to the scatter in the data, it is not clear whether further significant increase in Γ_{NP} occurs after 30 minutes immersion time and, if so, whether this increase ceases before 120 minutes immersion time.

Downard has shown that electrochemically prepared NP films at GC reach a limiting surface concentration after applying a certain fixed potential for a sufficient period of time.[32] It was suggested that film growth is limited because the films reach a thickness at which electron transfer through the film to the NBD in solution is no longer possible due to the blocking effect of the film. This prevents the production of aryl radicals, and hence, further film growth. The limiting surface concentration was shown to depend on the potential applied to achieve modification, with higher limiting surface concentrations found for films prepared at more negative applied potentials. It was proposed that, at more negative applied potentials, electron transfer through thicker films is possible, leading to higher limiting surface concentrations for films formed at more negative applied potentials.[32] If the spontaneous reaction proceeds via electron transfer from the surface to the diazonium cation, as suggested above, then spontaneously formed NP films would be expected to become self limiting after a certain immersion time with the limiting surface concentration being determined by the OCP of the substrate. Figure 4.7 does show some evidence of this behavior, with the rate of film growth significantly diminishing at longer immersion times. However, the scatter in the data prevents any conclusive analysis.

An alternative explanation for the slower increase in Γ_{NP} at longer immersion times is that NBD decomposes in solution. To test this possibility, two PPF samples were immersed in 10 mM NBD/0.14 M H_2SO_4 for 60 minutes, after which they were transferred to identical, freshly prepared, solutions of NBD and left to react for another 60 minutes. The surface concentrations were determined by cyclic voltammetry to be 6.3×10^{-10} and 9.7×10^{-10} mol cm^{-2}, no higher than the values determined for PPF samples after immersion in a single solution of NBD for 120 minutes (Figure 4.7). Hence it was concluded that decomposition of NBD is not responsible for the slower increase in Γ_{NP} at longer immersion times.

4.4.2 Atomic Force Microscope Film Thickness Measurements

Brooksby et al. have shown that that loosely packed NP multilayers are formed at PPF upon electrochemical reduction of NBD.[22] Hence, atomic force microscopy (AFM) film thickness measurements were undertaken to determine if loosely packed multilayers are also formed when the modification is undertaken spontaneously in aqueous conditions.

Samples prepared and analyzed as described in Section 4.4.1 were selected for film thickness analysis (see Section 2.5.3). For all samples a trench in the surface was seen after scratching with the AFM tip, indicating removal of the film. Figure 4.8 shows an AFM image of a section of a trench on a NP modified PPF sample, and the corresponding average cross section.

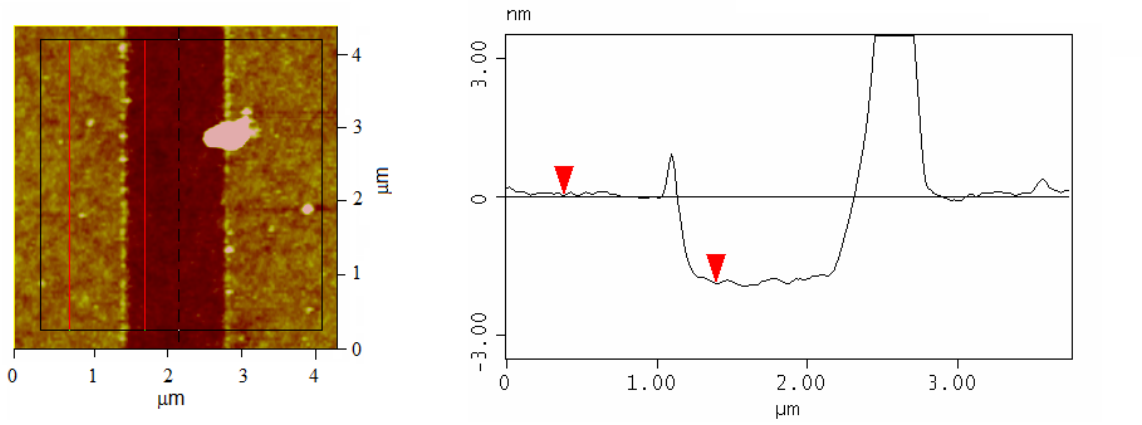

Figure 4.8. AFM image of a section of a trench made on a NP film on PPF (left) and average cross section taken across the scratch (right). The sample was prepared by immersion in 10 mM NBD/0.14 M H_2SO_4 for 60 minutes.

Figure 4.9 shows a plot of film thickness vs. immersion time in NBD used for sample preparation. The symbols correspond to samples of the same symbols as in Figure 4.7.

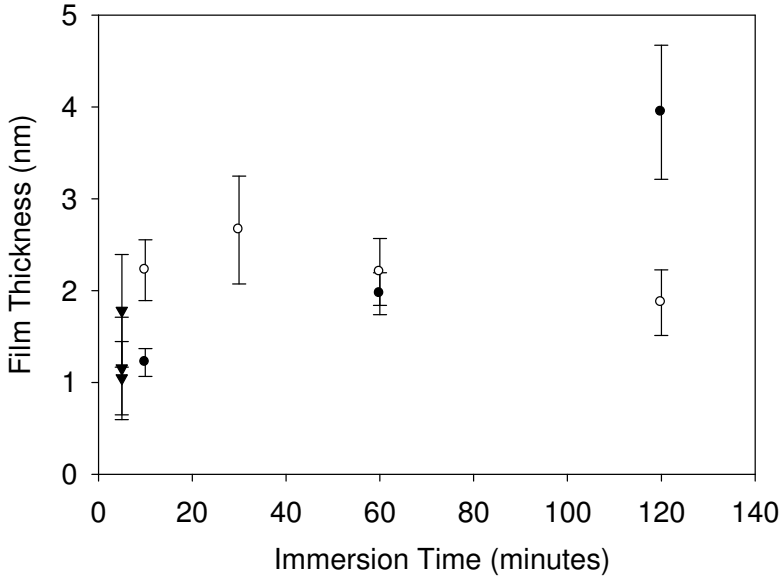

Figure 4.9. Plot of film thickness vs. immersion time for NP films at PPF prepared in 10 mM NBD/0.14 M H_2SO_4.

Film thicknesses ranging from ~1.1 to 3.9 nm were determined for the samples. The length of the NP modifier is 0.79 nm (as determined using Spartan),[22] hence it can be concluded that multilayer films had been formed. As described in Section 1.3.1, multilayers form when aryl radicals react with aryl moieties already bound to the surface. Figure 4.9 shows that the major increase in film thickness occurs between 0 and 5 minutes immersion time, with only a possible gradual increase in thickness thereafter. This supports the interpretation that the films become self limiting at longer immersion times (see Section 4.4.1) and also supports the OCP data which suggests rapid initial film growth which slows with immersion time.

Plotting Γ_{NP} against film thicknesses gives information concerning the average packing densities of the films. Figure 4.10 shows a plot of Γ_{NP} (from Section 4.4.1) vs. the corresponding film thicknesses for NP modified PPF samples.

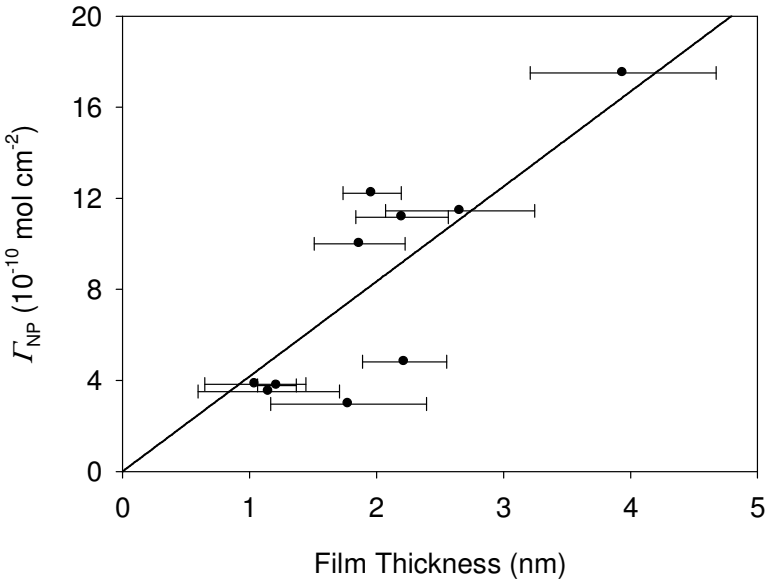

Figure 4.10. Plot of $\Gamma_{NP,}$ vs. film thickness. Slope = 4.2 ± 0.8 and R^2 = 0.69 with the regression line forced through origin. The error of the slope is given as two standard deviations.

The film thickness increases with Γ_{NP} and the relationship is close to linear, within the large uncertainties in the measurements and scatter in the data. Assuming a linear relationship, the average film density is given by the slope to be ~ (4.2 ± 0.8) × 10^{-10} mol cm^{-2} nm^{-1}. Using the theoretical value[22] for a monolayer thickness (0.79 nm) the surface concentration per monolayer thickness of NP groups is (3.3 ± 0.6) × 10^{-10} mol cm^{-2}. In comparison with the theoretical value[33] for a close packed monolayer of NP groups on a flat surface (12 × 10^{-10} mol cm^{-2}) it can be concluded that the films are loosely packed multilayers with a packing densities of ~30% of that of a closely packed monolayer on a flat surface. This result compares well with that obtained by Brooksby et al. who investigated the packing density of NP films prepared by electrochemical reduction of NBD at PPF. In their study, a linear relationship between Γ_{NP} and the film thickness was also found; and the surface concentration of NP groups per monolayer thickness was found to be (2.5 ± 0.5) × 10^{-10} mol cm^{-2}, ~20% of the close-packed value.[22] Hence the packing densities of the NP films formed spontaneously at PPF are similar to those for films prepared by electrochemical reduction of NBD at PPF.

4.4.3 Atomic Force Microscope Surface Roughness Analysis

To investigate the effect of the immersion time on surface roughness, PPF samples were immersed in 10 mM NBD/0.14 M H_2SO_4 for 10, 30, 60 and 120 minutes. After the standard post modification sonication procedure the surface roughness of the samples was measured by AFM, as described in Section 2.5.4. Figure 4.11 shows a plot of the surface roughness, R_a, of the samples vs. the immersion time. No statistically significant change in R_a was found, indicating that the roughness does not change during film growth (at least after 10 minutes).

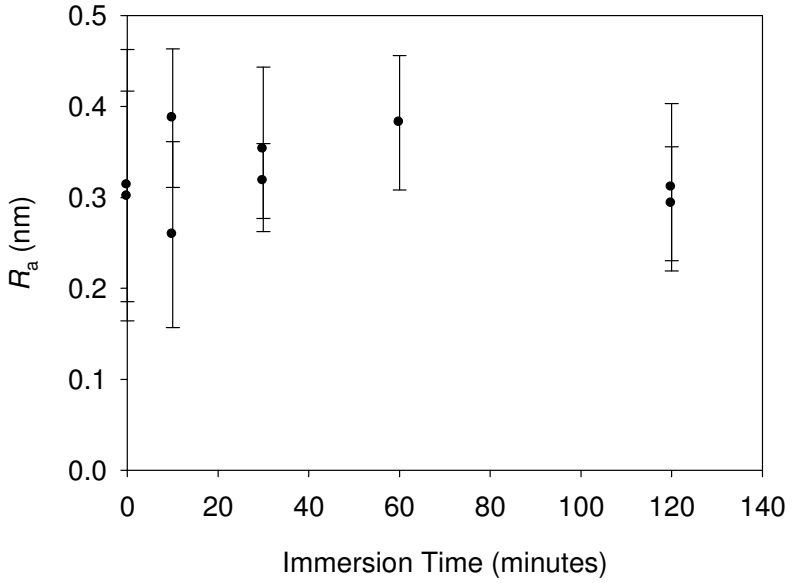

Figure 4.11. Plot of R_a of NP modified PPF vs. immersion time in 10 mM NBD/ 0.14 M H_2SO_4. The values at zero immersion time are for unmodified PPF.

4.4.4 Water Contact Angle Measurements

Water contact angle measurements were carried out to determine the effect of modification on the hydrophilicity of PPF. Figure 4.12 shows a plot of water contact angle vs. immersion time for NP films prepared in aqueous conditions. The data points at immersion time = 0 correspond to bare PPF not immersed in NBD solution. An increase of approximately 15º was observed upon modification of the samples with NP films, indicating a decrease in hydrophilicity. However, no

significant difference in the contact angles was observed with an increase in immersion time from 10 to 120 minutes, indicating that there is no significant change in hydrophilicity with immersion time.

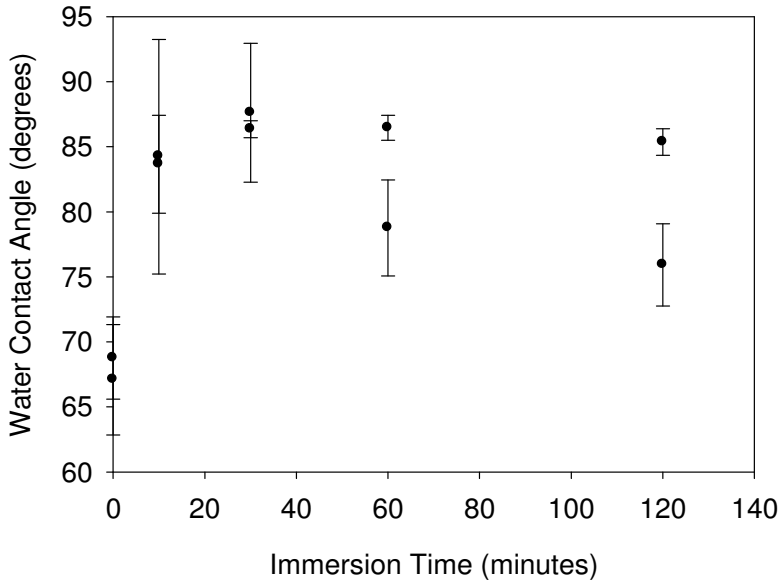

Figure 4.12. Plot of water contact angles vs. immersion time of PPF in 10 mM NBD/0.14 M H_2SO_4.

4.4.5 Stability of Spontaneously Prepared NP Films to Sonication

The stability of NP films spontaneously prepared at PPF in aqueous conditions to prolonged sonication in ACN was investigated. Two PPF substrates were modified with NP films by immersing in 10 mM NBD/0.14 M H_2SO_4 for 60 minutes. After the standard post modification sonication procedure, the samples were sonicated in ACN for a further 30 minutes. Cyclic voltammograms were then recorded between ~0.8 and -1.2 V in 0.14 M H_2SO_4 and Γ_{NP} was calculated. Surface concentrations of 12.3×10^{-10} and 14.1×10^{-10} mol cm^{-2} were found for the two samples. These concentrations are consistent with those after 60 minutes immersion time in Figure 4.7, suggesting negligible loss of NP groups from the surface upon prolonged sonication in ACN, and consequently, that the NP films are strongly bound. In fact, stability to prolonged sonication is often assumed to indicate covalent bonding between the films and the surface.[34-36]

Hence, it can be tentatively assumed that the spontaneously formed films are covalently bound to the surface.

4.4.6 OCP of PPF during Modification with NP Films.

A series of experiments were conducted at PPF, similar to those carried out at GC (Section 4.3.2), to look for evidence of the spontaneous modification via reduction of NBD by the PPF surface. To test the plausibility of this mechanism, cyclic voltammograms were recorded in 1 mM solutions of NBD in both in 0.1 M $[Bu_4N]BF_4$/ACN and 0.14 M H_2SO_4 at PPF electrodes.

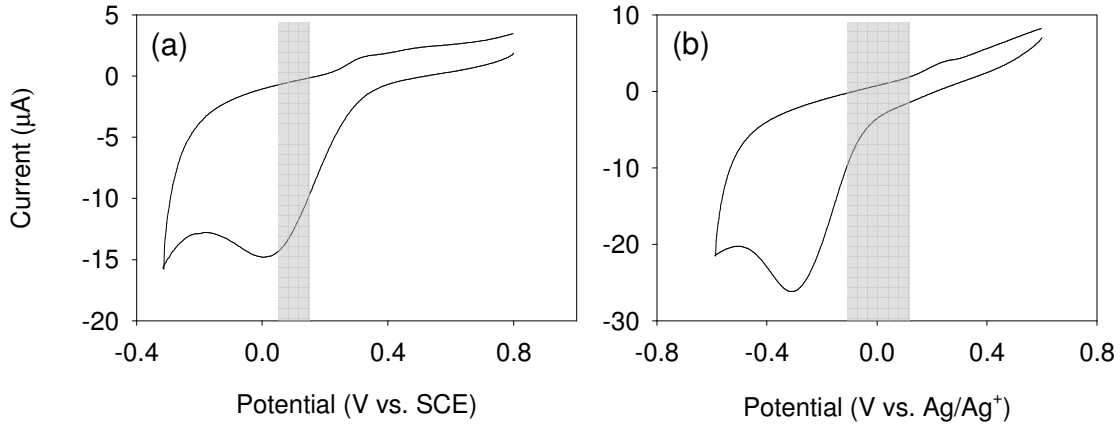

Figure 4.13. Electrochemical reduction of 1 mM NBD at a PPF working electrode in 0.14 M H_2SO_4 (a) and 0.1 M $[Bu_4N]BF_4$/ACN (b); scan rate = 100 mV s^{-1} .The range of OCP values of PPF after 60 minutes equilibration (for each medium) are shown by the vertical shaded bands (see Figure 4.14).

In aqueous conditions (Figure 4.13(a)) the OCP of the PPF (shaded area) is seen to be consistently and significantly negative of the beginning of the peak assigned to the reduction of NBD. Hence, under these conditions, PPF would be expected to spontaneously reduce NBD to an aryl radical leading to film formation. However, in 0.1 M $[Bu_4N]BF_4$/ACN (Figure 4.13(b)) the OCP of the PPF was seen to extend from the beginning of the peak assigned to the reduction of NBD to potentials positive of the reduction peak. This could explain why modification in ACN is irreproducible. For those cases where the OCP of the PPF in ACN is significantly positive of the beginning of the NBD reduction peak, no modification occurs. For other samples

the OCP is sufficiently low to lead to modification with low surface concentrations (relative to those obtained in aqueous conditions).

The effect of the addition of NBD on the OCP of PPF was investigated in 0.1 M $[Bu_4N]BF_4$/ ACN and 0.14 M H_2SO_4, in the same manner as for GC electrodes (Section 4.3.2). In brief, after allowing the PPF electrodes to "equilibrate" in blank electrolyte for 60 minutes, 10 mL of 20 mM NBD/electrolyte was added to give a solution of 10 mM NBD and the OCP was monitored for a further 120 minutes. Controls were carried out by adding "blank" electrolyte, and *p*-nitroaniline, rather than NBD.

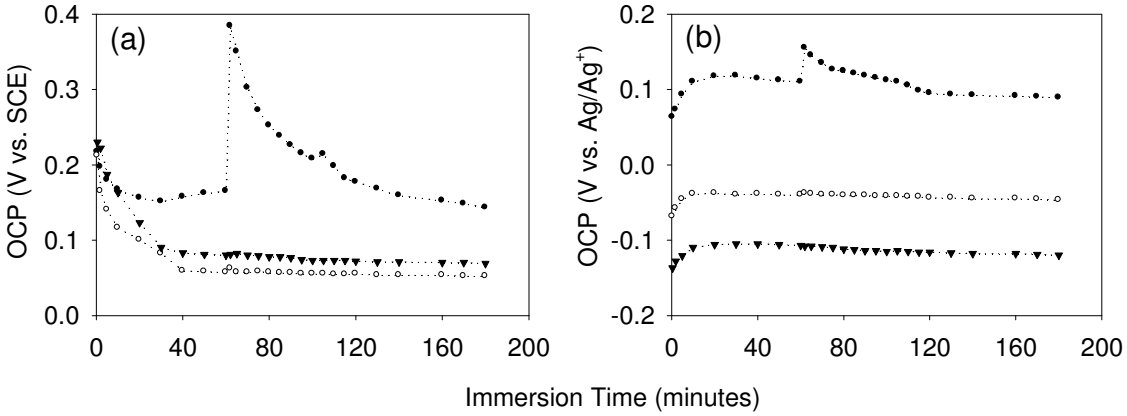

Figure 4.14. Plot of OCP vs. immersion time in 0.14 M H_2SO_4 (a) and 0.1 M $[Bu_4N]BF_4$/ACN (b) for PPF electrodes. After an equilibration period of 60 minutes 10 mL solutions of 20 mM NBD/electrolyte (●), 20 mM *p*-nitroanaline/electrolyte (▼) or 10 mL electrolyte (○) were added to the solution.

Figure 4.14 shows the effect of adding NBD (●), *p*-nitroanaline (▼) or blank electrolyte (○) on the OCP of PPF in 0.14 M H_2SO_4 (a) and 0.1 M $[Bu_4N]BF_4$/ACN (b). In both media the OCP is seen to increase on the addition of NBD at 60 minutes immersion time. No significant change in OCP is seen in either medium upon the addition of either blank electrolyte or *p*-nitroanaline, indicating that the diazonium cation moiety is responsible for the increase when NBD is added. The increase in ACN ($\Delta E \approx 0.04$ V) was significantly smaller than that in aqueous conditions ($\Delta E \approx 0.22$ V), indicating less reduction in ACN. This is consistent with the results presented in Section 4.4.1, where low surface concentrations of NP groups were found after immersion of

PPF substrates in NBD/ACN. Furthermore, it is also consistent with the data shown in Figure 4.13 (b) where the OCP of the PPF is close to the beginning of the NBD reduction peak in ACN.

4.5 Spontaneous Modification of PPF with CP Films

To demonstrate that the spontaneous reaction of diazonium salts with PPF is not limited to NBD, the spontaneous reaction of a second diazonium salt was investigated. *p*-Carboxybenzene diazonium tetrafluoroborate salt (CBD) was chosen for this purpose. Modification using CBD would be expected to lead to the formation of *p*-carboxyphenyl (CP) films, which are convenient for further coupling reactions and thereby amenable to many applications. Furthermore, CP layers would be expected to be significantly more hydrophilic than bare PPF, making their detection by contact angle measurements straightforward.

Four PPF samples were immersed in 10 mM CBD in 0.14 M H_2SO_4 for 180 minutes. After immersion the samples were analyzed using water contact angle measurements and $Fe(CN)_6^{3-/4-}$ redox probe voltammetry.

4.5.1 Water Contact Angles of CP Modified PPF

After immersion in CBD the PPF samples gave an average water contact angle of (48 ± 7)º, lower than the value of (68 ± 4)º found for bare PPF (Section 4.4.5). The decrease in contact angle indicates that the surface has become more hydrophilic, and is consistent with the presence of CP groups. Similar results have been reported by other workers after modification of PPF with CP functionalities via electro-reduction of CBD.[37] Hence, the water contact angle measurements indicate that spontaneous modification of PPF with CP films upon immersion in CBD/0.14 M H_2SO_4 was successful.

4.5.2 $Fe(CN)_6^{3-}$ Redox Probe Voltammetry of CP Modified PPF

$Fe(CN)_6^{3-/4-}$ redox probe voltammetry was employed to obtain further evidence for the presence of CP groups after immersion of the PPF samples in CBD.

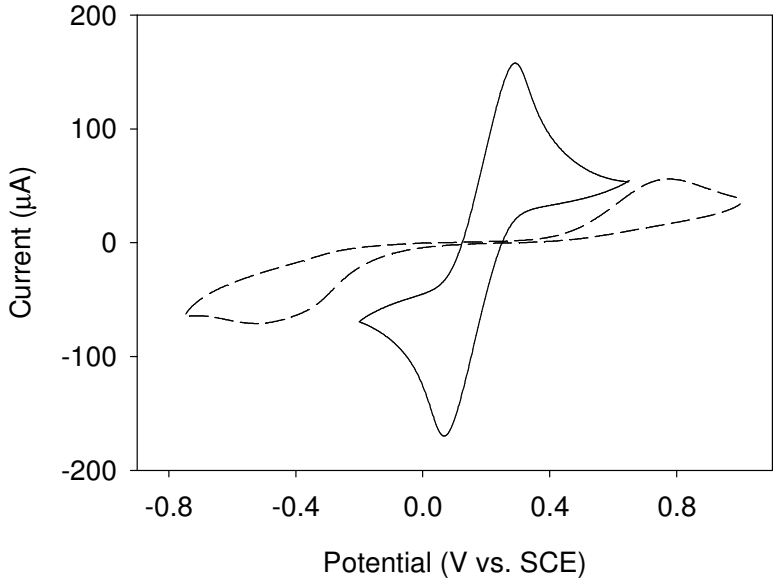

Figure 4.15. Cyclic voltammograms recorded in the presence of 5 mM $K_3Fe(CN)_6$/0.1 M phosphate buffer, pH 7.4, at bare PPF (—) and after immersion in 10 mM CBD/0.14 M H_2SO_4 for 180 minutes (---).

Figure 4.15 shows cyclic voltammograms of bare PPF (—) and PPF after immersion in CBD (---), recorded in the presence of $Fe(CN)_6^{3-/4-}$ (by scanning in the negative direction). The bare PPF electrode shows the quasi-reversible $Fe(CN)_6^{3-/4-}$ redox couple at $E_{1/2} \approx 0.15$ V vs. SCE with a peak separation of $\Delta E_p = 0.25$ V. Upon immersion in CBD the peak separation was seen to increase to $\Delta E_p = 1.24$ V. This suppressed $Fe(CN)_6^{3-/4-}$ response is consistent with the presence of an insulting film at the electrode surface and is further evidence for the presence of a CP film on the surface after spontaneous modification.

4.5.3 Potential of Reduction of CBD

Cyclic voltammetry was used to assess if PPF would be expected to reduce CBD at OCP. A cyclic voltammogram of a PPF electrode was recorded by scanning in the negative direction from an initial potential of 0.6 V vs. SCE in 1 mM CBD/0.14 M H_2SO_4.

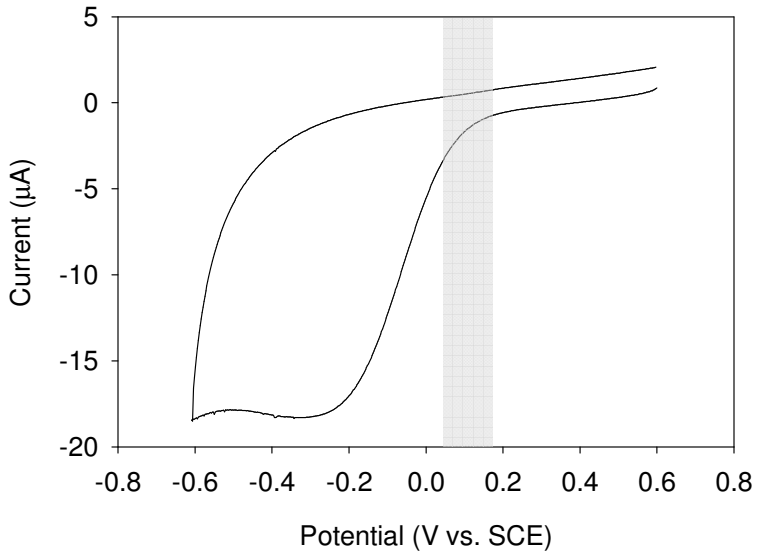

Figure 4.16. Cyclic voltammogram recorded at PPF in 1 mM CBD/0.14 M H_2SO_4, initial potential = 0.6 V; scan rate = 100 mV s^{-1}. The range of OCP values of PPF after 60 minutes equilibration in 0.14 M H_2SO_4 are shown by the vertical band (see Figure 4.14 (a)).

Figure 4.16 shows the chemically irreversible CBD reduction at $E_{p,c} \approx$ -0.3 V vs. SCE. The lower peak potential for the reduction of CBD compared to NBD (0.0 V vs. SCE from Figure 4.13(a)) is expected due to the more electron withdrawing nature of the -NO_2 substituent compared to -CO_2H.[6, 38] Nevertheless, the OCP of the PPF surface (vertical band) is seen to be negative of the start of the CBD reduction peak, indicating that spontaneous modification of PPF by reaction with CBD at OCP is expected.

4.6 Conclusion

The spontaneous modification of GC with NP films via reaction with NBD proceeds in both ACN and aqueous conditions. Cyclic voltammetric measurements show that films formed in aqueous conditions are denser than those formed in ACN, as previously found for electrochemically prepared NP films at PPF.[22] At PPF, significant modification occurs reliably only in aqueous conditions. OCP measurements suggest that the carbon surface acts as an electron donor during modification, reducing the diazonium cation to an aryl radical, leading to film formation. The spontaneous modification of PPF with CP film was also observed via immersion of the substrate in aqueous CBD solution. CBD is more difficult to reduce than NBD, hence the modification indicates that the spontaneous reaction is not limited to the relatively easily reduced NBD cation.

The reason for sensitivity of the reaction at PPF to the medium is not clear. One possible explanation is that the OCP of PPF in ACN is not always sufficiently negative to reduce NBD. OCP measurements are consistent with this interpretation. A further possibility is that a physisorption step of the diazonium cation is required prior to modification, but that physisorption does not occur in ACN.

Analysis of NP films spontaneously prepared at PPF from aqueous media show the formation of loosely packed multilayers with an average packing density similar to that previously determined for NP films prepared by electrochemical reduction at PPF.[22] Furthermore, the resulting films appear to be highly stable, thus exhibiting one of the key attractive features of films formed at carbon by electro-reduction of aryldiazonium salts. The films formed by spontaneous reaction of NBD with PPF showed poorly reproducible surface concentrations and film thicknesses, even when prepared under identical conditions. This is one disadvantage of spontaneous modification compared to electrochemical modification, where surface concentrations and film thickness are relatively reproducible.[22] This is probably due to the fact that the potential is controlled during electrochemical modification, whereas the OCP drifts during spontaneous modification. Furthermore, prior to modification the OCP of the PPF was found to vary considerably between

individual samples. Nevertheless, the spontaneous modification may be a useful technique in situations where electrochemical modification is impractical or impossible (see Chapter 6).

4.7 References

1. Fan, F. R. F.; Yang, J. P.; Dirk, S. M.; Price, D. W.; Kosynkin, D.; Tour, J. M.; Bard, A. J., Determination of the molecular electrical properties of self-assembled monolayers of compounds of interest in molecular electronics. *J. Am. Chem. Soc.* **2001,** 123, 2454-2455.

2. Hurley, B. L.; McCreery, R. L., Covalent bonding of organic molecules to Cu and Al alloy 2024 T3 surfaces via diazonium ion reduction. *J. Electrochem. Soc.* **2004,** 151, B252-B259.

3. Stewart, M. P.; Maya, F.; Kosynkin, D. V.; Dirk, S. M.; Stapleton, J. J.; McGuiness, C. L.; Allara, D. L.; Tour, J. M., Direct covalent grafting of conjugated molecules onto Si, GaAs, and Pd surfaces from aryldiazonium salts. *J. Am. Chem. Soc.* **2004,** 126, 370-378.

4. Adenier, A.; Cabet-Deliry, E.; Chausse, A.; Griveau, S.; Mercier, F.; Pinson, J.; Vautrin-Ul, C., Grafting of nitrophenyl groups on carbon and metallic surfaces without electrochemical induction. *Chem. Mater.* **2005,** 17, 491-501.

5. Combellas, C.; Delamar, M.; Kanoufi, F.; Pinson, J.; Podvorica, F. I., Spontaneous grafting of iron surfaces by reduction of aryldiazonium salts in acidic or neutral aqueous solution. Application to the protection of iron against corrosion. *Chem. Mater.* **2005,** 17, 3968-3975.

6. Adenier, A.; Barre, N.; Cabet-Deliry, E.; Chausse, A.; Griveau, S.; Mercier, F.; Pinson, J.; Vautrin-Ul, C., Study of the spontaneous formation of organic layers on carbon and metal surfaces from diazonium salts. *Surf. Sci.* **2006,** 600, 4801-4812.

7. Chamoulaud, G.; Bélanger, D., Spontaneous derivatization of a copper electrode with in situ generated diazonium cations in aprotic and aqueous media. *J. Phys. Chem. C* **2007,** 111, 7501-7507.

8. Liang, H. H.; Tian, H.; McCreery, R. L., Normal and surface-enhanced Raman spectroscopy of nitroazobenzene submonolayers and multilayers on carbon and silver surfaces. *Appl. Spectrosc.* **2007,** 61, 613-620.

9. Seinberg, J. M.; Kullapere, M.; Maeorg, U.; Maschion, F. C.; Maia, G.; Schiffrin, D. J.; Tammeveski, K., Spontaneous modification of glassy carbon surface with anthraquinone from the solutions of its diazonium derivative: An oxygen reduction study. *J. Electroanal. Chem.* **2008,** 624, 151-160.

10. Le Floch, F.; Simonato, J. P.; Bidan, G., Electrochemical signature of the grafting of diazonium salts: A probing parameter for monitoring the electro-addressed functionalization of devices. *Electrochim. Acta* **2009,** 54, 3078-3085.

11. Podvorica, F. I.; Kanoufi, F.; Pinson, J.; Cornbellas, C., Spontaneous grafting of diazoates on metals. *Electrochim. Acta* **2009,** 54, 2164-2170.

12. Lu, M.; Nolte, W. A.; He, T.; Corley, D. A.; Tour, J. M., Direct Covalent Grafting of Polyoxometalates onto Si Surfaces. *Chem. Mater.* **2009,** 21, 442-446.

13. Chen, B.; Lu, M.; Flatt, A. K.; Maya, F.; Tour, J. M., Chemical reactions in monolayer aromatic films on silicon surfaces. *Chem. Mater.* **2008,** 20, 61-64.

14. Combellas, C.; Kanoufi, F.; Pinson, J.; Podvorica, F. I., Time-of-flight secondary ion mass spectroscopy characterization of the covalent bonding between a carbon surface and aryl groups. *Langmuir* **2005,** 21, 280-286.

15. Toupin, M.; Bélanger, D., Spontaneous functionalization of carbon black by reaction with 4-nitrophenyldiazonium cations. *Langmuir* **2008,** 24, 1910-1917.

16. Smith, R. D. L.; Pickup, P. G., Voltammetric quantification of the spontaneous chemical modification of carbon black by diazonium coupling. *Electrochim. Acta* **2009,** 54, 2305-2311.

17. Bahr, J. L.; Tour, J. M., Highly functionalized carbon nanotubes using in situ generated diazonium compounds. *Chem. Mater.* **2001,** 13, 3823-+.

18. Dyke, C. A.; Tour, J. M., Unbundled and highly functionalized carbon nanotubes from aqueous reactions. *Nano Lett.* **2003,** 3, 1215-1218.

19. Strano, M. S.; Dyke, C. A.; Usrey, M. L.; Barone, P. W.; Allen, M. J.; Shan, H. W.; Kittrell, C.; Hauge, R. H.; Tour, J. M.; Smalley, R. E., Electronic structure control of single-walled carbon nanotube functionalization. *Science* **2003,** 301, 1519-1522.

20. Abiman, P.; Wildgoose, G. G.; Compton, R. G., Investigating the mechanism for the covalent chemical modification of multiwalled carbon nanotubes using aryl diazonium salts. *Int. J. Electrochem. Sci.* **2008,** 3, 104-117.

21. Brooksby, P. A.; Downard, A. J., Multilayer nitroazobenzene films covalently attached to carbon. An AFM and electrochemical study. *J. Phys. Chem. B* **2005,** 109, 8791-8798.

22. Brooksby, P. A.; Downard, A. J., Electrochemical and atomic force microscopy study of carbon surface modification via diazonium reduction in aqueous and acetonitrile solutions. *Langmuir* **2004,** 20, 5038-5045.

23. Zhong, C. J.; Woods, N. T.; Dawson, G. B.; Porter, M. D., Formation of thiol-based monolayers on gold: implications from open circuit potential measurements. *Electrochem. Commun.* **1999,** 1, 17-21.

24. Bard, A. J.; Faulkner, L. R., *Electrochemical Methods: Fundamentals and Applications*. 2nd ed.; John Wiley & Sons, Inc: Danvers, 2001.

25. Engstrom, R. C., Electrochemical Pretreatment of Glassy-Carbon Electrodes. *Anal. Chem.* **1982,** 54, 2310-2314.

26. Kepley, L. J.; Bard, A. J., Ellipsometric, Electrochemical, and Elemental Characterization of the Surface Phase Produced on Glassy-Carbon Electrodes by Electrochemical Activation. *Anal. Chem.* **1988,** 60, 1459-1467.

27. Bowling, R. J.; Packard, R. T.; McCreery, R. L., Activation of Highly Ordered Pyrolytic-Graphite for Heterogeneous Electron-Transfer - Relationship between Electrochemical Performance and Carbon Microstructure. *J. Am. Chem. Soc.* **1989,** 111, 1217-1223.

28. Zhao, Q. L.; Zhang, Z. L.; Bao, L.; Pang, D. W., Surface structure-related electrochemical behaviors of glassy carbon electrodes. *Electrochem. Commun.* **2008,** 10, 181-185.

29. Usrey, M. L.; Lippmann, E. S.; Strano, M. S., Evidence for a two-step mechanism in electronically selective single-walled carbon nanotube reactions. *J. Am. Chem. Soc.* **2005,** 127, 16129-16135.

30. Wang, H. M.; Xu, J. S., Theoretical evidence for a two-step mechanism in the functionalization single-walled carbon nanotube by aryl diazonium salts: Comparing effect of different substituent group. *Chem. Phys. Lett.* **2009,** 477, 176-178.

31. Ranganathan, S.; McCreery, R. L., Electroanalytical performance of carbon films with near-atomic flatness. *Anal. Chem.* **2001,** 73, 893-900.

32. Downard, A. J., Potential-dependence of self-limited films formed by reduction of aryldiazonium salts at glassy carbon electrodes. *Langmuir* **2000,** 16, 9680-9682.

33. Liu, Y. C.; McCreery, R. L., Reactions of Organic Monolayers on Carbon Surfaces Observed with Unenhanced Raman-Spectroscopy. *J. Am. Chem. Soc.* **1995,** 117, 11254-11259.

34. Delamar, M.; Hitmi, R.; Pinson, J.; Savéant, J. M., Covalent Modification of Carbon Surfaces by Grafting of Functionalized Aryl Radicals Produced from Electrochemical Reduction of Diazonium Salts. *J. Am. Chem. Soc.* **1992,** 114, 5883-5884.

35. Shewchuk, D. M.; McDermott, M. T., Comparison of Diazonium Salt Derived and Thiol Derived Nitrobenzene Layers on Gold. *Langmuir* **2009,** 25, 4556-4563.

36. Allongue, P.; Delamar, M.; Desbat, B.; Fagebaume, O.; Hitmi, R.; Pinson, J.; Savéant, J. M., Covalent modification of carbon surfaces by aryl radicals generated from the electrochemical reduction of diazonium salts. *J. Am. Chem. Soc.* **1997,** 119, 201-207.

37. Yu, S. C., *PhD thesis: covalent attachment of nanoscale organic films to carbon electrodes*. University of Canterbury: 2008.

38. Elofson, R. M.; Gadallah, F. F., Substituent Effects in the Polarography of Aromatic Diazonium Salts. *J. Org. Chem.* **1969,** 34, 854-857.

Chapter 5. Modification of Gold Surfaces by Spontaneous Reaction of Aryldiazonium Salts

5.1 Introduction

The modification of gold surfaces has been a subject of extensive research,[1-5] in part because gold is an attractive substrate for electrochemical sensing applications. The low capacitance of gold electrodes (in comparison to graphitic carbon) results in good sensitivity. Furthermore, gold is a relatively homogeneous material, which is an advantage for many applications where accuracy and surface reproducibility are of importance.[6] Gold surfaces have been most commonly modified by adsorption of alkanethiols, resulting in the formation of partial covalent Au-S bonds between the modifier and the surface.[1, 2, 5, 7-9] Films formed by this method are often well ordered monolayers and are generally referred to in the literature as self-assembled monolayers (SAMs). However, SAMs formed by gold-thiol chemistry have been shown to exhibit a degree of instability that is undesirable for some applications.[6] For example, they have been shown to be stable only in a relatively small potential window (typically 0.8 to -0.8 V) and to have poor thermal stability, some desorbing from the surface at temperatures as low as 100 ºC.[10]

These considerations have prompted a number of workers to investigate the electro-reduction of aryldiazonium salts as an alternative method of modifying gold.[3, 4, 6, 11-18] There is some evidence that the films formed at gold via electro-reduction of diazonium salts are covalently bound. Several workers have noted the absence of the diazonium cation moiety in XPS and infrared spectroscopy spectra of the surface after modification, indicating the diazonium cation had reacted, possibly with the surface.[3, 11] Bèlanger and coworkers investigated the C1s core level spectra of gold modified with *p*-carboxyphenyl (CP), *p*-diethylaniline and *p*-nitrophenyl (NP) moieties. In the case of the CP modified electrode, the spectrum could be conclusively fitted with an Au-C component. However, since the C1s peak depends on the nature of the aryl substituents, in the case of the *p*-diethylaniline and NP modifiers no conclusions about the presence of a Au-C bond could be reached.[3] Using polarized infrared reflectance absorption spectroscopy (IRRAS),

Calvo and coworkers confirmed that NP groups deposited on Au via electro-reduction of the corresponding diazonium salt are orientated perpendicular to the surface, consistent with covalent attachment.[11]

Several studies have examined the stability of films at gold prepared by electro-reduction of diazonium salts. Bèlanger and coworkers prepared NP, CP and *p*-diethylaniline films at gold by electrochemical reduction of the corresponding diazonium salts in ACN. The stabilities of the films to sonication in ACN were investigated using electrochemical impedance spectroscopy. Although some material was lost during sonication, film material remained at the gold surface even after 30 minutes sonication.[3] In a separate study, Gooding and coworkers compared the stability of diazonium cation derived CP films and short-chain alkanethiol films at gold to potential cycling in 0.1 M H_2SO_4.[6] The diazonium cation derived films were shown, by monitoring gold oxide formation, to have a higher stability to potential cycling than those derived from the thiols.

In a related study, McDermott and coworkers compared the stability of *p*-nitrobenzene diazonium salt (NBD) derived NP layers with NP films derived from thiols.[18] The stabilities of the films to sonication, refluxing in ACN, and displacement by octadecanethiol (ODT) were investigated by IRRAS. (Long-chain alkane thiols, such as ODT, are known to displace short-chain thiols[8]). Upon sonication in ACN, the percentage loss of NP groups for the thiol and diazonium derived films was found to be 8 % and 35 % respectively. Qualitatively similar results were found upon refluxing in ACN with 64 % loss observed for the diazonium cation derived films and 48 % loss for the thiol films. However, upon immersion in an ethanol solution of ODT, all of the initial thiol films were lost; while 27 % of the NBD derived NP film remained on the surface. This indicates that some of the diazonium cation derived NP groups are more stable on the surface than their thiol counterparts.

In a recent computational study Scherlis and coworkers compared the strengths of C-Au (111) bonds (such as those formed by the reaction of diazonium salts with gold) and S-Au(111) bonds (such as those formed by thiol-gold chemistry). It was found that the aryl C-Au(111) binding

energy (31.8 kcal mol^{-1}) is greater than that for aryl S-Au(111) (28.4 kcal mol^{-1}). However, both of these were found to be lower than the CH_3-S-Au binding energy (36.8 kcal mol^{-1}).[19]

Based on these binding energies, and their own results, McDermott and coworkers suggested that both physisorbed oligomer and covalently attached NP groups are present in the NBD derived NP films, and that the reflux and sonication treatments remove the majority of the physisorbed species.[18] This explains the loss of more material from the diazonium cation derived films than from the thiol films upon sonication and reflux, despite the theoretically stronger covalent bond for the diazonium cation derived film. However, based on the higher binding energy for the CH_3-S-Au(111) than for the aryl C-Au(111), the covalently attached NP groups would be expected to be displaced by ODT. To explain why a significant fraction of the NBD derived NP groups remain bound after exposure to ODT, it was suggested that the remaining NP groups were bound to higher-energy step sites on the gold surface.

Several workers have reported the spontaneous modification of gold by reaction with aryldiazonium salts.[20-22] Tour and coworkers reported the modification of gold via spontaneous reaction with diazonium salt in ACN. A reaction time of 24 hours was used and a film thicknesses indicative of surface concentrations of 10-20 % of a monolayer were found by ellipsometry.[22] In a study by Combellas and coworkers, multilayer formation was observed by ellipsometry after spontaneous modification of Au with NP and *p*-bromophenyl films in aqueous acid.[21] However, due to the difference in reaction times (one hour was used by Combellas and coworkers), diazonium salts species and diazonium salt concentrations, it is difficult to draw conclusions concerning the effect of the medium on the modification process. Furthermore, in general, there has been little film characterization work undertaken on spontaneously formed diazonium cation derived films on gold. The stabilities of the films and the mechanism of their formation have also not been addressed to date.

The aim of the current chapter is to investigate the spontaneous modification of gold using aryldiazonium salts. This study has several specific objectives. Firstly, the effect of the solvent on film formation is investigated. Secondly, the surface concentrations, thicknesses and densities of the films are determined. Thirdly, the role of the surface in film formation is investigated;

more specifically, the possibility that the gold surface acts as an electron donor to promote the reduction of the aryldiazonium salt is explored. Fourthly, the stability of films formed by the spontaneous modification of gold using diazonium salts is investigated. Finally, the effect of the *para* substituent on the benzene diazonium cation on the spontaneous reaction with gold is explored.

5.2 Experimental

All modification was conducted using 10 mM solutions of aryldiazonium salts. 0.1 M H_2SO_4 was used for modification in aqueous conditions. Modification in ACN was investigated in 0.1 M $[Bu_4N]BF_4$/ACN and ACN only. Reduction of NP films was carried out in by recording two consecutive cyclic voltammetric scans between ~ 0.6 and -1.2 V vs. SCE in 0.1 M solution of $NaClO_4$ in 1:9 (by volume) EtOH-H_2O. Potassium ferricyanide ($K_3Fe(CN)_6$) redox probe voltammetry was carried out using 1 mM of $K_3Fe(CN)_6$ in 0.1 M phosphate buffer pH 7.4. All cyclic voltammograms were recorded at a scan rate of 100 mV s^{-1}.

NP reduction on Au/NiCr/Si gold was carried out by exposing the entire gold electrode area (0.785 cm^2) to electrolytic solution. All other electrochemical measurements were undertaken by horizontally mounting the working gold electrode between an insulated metal base plate and a glass solution cell and using a 008 O-ring (Viton) to define the working area of the electrode (0.18 cm^2, see Section 2.4.2). All experiments were conducted on Au/NiCr/Si substrates, except atomic force microscopy film thickness measurements and the accompanying electrochemical experiments, which were undertaken using Au/mica substrates. For methods of preparing Au/NiCr/Si and Au/mica substrates see Section 2.3.3.

Two water-contact-angle measurements were taken per sample. Reported angles are arithmetic means of all measurements performed on samples prepared under a specific set of conditions. The errors are given as two standard deviations of the mean.

5.3 Spontaneous Modification of Gold with NP Films

5.3.1 Effect of Solvent on Modification

The spontaneous modification of gold surfaces with NP films was investigated in ACN and 0.1 M H_2SO_4 by immersing Au/NiCr/Si substrates in 10 mM NBD/ACN and 10 mM NBD/0.1 M H_2SO_4 for 60 minutes. After the standard post modification sonication procedure the surfaces were transferred to a cell containing 0.1 M $NaClO_4$ in 1:9 v/v EtOH-H_2O and consecutive cyclic voltammograms were recorded between 0.6 and -1.2 V vs. SCE (initial potential = 0.6 V).

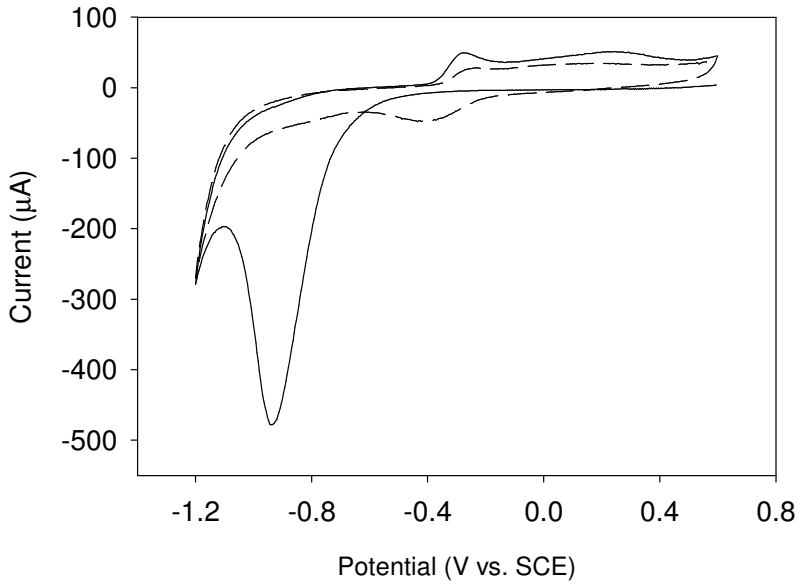

Figure 5.1. Consecutive cyclic voltammograms of Au/NiCr/Si electrodes in 0.1 M $NaClO_4$ in 1:9 v/v EtOH-H_2O after immersion in 10 mM NBD/0.1 M H_2SO_4 for 60 minutes; first scan (—)and second scan(---). Scan rate = 100 mV s^{-1}; initial potential 0.6 V.

Figure 5.1 shows cyclic voltammograms of Au/NiCr/Si substrates after immersion in 10 mM NBD/0.1 M H_2SO_4. The characteristic irreversible NP reduction (~ -0.9 V) and the chemically reversible hydroxyaminophenyl (APOH)/nitrosophenyl redox couple (~ -0.3 V) are observed, indicating NP groups are present at the surface. When the experiments were repeated by immersing the gold substrates in 10 mM NBD/ACN (both in the presence and absence of 0.1 M

$[Bu_4N]BF_4$), no redox processes were observed between 0.6 and -1.2 V, even when the immersion time was extended from 60 to 120 minutes. Hence, under the conditions used here, modification was observed to occur in aqueous conditions, but not in ACN. In contrast, Tour and coworkers reported the spontaneous modification of gold using aryldiazonium salts in ACN.[20, 22] However, their conditions (0.12 mM of diazonium salt with an immersion time of 24 hours) differed significantly from those used here and, even after a relatively long immersion time, only sub (10-20 %) monolayer surface concentrations were observed.[22] The films formed in aqueous conditions in the present work have much higher surface concentrations, even at relatively short (~ 60 minutes) immersion times (see below). Hence, the remainder of the present chapter focuses on the more facile aqueous reaction.

To test the role of the diazonium cation moiety in the formation of the film, Au/NiCr/Si substrates were immersed in 10 mM *p*-nitroaniline/0.1 M H_2SO_4 for 60 minutes. After post-immersion sonication, cyclic voltammograms were recorded between 0.6 and -1.2 V in 0.1 M $NaClO_4$ in EtOH-H_2O (initial potential 0.6 V). No redox systems were observed, indicating that no NP groups were present at the surface. *p*-Nitroaniline is structurally analogous to NBD, but lacks a diazonium cation functionality. This shows that the diazonium cation functionality is essential for the formation of the NP surface layers, described above.

Further evidence of the role of the diazonium cation moiety was found by close inspection of the cyclic voltammogram of the NP modified gold (Figure 5.1). To ensure that the presence of the functionality would be revealed in the scanned range of potential, a cyclic voltammogram of a gold surface was recorded in the presence of 1 mM NBD/0.1M $NaClO_4$ in EtOH-H_2O. A peak due to the irreversible reduction of the aryldiazonioum salt was observed at $E_{p,c}$ = 0.17 V vs. SCE. Hence, if the diazonium cation moiety were present in the spontaneously formed film, it would be observed in the cyclic voltammograms. The first scan in Figure 5.1 shows no peak due to the reduction of the diazonium cation moiety, hence it can be concluded that the diazonium cation moiety has reacted during the film formation process. However, it should be noted that the absence of the diazonium cation functionality in the film, while being a necessary condition for covalent attachment of the NP groups to the gold surface, is not alone sufficient evidence. The

result is consistent with covalent attachment of NP groups to gold, but also with the formation of a physisorbed film of NP dimers and oligormers.

5.3.2 Effect of Immersion Time on Surface Concentration of NP Groups

To investigate the effect of immersion time on the surface concentration of electro-active NP functionalities, multiple Au/NiCr/Si and Au/mica substrates were immersed in 10 mM NBD/0.1 M H_2SO_4 for times of 10, 30 60, 120 and 240 minutes. After sonication, NP reduction was examined at each surface in 0.1 M $NaClO_4$/EtOH-H_2O. The surface concentration of electro-active NP groups, Γ_{NP}, was determined for each of the samples, as described in Section 3.3.3.

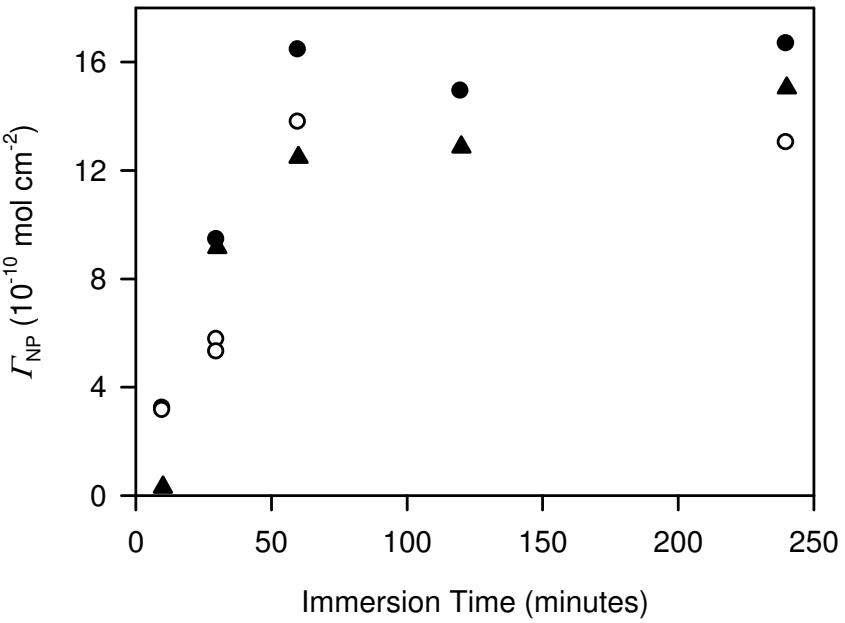

Figure 5.2. Plot of Γ_{NP} vs. immersion time in 10 mM NBD/0.1 M H_2SO_4 for Au/mica (○) and Au/NiCr/Si (●,▲) substrates. Each symbol shows the results of a separate set of experiments.

Figure 5.2 shows a plot of Γ_{NP} at Au/mica (○) and Au/NiCr/Si (●,▲) substrates vs. the immersion time used to achieve modification. Different symbols (○, ● and▲) denote experiments conducted on different days using different solutions of 10 mM NBD/0.1 M H_2SO_4. Γ_{NP} increases with immersion time up to ~60 minutes, where it reaches a maximum of ~14 × 10^{-}

^{10} mol cm^{-2} with no further significant changes up to 240 minutes immersion time. Hence, the surface concentration of electro-active NP groups appears to be limited at ~14 × 10^{-10} mol cm^{-2} under the conditions used.

A similar observation was made by previous workers who investigated the formation of NP films by electro-reduction of NBD at PPF in aqueous conditions at an applied potential 0.15 V to the negative of the NBD reduction peak.[23] In that study, a limiting surface concentration of ~6 × 10^{-10} mol cm^{-2} was reached after ~300 seconds electrolysis time. It was suggested that the films become self limiting when they reach a thickness at which electron transfer from the surface to the NBD in solution is no longer possible. This would prevent reduction of NBD and limit film growth. The fact that films formed spontaneously at gold also have a limiting surface concentration suggests that the spontaneous reaction occurs via electron transfer from the gold substrate to the NBD in solution. However, there are other possible explanations, as discussed below.

As discussed in Section 1.2, aryldiazonium salts are known to undergo thermal decomposition. Hence, it is possible that significant decomposition of NBD in solution over the first 60 minutes of the modification is responsible for limited film growth. To test this possibility, gold samples were immersed in 10 mM NBD/0.1 M H_2SO_4. After 60 minutes the samples were transferred to freshly prepared solutions of NBD and left for a further 180 minutes. The surface concentrations of NP groups were determined (by cyclic voltammetry) to be 12-14 × 10^{-10} mol cm^{-2}, the same as those for samples immersed in a single NBD solution for 60 to 240 minutes, indicating that the surface concentration is not limited by depletion of NBD in solution.

Another possible explanation for the apparently limiting surface concentration is that any NP groups that attach to the film after 60 minutes immersion cannot be detected by cyclic voltammetry. This could occur, for example, if groups that attached after 60 minutes are too far from the surface for effective electron transfer, or if they prevent (for example, by inhibiting ion diffusion) the reduction of groups attached earlier. These possibilities were investigated by immersing a Au/NiCr/Si substrate in 5 mL of 10 mM NBD/0.1 M H_2SO_4 for 60 minutes then adding 100 μL of 1 M hypophosphorous acid, which is known to reduce diazonium salts to aryl

radicals, leading to film growth without the requirement of electron donation from the surface.[24-28] After addition of the hypophosphorous acid and immersion for an additional 180 minutes, the NP surface concentration was determined by cyclic voltammetry to be 51×10^{-10} mol cm^{-2}. This clearly indicates that surface concentrations above the $\sim 14 \times 10^{-10}$ mol cm^{-2} limit would be detected. These results provide strong evidence that the NP films formed at gold by spontaneous reaction with NBD are genuinely self limiting; and they also provide indirect evidence that the reaction takes place by electron transfer from the gold surface to the NBD in solution.

5.3.3 XPS Characterization of NP and Reduced NP Films

The compositions of NP films and electro-reduced NP films were investigated using x-ray photoelectron spectroscopy (XPS). Two samples were prepared by immersing Au/NiCr/Si in 10 mM NBD/0.1 M H_2SO_4 for 240 minutes. One sample was subsequently electro-reduced in 0.1 M $NaClO_4$/EtOH-H_2O as described above. XPS analysis was carried out on both the reduced and the unreduced sample by recording narrow scans in the nitrogen 1s region.

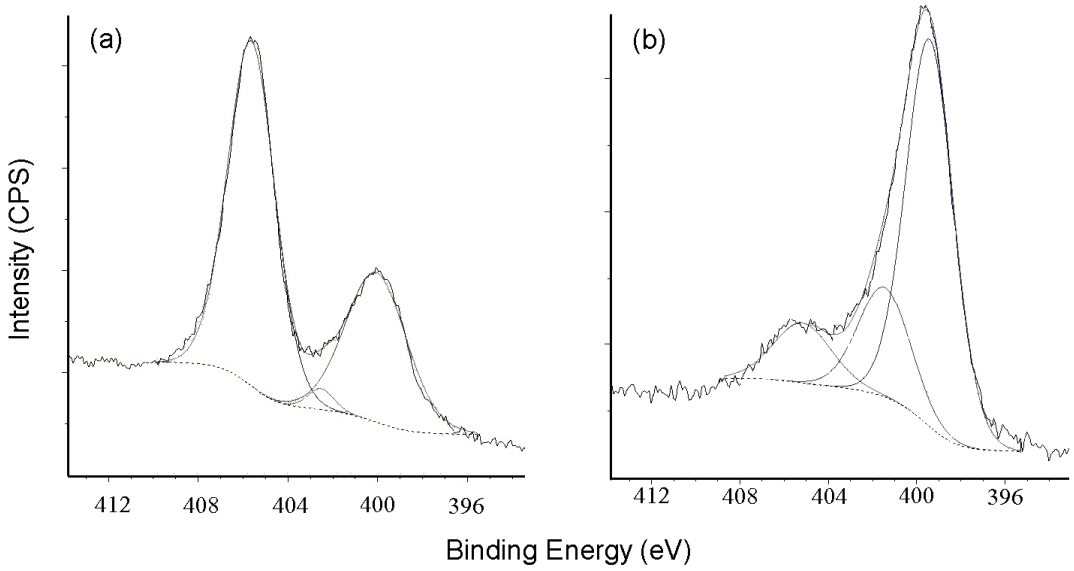

Figure 5.3. N1s core level spectra obtained at Au/NiCr/Si surfaces after immersion in NBD solution for 240 min (a) and after the same surface modification followed by reduction (two scans between 0.6 and -1.2V) in 0.1 M $NaClO_4$/EtOH-H_2O (b).

Figure 5.3 shows N1s core level spectra of the unreduced NP-modified gold (a) and the electro-reduced NP-modified gold (b). The spectrum of the unreduced NP film shows a strong signal at 405.6 eV, which is assigned to the NP nitrogen.[29] Another strong signal, at 400.1 eV, is assigned to the azo linkages[29] which are produced during film formation[29-31] and are discussed in Section 1.3.1 of this thesis. The relative peak areas indicate that 35 % of the total film nitrogen is present in the azo linkages. Yu et al. showed that 34-42 % of the total nitrogen of NP films prepared electrochemically at GC is present in the form of azo linkages.[29] Hence, NP films prepared spontaneously at gold have similar azo contents to those prepared electrochemically at GC. Since there are two nitrogen atoms per azo linkage, Spectrum 5.3 (a) indicates that 28 % of the NP groups present in the film have an azo linkage associated with them. The weak signal observed at 402.6 eV is assigned to a trace amount of hydroxyaminophenyl groups produced during film growth, and has also been observed for NP films prepared electrochemically at carbon.[29] Importantly, no peaks were observed at 403.8 and 405.1 eV, which would have been expected in the presence of unreacted diazonium cations.[32] This supports the electrochemical evidence (presented above) that the diazonium cation moiety has reacted during film formation.

The XPS spectrum of the reduced NP film (Figure 5.3 (b)) shows peaks at 399.4, 401.5 and 405.2 eV. The 399.4 eV peak is assigned to overlapping contributions from both azo groups and aminophenyl groups produced by electro-reduction of NP. The peak at 402.1 eV is assigned to hydroxylaminophenyl groups present in the film after electro-reduction, and the peak at 405.2 eV to NP groups that are electro-inactive, and hence, are not reduced during the cyclic voltammetry. After subtracting the 35 % azo groups contribution from the signal at 399.4 eV the relative concentrations of aminophenyl, hydroxyaminophenyl, and NP groups present in the reduced NP film were calculated to be 52 %, 31 % and 17 % respectively. Since 17 % of the NP groups are electro-inactive, the NP surface concentration determined by electro-reduction will be a corresponding underestimation. Yu et al. have detected the presence of similar amounts of electro-inactive NP groups for films formed on carbon by electro-reduction of NBD.[29] The fact that NP films prepared spontaneously at gold have azo and electro-inactive NP contents that are similar to those for films prepared electrochemically at carbon provides further evidence that the compositions of the two films are similar.

5.3.4 AFM Film Thickness Measurements

Atomic force microscopy (AFM) film thickness measurements were carried out on the NP modified Au/mica samples prepared and analyzed as described in Section 5.3.2. Figure 5.4 shows a plot of film thickness vs. immersion time in 10 mM NBD/0.1 M H_2SO_4.

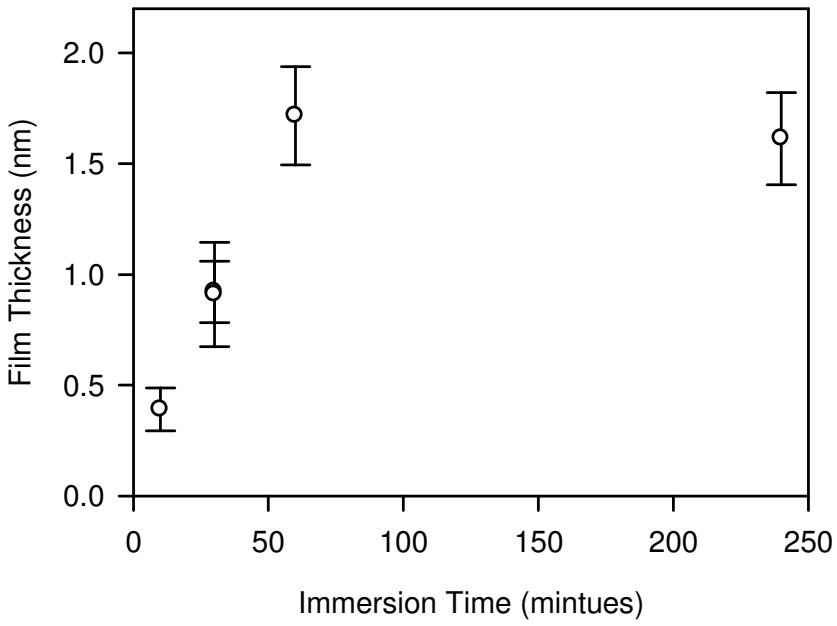

Figure 5.4. Plot of film thickness of NP modified Au/mica vs. immersion time in 10 mM NBD/0.1 M H_2SO_4. Note there are two nearly coincident datum points at 30 minutes immersion time.

The film thickness is seen to increase with immersion time reaching a maximum of approximately ~1.7 nm after 60 minutes, after which no further increase in thickness is observed. The trend is qualitatively similar to that in Figure 5.2, which shows an increase in surface concentration with immersion time, reaching a maximum at ~60 minutes. Hence the film thickness data support the electrochemical data, suggesting that the films become self limiting after ~60 minutes immersion time. Based on the theoretical length of the NP moiety (0.79 nm, calculated using Spartan)[23] the maximum film thickness of 1.7 nm indicates that multilayer films are formed. These results are in good agreement with those of Combellas and coworkers who determined the thicknesses of diazonium cation derived NP and *p*-bromophenyl films,

spontaneously prepared at gold under similar conditions, to be 1.3 and 1.7 nm, respectively, using ellipsometry.[21]

5.3.5 Packing Density of NP Films

Plotting the surface concentration of electro-active NP groups against the corresponding film thickness gives information concerning the structural uniformity and packing density of the films. Figure 5.5 shows a plot of the surface concentration of electro-active NP groups, Γ_{NP}, on Au/mica (prepared and analyzed as described in Section 5.3.2) vs. the film thickness (from Section 5.3.4).

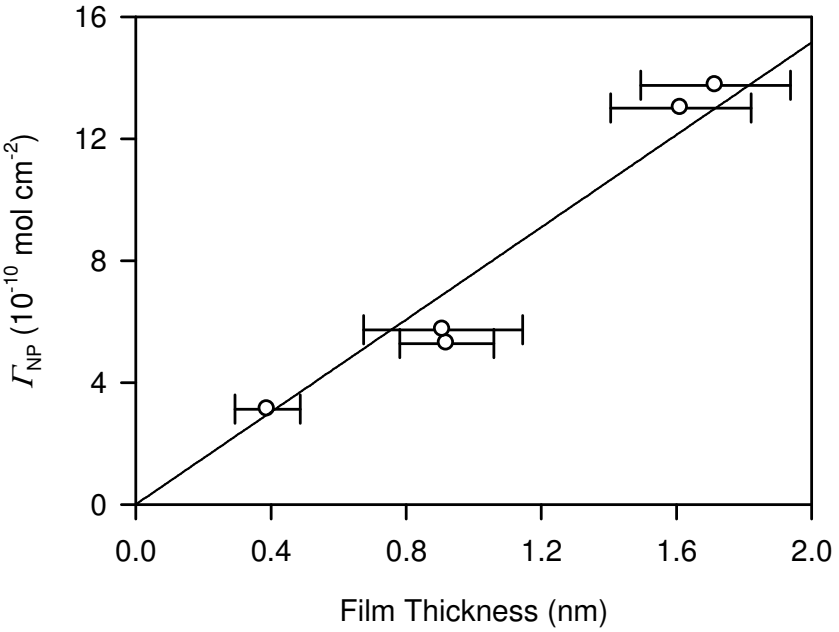

Figure 5.5. Plot of Γ_{NP} vs. film thickness for NP films spontaneously prepared at Au/mica. Regression line forced through origin with slope = (7.6 ± 0.43) $\times 10^{-10}$ mol cm^{-2} nm^{-1}. R^2 = 0.94. The error of the slope is given as two standard deviations.

The linear relationship between the film thickness and surface concentration indicates that spontaneously formed NP films on Au/mica are, on average, uniformly structured. From the slope of the regression line, the density of electro-active NP groups was determined to be (7.6 ± 0.4) × 10^{-10} mol cm^{-2} nm^{-1}. This corresponds to a packing density of (6.0 ± 0.3) × 10^{-10} mol cm^{-2}

per monolayer thickness. Considering that the theoretical value for a close-packed monolayer of NP groups on a flat surface is 12×10^{-10} mol cm^{-2}, it can be concluded that the films are loosely packed multilayers. In Section 5.3.3, ~17 % of NP units in the films were determined to be electro-inactive, so the total packing density of (electro-active and electro-inactive) NP groups is $(7.2 \pm 0.4) \times 10^{-10}$ mol cm^{-2} per monolayer thickness, which still indicates that loosely packed multilayers are formed. A similar conclusion was reached for NP films spontaneously prepared at carbon (Section 4.4.2), which have a packing density of $(3.3 \pm 0.3) \times 10^{-10}$ mol cm^{-2} per monolayer thickness. Furthermore, Brooksby et al. reported the formation of loosely packed multilayers with a packing density of $(2.5 \pm 0.5) \times 10^{-10}$ mol cm^{-2} per monolayer thickness upon electrochemical modification of carbon with NP films.[23] The higher effective packing densities reported here for NP films on gold could be due to differences in the surface roughness and the density of binding sites available on the substrate. Incorporation of physisorbed material into the film would also be expected to bring about an increase in film density (see Section 5.5.2).

5.4 Role of the Gold Surface in NP Film Formation Process

As discussed in Section 5.3, NP films formed by the spontaneous reaction of gold with NBD appear to have limiting surface concentrations and thicknesses. It was suggested above that a film become self limiting when it reaches a thickness at which spontaneous electron transfer through the film is no longer possible. This prevents the further generation of aryl radicals, and hence causes film growth to cease. In this section experiments are conducted to provide direct evidence of electron transfer from the gold surface to species (such as NBD) in solution.

5.4.1 OCP Behavior during NP Film Formation

Figure 5.6 shows a cyclic voltammogram of a Au/NiCr/Si substrate recorded in 1 mM NBD/0.1 M H_2SO_4. The OCP of the gold (vertical band, taken from Figure 5.7 after 60 minutes equilibration) is seen to be significantly on the negative side of the peak assigned to the reduction

of NBD. Hence the gold surface would be expected to reduce NBD at OCP under the conditions used.

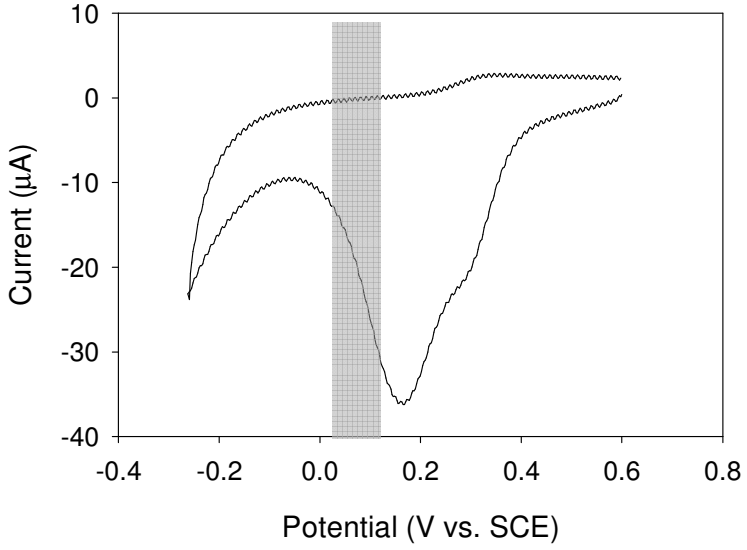

Figure 5.6. Electrochemical reduction of 1 mM NBD at a Au/NiCr/Si working electrode in 0.1 M H_2SO_4; scan rate = 100 mV s^{-1}. The range of OCP values of Au/NiCr/Si after 60 minutes equilibration is shown by the vertical band (see Figure 5.7).

To gain more direct evidence of electron transfer from the gold substrate to the NBD in solution, an Au/NiCr/Si substrate was immersed in 10 mL of 0.1 M H_2SO_4 and its OCP was monitored using an SCE reference electrode. After 60 minutes of "equilibration" a relatively stable OCP was reached and 10 mL of 20 mM NBD/0.1 M H_2SO_4 was added, resulting in a 10 mM solution of NBD. The OCP of the gold was then monitored for a further 240 minutes. Two control experiments were also carried out: one by adding 10 mL of 0.1 M H_2SO_4 (no NBD) after equilibration, and the second by adding 10 mL of a 20 mM solution of *p*-nitroaniline after equilibration. This second control experiment was conducted to test the effect on the OCP of a molecule that is structurally similar to NBD, but does not have diazonium cation functionality.

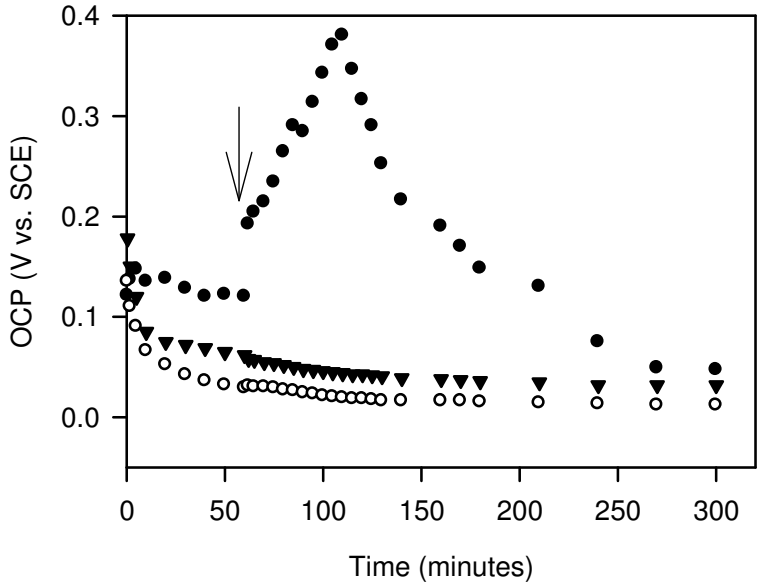

Figure 5.7. Plot of OCP vs. immersion time in 0.1 M H_2SO_4 for three different gold electrodes. After an equilibration period of 60 minutes a 10 mL solution of 20 mM NBD/0.1 M H_2SO_4 (●), 20 mM p-nitroaniline/ 0.1 M H_2SO_4 (▼), or 0.1 M H_2SO_4 (○) were each added to the solution of one of the three electrodes.

Figure 5.7 shows the effect of each of the additions on the OCP of the gold electrodes. When "blank" 0.1 M H_2SO_4 or *p*-nitroaniline is added (○ and ▲, respectively) no significant change in OCP is observed. However, upon addition of NBD (●) at 60 minutes immersion time (↓) the OCP is seen to jump from 0.13 to 0.19 V and then increase more slowly to a maximum of 0.39 V after 60 minutes; after this maximum the OCP decreases over the next 180 minutes. The fact that the increase in OCP is observed upon addition of NBD, but not *p*-nitroaniline, indicates that the diazonium cation substituent is associated with the increase.

An increase in OCP is consistent with the accumulation of positive charge on the surface, which would be expected if reduction of diazonium cation occurs via electron transfer from the gold substrate. Hence, it is proposed that the gold substrate reduces the diazonium cations, leading to the generation of an aryl radicals and film growth. As the film continues to grow for 60 minutes, the accumulation of positive charge on the surface results in a rise of the OCP. After 60 minutes the film reaches a thickness at which it inhibits electron transfer, and hence, both the increase in OCP, and (significant) film growth, cease. An increase in the OCP of a gold electrode upon

addition of sodium nitrite to a *p*-phenylenediamine solution (which results in the in situ formation of *p*-aminobenzene diazonium cations) was also observed by Bèlanger and coworkers.[33] However, they did not monitor the OCP for an extended period and did not report a discharge process (see below).

In another experiment using ACN/0.1 M $[Bu_4N]BF_4$ rather than 0.1 M H_2SO_4, no significant changes were seen in the OCP of the gold (vs. Ag wire) upon addition of NBD, *p*-nitroaniline or 0.1 M $[Bu_4N]BF_4$. This is consistent with the result in Section 5.3.1, where it was found that no significant spontaneous reaction of NBD with gold occurs in ACN.

The decay of the OCP that starts 60 minutes after the addition of NBD corresponds to a loss of positive charge by the surface, i.e., a discharge process. Porter and coworkers observed a discharge process (though in the opposite direction) when studying the OCP of gold during its reaction with butanethiol, and assigned it to a chemical process.[34] If (as proposed here) the spontaneous reaction of NBD with gold proceeds via electron transfer, then the gold is (in effect) oxidized. The "discharge" process could then involve the formation of gold oxidation products, brought about by the rise in OCP and the build-up of positive charge on the gold surface. Therefore, further experiments were conducted (Sections 5.4.2 and 5.4.3) to test for the presence of gold oxidation products.

5.4.2 Electrochemical Investigation of Gold Oxide Formation

Stable oxide layers form on the surfaces of most metals under ambient conditions. Gold is not typical in this sense; being a relatively inert metal it does not undergo oxidation under ambient conditions. However, the electrochemically induced oxidation of gold to gold oxide is known to occur upon application of a positive potential to a gold electrode in aqueous conditions.[35-39] Equation 5.1 shows the accepted reaction scheme for the electrochemically induced formation of gold oxide. The scheme for the corresponding reduction of the gold oxide is given by Equation 5.2, where subscript '(sur)' indicates a surface species.[39]

$$Au.H_2O(sur) + 2H_2O \leftrightarrow (Au(OH)_3)(sur) + 3H^+ + 3e^- \quad (5.1)$$

$$Au(OH)_3(sur) + 3e^- \rightarrow Au(sur) + 3OH^- \quad (5.2)$$

In Figure 5.8, the dashed curve (---) shows the gold oxide redox system in 0.1 M H_2SO_4 at an Au/NiCr/Si electrode. The oxidation peak at ~1.1 V and reduction peak at ~0.7 V, are assigned to gold oxide formation (Equation 5.1) and reduction (Equation 5.2), respectively.

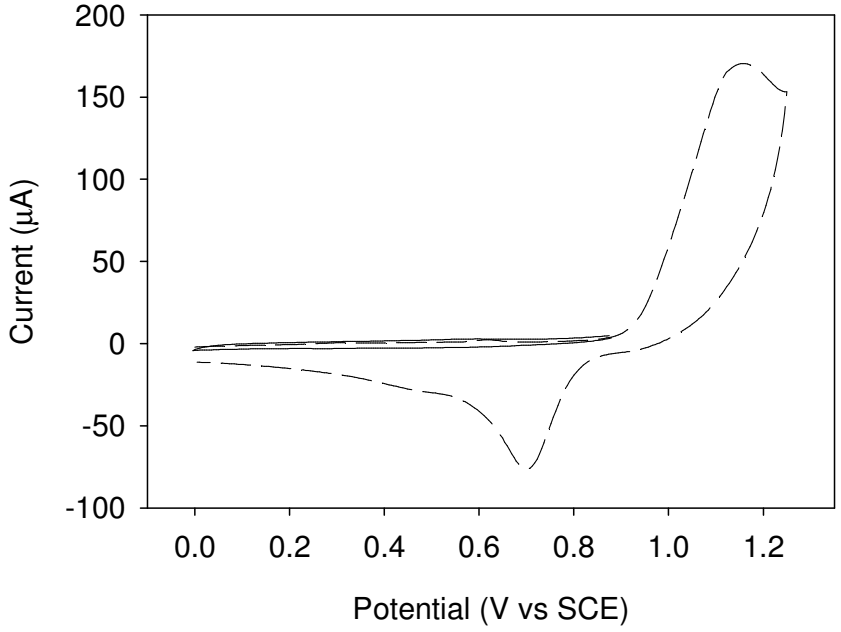

Figure 5.8. Cyclic voltammograms of an Au/NiCr/Si electrode in 0.1 M H_2SO_4, before reaction with NBD (---), initial potential 0 V; and in 10 mM NBD/0.1 M H_2SO_4 after immersion in 10 mM NBD/0.1 M H_2SO_4 for 120 minutes (—), initial potential 0.9 V.

The formation of gold oxides could explain the decrease in OCP that is observed after the initial 60 minute period of film growth. Equation 5.3 shows a proposed scheme for the formation of gold oxides following the spontaneous oxidation of gold by NBD. Under this scheme, as the gold reduces NBD, positive charge builds up on the gold surface and the OCP rises. Subsequently, an interaction between positively charged gold species (Au_n^{x+}(sur) in Equation 5.3) and water molecules results in the formation of gold oxide and loss of positive charge in the form of H^+. The loss of positive charge is observed as a decrease in the OCP.

$$Au_n^{x+}(sur) + xnH_2O \leftrightarrow (Au(OH)_x)_n(sur) + xnH^+ \qquad (5.3)$$

This possibility was explored by using cyclic voltammetry to test for the presence of gold oxides after spontaneous modification. Having established the precise positions of the gold redox peaks as in Figure 5.8 (---), 10 mM NBD/0.1 M H_2SO_4 was left to react with the gold surface of a Au/NiCr/Si electrode for 120 minutes under standard conditions. After this time a cyclic voltammogram was recorded by scanning between 0.9 and 0.0 V vs. SCE, from an initial potential of 0.9 V, with the results shown by the full curve (—) in Figure 5.7. The initial potential was chosen because it is sufficiently low to avoid the production of gold oxides during the scan, thereby avoiding the possibility of a false positive. It is also sufficiently positive to allow for observation of the reduction of any gold oxide that might have formed on the surface during spontaneous modification. No gold oxide reduction was observed. The experiment was repeated on another Au/NiCr/Si sample using a reaction time of 30 minutes with NBD rather than 120, but again no gold oxide reduction was observed after modification. Hence, there is no evidence that gold oxide is formed as an oxidation product during the spontaneous reaction of NBD with gold.

5.4.3 AAS Investigation of Gold Ion Formation

Another possible mechanism for the loss of positive charge is oxidative desorption of gold ions (Equation 5.4), which could occur at a sufficiently positive potential in aqueous conditions.

$$Au(s) \rightarrow Au^{3+}(sur) \rightarrow Au^{3+}(aq) \qquad (5.4)$$

To investigate this possibility, a high-surface-area (28 cm^2) gold electrode was prepared by crumpling gold wire into a small vial and the entire area was immersed in 2.5 mL of 10 mM NBD/0.1 M H_2SO_4 solution. After 240 minutes the wire was removed and the solution was analyzed for gold using atomic absorption spectroscopy (AAS). Two controls were also prepared and analyzed. In the first case, the gold wire was immersed in 2.5 mL of 0.1 M H_2SO_4 for 240 minutes; in the other, a blank was a solution of 10 mM NBD/0.1 M H_2SO_4 was analyzed

without having been in contact with the gold wire. (Note: the gold wire was cleaned with Piranha solution prior to each experiment).

The AAS results were compared with a calibration curve prepared using standards containing 100, 200, 400 and 600 ppb of gold ions. The analysis revealed ~20 ppb of gold in both blanks and in the sample. If each NP unit attached to the gold accepts one electron from the surface, then three attached NP units would account for the formation of one Au(III) ion. Hence, with the expected surface concentration of NP groups (14×10^{-10} mol cm^{-2}) under the conditions used, more than 1000 ppb of gold would be expected. Considering that the same concentrations of only 20 ppb were detected for the sample and the blanks, it can be concluded that any gold ions in solution are not the product of the spontaneous reaction of NBD with gold. Consequently, oxidative desorption is not responsible for the discharge process.

The results of sections 5.4.2 and 5.4.3 indicate that the discharge process does not involve oxide formation or oxidative gold ion desorption. Its origin remains unknown, but is tentatively attributed to the oxidation of solution impurities.

5.5 Stability of Spontaneously Prepared NP Films at Gold

Diazonium cation derived films at carbon are known to be very stable, owing to the strength of the C-C bond between the modifier and the surface. As discussed in Section 5.1, several studies have investigated the stability of diazonium cation derived films formed at gold by electro-reduction of diazonium salts. However, the stability of such films formed *spontaneously* at gold has not been studied. In this section the stability of NP films formed via spontaneous reaction of NBD with a gold surface is investigated and compared with the stability of the corresponding electrochemically prepared films.

5.5.1 Stability in Vacuum

To determine the stability of spontaneously prepared NP films at gold in vacuum, four Au/NiCr/Si substrates were immersed in 10 mM NBD/0.1 M H_2SO_4 for 60 minutes. After the standard post modification sonication procedure, two samples were subjected to a vacuum of 1×10^{-7} torr for 180 minutes while the other two samples served as controls. The surface concentrations of NP groups, determined using cyclic voltammetry as described in Section 5.3, were 11-14 $\times 10^{-10}$ mol cm^{-2} for the samples subject to vacuum and 13-14 $\times 10^{-10}$ mol cm^{-2} for the controls. Hence there was no evidence that the NP films are unstable in vacuum.

5.5.2 Stability to Sonication

The stability to extended sonication of spontaneously formed NP films prepared at gold was investigated and compared with NP films of similar surface concentrations generated by electrochemical reduction. Two spontaneously prepared films were prepared by immersing Au/NiCr/Si substrates in 10 mM NBD/0.1 M H_2SO_4 for 60 minutes. Another pair of NP films were formed by 10 minutes electro-reduction of 1 mM NBD in 0.1 M $[Bu_4N]BF_4$/ACN at a potential of -0.2 V vs. Ag wire. A third pair was prepared by electro-reduction of 1 mM NBD in 0.1 M H_2SO_4 by applying a potential of -0.25 V vs. SCE for 15 minutes. All samples were subjected to the standard post modification sonication procedure (5 minutes sonication in Milli Q water) and then one sample from each pair was sonicated in ACN for a further 30 minutes. The NP groups were electro-reduced and the corresponding surface concentrations were calculated as described in Section 5.3.

Table 5.1. Surface concentrations of film remaining on the surface after sonication procedures for films prepared spontaneously and electrochemically at Au/NiCr/Si substrates.

Film	Surface Concentration (10^{-10} mol cm^{-2})	
Preparation	5 minutes, H_2O	30 minutes, ACN
Electrochemically in ACN	10.9	4.3
Electrochemically in Aqueous	11.5	1.8
Spontaneously in Aqueous	11	1.9

Table 5.1 shows that, for all types of films, 30 minutes sonication in ACN removes a large amount of film material. However, substantially more material was removed from films prepared in aqueous conditions, both spontaneously (83 % removed) and electrochemically (84 % removed), than from the film prepared electrochemically in ACN (61 % lost). Hence, the medium used for film preparation, rather than the preparation method (electrochemical or spontaneous), appears to determine the stability of the films to sonication in ACN. As discussed in Section 5.1, other workers have found evidence of physisorbed material in diazonium cation derived films prepared electrochemically in ACN.[18] The present results suggest that films prepared in aqueous conditions have a higher proportion of physisorbed material than those prepared in ACN, possibly due to the lower solubility of aryl dimers and oligomers in aqueous solutions. Physisorbed material would be expected to block the attack of aryl radicals at the gold surface, leading to a lower surface concentration of the strongly bound material that can resist extended sonication.

An alternative explanation for the formation of less stable films in aqueous conditions is that the bonding of the aryl groups is predominant at different sites of the gold surface in the two media. As discussed in Section 5.1, McDermott and coworkers have suggested that different aryl-Au bond strengths are expected for different sites on the gold surface.[18] More specifically, they suggested that the more strongly bound film material was present at step sites, with more weakly (but still covalently) bound material at terrace sites.[18] The data presented in the current work could also be interpreted along these lines. It is possible that solvent effects or different surface reorganization in ACN brings about more binding to step sites than in aqueous conditions, leading to a larger number of strongly bound NP groups.

5.6 Spontaneous Modification of Gold with CP and MP Films

As discussed in Section 1.2, the ability of a substituent *para* to the diazonium cation moiety to donate or withdraw electrons affects the potential at which the diazonium cation moiety is reduced. Electron donating *para* substituents shift the potential in the negative direction while

electron withdrawing substituents shift the potential in the positive direction. If (as proposed above) spontaneous reaction takes place by reduction of the diazonium cation by the substrate, then it will proceed only if the potential at which the diazonium cation is reduced is sufficiently positive, in relation to the OCP of the surface, for reduction to occur.[40] NBD is reduced at a relatively positive potential compared to most aryldiazonium salts, owing to the electron withdrawing nature of the *para*-NO_2 substituent. However, there is a question as to whether the OCP of gold is sufficiently negative to reduce diazonium cations with other *para* substituents. Hence the potentials of the reduction peak of a number of diazonium salts were determined, and the spontaneous reaction of some of these diazonium salts with gold, at OCP, was investigated.

5.6.1 Potential of Reduction for Various Aryldiazonium Salts at Gold

The potentials of the reduction peaks for a number of different *para* substituted diazonium salts were investigated. This was achieved by recording cyclic voltammograms between ~0.5 and -0.5 V vs. SCE (initial potential 0.5 V) in the presence of 1 mM of the diazonium salt in 0.1 M H_2SO_4. The potential of the reduction peak was determined for benzenediazonium salts with *p*-NO_2, *p*-Br, *p*-F, *p*-CF3, *p*-CO_2H, and *p*-MeO substituents.

Table 5.2. Potentials of reduction peaks, $E_{p,c}$, for the diazonium moiety of *para*-substituted benzenediazonium salts. Cyclic voltammograms were recorded in 1mM diazonium salt/0.1 M H_2SO_4 at Au/NiCr/Si; scan rate = 100 mV s^{-1}.

Substituent	$E_{p,c}$ (V vs. SCE)
p-NO_2	0.15
p-Br	0.12
p-F	0.04
p-CF_3	0.00
p-CO_2H	-0.04
p-OMe	-0.11

As shown in Table 5.2, as the *para* substituent becomes more electron donating the potential of the diazonium cation reduction peak shifts more negative, with NBD (*p*-NO_2 in Table 5.2) being the "most easily" reduced of the diazonium salts investigated here. In this section, the spontaneous reactions of *p*-methoxybenzene diazonium salt (*p*-MeO; MBD) and *p*-carboxybenzene diazonium salt (*p*-CO_2H; CBD) with gold were investigated since they are the

"most difficult" to reduce. If the spontaneous reaction proceeds with these reagents, it would be expected to proceed for the large number of diazonium salts that are reduced at more positive potentials. CBD is also of interest since it gives CP-containing layers that can be used for attachment of further molecules via coupling reactions.

In Figure 5.9, the cyclic voltammograms of CBD (a) and MBD (b) are compared to the OCP of Au/NiCr/Si in 0.1 M H_2SO_4 (vertical bands, obtained from Figure 5.7) after 60 minutes immersion time.

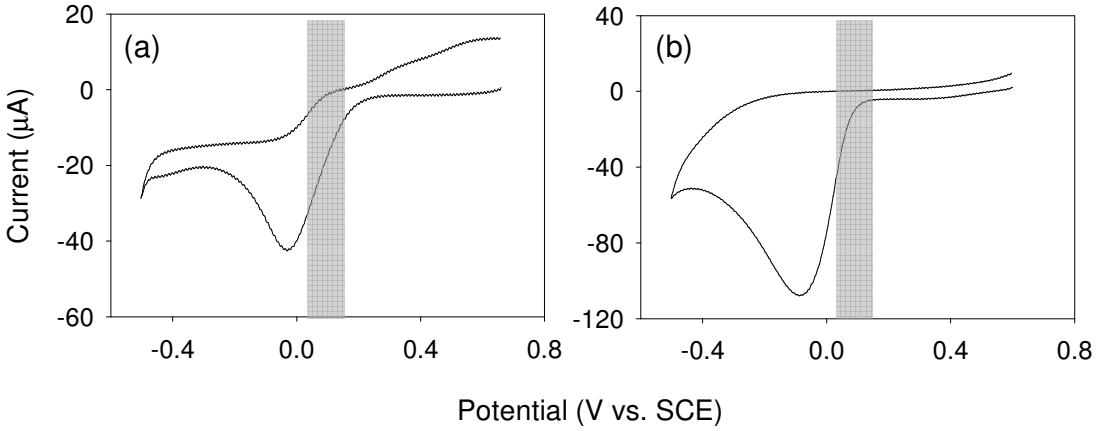

Figure 5.9. Electrochemical reduction of 1 mM CBD (a) and 1 mM MBD (b) at a Au/NiCr/Si working electrode in 0.1 M H_2SO_4; scan rate = 100 mV s^{-1}. The range of OCP values of Au/NiCr/Si after 60 minutes equilibration are shown by the vertical bands (see Figure 5.7).

In the case of CBD, the OCP range falls entirely to the negative of the high-potential edge (~0.2 V) of the reduction peak. Hence, the gold substrate would be expected to reduce CBD at OCP. For MBD, the high-potential edge of the reduction peak (~0.1 V) is in the centre of the OCP range.

5.6.2 Spontaneous Modification of Gold with CP Films

Three Au/NiCr/Si substrates were immersed in 10 mM CBD/0.1 M H_2SO_4 for 240 minutes. Two controls were prepared by immersing Au/NiCr/Si substrates in 0.1 M H_2SO_4 for the same period

of time. After the standard post modification sonication procedure, the water contact angles were found to be (36 ± 6) º for samples immersed in CBD solution compared to (67 ± 6) º for the controls. The smaller contact angle for the samples immersed in CBD is consistent with the presence of hydrophilic CP groups at the surface, and indicates that modification was successful, as expected from the comparison of the CBD reduction peak and gold OCP values (Figure 5.9 (a)).

5.6.3 Spontaneous Modification of Gold with MP Films

Three Au/NiCr/Si substrates were immersed in 10 mM MBD/0.1 M H_2SO_4 for 240 minutes. After the standard post modification sonication procedure, the water contact angles of the samples were found to be (60± 7) º. The difference from the value of (67 ± 6) º for the controls is not statistically significant, and hence, the contact angle measurements provided no evidence for modification.

Ferricyanide ($Fe(CN)_6^{3-}$) redox-probe voltammetry was carried out on the samples that had been immersed in MBD to look for evidence of a passivating *p*-methoxyphenyl (MP) film. The $Fe(CN)_6^{3-/4-}$ response was highly irreproducible; some cyclic voltammograms were essentially the same as those recorded at bare gold ($\Delta E_p \approx 0.17$ V), while others showed larger peak separations and still others showed no evidence of the $Fe(CN)_6^{3-/4-}$ redox response. This suggests that MP film formation was highly variable from sample to sample, which can be attributed to variations in the base OCP of the individual gold surfaces in comparison with the MBD reduction potential. As predicted by the comparison of the MBD reduction peak and the gold OCP range (Figure 5.9 (b)), it appears that some gold substrates have an OCP sufficiently low to reduce MBD while others do not.

5.7 Conclusion

The spontaneous reaction of aryldiazonium salts with gold surfaces was investigated using NBD. NP films were formed when modification was carried out in aqueous conditions, but not when it was attempted in ACN. This is consistent with the results found at PPF, and may arise from a higher OCP of gold in ACN than in aqueous conditions or from the requirement for an adsorption step prior to modification (see Section 4.4). Other workers have reported the spontaneous modification of gold in ACN, but only with much longer immersion times than used here, and with significantly lower surface concentrations than for the films formed in aqueous conditions in the present work.[22]

NP films prepared spontaneously at gold were found to be similar to those formed at carbon. XPS measurements indicated that films formed at gold have a similar percentage (~28 %) of azo groups per NP groups and a similar proportion (~17 %) of electro-inactive NP groups to those formed by electrochemical induction at carbon.[29] Furthermore, AFM measurements indicate that the films are loosely packed multilayers up to approximately 2-3 monolayers thick. The packing density of NP groups was found to be ~6 × 10^{-10} mol cm^{-2} per monolayer thickness, approximately twice those of NP films formed at carbon, both spontaneously (Section 4.4) and electrochemically.[23] This could be due to the incorporation of more physisorbed material in the films formed at gold than those prepared at carbon. Stability tests indicated that significant amounts (~80 %) of film material is lost upon extended sonication in ACN. Similar results were found for NP films prepared in aqueous conditions by electrochemical induction at gold, while those prepared electrochemically in ACN showed considerably better stability. In light of these results, it might reasonably be expected that films formed spontaneously in ACN would also exhibit the relatively high stability of their electrochemically prepared counterparts. However, the spontaneous reaction in ACN leads to very low surface concentrations, even at long immersion times, and hence it is likely that there would be a lower final concentration on the surface than for the films spontaneously prepared in aqueous conditions, even after extended sonication. While incorporation of more physisorbed material in the film is one possible cause of the relatively low stability of films formed at gold in aqueous conditions compared to those formed in ACN, different surface rearrangement in the two media, leading to different binding

sites, is also possible.[18] Whatever the cause, the low stability will limit the potential applications of the films, and points to one clear advantage of using carbon substrates. However, it is worth noting that surface concentrations of spontaneously prepared films were much more reproducible at gold than at carbon. This allowed for a more successful investigation into the nature of the film growth process, and the mechanism of film formation.

Despite the doubts of previous workers,[21] considerable evidence is presented here that spontaneous modification of gold using aryldiazonium salts proceeds via reduction of the diazonium cation by the substrate. Firstly, the surface concentrations and film thicknesses are shown to be self-limiting, indicating the ability of the surface to donate electrons to the NBD in solution is required for film growth. Secondly, the OCP of the surface is seen to increase upon addition of diazonium salts, consistent with electron transfer from the substrate to the diazonium in solution. Thirdly, modification does not occur reliably if the OCP of the gold is higher than the high-potential edge of the diazonium cations reduction peak. One consequence of the proposed mechanism is that spontaneous modification will be possible only using diazonium salts whose reduction potentials are sufficiently positive. However, many useful diazonium salts (e.g., NBD and CBD) fall into this category.

5.8 References

1. Nuzzo, R. G.; Allara, D. L., Adsorption of Bifunctional Organic Disulfides on Gold Surfaces. *J. Am. Chem. Soc.* **1983,** 105, 4481-4483.
2. Schreiber, F., Structure and growth of self-assembling monolayers. *Prog. Surf. Sci.* **2000,** 65, 151-256.
3. Laforgue, A.; Addou, T.; Belanger, D., Characterization of the deposition of organic molecules at the surface of gold by the electrochemical reduction of aryldiazonium cations. *Langmuir* **2005,** 21, 6855-6865.
4. Liu, G. Z.; Liu, J. Q.; Bocking, T.; Eggers, P. K.; Gooding, J. J., The modification of glassy carbon and gold electrodes with aryl diazonium salt: The impact of the electrode materials on the rate of heterogeneous electron transfer. *Chem. Phys.* **2005,** 319, 136-146.
5. Love, J. C.; Estroff, L. A.; Kriebel, J. K.; Nuzzo, R. G.; Whitesides, G. M., Self-assembled monolayers of thiolates on metals as a form of nanotechnology. *Chem. Rev.* **2005,** 105, 1103-1169.
6. Liu, G. Z.; Bocking, T.; Gooding, J. J., Diazonium salts: Stable monolayers on gold electrodes for sensing applications. *J. Electroanal. Chem.* **2007,** 600, 335-344.
7. Bain, C. D.; Evall, J.; Whitesides, G. M., Formation of Monolayers by the Coadsorption of Thiols on Gold - Variation in the Head Group, Tail Group, and Solvent. *J. Am. Chem. Soc.* **1989,** 111, 7155-7164.
8. Laibinis, P. E.; Nuzzo, R. G.; Whitesides, G. M., Structure of Monolayers Formed by Coadsorption of 2 Normal-Alkanethiols of Different Chain Lengths on Gold and Its Relation to Wetting. *J. Phys. Chem.* **1992,** 96, 5097-5105.
9. Lahann, J.; Mitragotri, S.; Tran, T. N.; Kaido, H.; Sundaram, J.; Choi, I. S.; Hoffer, S.; Somorjai, G. A.; Langer, R., A reversibly switching surface. *Science* **2003,** 299, 371-374.
10. Delamarche, E.; Michel, B.; Kang, H.; Gerber, C., Thermal-Stability of Self-Assembled Monolayers. *Langmuir* **1994,** 10, 4103-4108.
11. Ricci, A.; Bonazzola, C.; Calvo, E. J., An FT-IRRAS study of nitrophenyl mono- and multilayers electro-deposited on gold by reduction of the diazonium salt. *Phys. Chem. Chem. Phys.* **2006,** 8, 4297-4299.

12. Harper, J. C.; Polsky, R.; Dirk, S. M.; Wheeler, D. R.; Brozik, S. M., Electroaddressable selective functionalization of electrode arrays: Catalytic NADH detection using aryl diazonium modified gold electrodes. *Electroanalysis* **2007,** 19, 1268-1274.

13. Paulik, M. G.; Brooksby, P. A.; Abell, A. D.; Downard, A. J., Grafting aryl diazonium cations to polycrystalline gold: Insights into film structure using gold oxide reduction, redox probe electrochemistry, and contact angle behavior. *J. Phys. Chem. C* **2007,** 111, 7808-7815.

14. Benedetto, A.; Balog, M.; Viel, P.; Le Derf, F.; Salle, M.; Palacin, S., Electro-reduction of diazonium salts on gold: Why do we observe multi-peaks? *Electrochim. Acta* **2008,** 53, 7117-7122.

15. Haccoun, J.; Vautrin-Ul, C.; Chausse, A.; Adenier, A., Electrochemical grafting of organic coating onto gold surfaces: Influence of the electrochemical conditions on the grafting of nitrobenzene diazonium salt. *Prog. Org. Coat.* **2008,** 63, 18-24.

16. Harper, J. C.; Polsky, R.; Wheeler, D. R.; Lopez, D. M.; Arango, D. C.; Brozik, S. M., A Multifunctional Thin Film Au Electrode Surface Formed by Consecutive Electrochemical Reduction of Aryl Diazonium Salts. *Langmuir* **2009,** 25, 3282-3288.

17. Kullapere, M.; Marandi, M.; Sammelselg, V.; Menezes, H. A.; Maia, G.; Tammeveski, K., Surface modification of gold electrodes with anthraquinone diazonium cations. *Electrochem. Commun.* **2009,** 11, 405-408.

18. Shewchuk, D. M.; McDermott, M. T., Comparison of Diazonium Salt Derived and Thiol Derived Nitrobenzene Layers on Gold. *Langmuir* **2009,** 25, 4556-4563.

19. de la Llave, E.; Ricci, A.; Calvo, E. J.; Scherlis, D. A., Binding between Carbon and the Au(111) Surface and What Makes It Different from the S-Au(111) Bond. *J. Phys. Chem. C* **2008,** 112, 17611-17617.

20. Fan, F. R. F.; Yang, J. P.; Dirk, S. M.; Price, D. W.; Kosynkin, D.; Tour, J. M.; Bard, A. J., Determination of the molecular electrical properties of self-assembled monolayers of compounds of interest in molecular electronics. *J. Am. Chem. Soc.* **2001,** 123, 2454-2455.

21. Podvorica, F. I.; Kanoufi, F.; Pinson, J.; Cornbellas, C., Spontaneous grafting of diazoates on metals. *Electrochim. Acta* **2009,** 54, 2164-2170.

22. Fan, F. R. F.; Yang, J. P.; Cai, L. T.; Price, D. W.; Dirk, S. M.; Kosynkin, D. V.; Yao, Y. X.; Rawlett, A. M.; Tour, J. M.; Bard, A. J., Charge transport through self-assembled monolayers of compounds of interest in molecular electronics. *J. Am. Chem. Soc.* **2002,** 124, 5550-5560.

23. Brooksby, P. A.; Downard, A. J., Electrochemical and atomic force microscopy study of carbon surface modification via diazonium reduction in aqueous and acetonitrile solutions. *Langmuir* **2004,** 20, 5038-5045.

24. Kornblum, N.; Cooper, G. D.; Taylor, J. E., The Chemistry of Diazo Compounds .2. Evidence for a Free Radical Chain Mechanism in the Reduction of Diazonium Salts by Hypophosphorous Acid. *J. Am. Chem. Soc.* **1950,** 72, 3013-3020.

25. Wildgoose, G. G.; Pandurangappa, M.; Lawrence, N. S.; Jiang, L.; Jones, T. G. J.; Compton, R. G., Anthraquinone-derivatised carbon powder: reagentless voltammetric pH electrodes. *Talanta* **2003,** 60, 887-893.

26. Abiman, P.; Wildgoose, G. G.; Compton, R. G., Investigating the mechanism for the covalent chemical modification of multiwalled carbon nanotubes using aryl diazonium salts. *Int. J. Electrochem. Sci.* **2008,** 3, 104-117.

27. Toupin, M.; Belanger, D., Spontaneous functionalization of carbon black by reaction with 4-nitrophenyldiazonium cations. *Langmuir* **2008,** 24, 1910-1917.

28. Smith, R. D. L.; Pickup, P. G., Voltammetric quantification of the spontaneous chemical modification of carbon black by diazonium coupling. *Electrochim. Acta* **2009,** 54, 2305-2311.

29. Yu, S. S. C.; Tan, E. S. Q.; Jane, R. T.; Downard, A. J., An electrochemical and XPS study of reduction of nitrophenyl films covalently grafted to planar carbon surfaces *Langmuir* **2008,** 24, 7038-7038.

30. Saby, C.; Ortiz, B.; Champagne, G. Y.; Belanger, D., Electrochemical modification of glassy carbon electrode using aromatic diazonium salts .1. Blocking effect of 4-nitrophenyl and 4-carboxyphenyl groups. *Langmuir* **1997,** 13, 6805-6813.

31. Doppelt, P.; Hallais, G.; Pinson, J.; Podvorica, F.; Verneyre, S., Surface modification of conducting substrates. Existence of azo bonds in the structure of organic layers obtained from diazonium salts. *Chem. Mater.* **2007,** 19, 4570-4575.

32. Finn, P.; Jolly, W. L., Nitrogen 1s Binding-Energies of Some Azide, Dinitrogen, and Nitride Complexes of Transition-Metals. *Inorg. Chem.* **1972,** 11, 1434-1440.

33. Lyskawa, J.; Belanger, D., Direct modification of a gold electrode with aminophenyl groups by electrochemical reduction of in situ generated aminophenyl monodiazonium cations. *Chem. Mater.* **2006,** 18, 4755-4763.

34. Zhong, C. J.; Woods, N. T.; Dawson, G. B.; Porter, M. D., Formation of thiol-based monolayers on gold: implications from open circuit potential measurements. *Electrochem. Commun.* **1999,** 1, 17-21.

35. Angersteinkozlowska, H.; Conway, B. E.; Hamelin, A.; Stoicoviciu, L., Elementary Steps of Electrochemical Oxidation of Single-Crystal Planes of Au .1. Chemical Basis of Processes Involving Geometry of Anions and the Electrode Surfaces. *Electrochim. Acta* **1986,** 31, 1051-1061.

36. Angersteinkozlowska, H.; Conway, B. E.; Hamelin, A.; Stoicoviciu, L., Elementary Steps of Electrochemical Oxidation of Single-Crystal Planes of Au .2. a Chemical and Structural Basis of Oxidation of the (111) Plane. *J. Electroanal. Chem.* **1987,** 228, 429-453.

37. Hamelin, A., Cyclic voltammetry at gold single-crystal surfaces .1. Behaviour at low-index faces. *J. Electroanal. Chem.* **1996,** 407, 1-11.

38. Hamelin, A.; Martins, A. M., Cyclic voltammetry at gold single-crystal surfaces .2. Behaviour of high-index faces. *J. Electroanal. Chem.* **1996,** 407, 13-21.

39. Juodkazis, K.; Juodkazyte, J.; Sebeka, B.; Lukinskas, A., Cyclic voltammetric studies on the reduction of a gold oxide surface layer. *Electrochem. Commun.* **1999,** 1, 315-318.

40. Adenier, A.; Barre, N.; Cabet-Deliry, E.; Chausse, A.; Griveau, S.; Mercier, F.; Pinson, J.; Vautrin-Ul, C., Study of the spontaneous formation of organic layers on carbon and metal surfaces from diazonium salts. *Surf. Sci.* **2006,** 600, 4801-4812.

Chapter 6. Patterning Surfaces by Microcontact Printing Using Aryldiazonium Salts

6.1 Introduction

Many of the envisaged applications of modified surfaces require molecular level patterning whereby only certain, well defined, regions of the surface are modified.[1] The patterning of surfaces with specific chemical functionalities can be achieved by soft-lithography. "Soft lithography" refers to a group of techniques for patterning surfaces using elastomeric stamps or molds. The elastomeric stamps and molds are prepared by casting a liquid pre-polymer onto a patterned hard master, which is generally fabricated using standard photolithography. After the polymer has set and is removed from the master, the resulting stamp/mold has the inverse of the pattern on the master (Scheme 6.1). The most commonly used elastomer in soft lithography is polydimethylsiloxane (PDMS).

Scheme 6.1. General procedure for fabricating stamps and molds for use in soft lithography.

One of the most commonly used forms of soft lithography is microcontact printing (μCP).[1-3] Patterning surfaces by μCP is remarkably simple: a PDMS stamp is inked by being placed in a solution containing the modifier, and then placed in contact with the surface. The modifier is transferred to only those regions of the surface that make contact with the stamp, resulting in a patterned surface (Scheme 6.2).

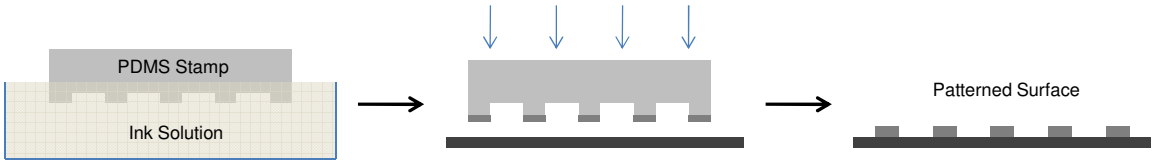

Scheme 6.2. Schematic of the general procedure for μCP.

Microcontact printing was originally developed by Whitesides and coworkers to prepare self assembled monolayer (SAM) patterns on gold using thiol chemistry[4-14] It was later extended to the patterning of alkanethiol layers on Ag,[15, 16] Cu[17] and Pd,[18, 19] and alkylsiloxanes on silicon oxide.[20] Surfaces patterned by μCP have been shown to have a wide range of applications. Patterns of alkanethiols on Au, Ag, Cu, and Pd have been used as resists for selective wet etching processes.[4, 5, 11, 16-18] Patterns formed by μCP on gold and silicon have been used in a number of biological applications such as the development of biosensors[21, 22] and cell studies[6, 22-25]. Further possible applications include the development of optical diffraction gratings,[7] light emitting diodes[26] and molecular electronics.[27]

Only a few examples exist of the preparation of patterns on surfaces using aryldiazonium salt chemistry. Downard and coworkers described a method where a film was deposited on a surface via electro-reduction of a aryldiazonium salt, and then removed in certain regions by scratching with an AFM tip (see Section 2.5.3).[28] Subsequent electro-reduction of a second aryldiazonium salt, at the same surface, modified only those areas where the initial film had been removed. The result was a surface with specific chemical functionalities immobilized in different, well-defined, regions.[28] In other work by the same group, micro-channels, formed by adhering a PDMS mold to the surface, were filled with aryldiazonium salt solution, which was subsequently reduced resulting in localized modification.[29] In the same report, patterning by region-specific electro-reduction of a *p*-nitrophenyl (NP) film was also demonstrated using micro-channels. Cougnon and coworkers achieved patterning by localized reduction of aryldiazonium cations using scanning electrochemical microscopy.[30] Non-localized spontaneous modification was avoided by carrying out the modification using a nitrophenyl precursor of the diazonium cation in sodium nitrite. Localized reduction of the nitrophenyl to aminophenyl at the SECM tip, in the presence of sodium nitrite, resulted in the formation of the diazonium cation, which was reduced leading to localized modification.[30] Charlier and coworkers patterned Si by doping of the substrate in selected regions. Under certain conditions, modification by electro-reduction of a diazonium salt occurred only in the doped areas.[31] The same researchers also reported patterning by selectively illuminating p-type Si through a mask. The illumination results in an increase in the conductivity of the Si, and electro-reduction of diazonium salts occurred only in the illuminated areas.[32]

The spontaneous reaction of aryldiazonium salts with surfaces (Chapters 4 and 5) points to the possibility of μCP using aryldiazonium salts. This printing method may have a number of advantages over methods using alkanethiol and alkylsiloxanes. Firstly, since surface modification using diazonium salts proceeds via a highly reactive aryl radical intermediate, the method should, in principle, be applicable to a wider range of surfaces. Secondly, due to the strength of the C-C bond, patterns prepared on carbon surfaces by printing of diazonium salts should be more stable than those formed using thiol inks on metal substrates. Microcontact printing is also a much simpler method than those used in previous reports of patterning using aryldiazonium salts. Hence, the aim of the current chapter is to develop μCP techniques for patterning carbon, metallic and semiconducting surfaces via the spontaneous reaction with aryldiazonium salts.

6.2 Experimental

Hard SU-8 masters, with pattern features ranging from 50-120 μm (Figure 6.1), were prepared by David J. Garrett from silicon wafers and SU8-50 negative photoresist (Microlithography Chemicals Corporation) using previously published methods.[29]

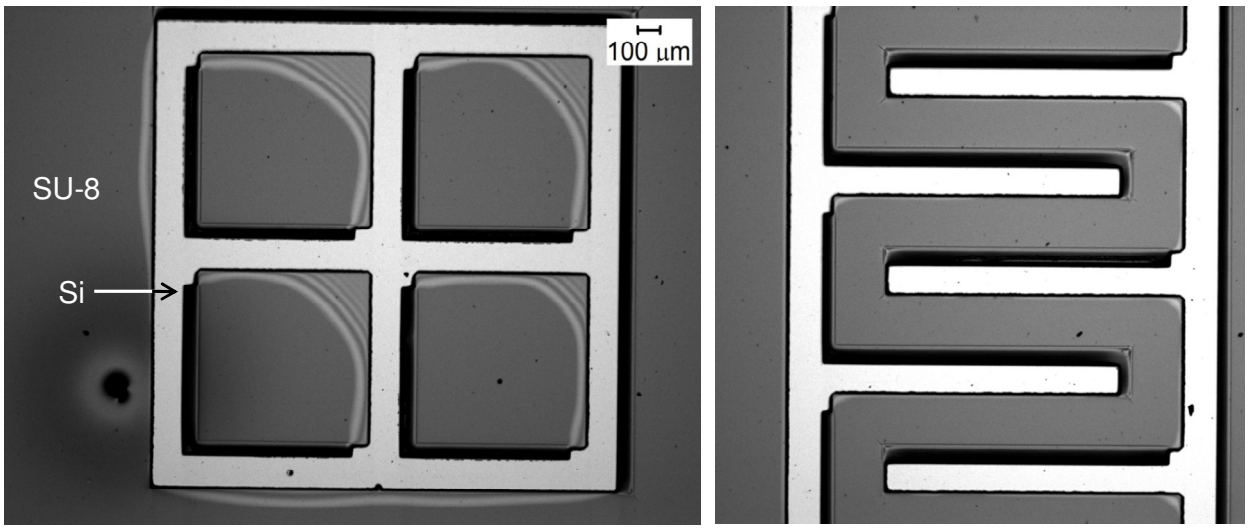

Figure 6.1. Optical microscope images of some of the patterns on the SU-8 master.

10:1 mixtures of Sylgard 184 (Dow Corning) prepolymer and curing agent were cast into the patterned master (for patterned stamps) and onto flat bare Si wafers (for non-patterned stamps). The polymers were cured in an oven at 95 ºC for 30 minutes, before being peeled from the master and cut into approximately 1.5 × 1.5 cm in size stamps. Stamps were solvent extracted by soaking successively in pentane (two days), toluene (one day), ethyl acetate (one day) and acetone (one day) to remove uncrosslinked oligomers. The soaking process reduces contamination during printing and leads to greater hydrophilicity of the PDMS stamp after oxygen plasma treatment (see below). [33] The stamps were dried in an oven at 60 ºC for two days and stored in ethanol between experiments.

Within two hours prior to printing, the stamps were subjected to oxygen plasma treatment (at 0.1 Torr for 5 minutes with a power of 100 W using a K1050X Emitech plasma asher) to make them compatible with polar inks.[33-35] Printing was undertaken by immersing the stamps in the inking solution for two minutes and then drying in a stream of N_2 gas for approximately 15 seconds until nearly dry. They were then placed on the modification substrate for the selected printing time. Each stamp was used with just one inking solution to avoid cross-contamination.

Printing on gold was undertaken on Au/NiCr/Si substrates, prepared as described in Section 2.3.3. Experiments using silicon were conducted using both low-conductivity ($Si_{LC;}$ Silicon Quest and Micro Materials, resistivity = 1-20 Ω.cm) and high-conductivity ($Si_{HC;}$ Virginia Semiconductor, Inc. USA, resistivity = 0.01 -0.05 Ω.cm) Si (100) wafers cut into 1.5 × 1.5 cm squares. Prior to modification the Si squares were placed in 40 % hydrofluoric acid (Sigma-Aldrich) for three minutes to remove the native silicon oxide and hydrogenate the underlying Si surface. The Si surfaces were then washed with methanol and dried under a stream of N_2 gas. The surfaces were used within 10 minutes of the hydrofluoric acid treatment, which was carried out by Benjamin S. Flavel. Copper of unknown origin was obtained from the mechanical workshop of the University Of Canterbury Department of Chemistry. Prior to printing, the copper oxide layer was removed by immersing in 16 M nitric acid for 10 seconds. The substrates were then washed with water, immersed in 17 M acetic acid for 30 seconds, and washed again with water again prior to drying with a stream of N_2 gas.

All printing was undertaken using aqueous inks whose compositions will be indicated as "diazonium salt/medium". Due to the difficulty of isolating *p*-aminobenzene diazonium salt (ABD), printing with ABD was undertaken using *in situ*-generated ABD. [36, 37] 5 ml of a 20 mM solution of *p*-phenylenediamine in 0.5 M HCl was mixed with an equimolar amount of sodium nitrite dissolved in a minimal volume (< 1 ml) of 0.5 M HCl. The mixture was stirred by bubbling nitrogen gas through it for two minutes and used as an ink within 10 minutes of the initial mixing.[37] This ink will be referred to as 20 mM ABD/0.5 M HCl.

At pyrolyzed photoresist film (PPF) substrates *p*-nitrophenyl (NP) films were electro-reduced in 0.1 M H_2SO_4; the area of the working electrode was 0.18 cm^2. At gold the reduction was carried out in 0.1 M solutions of $NaClO_4$ in 1:9 (by volume) EtOH-H_2O; working electrode area = 0.785 cm^2. A scan rate of 100 mV s^{-1} was used for all cyclic voltammetry.

Atomic force microscopy (AFM) film thickness measurements of *p*-carboxyphenyl (CP) films after coupling of *p*-nitroaniline (NA), and associated blanks, were performed, by preparing two samples of each type. AFM thickness measurements were made on each sample as described in Section 2.5.3. The values given are an average all of the values (24 values) obtained over the two samples for each sample type. All other AFM film thickness measurements were performed as described in Section 2.5.3, with values given being representative of the thickness of individual samples (rather than two samples prepared by the same method).

Contact angle measurements of CP films reported in Section 6.5.1 were carried out by delivering two drops onto each sample and recording the contact angle. Two samples and two blanks were prepared. Hence the values given, for both the samples and the blanks, are arithmetic means of four measurements. Contact angle measurements in Section 6.5.2 were carried out by preparing duplicates of the samples and each of the blanks. Three drops were delivered onto each sample and blank. Hence the value given for each type of sample and blank is the arithmetic mean of the six measurements obtained for that sample/blank type. The uncertainty for all contact angle values is given as two standard deviations of the mean.

Condensation figures were obtained as reported previously.[29] Briefly, a patterned PPF surface was breathed on and an optical microscope image (Section 2.7) was taken within two seconds. Water droplets with larger diameters form on areas with higher hydrophilicity, allowing for the imaging of patterns that vary from the substrate in hydrophilicity.

6.3 Microcontact Printing of NP Films on PPF

Pyrolyzed photoresist film (PPF) was chosen as the substrate to investigate the μCP of carbon with aryldiazonium salts since its low surface roughness (in comparison to GC) is expected to lead to sharper and better-defined patterns. Initial investigations used non-patterned stamps and aqueous *p*-nitrobenzene diazonium tetrafluoroborate salt (NBD) inks. NBD was chosen because it reacts spontaneously with PPF in aqueous conditions (but not in ACN) to form *p*-nitrophenyl (NP) films (see Chapter 4), which can be easily detected electrochemically. Non-patterned stamps were used to modify the entire surface, thereby simplifying calculations of surface concentrations from cyclic voltammetric data.

6.3.1 Electro-Reduction of Printed NP Films

A PPF substrate was printed by contacting a 20 mM NBD/1 M H_2SO_4 inked (non-patterned) PDMS stamp with the surface for 30 minutes. (1 M H_2SO_4 was used, rather than the 0.14 M H_2SO_4 used for spontaneous modification in Chapter 4, because preliminary results suggested that the higher acid concentration leads to more effective modification by μCP.) After standard post modification sonication, the surface was analyzed by consecutive cyclic voltammograms between ~0.8 and -1.1 V vs. SCE in 0.1 M H_2SO_4, from an initial potential of ~0.8 V.

Figure 6.2 shows consecutive cyclic voltammograms after printing. The characteristic irreversible NP reduction and hydroxyaminophenyl (APOH)/nitrosophenyl redox couple occur at ~-0.6 and ~0.3 V, respectively. The first scan shows no evidence of the reduction of the diazonium cation moiety, which would be expected at $E_{p,c} \approx 0$ V vs. SCE if present, indicating

that it has reacted. The surface concentration of the electro-active NP groups, Γ_{NP}, was determined (as described in Section 3.3.3) to be 16.4×10^{-10} mol cm^{-2}.

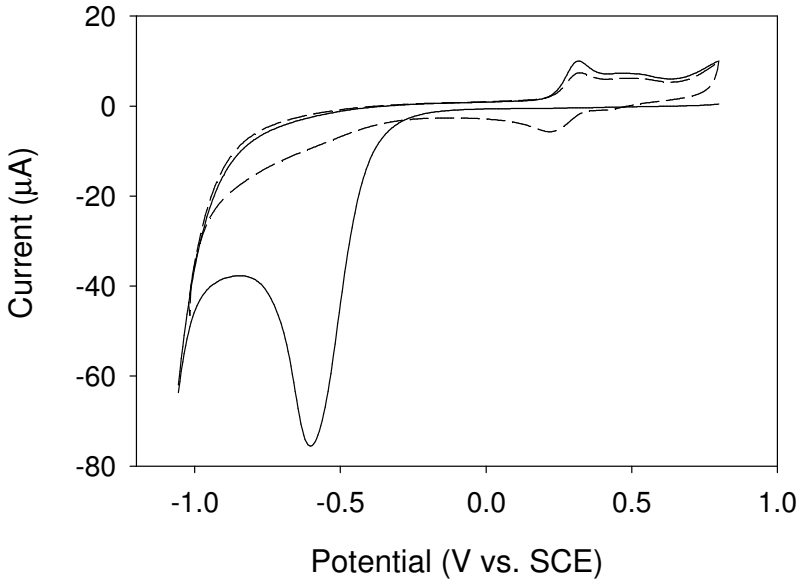

Figure 6.2. Consecutive cyclic voltammograms in 0.1 M H_2SO_4 of a PPF surface printed with 20 mM NBD/1 M H_2SO_4 for 30 minutes; first scan (—) and second scan(---). Initial potential = 0.8 V; scan rate = 100 mV s^{-1}.

6.3.2 Effect of Printing Time on Surface Concentration

The effect of the printing time on the surface concentration of electro-active NP groups, $\Gamma_{NP,}$ was investigated. Samples were prepared by printing for 5, 10, 30, 60 and 120 minutes. After printing the samples were subjected to the standard post-modification sonication procedure. Consecutive cyclic voltammograms of each sample were recorded between ~0.8 and -1.0 V vs. SCE in 0.1 M H_2SO_4 (initial potential = 0.8 V). The corresponding Γ_{NP} values (calculated as described in Section 3.3.3) are listed in Table 6.1, where the symbols (●,▼,○) represent different sets of samples prepared on different days.

Table 6.1. Surface concentrations and film thicknesses of NP films prepared by printing 20 mM NBD/1 M H_2SO_4 on PPF for various times. The symbols (●,▼,○) represent sample sets printed on different days. No film thickness measurements were preformed on the sample set represented by the symbol ○.

Data Set	Printing Time (minutes)	Γ_{NP} (10^{-10} mol cm^{-2})	Film Thickness (nm)
●	5	9.0	2.2 (± 0.7)
	30	16.4	1.7 (± 0.4)
	60	15.4	1.7 (± 0.4)
▼	30	6.2	2.4 (± 0.6)
	30	4.8	1.5 (± 0.4)
	60	2.2	0.9 (± 1.0)
	120	8.9	0.9 (± 1.0)
	120	4.8	0.3 (± 0.5)
○	5	20.5	—
	10	20.9	—
	30	21.7	—
	60	21.1	—

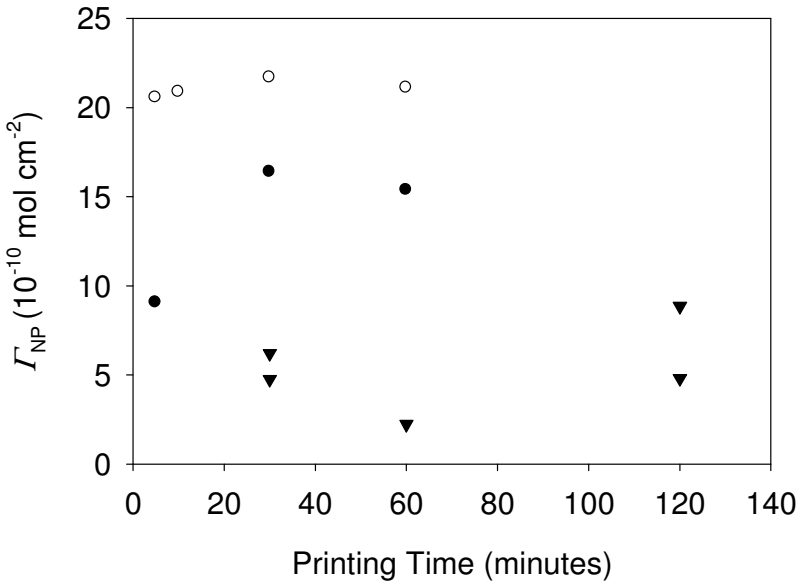

Figure 6.3. Plot of Γ_{NP} groups vs. printing time for NP films printed using NBD/1 M H_2SO_4. The different symbols (●,▼,○) represent experiments conducted on different days.

The data are also shown as a plot of Γ_{NP} vs. printing time in Figure 6.3. Significant variations in Γ_{NP} values were observed, even after identical printing times. These variations appeared to be systematic, with low concentrations (~5 to 10 × 10^{-10} mol cm^{-2}) observed for films printed on some days (▼) and higher concentrations (~10 to 20 × 10^{-10} mol cm^{-2}) observed on other days (○,●). These variations may be due to contamination during plasma ashing, leading to less effective oxygen plasma treatment on certain days, and could be related to the large number of users and their types of use of the machine. Nevertheless, Figure 6.3 shows tentative evidence for an increase in Γ_{NP} between 5 and 30 minutes printing time. However, no increase was observed after 30 minutes, suggesting that 30 minutes is sufficient to obtain the maximum Γ_{NP} under the conditions used.

6.3.3 AFM Thickness Measurements of Printed NP Films

AFM film thickness measurements (Section 2.5.3) were undertaken on selected printed NP films. The data are listed in Table 6.1 and are also represented in Figure 6.4 (using the same symbols as in Figure 6.3).

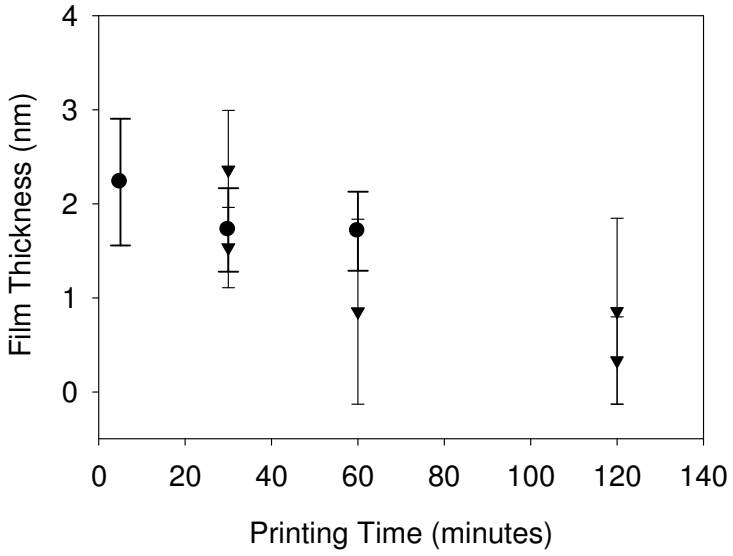

Figure 6.4. Plot of film thickness vs. printing time for PPF substrates printed with NP films using a 20 mM NBD/1 M H_2SO_4 inking solution.

Film thicknesses were found to be quite variable at all printing times. For some samples, thicknesses greater than ~0.79 nm indicated the formation of multilayer films. This is consistent with the data in Section 4.4.2, where multilayer films were found for NP films formed spontaneously at PPF immersed in NBD/H_2SO_4 solution. No significant change in film thickness was observed between 5 and 30 minutes printing time, but there is tentative evidence for a decrease between 30 and 120 minutes. This could be due to drying of the stamp at longer printing times, leading to mechanical perturbations of the film on removal of the stamp. Since both the surface concentrations and film thicknesses are at a maximum after a printing time of 30 minutes, this printing time was used for the remainder of the PPF samples prepared in this work. Maximum concentrations and film thicknesses are desirable because patterns of thicker films are expected to be imaged more easily using microscopy techniques.

The large uncertainties for the film thicknesses seen in Figure 6.4 arise not only from the differences in the thickness determined from the two duplicate scratches carried out for each sample, but also from difference in thickness values obtained from an individual scratch. Hence, the films were seen to be highly variable in thickness even over the length of a single scratch (10 µm), as shown by the average line profile taken across a scratch (Figure 6.5).

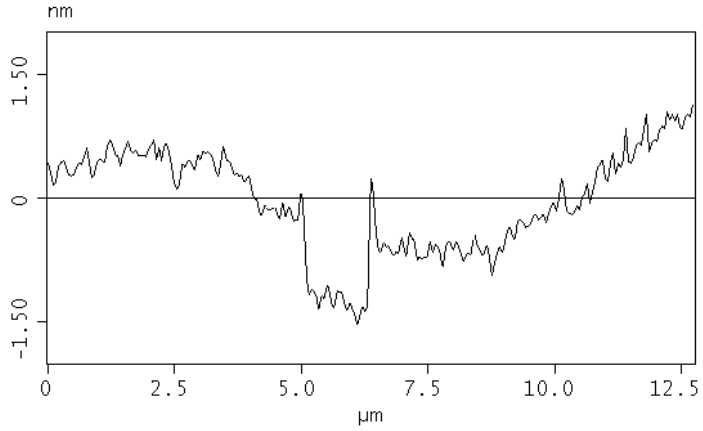

Figure 6.5 Average line profile across a scratch in an NP film on PPF prepared by printing with 20 mM NBD/1 M H_2SO_4 using a printing time of 120 minutes

The highly variable thickness of the printed NP films (Figure 6.5) may be caused by inhomogeneities in the stamps. This interpretation is supported by the fact that the average error in thickness for printed NP films (0.63 nm) is higher than the average error associated with the

thickness of NP films formed spontaneously in solution (0.43 nm, Section 4.4.2). However, printing does not always to lead to films of highly variable thickness. For example, homogeneous films with much smaller uncertainties in thickness were found for CP films prepared by printing *p*-carboxybenzene diazonium salt (CBD) on PPF (Section 6.5); and when NBD was printed onto a CP modified PPF surface, reproducible film thicknesses were also obtained (Section 6.6.2). Vautrin-Ul and coworkers have shown that the more positive the diazonium reduction peak relative to the surface open circuit potential (OCP), the less uniform the resulting spontaneously prepared film.[38] This may explain the differences between the NP films described here and the CP films (Section 6.5). It would also explain why the printing of NBD on a (passivated) CP modified PPF surface (Section 6.6.2) leads to reproducible film thicknesses with relatively small uncertainties. Hence, the high reduction potential of NBD, together with possible inhomogeneities in the PDMS stamp, can account for the inhomogeneous films observed upon printing NBD on PPF.

6.3.4 Density of Printed NP Films

As discussed in Sections 4.4.2 and 5.3.5, plotting Γ_{NP} against the corresponding film thicknesses can give information about the packing densities of NP groups in the films.

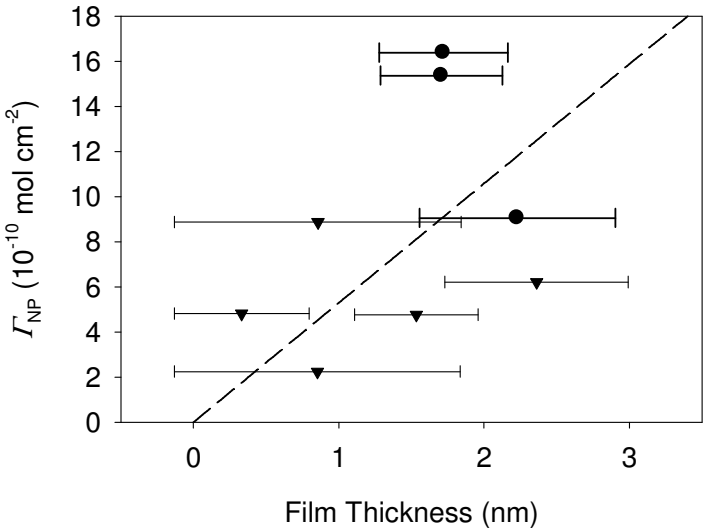

Figure 6.6. Plot of Γ_{NP} vs. film thickness for PPF substrates printed with NP films using a 20 mM NBD/1 M H_2SO_4 inking solution. Regression line (---) forced through zero. Slope = (5.3 ± 2.2) × 10^{-10} mol cm^{-2} nm^{-1}. R^2= 0.14.

Figure 6.6 shows a plot of Γ_{NP} vs. film thickness for PPF surfaces printed with NP films, using the data in Table 1.1. The data do not fall on a straight line. This is not surprising considering the high uncertainties associated with film thickness measurements for individual NP films.

6.3.5 Patterning of NP Films on PPF by μCP

Patterning of PPF with NP films was investigated by printing with patterned stamps and using 20 mM NBD/1 M H_2SO_4 solution as the ink. Blanks were prepared by printing PPF with 1 M H_2SO_4 ink. After post modification sonication the printed samples and blanks were analyzed using SEM, as described in Section 2.6.

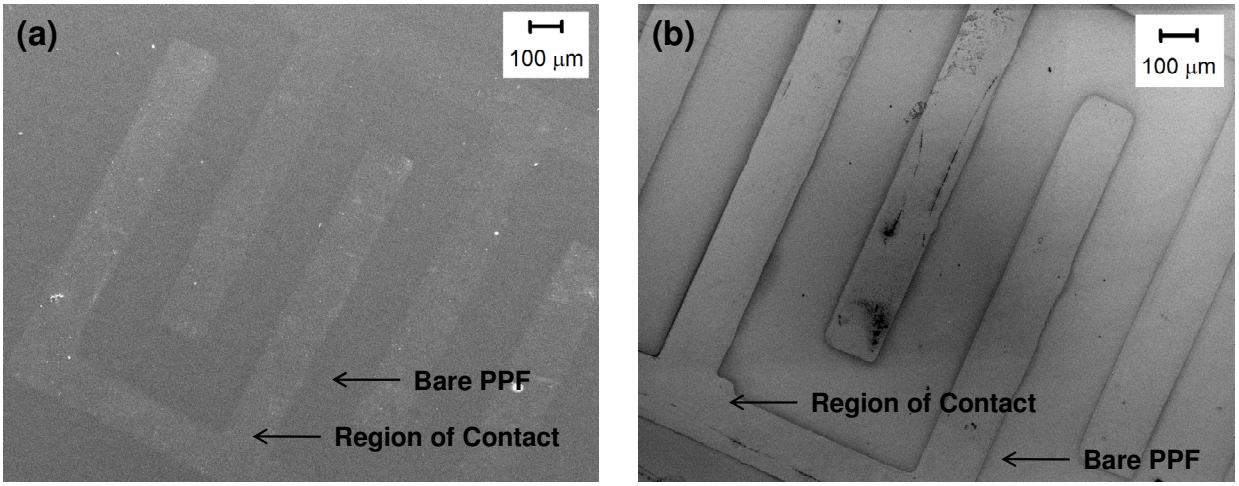

Figure 6.7. SEM images of PPF surface printed with 20 mM NBD/1 M H_2SO_4 (a) and 1 M H_2SO_4 (b). Printing time = 30 minutes.

Patterns matching the features of the master (Figure 6.1) were seen both on the printed samples and the blanks. On the samples (Figure 6.7 (a)), the areas of the surface that had contacted the stamp are seen to be lighter, demonstrating that patterning by μCP of NBD was successful. On the blanks (Figure 6.7 (b)) there was no contrast between the contacted and unstamped areas; the dark lines seen on the edges of the stamped areas could be due to solvent and PDMS residues.

6.4 Microcontact Printing of Aminophenyl Films on PPF

p-Aminophenyl (AP) films have the advantage that they can be used to assemble citrate-capped gold nanoparticles under acidic conditions, due to the electrostatic interaction between the negatively charged nanoparticles and the positive charge of the protonated AP groups. The assembled gold nanoparticles act as highly efficient contrasting agents for electron microscopy, allowing for more effective imaging of patterns.

6.4.1. Electrochemistry of Printed AP Films

μCP of PPF with *p*-aminobenezene diazonium salt (ABD) was initially investigated by printing the surface with 20 mM ABD/0.5 M HCl using non-patterned stamps and a printing time of 30 minutes. Blanks were prepared in the same manner, but by printing with 0.5 M HCl.

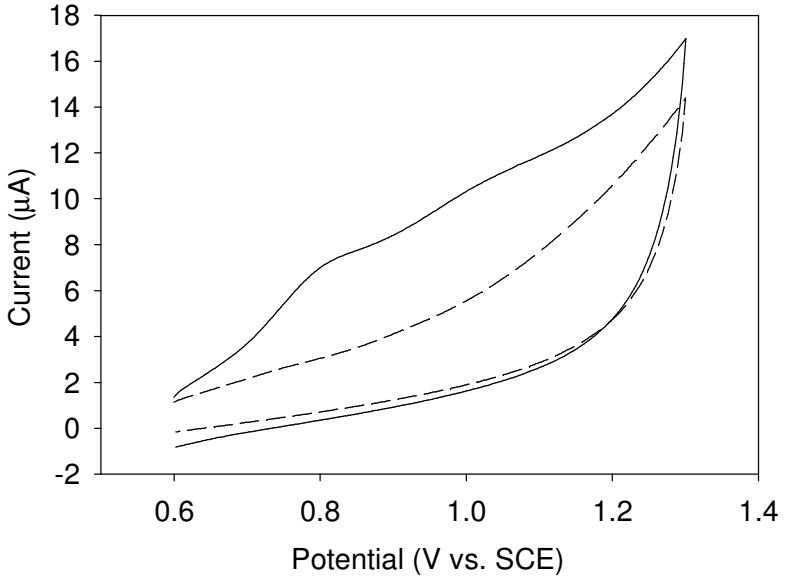

Figure 6.8. Cyclic voltammograms of PPF substrates printed with 20 mM ABD/0.5 M HCl (—) and 0.5 M HCl (---). Initial potential = 0.6 V, scan rate = 100 mV s^{-1}.

Figure 6.8 shows cyclic voltammograms recorded in 0.1 M H_2SO_4 of PPF surfaces printed with ABD/HCl solution (—) and "blank" HCl (---). AP films are known to undergo oxidation at potentials between 0.7 and 1.2 V vs. SCE in aqueous conditions,[39] and the ABD printed surface shows two oxidation peaks (at 0.8 and 1.0 V) in this range. Since no peaks are observed for the blank, it is very likely that both peaks for the ABD printed sample are due to the AP groups at the surface. The existence of two oxidation peaks may indicate AP groups in different environments. Cyclic voltammograms of the surface printed with ABD were also recorded by scanning in the negative direction between 0.6 and -0.6 V vs. SCE, the region where the reduction of the diazonium cation moiety would have been expected. The absence of reduction peaks indicates that there is no unreacted ABD present at the surface. These results are consistent with the formation of a covalently bound AP film at the surface after printing.

6.4.2 *Patterning of AP Films on PPF by μCP*

Patterning of PPF with AP films was undertaken using patterned stamps with 20 mM ABD/0.5 M HCl inking solution. After standard post modification sonication, the printed surfaces were immersed in a solution of citrate capped gold nanoparticles (prepared as described in Section 2.2.4) for 40 minutes. After immersion the samples were sonicated for 30 seconds in Milli Q water and then dried with a stream of N_2 gas prior to analysis by SEM. Blanks were prepared in the same manner, except the initial printing step was carried out by inking the stamps with 0.5 M HCl (no ABD).

Figures 6.9 (a) and (c) show SEM images of PPF samples prepared by printing with ABD. Substantial assembly of gold nanoparticles is seen in the areas where the stamp has made contact with the surface, with much smaller amounts in other areas. Figures 6.9 (b) and (d) show that there is little gold nanoparticle assembly on the blanks, indicating that the ABD printing ink is responsible for the assembly observed in (a) and (c). Since the diazonium moiety was not present after printing (Section 6.4.1) it cannot be responsible for the electrostatic interactions leading to nanoparticle assembly. It is reasonable to conclude that the negatively charged citrated capped

nanoparticles are interacting with the positively charged protonated AP film; in other words, that that patterning of AP films on PPF by μCP of ABD was successful.

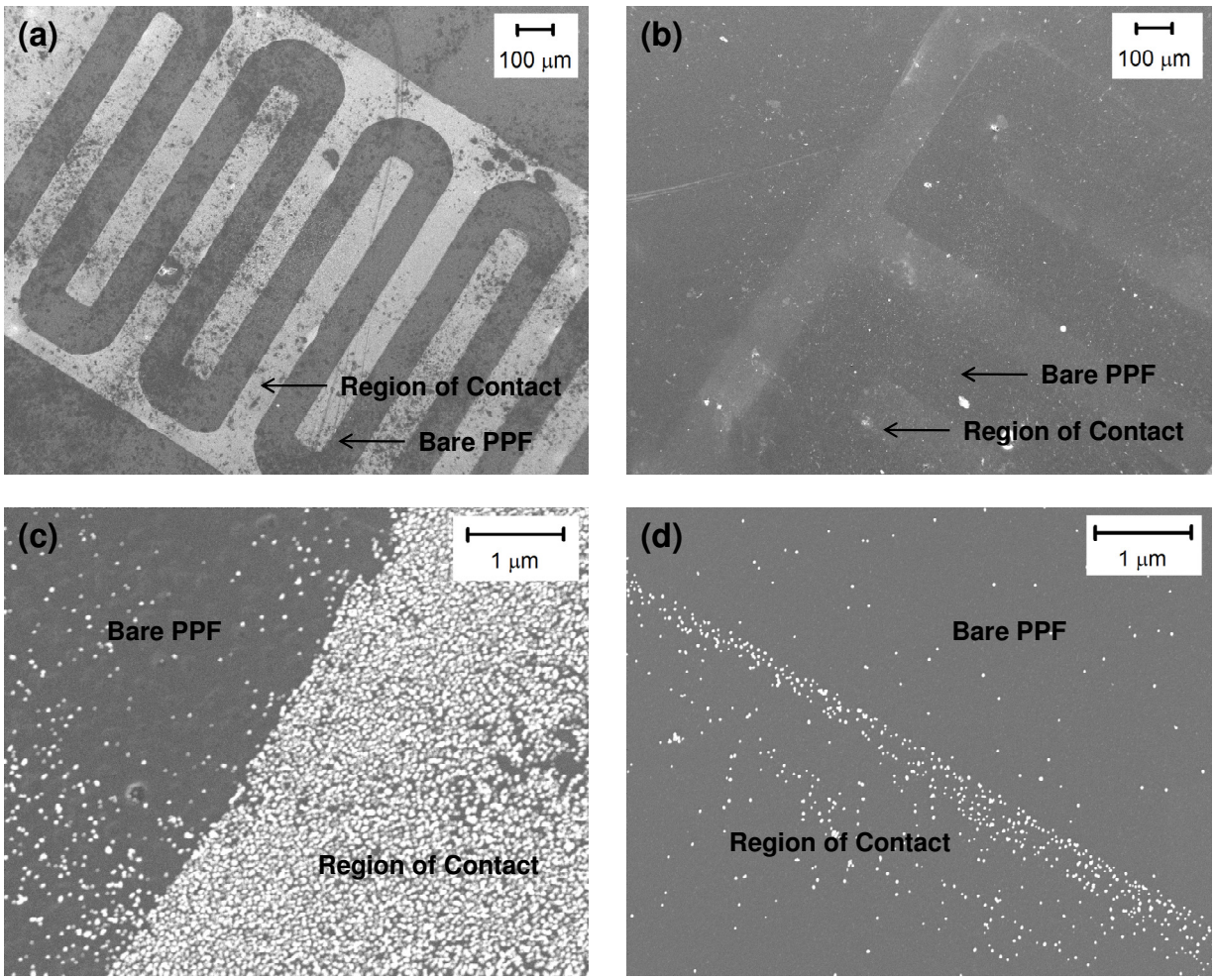

Figure 6.9. PPF substrates printed with 20 mM ABD/0.5 M HCl solution (a and c) and 0.5 M HCl (b and d). All surfaces were subsequently immersed in citrate capped gold nanoparticle solution for 40 minutes.

6.5 Microcontact Printing of CP Films on PPF

As mentioned in Sections 4.5 and 5.6, *p*-carboxyphenyl (CP) films are of interest due to their ability to serve as electrophilic sites for coupling reactions. Some applications of patterned surfaces are likely to involve the coupling of further molecules to the patterned films. Hence, in the present section, modification of PPF with CP films by μCP of CBD is investigated. Subsequently, the coupling of *p*-nitroaniline (NA) to the films is explored.

6.5.1 Printing of CP Films

PPF substrates were printed with non-patterned stamps using a 20 mM CBD/1 M H_2SO_4 ink solution and a printing time of 30 minutes. After standard post modification sonication, the samples were analyzed using cyclic voltammetry, contact angle measurements and AFM film thickness measurements. Blanks were prepared by printing PPF samples with 1 M H_2SO_4.

PPF samples printed with CBD/H_2SO_4 gave a water contact of (31 ± 2) º compared to (64 ± 11) º for the blanks printed with only H_2SO_4. The results are indicative of the formation of a hydrophilic CP film on the surface after printing with CBD. AFM measurements revealed a film with a thickness of (1.0 ± 0.2) nm on a PPF substrate printed with CBD, but no measurable film on the blank, thereby supporting the contact angle measurements.

Cyclic voltammetry was performed on the printed CP films to test for the reduction of the CBD's diazonium cation moiety, which is expected at -0.3 V vs. SCE in 0.1 M H_2SO_4. Scans in the negative direction between 0.8 and -0.5 V vs. SCE in 0.1 M H_2SO_4 revealed no peaks, indicating that the diazonium cation moiety has reacted. This is consistent with the covalent attachment of CP functionalities to the PPF surface.

6.5.2 Coupling of NA onto Printed CP Films

PPF substrates were printed for 30 minutes with non-patterned stamps using 20 mM CBD/1 M H_2SO_4 ink solution. After the standard post modification sonication, the CP films were activated to form acyl chloride films by immersion in thionyl chloride ($SOCl_2$) for 30 minutes. The samples were transferred to a 20 mM *p*-nitroaniline (NA)/ACN solution, and left to react for 24 hours. After removal from the NA solution, they were sonicated for 5 minutes in ACN prior to analysis. These samples will be referred to as PPF-CP+$SOCl_2$+NA.

A number of blanks were also prepared. One type, referred to as PPF-CP, was prepared by printing PPF substrates with 20 mM CBD/1 M H_2SO_4 for 30 minutes. Another type of blank

was prepared by in the same manner as the PPF-CP+$SOCl_2$+NA samples but without the $SOCl_2$ activation step; these will be referred to as PPF-CP+NA. The final type was prepared by printing PPF with 1 M H_2SO_4 (no CBD) activating with $SOCl_2$ (as described above) and subsequently placing in NA/ACN for 24 hours; these blanks will be referred to as PPF + $SOCl_2$ + NA. All blanks were sonicated for five minutes in ACN after preparation.

Analysis of samples and blanks was undertaken by recording cyclic voltammograms in 0.1 M H_2SO_4 between 0.7 and -1.0 V vs. SCE (initial potential 0.7 V).

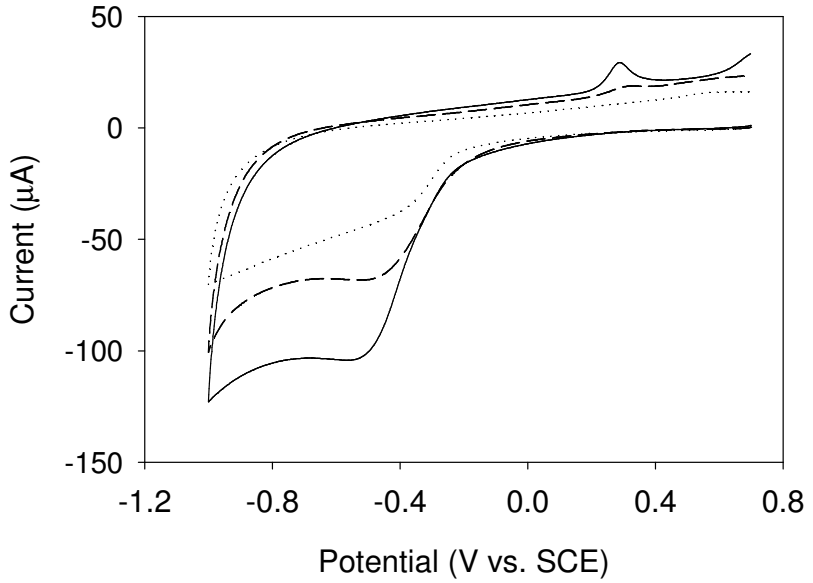

Figure 6.10. Cyclic voltammograms of PPF-CP+$SOCl_2$+NA (—), PPF+$SOCl_2$+NA (---) and PPF-CP+NA (⋯) recorded in 0.1 M H_2SO_4, initial potential 0.7 V. Scan rate 100 mV s^{-1}.

Figure 6.10 shows cyclic voltammograms in 0.1 M H_2SO_4 between 0.7 and -1.0 V vs. SCE (initial potential 0.7 V) of PPF-CP+$SOCl_2$+NA (—), PPF+$SOCl_2$+NA (---) and PPF-CP+NA (⋯) surfaces. The cyclic voltammogram of the PPF-CP+$SOCl_2$+NA sample shows the characteristic NP reduction and APOH oxidation at -0.5 V and 0.3 V, respectively, indicating the presence of the NP moiety after coupling of NA. A smaller NP reduction peak was observed for the PPF+$SOCl_2$+NA blank. This could be a result of NA groups coupling to carboxylic acid functionalities, which are known to exist at bare PPF surfaces. The PPF-CP+NA blank also showed a small reduction peak at the same potential, presumably due to the physisorption of NA

onto (or absorption into) the CP film. The surface concentrations of NP groups for the three surfaces were calculated from the voltammograms in the manner described in Section 3.3.3, and are summarized in Table 6.2.

Table 6.2. Surface concentration of NP groups after reaction of NA with the surfaces listed.

Sample Type	Surface Concentration (10^{-10} mol cm^{-2})
PPF-CP+$SOCl_2$+NA	12.8
PPF+$SOCl_2$+NA	4.9
PPF-CP+ NA	2.5

The surface concentration of 12.8×10^{-10} mol cm^{-2} for the PPF-CP+$SOCl_2$+NA sample is consistent with the theoretical value for a closely packed monolayer on a flat surface (12×10^{-10} mol cm^{-2}), providing strong evidence that the covalent coupling of NA with the printed CP film has occurred. As expected from the cyclic voltammograms, the surface concentrations for the two blanks are much lower.

Table 6.3. Film thicknesses for NA layer coupled on CP film, and associated blanks.

Sample Type	Film thickness (nm)
PPF-CP	1.0 (± 0.3)
PPF-CP+$SOCl_2$+NA	2.0 (± 0.5)
PPF+$SOCl_2$+NA	0.4 (± 0.2)
PPF-CP+NA	1.0 (± 0.4)
PPF+H_2SO_4	0

Table 6.3 shows the film thicknesses, determined by AFM, for the coupled samples and the associated blanks. The thickness of (1.0 ± 0.3) nm for the printed PPF-CP films is consistent with the measurements in Section 6.5.1 for samples that were subjected to standard post modification sonication, but not to an additional five minutes sonication in ACN. The PPF-CP+$SOCl_2$+NA samples are significantly thicker (2.0 ± 0.5 nm), consistent with the coupling of NA groups to the activated acyl chloride film. The PPF-CP+NA control has a (1.0 ± 0.4) nm film, the same as the PPF-CP samples, indicating an insignificant contribution from NP groups. These results provide evidence for the occurrence of a coupling reaction in the preparation of the PPF-CP+$SOCl_2$+NA samples. Finally a (0.4 ± 0.2) nm thick film for PPF+$SOCl_2$+NA is

consistent with coupling of NA due to a low concentration of carboxylic acid functionalities on the PPF surface.

Table 6.4. Water angle measurements for NA layer coupled on CP film, and corresponding blanks.

Sample	Contact Angle (degrees)
PPF-CP	41 (± 6)
PPF-CP + $SOCl_2$ + NA	71 (± 4)
PPF-CP + NA	49 (± 10)
PPF + $SOCl_2$ + NA	73 (± 8)
PPF + H_2SO_4	64 (± 11)

Water contact angles for the coupled samples and blanks are listed in Table 6.4. The low value of (41 ± 6) º for PPF-CP indicates the presence of hydrophilic surface film. The fact that it is slightly higher than the (31 ± 2) º for CP films printed on PPF (Section 6.5.1) is probably due to the additional ACN sonication step, which could bring about rearrangement of the film or entrapment of solvent in the film. The PPF-CP+$SOCl_2$+NA samples are significantly less hydrophilic than the PPF-CP blanks, with a water contact angle of 71 (± 4) º. The increase is consistent with the coupling of NA groups to the acyl chloride layer, in support of the electrochemical and AFM measurements, indicating that the coupling reaction was successful. PPF-CP+NA blanks showed a contact angle of 49 (± 10) º. This is higher than for PPF-CP, possibly due to physisorption/absorption of a small amount of NA onto/into the CP film, as detected electrochemically above. The PPF+$SOCl_2$+NA samples have a contact angle of 73 (± 8) º, consistent with both the coupling of NA molecules to native CP on bare PPF (contact angles of NP films are in the range of 75-93 º; Section 4.4.5) and the water contact angle of (64 ± 11) º for PPF printed with blank 1 M H_2SO_4 (Section 6.5.1).

6.5.3 Patterning of CP Films on PPF by µCP

PPF substrates were printed using patterned stamps and 20 mM CBD/1 M H_2SO_4 ink. After the standard post modification sonication procedure the condensation image (Figure 6.11) revealed patterns matching the stamp on the surface.

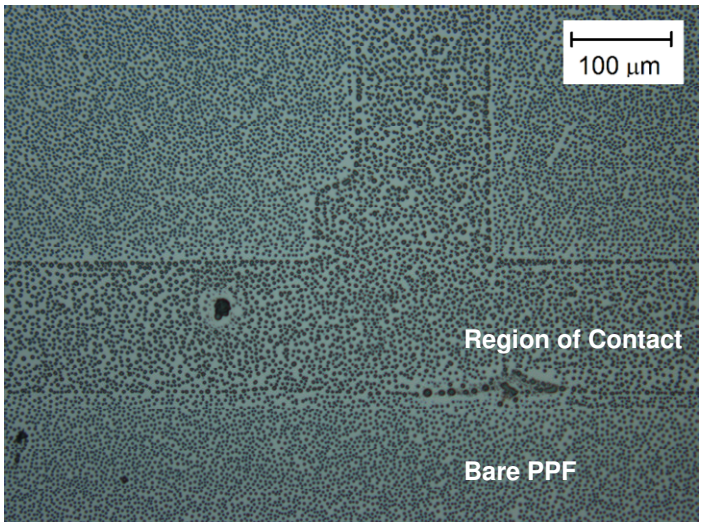

Figure 6.11. Condensation image of CP film patterned on a PPF surface using 20 mM CBD/ 1M H_2SO_4 ink solution.

6.6 Preparation of Multi-Component Systems on PPF

Further work focused on the preparation of multicomponent surfaces on PPF substrates by µCP of diazonium salts. The aim was to prepare surfaces where specific areas are modified with different chemical functionalities. Two strategies, referred to as "fill-in" and "build-up", were investigated.

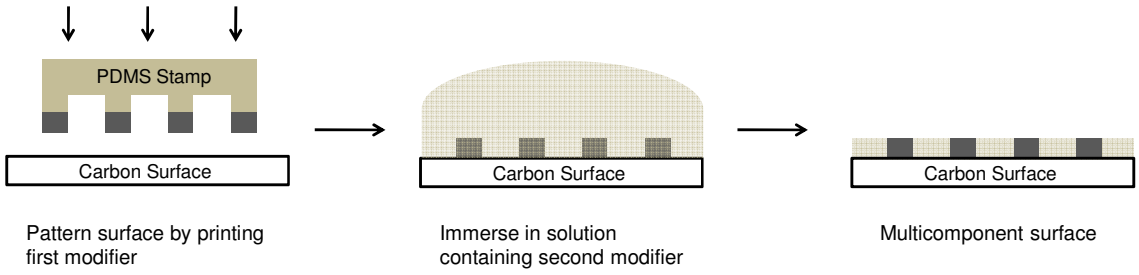

Scheme 6.3. Preparation of multicomponent surfaces by the fill-in method.

In the fill-in method (Scheme 6.3) printing is used to modify well-defined regions of the surface. The patterned surface is then immersed in a solution of a second modifier, which reacts with the areas left bare by the printing process. This general approach has been used to prepare multicomponent systems of SAMs on gold using thiol chemistry.[7, 10] A variation of fill-in method has also been employed by Downard and coworkers to prepare multicomponent surfaces

on carbon substrates.[29] In that work, an initial pattern was prepared on a PPF surface by oxidation of tetraethylene glycol diamine within the microchannels of a PDMS mold. Subsequently, *p*-methylbenzene diazonium cation was reduced at the surface leading to the formation of a *p*-methylphenyl film in the non-patterned areas.

The first step of the build-up approach is to modify an entire surface in a solution of the first modifier. A second modifier is then printed onto the pre-modified surface, resulting in a surface where different chemical functionalities are exposed in different, well-defined, regions (Scheme 6.4).

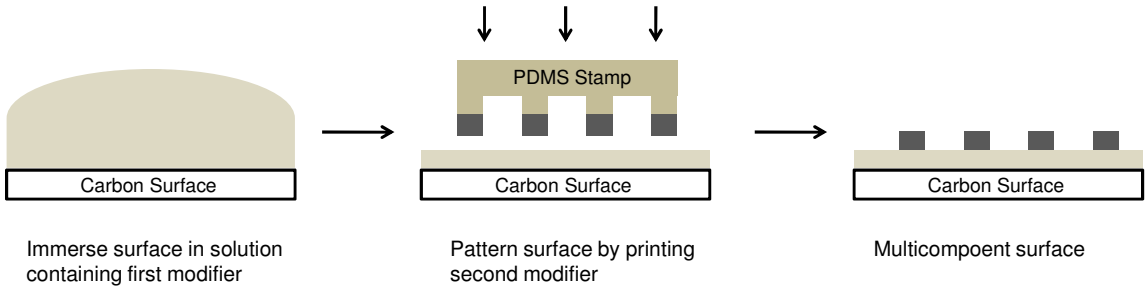

Scheme 6.4. Preparation of multicomponent surfaces by the build-up approach.

Variations of the build-up approach have been used by a number of research groups. Bowden and coworkers used microchannels in a PDMS mold to pattern amine-terminated groups on an underlying carboxylic acid film on Si via a coupling reaction.[40] A similar strategy was employed by Downard and coworkers who used microchannels to couple ethylenediamine patterns onto a PPF surface functionalized with a CP film.[29] The build-up approach used in this thesis differs from the variations described above in that μCP is used to attach the second layer. Furthermore, rather than coupling the second modifier via activation of a carboxylic acid group, the method investigated here relies on attachment of the second modifier by spontaneous radical coupling onto the primary film. Since radical coupling should take place for a large number of aryl systems, the current method allows for a larger range of modifiers for the first modification step.

6.6.1 Multicomponent Surfaces by the Fill-In Method

Initially experiments were carried out to determine whether attachment of a second modifier will occur over a patterned film or will be confined to the areas that are left bare after printing with the first modifier. One half of two large PPF plates (~3.0 × 1.5 cm) were printed with non-patterned stamps using inking solutions of 20 mM CBD/1 M H_2SO_4 in one case and 20 mM ABD/1 M H_2SO_4 in the other. The full surfaces were immersed in 10 mM NBD/0.1 M H_2SO_4 for 60 minutes then each half (i.e. the initially printed and unprinted areas) were analyzed separately by recording cyclic voltammograms between ~0.8 and -1.2 V vs. SCE in 0.1 M H_2SO_4 from an initial potential of ~0.8 V. Irreversible NP reduction and APOH oxidation were observed for both regions of both samples, indicating the NBD reacts not only with the bare PPF surface, but also with the areas printed with CP and AP films. The surface concentrations of electro-active NP groups, Γ_{NP}, for each region of each surface are given in Table 6.5.

Table 6.5. Γ_{NP} for printed and non-printed regions of PPF substrates. One half of each sample was printed with 20 mM CBD/1M H_2SO_4 (PPF-CP+NP) or 20 mM ABD/0.5 M HCl (PPF-AP+NP). Samples were subsequently immersed in 10 mM NBD/0.1 M H_2SO_4.

	Γ_{NP} (10^{-10} mol cm^{-2})	
Sample	Printed Region	Non-Printed Region
PPF-CP+NP	2.3	7.0
PPF-AP+NP	7.5	12.7

Lower values of Γ_{NP} were determined for the regions that were initially printed. This is an expected result, since the printed films should inhibit electron transfer from the surface to NBD in solution, thereby impeding film growth. However, the fact that some NP is present in the areas that were initially printed limits the usefulness of this approach and it was not investigated further.

6.6.2 Multicomponent Surfaces by the Build-Up Method

The feasibility of the build-up approach was initially investigated by determining whether a layer could be successfully printed on top of a pre-modified surface. The first step was immersion of

two large (~3.0 x 1.5 cm) PPF samples in 10 mM CBD/0.1 M H_2SO_4 solution for 30 minutes. Immersion of PPF in 10 mM CBD/0.1 M H_2SO_4 has previously been shown to lead to the formation of a CP film on the surface (see Section 4.5). Subsequently, one half of each of the samples was printed with non-patterned stamps using 20 mM NBD/1 M H_2SO_4 inking solution and a printing time of 30 minutes. Cyclic voltammograms were carried out on the region that had been printed with NBD (after immersion in CBD) by cycling between 0.8 and -1.0 V vs. SCE in 0.1 M H_2SO_4 from an initial potential of 0.8 V (Figure 6.12).

The irreversible NP reduction and APOH/nitrosophenyl redox couple were observed at $E_{p,c} \approx$ -0.5 and $E_{1/2} \approx 0.3$ V respectively, indicating the presence of the NP moiety at the surface after printing. During the first scan, no peak was observed in the region where the reduction of the diazonium cation moiety would appear ($E_{p,c} \approx$ 0.0 V vs. SCE). Hence the diazonium cation moiety of the NBD has reacted during printing. These results are consistent with the attachment of NP groups to the spontaneously formed CP layer upon printing with NBD.

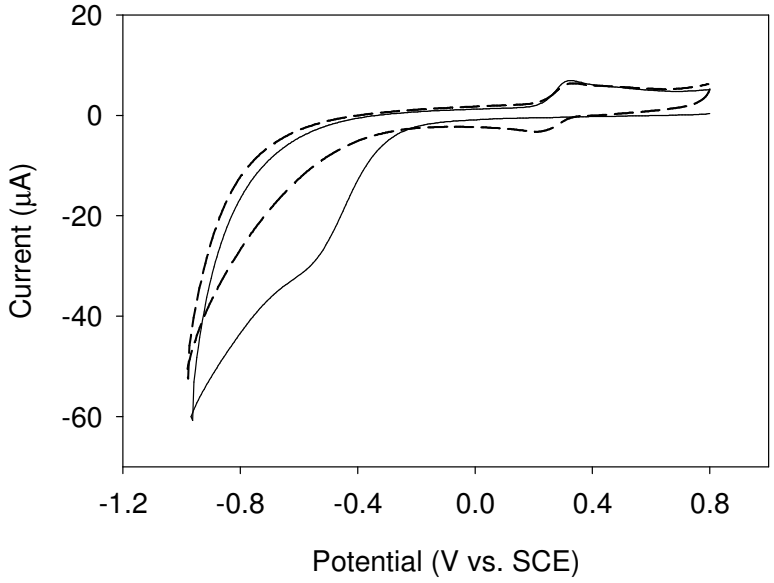

Figure 6.12. Consecutive cyclic voltammograms recorded in 0.1 M H_2SO_4 of PPF surface immersed in 10 mM CBD/0.1 M H_2SO_4 and subsequently printed for 30 minutes with 20 mM NBD/1 M H_2SO_4; first scan (—) and second scan (---).

AFM film thickness measurements were carried out in both regions of both samples. After an initial determination, the samples were sonicated in ACN for 30 minutes and the measurements were repeated to test the stability of the layers. The results are tabulated in Table 6.6.

Table 6.6. Film thickness (determined by AFM) of PPF substrates immersed in CBD and subsequently printed with NBD on approximately half the sample. Thicknesses were determined for both regions after sonication in H_2O for 5 minutes and after additional sonication in ACN for 30 minutes.

		Film Thickness (nm)		
Sonication	Sample	CBD only region	CBD+NBD region	Change
H_2O (5 min)	1	1.6 (± 0.3)	2.2 (± 0.3)	0.6
	2	1.4 (± 0.3)	2.1 (± 0.2)	0.7
H_2O (5 min)+	1	1.7 (± 0.6)	2.1 (± 0.3)	0.4
ACN (30 min)	2	1.5 (± 0.4)	2.0 (± 0.2)	0.5

After the standard post modification sonication procedure (five minutes in H_2O) the regions of the PPF that had only been immersed in CBD (no NBD printing) had a film thickness of ~1.5 nm while the areas in which NBD was printed on the CP film had a thickness of ~2.1 nm. The increase of ~ 0.6 nm upon printing NBD is consistent with a layer of NP groups attached on top of the spontaneously prepared CP film. After sonication in ACN for 30 minutes the CP-only areas had a film thickness of ~1.6 nm, while the thickness of the areas where NBD was printed on the CP film were found to be ~ 2.0 nm. These results show that the multi component surfaces prepared by the build-up method using μCP are stable to extended sonication. Stability to extended sonication is taken as evidence for covalent attachment.

Patterning using the build-up approach was investigated by printing an AP film on an underlying CP layer. AP was chosen since it assembles citrate-capped gold nanoparticles, which can be detected very easily by SEM. Primary layers were prepared by immersing PPF substrates in 10 mM CBD/0.1 M H_2SO_4 for 30 minutes. These surfaces were printed for 30 minutes with 20 mM ABD/0.5 M HCl using patterned stamps, immersed in a solution of citrate-capped gold nanoparticle for 40 minutes, and then sonicated in H_2O for 30 seconds prior to SEM analysis.

Blanks were prepared in the same manner except that printing was carried out with 0.5 M HCl (no ABD present).

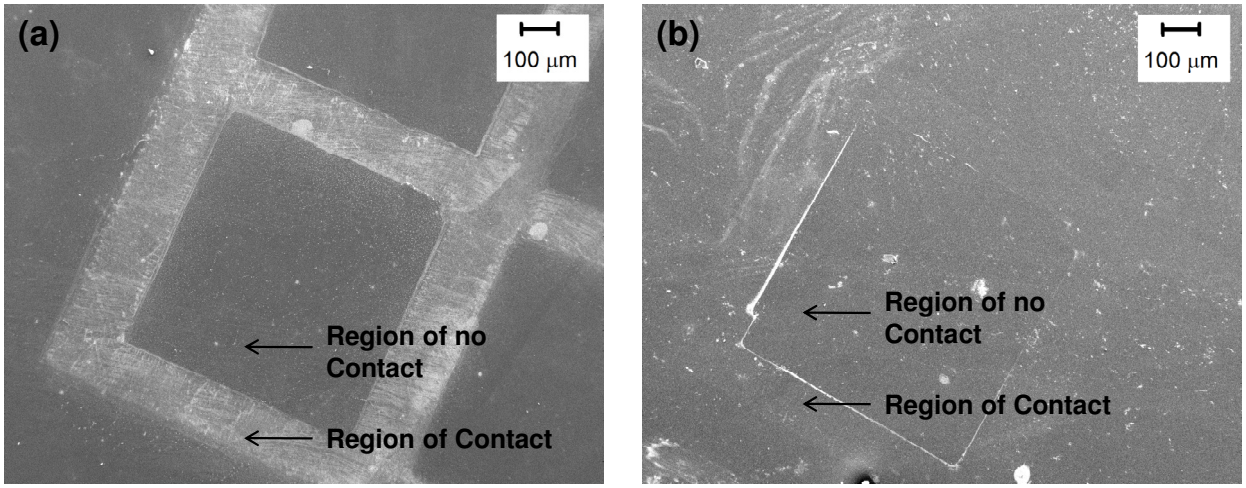

Figure 6.13. SEM images of surfaces that were immersed in 10 mM CBD/0.1 H_2SO_4 for 30 minutes and subsequently printed with 20 mM ABD/0.5 M HCl (a) and 0.5 M HCl (b). After printing the surfaces were immersed in gold nanoparticle solution for 40 minutes and then sonicated in H_2O for 30 seconds.

Figure 6.13 shows SEM images of PPF surfaces after immersion in CBD and printing with 20 mM ABD/0.5 M HCl (a) and 0.5 M HCl (b). Significant gold nanoparticle assembly was observed in the areas where the ABD-inked stamp had made contact with the surface (Figure 6.13 (a)) but not in the areas printed with only 0.5 M HCl (Figure 6.13 (b). This is consistent with the assembly of negatively charged citrate capped gold nanoparticles on a protonated AP film. The results indicate that multicomponent patterns, with specific chemical functionalities in different regions of the surface, can be formed by μCP using the build-up methodology.

6.7 Microcontact Printing on Gold

In Chapter 5, the reaction of aryldiazonium salts with gold surfaces was demonstrated to proceed spontaneously at OCP. In the present section, the application of the reaction to μCP of gold surfaces using aryldiazonium salts is described.

6.7.1 Printing of NP Films

The effect of printing time on the surface concentration of electro-active NP groups, Γ_{NP} was investigated by printing Au/NiCr/Si substrates with non-patterned stamps using a 20 mM NBD/1 M H_2SO_4 solution and printing times of 5, 10, 20, 30 and 60 minutes. Consecutive cyclic voltammograms were recorded between 0.6 and -1.2 V vs. SCE in 0.1 M $NaClO_4$ in EtOH-H_2O (1:9 by volume) from an initial potential of 0.6 V. The irreversible NP reduction was observed at approximately -0.9 V vs. SCE for all printed samples. The reversible APOH/nitrosophenyl redox couple appeared at approximately -0.3 V vs. SCE (Figure 6.14). Hence it can be concluded that NP functionalities are present at the surfaces after printing. During the first scans of the cyclic voltammograms no reduction peak was observed at ~0.17 V vs. SCE where reduction of the NBD's diazonium cation moiety would have been expected. This indicates that the diazonium cation substituent has reacted during printing, and is consistent with covalent modification.

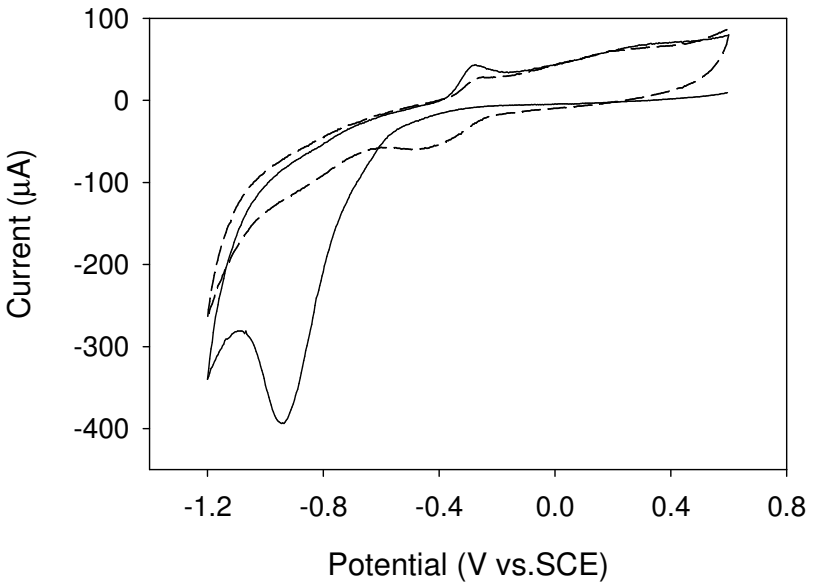

Figure 6.14. Consecutive cyclic voltammograms in 0.1 M $NaClO_4$/EtOH-H_2O (1:9 by volume) of a Au/NiCr/Si substrate printed with 20 mM NBD/1 M H_2SO_4 for 30 minutes; first scan (—) and second scan (---). Initial potential = 0.6 V vs. SCE. Scan rate = 100 mV s^{-1}.

The surface concentrations of electro-active NP groups, $\Gamma_{NP,}$ on Au/NiCr/Si substrates printed with 20 mM NBD/1 M H_2SO_4 were calculated from the corresponding cyclic voltammograms as

described in Section 3.3.3, and are shown in Figure 6.15 as a plot against printing time. Γ_{NP} increases to maximum of ~12 × 10^{-10} mol cm^{-2} after 30 minutes, but no further increase is observed when the printing time is extended to 60 minutes. This behavior is qualitatively similar to that observed in Section 5.3.2 for the same substrate, where Γ_{NP} reached a maximum of ~14 × 10^{-10} mol cm^{-2} after 60 minutes immersion in 10 mM NBD/0.1 M H_2SO_4 with no further increase thereafter. The fact that the maximum is reached more quickly for the printed samples could be due to the greater NBD and/or H_2SO_4 concentrations. Considering the results depicted in Figure 6.15, and to ensure the formation substantial films that could be easily detected by SEM, a printing time of 30 minutes was used for all further printing on gold surfaces.

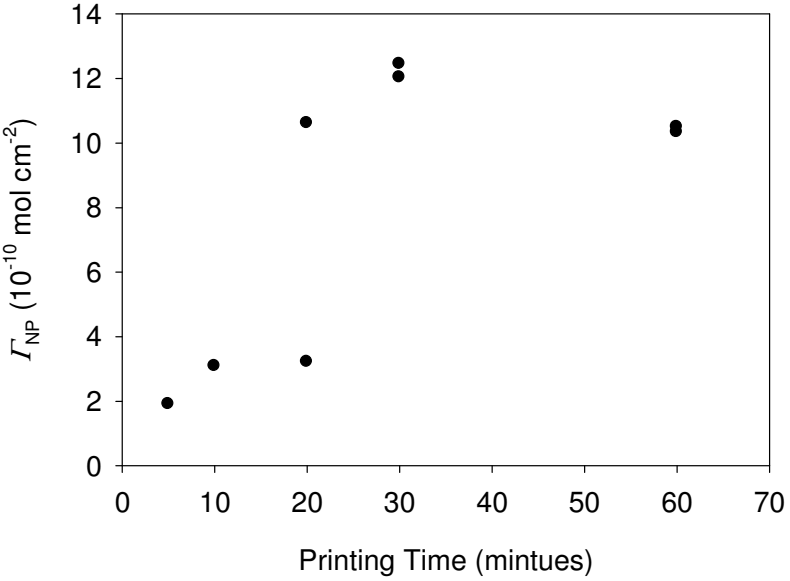

Figure 6.15. Plot of Γ_{NP} vs. printing time for Au/NiCr/Si substrates printed with 20 mM NBD/1 M H_2SO_4. There are two nearly coincident points at $\Gamma_{NP} \approx 10.5 \times 10^{-10}$ mol cm^{-2} and 60 minutes immersion time.

6.7.2 Patterning of Gold Surfaces

Au/NiCr/Si substrates were printed with patterned stamps using an inking solution containing 20 mM of one of three diazonium salts: NBD, CBD and *in situ*-prepared ABD. The NBD and CBD inking solutions were prepared by dissolving the diazonium salts in 1 M H_2SO_4. The ABD

solution was generated *in situ* in 0.5 M HCl as described in Section 6.2. Blanks were prepared by printing with 1 M H_2SO_4 and 0.5 M HCl.

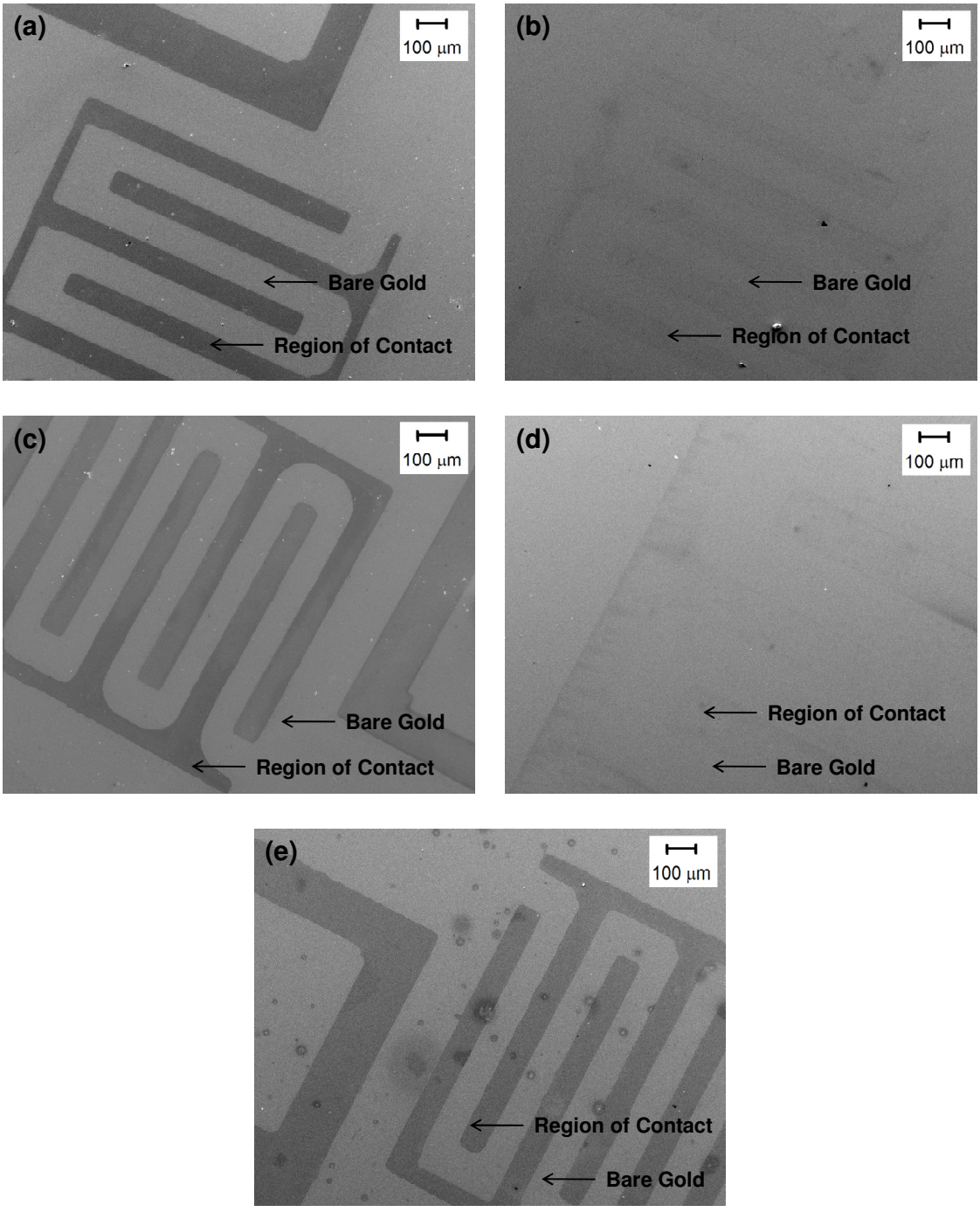

Figure 6.16. SEM images of Au/NiCr/Si substrates printed with patterned stamps using inking solutions of 20 mM NBD/1M H_2SO_4 (a), 1 M H_2SO_4 (b), 20 mM ABD/0.5 M HCl (c), 0.5 M HCl (d), 20 mM CBD/1 M H_2SO_4 (e). A printing time of 30 minutes was used.

SEM images after printing with diazonium inks (Figure 6.16 (a), (c) and (e)) showed strong contrast between the bare gold surface and the areas where the stamp had made contact with the surface. This gives strong evidence that modification occurs only in the stamped areas. Surfaces printed with blank 1 M H_2SO_4 (Figure 6.16 (b)) or 0.5 M HCl (Figure 6.16 (d)) showed only very faint patterns, probably due to solvent and/or PDMS residues.

6.8 Microcontact Printing of Silicon

The modification of hydrogen-terminated silicon by spontaneous reaction with aryldiazonium salts has been demonstrated by Tour and coworkers.[41] In principle, μCP of silicon using aryldiazonium salts should therefore be possible, and experiments were undertaken to test this. Preliminary experiments focused on the spontaneous modification of Si by immersion in NBD/0.1 M H_2SO_4 solution. Subsequently, μCP of Si with aryldiazonium salts was investigated.

6.8.1 Spontaneous Modification of Silicon with NP Films

The spontaneous reaction of NBD with Si was investigated with both high-conductivity (Si_{HC}) and low-conductivity (Si_{LC}) silicon (specifications in Section 6.2). After HF treatment (see Section 6.2), two samples of each type were immersed in 10 mM NBD/0.1 M H_2SO_4 for 240 minutes. AFM measurements gave film thicknesses of (4.2 ± 0.7) and (4.2 ± 0.6) nm for the two Si_{HC} surfaces, and (4.6 ± 1.1) and (4.5 ± 0.6) nm for the two Si_{LC} substrates. These results indicate that multilayer films are formed under the conditions used here, and that the differing conductivity of the two Si types does not significantly affect the thicknesses of the films.

6.8.2 Printing of NP Films on Silicon

A Si_{LC} substrate was printed for 30 minutes with a non-patterned stamp using an inking solution of 20 mM NBD/1 M H_2SO_4. AFM measurements indicated the presence of a (3.1 ± 0.4) nm thick

film, slightly thinner than that found upon immersion of Si substrates in NBD solution for 240 minutes. The lower film thickness for the film formed by printing, than for those formed by immersion in solution, can be accounted for by the shorter reaction time used for the sample prepared by printing.

6.8.3 Patterning of Silicon Surfaces

Patterning of Si_{LC} was carried out with pattered stamps using 20 mM NBD/1 M H_2SO_4 and 20 mM ABD/ 0.5 M HCl ink solutions and a printing time of 30 minutes. Corresponding blanks were prepared by printing with 1 M H_2SO_4 and 0.5 M HCl for 30 minutes.

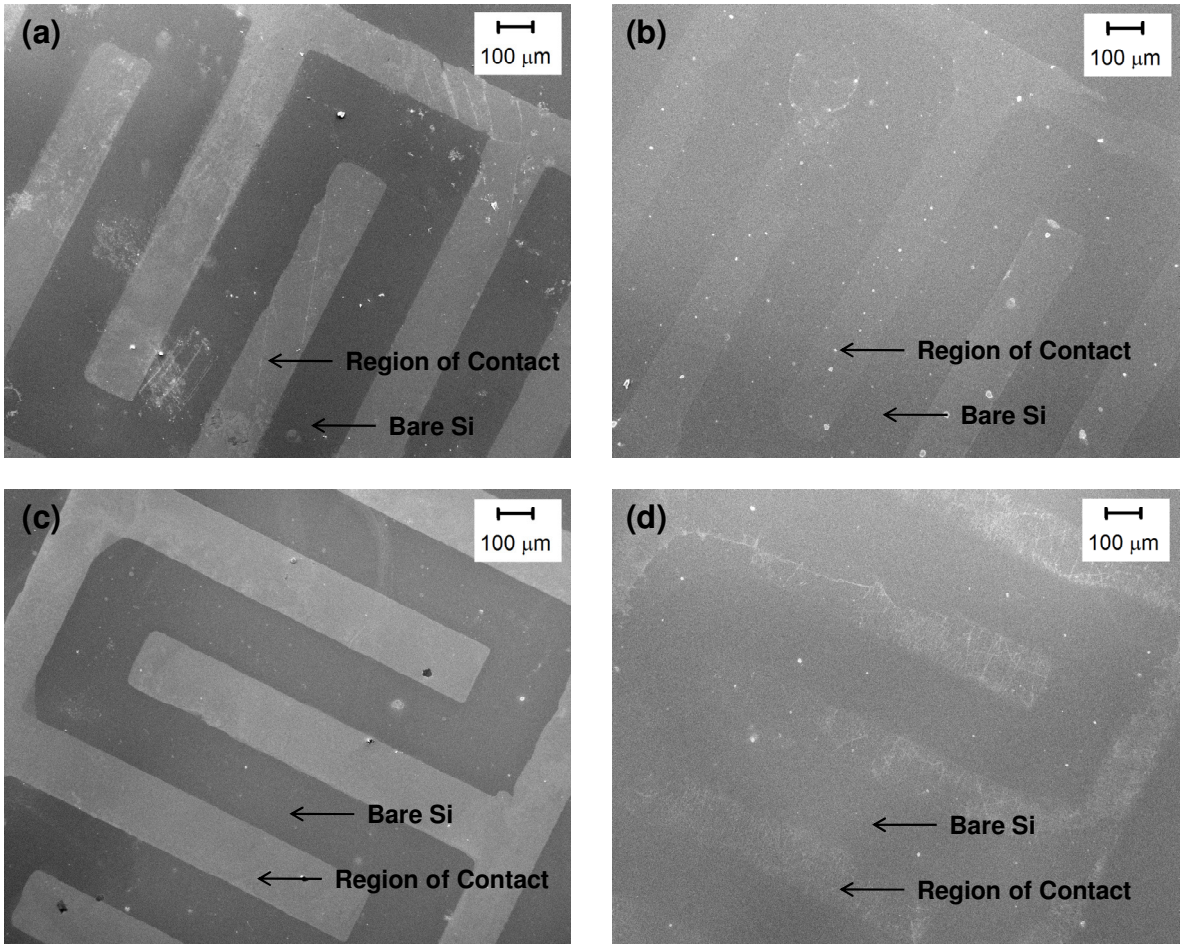

Figure 6.17. SEM images of Si_{LC} substrates printed for 30 minutes with patterned stamps using inking solutions of 20 mM NBD/1M H_2SO_4 (a), 1 M H_2SO_4 (b), 20 mM ABD/0.5 M HCl (c), and 0.5 M HCl (d).

The SEM images of surfaces printed with ink containing NBD (Figure 6.17 (a)) or ABD (Figure 6.17 (c)) show clear patterns matching the features on the stamp. Those for "blank" 1 M H_2SO_4 (Figure 6.17 (b) or 0.5 M HCl (Figure 6.17 (d)) showed very faint patterns, possibly due to solvent and/or PDMS residues. These results indicate μCP had been successful, with modification having occurred only in the regions where the stamp has made contact with the surface.

6.9 Microcontact Printing on Copper

One of the attractive features of μCP using aryldiazonium salts is that it should be applicable to a large number of different substrates due to the high reactivity of aryldiazonium salts. The modification of copper via spontaneous reaction with NBD has been demonstrated by other workers.[42, 43] Accordingly, the μCP of copper using NBD was investigated here to further demonstrate this versatility of the method.

Native copper oxide was removed from the surface prior to printing, as described in Section 6.2. Printing was undertaken with patterned stamps using a 20 mM NBD/1 M H_2SO_4 inking solution and a printing time of 30 minutes. Blanks were prepared in the same manner, except by printing with 1 M H_2SO_4 (no NBD).

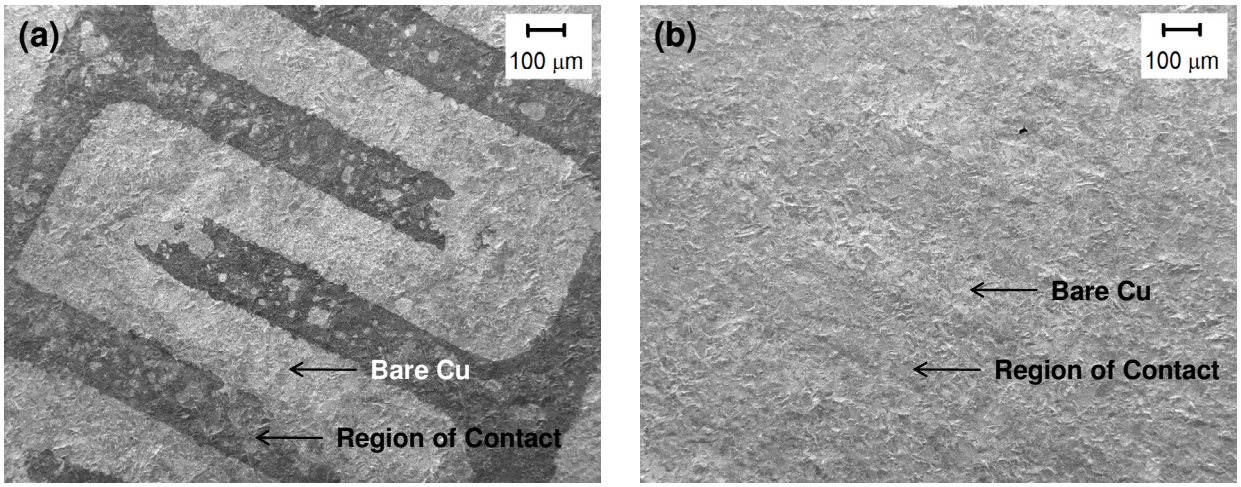

Figure 6.18. SEM images of Cu substrates printed with stamps with features using inking solutions of 20 mM NBD/1M H_2SO_4 (a) and 1 M H_2SO_4 (b). A printing time of 30 minutes was used.

Figure 6.18 (a) shows that a distinct pattern in the SEM image of Cu that was printed with 20 mM NBD/1M H_2SO_4. In contrast, when printing was carried out using 1 M H_2SO_4 only, very faint patterns were seen on the surface (Figure 6.18 (b)). This indicates that the μCP of copper with NBD is successful. However, the NP films formed by printing were inhomogeneous, containing defects that are visible in the SEM image. This can be accounted for by the high surface roughness of the copper, which permits only partial contact of the patterns on the stamp with the surface. It demonstrates that surfaces selected for printing must be sufficiently smooth for consistent transfer of the modifier to the surface.

6.10 Conclusion

In this chapter microcontact printing using aryldiazonium salts has been demonstrated at carbon, gold, silicon and copper surfaces. The majority of the work focused on printing of carbon (PPF) substrates with diazonium salts, primarily due to the strength of the C-C bond formed between the modifier and the surface, an attractive feature for many applications.

Modification of PPF with NP films by printing of NBD was confirmed by cyclic voltammetry and AFM film thickness measurements. The surface concentrations, film thicknesses and film densities on carbon substrates were found to be highly irreproducible. SEM visualization of NP patterns on PPF demonstrated that patterning was successful. The selective assembly of citrate-capped gold nanoparticles on a printed AP pattern on PPF was also observed by SEM. Printing of CP films on PPF was demonstrated by water contact angle and AFM film thickness measurements. Successful coupling of *p*-nitroaniline to the activated CP film was confirmed by cyclic voltammetry, AFM film thickness measurements and contact angle measurements. This demonstrates that printed CP films are suitable for coupling reactions, making them relevant to applications involving the tethering of molecules to patterned surfaces.

The formation of multi- (two-) component films by μCP of aryldiazonium salts was investigated using two methods. The fill-in method, proved to be problematic due to reaction of the second modifier in the regions where the first had been printed. The second, build-up, method proved

more promising, with evidence of different chemical functionalities located in different areas of the surface. Furthermore, both modifiers were attached to the surface, remaining after prolonged sonication in ACN. Future work could focus on determining whether coupling reactions will occur selectively to particular regions of the surface.

Patterning by μCP using aryldiazonium salts was shown to be successful at gold, silicon and copper substrates; and, in principle it should be applicable at a large range of other conducting and semiconducting surfaces. This is one of the primary advantages of patterning by μCP using aryldiazonium salts rather than thiols.

6.11 References

1. Xia, Y. N.; Whitesides, G. M., Soft lithography. *Angew. Chem., Int. Ed.* **1998,** 37, 551-575.

2. Quist, A. P.; Pavlovic, E.; Oscarsson, S., Recent advances in microcontact printing. *Anal. Bioanal. Chem.* **2005,** 381, 591-600.

3. Perl, A.; Reinhoudt, D. N.; Huskens, J., Microcontact Printing: Limitations and Achievements. *Adv. Mater.* **2009,** 21, 2257-2268.

4. Kumar, A.; Whitesides, G. M., Features of Gold Having Micrometer to Centimeter Dimensions Can Be Formed through a Combination of Stamping with an Elastomeric Stamp and an Alkanethiol Ink Followed by Chemical Etching. *Appl. Phys. Lett.* **1993,** 63, 2002-2004.

5. Kumar, A.; Biebuyck, H. A.; Whitesides, G. M., Patterning Self-Assembled Monolayers - Applications in Materials Science. *Langmuir* **1994,** 10, 1498-1511.

6. Singhvi, R.; Kumar, A.; Lopez, G. P.; Stephanopoulos, G. N.; Wang, D. I. C.; Whitesides, G. M.; Ingber, D. E., Engineering Cell-Shape and Function. *Science* **1994,** 264, 696-698.

7. Kumar, A.; Whitesides, G. M., Patterned Condensation Figures as Optical Diffraction Gratings. *Science* **1994,** 263, 60-62.

8. Biebuyck, H. A.; Whitesides, G. M., Autophobic Pinning of Drops of Alkanethiols on Gold. *Langmuir* **1994,** 10, 4581-4587.

9. Xia, Y. N.; Whitesides, G. M., Use of Controlled Reactive Spreading of Liquid Alkanethiol on the Surface of Gold to Modify the Size of Features Produced by Microcontact Printing. *J. Am. Chem. Soc.* **1995,** 117, 3274-3275.

10. Wilbur, J. L.; Biebuyck, H. A.; Macdonald, J. C.; Whitesides, G. M., Scanning Force Microscopies Can Image Patterned Self-Assembled Monolayers. *Langmuir* **1995,** 11, 825-831.

11. Jackman, R. J.; Wilbur, J. L.; Whitesides, G. M., Fabrication of Submicrometer Features on Curved Substrates by Microcontact Printing. *Science* **1995,** 269, 664-666.

12. Xia, Y. N.; Whitesides, G. M., Reduction in the Size of Features of Patterned SAMs Generated by Microcontact Printing with Mechanical Compression of the Stamp. *Adv. Mater.* **1995,** 7, 471-473.

13. Kim, E.; Whitesides, G. M.; Freiler, M. B.; Levy, M.; Lin, J. L.; Osgood, R. M., Fabrication of micrometer-scale structures on GaAs and GaAs/AlGaAs quantum well material using microcontact printing. *Nanotechnology* **1996,** 7, 266-269.

14. Wilbur, J. L.; Kumar, A.; Biebuyck, H. A.; Kim, E.; Whitesides, G. M., Microcontact printing of self-assembled monolayers: Applications in microfabrication. *Nanotechnology* **1996,** 7, 452-457.

15. Xia, Y.; Kim, E.; Whitesides, G. M., Microcontact printing of alkanethiols on silver and its application in microfabrication. *J. Electrochem. Soc.* **1996,** 143, 1070-1079.

16. Xia, Y. A.; Venkateswaran, N.; Qin, D.; Tien, J.; Whitesides, G. M., Use of electroless silver as the substrate in microcontact printing of alkanethiols and its application in microfabrication. *Langmuir* **1998,** 14, 363-371.

17. Xia, Y. N.; Kim, E.; Mrksich, M.; Whitesides, G. M., Microcontact printing of alkanethiols on copper and its application in microfabrication. *Chem. Mater.* **1996,** 8, 601-&.

18. Wolfe, D. B.; Love, J. C.; Paul, K. E.; Chabinyc, M. L.; Whitesides, G. M., Fabrication of palladium-based microelectronic devices by microcontact printing. *Appl. Phys. Lett.* **2002,** 80, 2222-2224.

19. Carvalho, A.; Geissler, M.; Schmid, H.; Michel, B.; Delamarche, E., Self-assembled monolayers of eicosanethiol on palladium and their use in microcontact printing. *Langmuir* **2002,** 18, 2406-2412.

20. Xia, Y. N.; Mrksich, M.; Kim, E.; Whitesides, G. M., Microcontact Printing of Octadecylsiloxane on the Surface of Silicon Dioxide and Its Application in Microfabrication. *J. Am. Chem. Soc.* **1995,** 117, 9576-9577.

21. Wilhelm, T.; Wittstock, G., Generation of periodic enzyme patterns by soft lithography and activity imaging by scanning electrochemical microscopy. *Langmuir* **2002,** 18, 9485-9493.

22. Kane, R. S.; Takayama, S.; Ostuni, E.; Ingber, D. E.; Whitesides, G. M., Patterning proteins and cells using soft lithography. *Biomaterials* **1999,** 20, 2363-2376.

23. Mrksich, M.; Dike, L. E.; Tien, J.; Ingber, D. E.; Whitesides, G. M., Using microcontact printing to pattern the attachment of mammalian cells to self-assembled monolayers of alkanethiolates on transparent films of gold and silver. *Exp. Cell Res.* **1997,** 235, 305-313.

24. Chen, C. S.; Mrksich, M.; Huang, S.; Whitesides, G. M.; Ingber, D. E., Geometric control of cell life and death. *Science* **1997,** 276, 1425-1428.

25. Endler, E. E.; Duca, K. A.; Nealey, P. F.; Whitesides, G. M.; Yin, J., Propagation of viruses on micropatterned host cells. *Biotechnol. Bioeng.* **2003,** 81, 719-725.

26. Grace, A. N.; Pandian, K., A polypyrrole/polymethylene pattern on gold using a micro-contact printing technique. *J. Solid State Electrochem.* **2003,** 7, 296-300.

27. Brondijk, J. J.; Li, X.; Akkerman, H. B.; Blom, P. W. M.; de Boer, B., Microcontact printing of self-assembled monolayers to pattern the light-emission of polymeric light-emitting diodes. *Applied Physics a-Materials Science & Processing* **2009,** 95, 1-5.

28. Brooksby, P. A.; Downard, A. J., Nanoscale patterning of flat carbon surfaces by scanning probe lithography and electrochemistry. *Langmuir* **2005,** 21, 1672-1675.

29. Downard, A. J.; Garrett, D. J.; Tan, E. S. Q., Microscale patterning of organic films on carbon surfaces using electrochemistry and soft lithography. *Langmuir* **2006,** 22, 10739-10746.

30. Cougnon, C.; Gohier, F.; Belanger, D.; Mauzeroll, J., In Situ Formation of Diazonium Salts from Nitro Precursors for Scanning Electrochemical Microscopy Patterning of Surfaces. *Angew. Chem., Int. Ed.* **2009,** 48, 4006-4008.

31. Charlier, J.; Palacin, S.; Leroy, J.; Del Frari, D.; Zagonel, L.; Barrett, N.; Renault, O.; Bailly, A.; Mariolle, D., Local silicon doping as a promoter of patterned electrografting of diazonium for directed surface functionalization. *J. Mater. Chem.* **2008,** 18, 3136-3142.

32. Charlier, J.; Clolus, E.; Bureau, C.; Palacin, S., Localized organic grafting on photosensitive semiconductors substrates. *J. Electroanal. Chem.* **2008,** 622, 238-241.

33. Lee, J. N.; Park, C.; Whitesides, G. M., Solvent compatibility of poly(dimethylsiloxane)-based microfluidic devices. *Anal. Chem.* **2003,** 75, 6544-6554.

34. Langowski, B. A.; Uhrich, K. E., Oxygen plasma-treatment effects on Si transfer. *Langmuir* **2005,** 21, 6366-6372.

35. Olander, B.; Wirsen, A.; Albertsson, A. C., Oxygen microwave plasma treatment of silicone elastomer: Kinetic behavior and surface composition. *J. Appl. Polym. Sci.* **2004,** 91, 4098-4104.

36. Baranton, S.; Belanger, D., Electrochemical derivatization of carbon surface by reduction of in situ generated diazonium cations. *J. Phys. Chem. B* **2005,** 109, 24401-24410.

37. Lyskawa, J.; Belanger, D., Direct modification of a gold electrode with aminophenyl groups by electrochemical reduction of in situ generated aminophenyl monodiazonium cations. *Chem. Mater.* **2006,** 18, 4755-4763.

38. Adenier, A.; Barre, N.; Cabet-Deliry, E.; Chausse, A.; Griveau, S.; Mercier, F.; Pinson, J.; Vautrin-Ul, C., Study of the spontaneous formation of organic layers on carbon and metal surfaces from diazonium salts. *Surf. Sci.* **2006,** 600, 4801-4812.

39. Yu, S. C., *PhD thesis: covalent attachment of nanoscale organic films to carbon electrodes*. University of Canterbury: 2008.

40. Perring, M.; Dutta, S.; Arafat, S.; Mitchell, M.; Kenis, P. J. A.; Bowden, N. B., Simple methods for the direct assembly, functionalization, and patterning of acid-terminated monolayers on Si(111). *Langmuir* **2005,** 21, 10537-10544.

41. Stewart, M. P.; Maya, F.; Kosynkin, D. V.; Dirk, S. M.; Stapleton, J. J.; McGuiness, C. L.; Allara, D. L.; Tour, J. M., Direct covalent grafting of conjugated molecules onto Si, GaAs, and Pd surfaces from aryidiazonium salts. *J. Am. Chem. Soc.* **2004,** 126, 370-378.

42. Hurley, B. L.; McCreery, R. L., Covalent bonding of organic molecules to Cu and Al alloy 2024 T3 surfaces via diazonium ion reduction. *J. Electrochem. Soc.* **2004,** 151, B252-B259.

43. Chamoulaud, G.; Belanger, D., Spontaneous derivatization of a copper electrode with in situ generated diazonium cations in aprotic and aqueous media. *J. Phys. Chem. C* **2007,** 111, 7501-7507.

Chapter 7. Covalent Attachment of Glucose Oxidase Hydrogel to Carbon Electrodes

7.1 Introduction

The development of miniaturized implantable medical devices, designed to monitor certain physiological conditions, has been an area of significant research in recent years.[1-3] These developments have produced a need for implantable power sources to drive the devices. One solution is the use of miniaturized batteries (galvanic cells). However, due to the toxicity of the chemicals involved, protective casings and seals are required, making battery miniaturization technically difficult and expensive. Furthermore, batteries cannot operate indefinitely and require regular replacement or recharging. An alternative solution is bio-fuel cells, which convert chemicals prevalent in biological systems into electrical energy via biocatalytic redox reactions.[1-3]

A generalized schematic of a bio-fuel cell is shown in Figure 7.1.[4-8] The cell consists of anodic and a cathodic components. At the anode, a catalyst (Cat 1) oxidizes a substrate (Sub 1) and is thereby reduced. Subsequent regeneration of the oxidized form of the catalyst results in donation of electrons to the anode via a redox mediator (Med 1). At the cathode a different catalyst (Cat 2) reduces another substrate (Sub 2) and is thereby oxidized. Cat 2 is regenerated in its reduced form by accepting electrons from the cathode via a redox mediator (Med 2). Since the substrates are species prevalent in biological systems, the catalysts are generally enzymes. The mediators are ideally carefully tailored complexes that undergo redox reactions at potentials that facilitate electron transfer between the catalysts and the electrodes and which maximize the voltage supplied by the bio-fuel cell. The catalytic redox processes cause a current to flow from the cathode to the anode. The result is the production of electrical energy which can be used to power electronic devices.

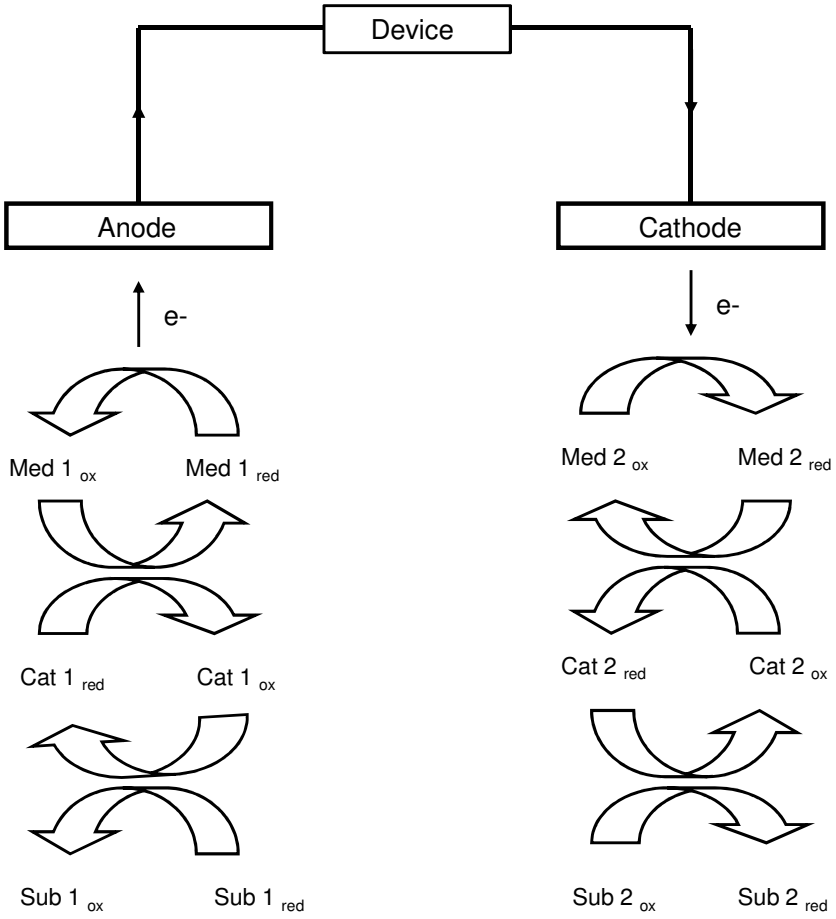

Scheme 7.1. General schematic of catalytic bio-fuel cell.

Assuming that the enzymes and mediators are effectively immobilized on the electrode, and that constant supplies of the substrates are available, a bio-fuel cell can, in principle, operate indefinitely. This eliminates the need for recharging, and hence, makes bio-fuel cells an attractive power source for biomedical implants. Furthermore, if the components of the bio-fuel cell are biocompatible, toxicity issues are avoided.

Immobilization of the enzymes on the electrode surface is often achieved by the incorporation of enzymes into hydrogels. The hydrogel is prepared by depositing a mixture of enzyme and a polymeric crosslinker on the electrode surface. Commonly used crosslinkers are diepoxides, such as poly(ethylene glycol) diglycidyl ether (PEGDGE). The crosslinking process consists of the reaction of the epoxide groups with primary amine functionalities of the enzyme (Scheme 7.2).

Redox mediators containing substituents that react with the crosslinker can also be incorporated into the hydrogel matrix.[4, 7, 9-15]

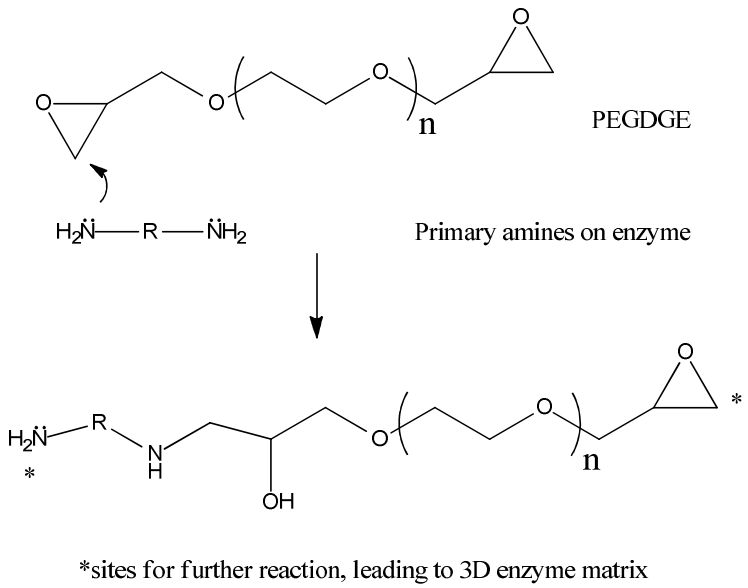

Scheme 7.2. Reaction between epoxide functionalities of PEGDGE and primary amines of an enzyme leading to the formation of a 3-dimensional enzyme hydrogel matrix.

Significant work on the fabrication of enzymatic hydrogel bio-fuel cells has been undertaken by Heller and coworkers.[3-7, 9, 10, 12-14, 16-19] Anodes have been fabricated by producing hydrogels incorporating glucose oxidase (GOx),[3-6, 9] which can oxidize glucose to gluconolactone. The preparation of cathodes has focused on the incorporation of enzymes such as bilirubin oxidase[4, 7, 12, 13] and laccase[5, 6] into hydrogels. These enzymes can reduce O_2 to H_2O by accepting electrons from the cathode. Anodic and cathodic hydrogel electrodes have been used to fabricate prototype bio-fuel cells,[3, 5-7, 14, 18, 19] and a miniature glucose oxidase/bilirubin oxidase bio-fuel cell has been demonstrated to operate inside a living plant.[4]

Barrière, Leech and coworkers have been developing and optimizing a glucose oxidase/laccase bio-fuel cell by tailoring redox mediators to maximize power output.[8] A prototype bio-fuel cell has been reported to operate in physiological buffer,[20] but with poor stability over time. A possible source of the instability is the leaching of enzymes and mediators from the hydrogel electrodes. Hence, a collaboration (reported here) was undertaken with Barrière and his group

with the aim of fabricating electrodes where the enzyme hydrogel is covalently bound to a carbon surface via modification involving aryldiazonium cation chemistry.

Previously, Barrière and coworkers have investigated covalently bound GOx hydrogels.[11] Their first preparation step was to modify GC electrodes with carboxylic acid terminated films (Scheme 7.3, n = 1, 2 and 3). Subsequently, carboxylic acid functionalities were activated and coupled to GOx. A GOx/PEGDGE crosslinker mixture was then deposited on the GOx modified electrode, resulting in crosslinking between the deposited PEGDGE and the amine terminated groups on the covalently coupled enzyme. The covalently bound hydrogels were reported to exhibit better long term stability than those which were physisorbed on the GC surface.[11]

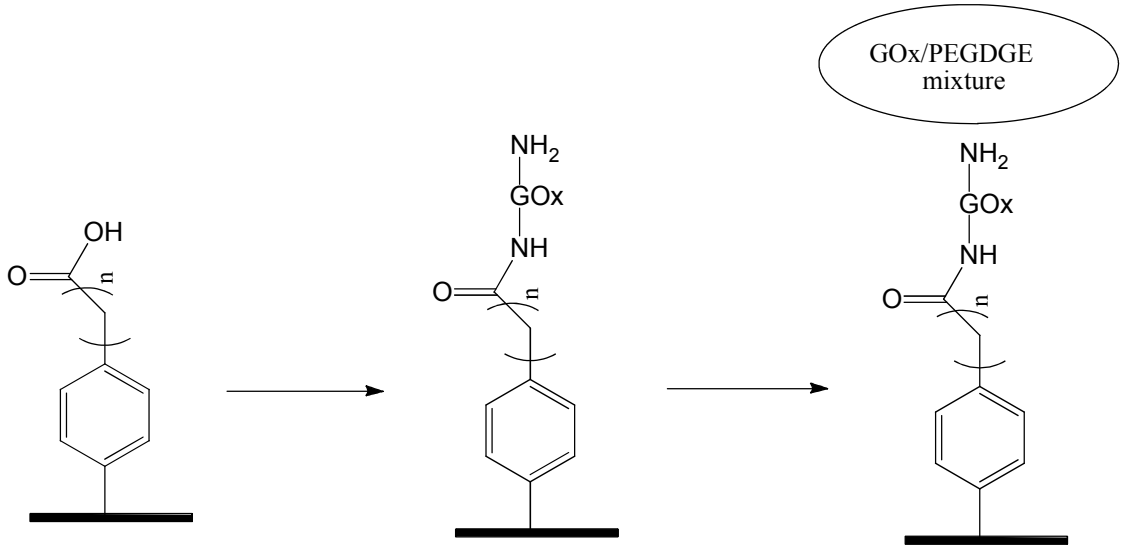

Scheme 7.3. Strategy used by Barrière and workers for covalent immobilization of GOx hydrogel.[11]

In another investigation, published after the work described in this chapter was completed, Leech and coworkers reported the modification of carbon electrodes with *p*-aminophenyl (AP) films using diazonium cation chemistry.[15] A GOx/PEGDGE crosslinker mixture (also containing a redox mediator) was deposited on the AP modified electrodes. They postulated that the surface-bound AP groups would react with the PEGDGE crosslinker, thereby rendering the hydrogel covalently bound to the surface (Scheme 7.4). These covalently bound hydrogels exhibited better long term stability than those physisorbed on the GC surface.[15]

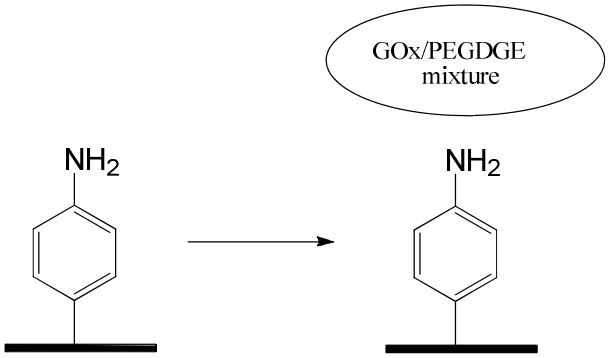

Scheme 7.4. Strategy used by Leech and coworkers to covalently GOx hydrogels.

The aim of the current chapter is threefold. Firstly to determine the factors that affect the activity and long-term stability of physisorbed GOx hydrogels at carbon electrodes, and to use the resulting data to optimize the performance of the physisorbed hydrogels. Secondly, to find evidence as to whether the immobilization methods depicted in schemes 7.3 and 7.4 really lead to covalent attachment of the hydrogel to the modified electrode. Thirdly, to investigate whether covalently bound GOx hydrogels exhibit better long-term stability than optimized physisorbed hydrogels.

7.2 Experimental

7.2.1 Materials and Reagents

The following chemicals were purchased from Sigma-Aldrich: glucose oxidase (GOx) type II-S from *Aspergillus niger*, polyoxyethylene bis(diglycidylether) (PEGDGE) of average MW ~ 526 g mol^{-1}, ferrocenemethanol, *N*-hydroxysuccinimide (NHS), *N*-ethyl-*N*'-(3-dimethylaminopropyl) diimide hydrochloride (EDC). 0.1 M phosphate buffer (PB) pH 7.4 was prepared as described in Section 2.2.1 and was used for all PB solutions.

7.2.2. Preparation of Hydrogels

The GOx/PEGDGE hydrogel electrodes were prepared by depositing 10 μL drops of a GOx-PEGDGE/PB solution onto the electrode surfaces (GC plates, GC rods, and PPF). The solution contained 300 μL of 8 mg mL^{-1} GOx/PB solution and 120 μL of 2 mg mL^{-1} PEGDGE/PB solution. The drops were left to cure (dry and react) for a designated time period in a temperature controlled room at (25 ± 2) ºC in the absence of light. After curing, hydrogels ~5.5 mm in diameter, were present on the GC plate and PPF surfaces.

7.2.3. Immersion of Hydrogel Electrodes Samples in Phosphate Buffer

Cured hydrogel electrodes made using PPF samples and GC plates were immersed in 20 mL PB in a 50 mL beaker with the modified side of the electrode oriented upwards. Those made using GC rods were suspended in 20 mL PB in a large vial with the modified side facing downwards. The samples were placed on an orbital shaker and agitated at 50 rpm for 24 hours at (25 ± 2) ºC in the absence of light. This procedure was undertaken immediately after curing and preceded all electrochemical measurements. After each electrochemical measurement samples were immersed in a fresh solution of PB. Stability measurements involving prolonged immersion in PB were carried out under the same immersion conditions.

7.2.4 Electrochemical Determination of Enzymatic Activity

Electrodes were mounted in electrochemical cells as described in Section 2.4.2. For PPF substrates and GC plates, a 012 Viton O-ring was used to define the area of the working electrode (~0.71 cm^2). When present, the hydrogel covered ~34 % of this area. Enzymatic activity was determined by first obtaining cyclic voltammograms between -0.1 and 0.4 V vs. SCE in 1.5 mM ferrocene methanol (FcOH)/PB, at a scan rate of 5 mV s^{-1} from an initial potential of -0.1 V. Subsequently, a second cyclic voltammogram was recorded in 1.5 mM

FcOH-0.2 M D-glucose/PB, using the same parameters. The same stock of FcOH was used to prepare both working solutions. The current amplification (CA) of the FcOH redox couple, due to the electrocataytic oxidation of glucose, was calculated as described below.

7.2.5 Modification via Reduction of Aryldiazonium Salts

All surface modifications were carried out in a 1 mM solution of diazonium salt in dry ACN with 0.1 M $[Bu_4N]BF_4$ electrolyte. The geometric area of the working carbon electrodes was defined using a 012 Viton O-ring. After modification, all surfaces were cleaned using the standard sonication procedure (five minutes in H_2O). Electrochemical modification of GC and PPF surfaces with *p*-carboxyphenyl (CP) functionalities was carried out by cycling fives time between 0.35 and -0.7 V (vs. Ag wire) at 20 mV s^{-1} in carboxybenzene diazonium salt (CBD)-0.1 M $[Bu_4N]BF_4$/ACN solution. Electrochemical modification of GC and PPF surfaces with AP films was achieved using a two-step process. Initially, the electrodes were electrochemically modified with *p*-nitrophenyl (NP) groups at a fixed potential of -0.1 V (vs. Ag wire) for 300 s (unless stated otherwise) in a solution of *p*-nitrobenzene diazonium salt (NBD) in 0.1 M $[Bu_4N]BF_4$/ACN. NP reduction was subsequently carried out by cycling twice from 0.6 to -1.2 vs. SCE in 0.1 M H_2SO_4 at 100 mV s^{-1}.

7.2.6 Coupling of GOx to CP Modified Surfaces

CP modified surfaces were activated by immersion in a solution of 30 mM EDC- 90 mM NHS/H_2O for 45 minutes. The electrodes were then rinsed with PB, then transferred to PB solution containing 1 mg mL^{-1} GOx and allowed to react for 180 minutes. The electrodes were rinsed thoroughly with the PB before further analysis.

7.2.7 Step Profilimetry

Determination of hydrogel thickness was carried out by step profilimetry using a Veeco Dektak 150 Profilimeter. The resulting data were processed using Vision (V 9.1.1.6) software. Two PPF-hydrogel samples were prepared for each curing time (24, 48, and 72 hours). After curing, the samples were immersed for 24 hours in PB as described in Section 7.2.3. Subsequently, the samples were dried for 21 days at 25 ºC. Two mutually perpendicular 7 mm long profilimeter scans, passing through the centre of the hydrogel, were recorded across the surface of each sample. These revealed a relatively thick outer ring (~200 μm wide) and a thinner central region. Each scan gave two thickness values for the outer ring and one for the central region. The stated outer thickness value for a particular curing time is the mean of the eight values obtained over the two scans performed on each of the two samples prepared at that curing time. The thickness values for the central regions are the means of four values. The errors are given as two standard deviations of the mean.

7.3 Activity and Stability of Physisorbed GOx Hydrogels

The reaction of PEGDGE with primary amine groups on the GOx is known to take place only after significant drying of the GOx/PEGDGE mixture has occurred.[10] However, tight control over curing times and/or other conditions generally has not been reported in the literature describing the preparation of enzyme/PEGDGE hydrogels.[4, 7, 11-13, 15] In the present section the effect of curing time (under controlled conditions) on the enzymatic activity of physisorbed GOx/PEGDGE hydrogels is investigated, along with the stability of that activity.

7.3.1 Dependence of Catalytic Activity on Glucose Concentration

Initial experiments were aimed at determining an appropriate concentration of D-glucose to use in investigations of hydrogel activity: a concentration at which glucose is in sufficiently large

excess to ensure that small variations in its concentration do not affect the apparent hydrogel activity.

Physisorbed hydrogels were prepared by curing 10 μL drops of GOx/PEGDGE on unmodified PPF samples for 24 hours. Their catalytic activities were determined by recording cyclic voltammograms in 1.5 mM ferrocene methanol (FcOH)/PB by cycling between -0.1 and 0.4 V vs. SCE in both the absence, and presence of serial additions of D-glucose. FcOH mediates the transfer of electrons from the GOx to the electrode surface.

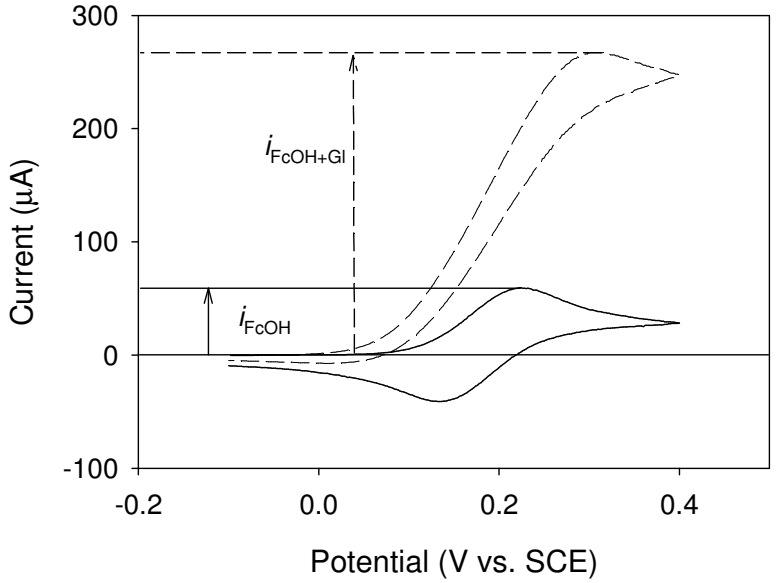

Figure 7.1. Cyclic voltammograms of PPF- GOx/PEGDGE hydrogel (curing time 24 hours) recorded in 1.5 mM FcOH/0.1 M PB pH 7.4 (—) and 0.2 M D-glucose-1.5 mM FcOH/0.1 M PB pH 7.4 (---) from an initial potential of -0.1 V vs. SCE; scan rate = 5 mV s^{-1}.

Figure 7.1 shows typical cyclic voltammograms obtained for a PPF-GOx/PEGDGE hydrogel in FcOH. The currents i_{FcOH} and $i_{FcOH+Gl}$, respectively represent the oxidation currents in the absence (—) and presence of glucose (---).The catalytic activity of the hydrogel is quantified in terms of a current amplification (CA) defined by Equation 7.1.[11]

$$CA = \frac{i_{FcOH+Gl} - i_{FcOH}}{i_{FcOH}} \qquad (7.1)$$

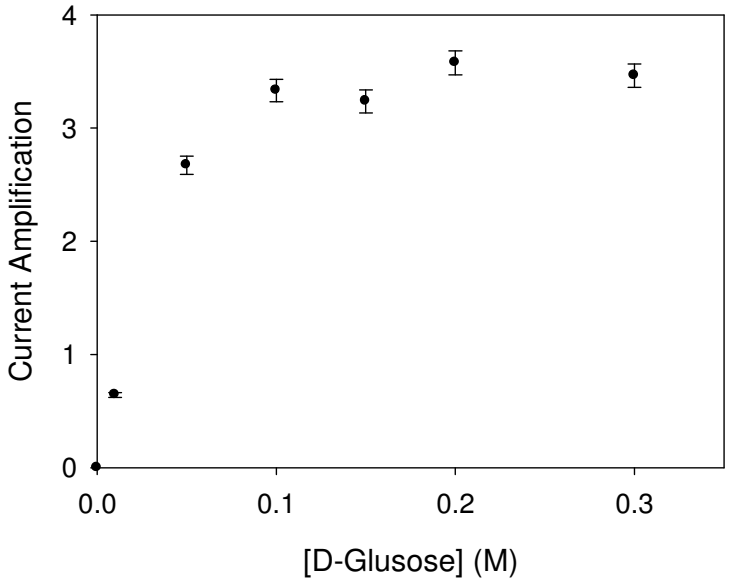

Figure 7.2. Plot of CA vs. [D-Glucose] for a GOx hydrogel physisorbed on a PPF substrate using a curing time of 24 hours.

Figure 7.2 shows that CA increases with the concentration of D-glucose reaching a plateau of ~3.5 at 0.1 M D-glucose. These results indicate that D-glucose is not limiting at concentrations above about 0.1 M; a D-glucose concentration of 0.2 M was used in all subsequent experiments where CA was determined.

7.3.2 Effect of Curing Time of Hydrogel on Enzymatic Activity

The effect of the curing time on CA was investigated by using hydrogels prepared by depositing 10 µL drops of GOx/PEGDGE mixture on PPF and curing for 6, 15, 24, 48 and 72 hours. Samples were prepared in duplicate at each curing time.

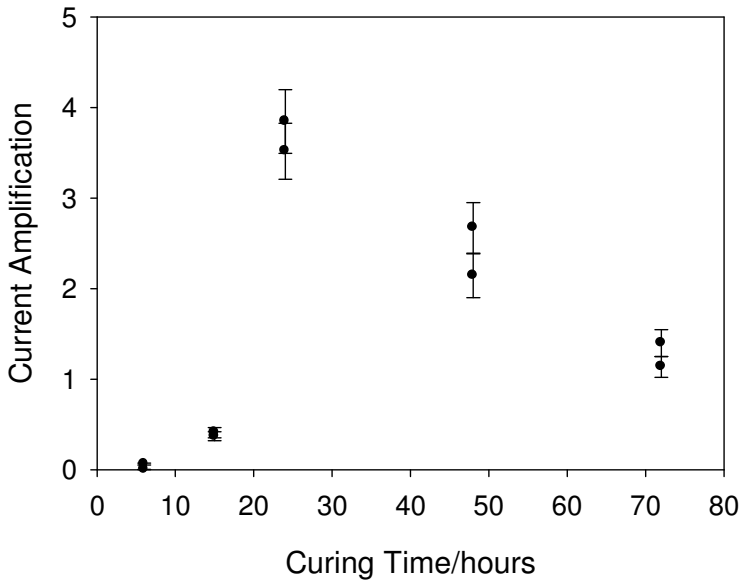

Figure 7.3. Plot of CA vs. curing time for GOx/PEGDGE hydrogels physisorbed on PPF by curing at (25 ± 2) ºC in the absence of light.

Figure 7.3 shows a strong dependence of CA on curing time; CA increasing between zero and 24 hours curing time and then decreasing between 24 and 72 hours. To further investigate this behavior, optical microscopy and step profilimetry were used.

Figure 7.4 shows optical microscopy images of four hydrogels prepared using different curing times, followed by the standard post-curing treatment (24 hours immersion in PB with gentle agitation). For the sample cured for 15 hours (a), only a small amount of hydrogel, in the form of a ring, was observed on the surface after immersion in PB. When the curing time was extended to 24 hours (b) more hydrogel material was observed but the film was still very inhomogeneous, with evident "gaps" in its structure. After 48 (c) and 72 hours (d) curing time a continuous hydrogel film is seen on the PPF surface. The hydrogel films in Figure 7.4 have all been subjected to the standard post-curing treatment, that is, 24 hours immersion in PB with gentle agitation, prior to imaging. In summary, the images show that the amount of hydrogel stable to the post-curing treatment increases up to 48 hours curing time (and possibly thereafter).

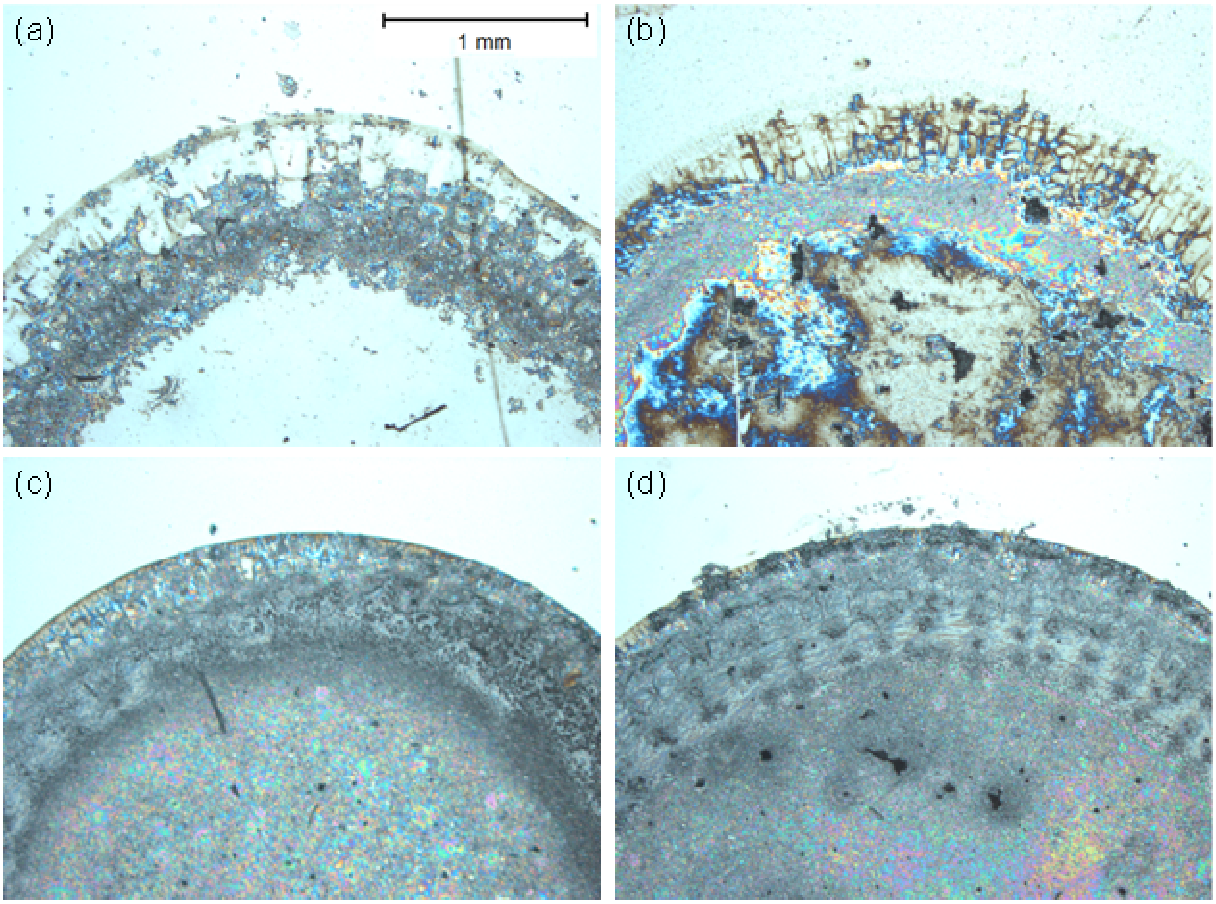

Figure 7.4. Optical microscope images of GOx/PEGDGE hydrogels physisorbed at PPF using curing times of 15 (a), 24 (b), 48 (c) and 72 (d) hours.

Step profilimetry was used to quantify the effect of curing time on hydrogel thickness. Line profiles were obtained by scanning across the PPF-hydrogel surface of samples prepared at curing times of 24, 48 and 72 hours. These revealed a relatively thick outer ring (~200 µm wide) and a thinner central region. The thicknesses of the outer and central regions were analysed separately, as described in section 7.2.7, and the results are shown in Figure 7.5. The uncertainties for hydrogel thicknesses are large for both the outer (a) and central (b) regions due to highly variable and rough hydrogel surfaces. However, in both regions the thickness clearly increases when the curing time was extended from 24 to 72 hours. This indicates that the amount of hydrogel material stable to the post-curing treatment increases from 24 to 72 hours curing time (and possibly thereafter).

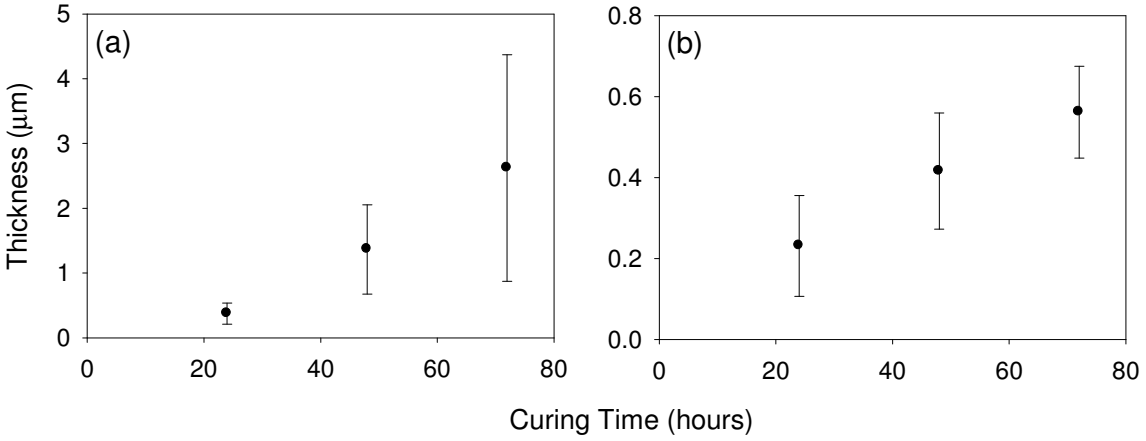

Figure 7.5. Plots of hydrogel thickness vs. curing time for GOx/PEGDGE hydrogels physisorbed at PPF using various curing times. The outer (a) and central regions (b) of the hydrogels were analyzed separately.

Considering the optical microscopy and step profilimetry data, along with the relationship between CA and curing time shown in Figure 7.3, it is proposed that the crosslinking reaction between GOx and PEGDGE continues for at least 72 hours after the deposition of the GOx/PEGDGE drop on to the PPF surface. More extensive crosslinking leads to a more stable hydrogel and less loss of material during post-curing immersion in PB. Hence, more hydrogel material at the surface, resulting from more crosslinking, accounts for the increase in CA between zero and 72 hours curing time.

The reason for the decrease in CA when curing is extended beyond 24 hours (Figure 7.3) is less clear. Optical microscopy and step profilimetry indicate that an increasing amount of stable film is formed for up to 72 hours during curing. Hence, the decease in CA cannot be attributed to the formation of thinner or less substantial hydrogels at longer curing times (>24 hours). One possibility is that more highly crosslinked hydrogels, which would be expected after longer curing times, have a less open structure which inhibits diffusion of FcOH and/or glucose through the hydrogel, thereby limiting the voltammetric response. However, FcOH voltammograms of PPF-hydrogel samples recorded in the absence of D-glucose show at most a 5 % decrease in the current when curing time was extended from 24 to 72 hours. Hence, it appears that FcOH diffusion is not significantly affected by an increase in curing time. Although the rate of diffusion of glucose was not measured, it is reasonable to assume (on the basis that glucose is

roughly the same size as FcOH) that the rate of diffusion of glucose through the hydrogel is also not significantly affected by the curing time. Furthermore, Heller and coworkers have shown that diffusion of glucose through GOx/PEGDGE films is not rate limiting for hydrogels formed under conditions similar to those used here.[9] Therefore it is unlikely that the decrease in CA observed at longer curing times is due to a decrease in the permeability of the hydrogel.

Another possible cause of the decrease of CA at curing times > 24 hours is decreased enzymatic activity at longer curing times. During the curing process, primary amine groups on the enzyme react with the epoxide groups of the PEGDGE crosslinker. It is possible that the activity of the GOx enzyme is compromised by this reaction. Furthermore, the higher degree of crosslinking in hydrogels formed at longer curing times would be expected to result in an increase in stiffness in the hydrogel which could affect enzymatic activity. Hence, it is tentatively proposed that the decrease in CA at longer curing times is due to a decrease in enzymatic activity, which either directly, or indirectly, results from more extensive crosslinking.

The results presented here show that tight control over curing time, and hence, over the extent of crosslinking in the hydrogel, is important to obtain surfaces with reproducible enzymatic activity. This is of particular importance in the preparation of electrodes for use in bio-fuel cells, where maximization of the enzymatic activity is desirable.

7.3.3 Long Term Stability of Activity of Physisorbed Hydrogels

Many of the anticipated applications of enzymatic hydrogels, including their use as bio-fuel cells, require that enzymatic activity is retained for a significant period of time. Although a curing time of 24 hours was seen to result in the highest CA for the samples prepared above, it is possible that hydrogels prepared at other curing times have better stability to extended immersion in solution. Hence, the stability of the activity of physisorbed hydrogels, prepared at different curing times, to prolonged immersion in PB was investigated.

For these experiments, the samples prepared in the previous section at curing times of 24, 48 and 72 hours were immersed in PB with gentle agitation on an orbital shaker (see section 7.2.3) for up to 102 days. The enzymatic activity of the samples was determined at approximately weekly intervals, by measuring the CA by cyclic voltammetry as described above.

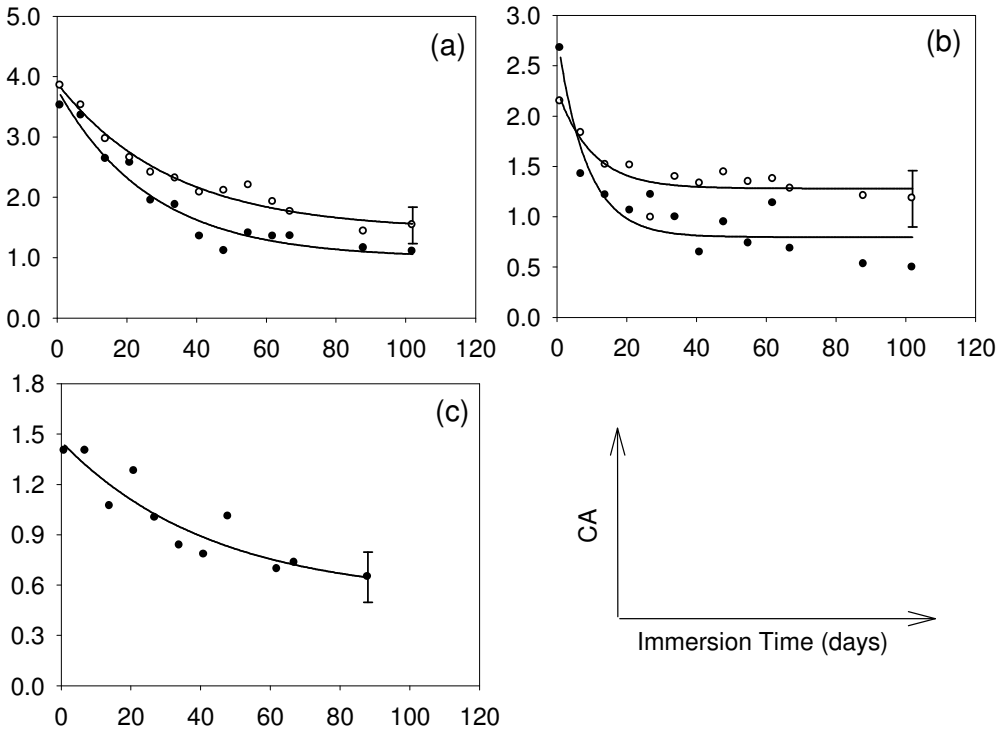

Figure 7.6. Plots of CA vs. immersion time in PB for GOx/PEGDGE hydrogels physisorbed at PPF using curing times of 24 (a), 48 (b), and 72 (c) hours. The error bars were calculated from the uncertainty in the concentration of FcOH and the uncertainties associated with the baselines for the cyclic voltammograms.

Figure 7.6 shows CA vs. immersion time for hydrogels cured for 24 (a), 48 (b), and 72 (c) hours; the symbols (●, ○) represent different individual PPF-hydrogel samples (the curves are least-squares fitted exponentials to guide the eye). For all samples, the CA decreases significantly during the full period of immersion in PB, but they all maintained significant activity even after immersion for > 80 days.

The decrease in CA (and enzymatic activity) with immersion time could be brought about by a number of factors. One possibility is that GOx leaches from the hydrogel during immersion in

PB. To test this possibility a 10 µL drop of GOx/PEGDGE mixture was deposited on a GC plate. The sample was cured for 24 hours and subjected to the standard post-curing treatment (immersion in 20 mL PB for 24 hours). Subsequently the sample was immersed in a fresh 10 mL solution of PB for 14 days. After removal of the sample from the second PB solution FcOH was added to give a 1.5 mM FcOH/PB solution. A cyclic voltammogram of the solution was recorded using a GC disk electrode by cycling between -0.1 and 0.4 V vs. SCE (initial potential -0.1 V). Subsequently D-glucose was added to the solution to give a solution of 0.2 M D-glucose-1.5 mM FcOH/0.1 M PB, and another cyclic voltammogram was recorded using the same parameters. Upon addition of D-glucose to the solution a small current amplification of 0.22 was obtained, indicating that GOx was present in the solution. The hydrogel-GC sample was immersed in fresh 10 mL solution PB for a further 14 days and the CA was of the solution was determined as described above. No CA was observed, indicating that no detectable amount of GOx was present in the solution after immersion for the second 14 day period. Hence, it can be concluded that GOx leaches from the hydrogel during the first 14 days of immersion in PB. This can partially account for the drop in CA of the PPF-hydrogel samples upon immersion in PB. However, since the CA is seen to decease at immersion times longer than 14 days, leaching of GOx from the hydrogel cannot be the only cause of the decrease in CA. A further possible cause of the decrease is depletion of GOx activity due to the presence of hydrogen peroxide (H_2O_2). Hydrogen peroxide is produced when oxygen competes with $FcOH^+$ to reoxidize the enzyme during monitoring of hydrogel activity in the presence of air. H_2O_2 is known to destroy the activity of GOx, and hence, H_2O_2 may be a further factor in the depletion of enzymatic activity seen in Figure 7.6.[21]

The significant remnant activity found here for physisorbed hydrogels after prolonged immersion in PB is inconsistent with the results of Barrière and coworkers who observed a drop of CA from ~ 2.0 to 0 (i.e., complete loss of catalytic activity) for GOx/PEGDGE hydrogels physisorbed on GC after 10 days immersion in unperturbed PB solution at 4 ° C.[11] A possible reason for the discrepancy is the difference in the type of carbon substrate. Barrière and coworkers used GC electrodes, whereas the results above were obtained on PPF. It is possible that the roughness of the substrate affects the adhesion of the hydrogel to the surface.[15] To test this possibility two samples were prepared using 10 µL drops of GOx/PEGDGE mixture deposited on GC plate

electrodes and cured for 24 hours. The samples were subjected to prolonged immersion in PB and their CA was monitored over 49 days at approximately weekly intervals.

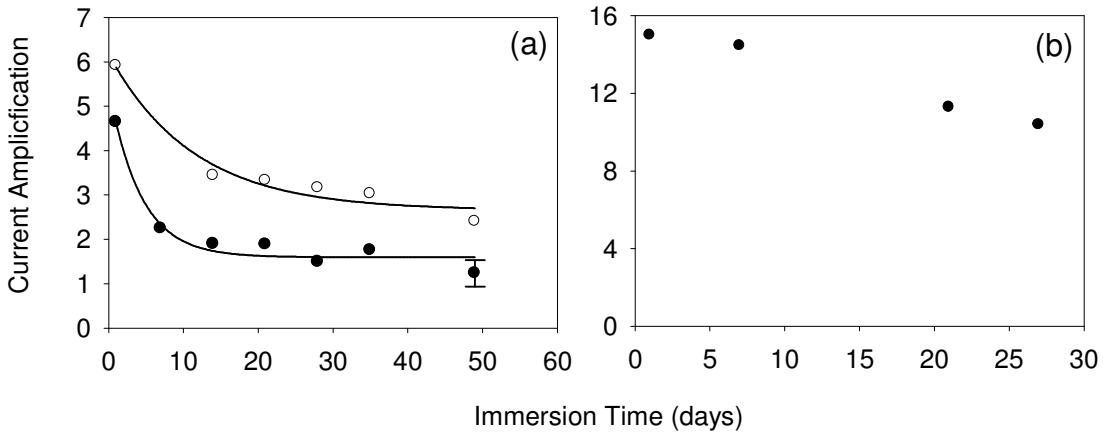

Figure 7.7. Plot of CA vs. immersion time in PB for GOx/PEGDGE hydrogels physisorbed on a GC plate (a) and GC disk electrode (b) after a curing time of 24 hours.

Figure 7.7 (a) shows that the CA vs. immersion time plots for GC-hydrogel electrodes follow a similar trend to that found for the PPF-hydrogel electrodes. Although the initial decrease in enzymatic activity is more rapid, it levels out at longer immersion times and a significant CA was observed after 49 days of immersion. This indicates that the difference in substrate cannot account for the differences in the stability of the activity of physisorbed hydrogels observed here and by Barrière and coworkers.[11]

Another possible explanation for the discrepancy is the orientation of the electrodes during immersion in PB. Barrière's group used GC rod electrodes suspended in PB with the electrode surface facing down. In the experiments presented here, the electrode surfaces were facing upwards during soaking. To test if this orientation difference could account for the conflicting results a 10 µL drop of GOx/PEGDGE mixture was deposited on a 0.071 cm^2 GC disk electrode and cured for 24 hours. The sample was subjected to prolonged immersion by suspension in PB with the hydrogel surface orientated downward and the CA was monitored over 27 days at approximately weekly intervals.

Figure 7.7 (b) shows a plot of CA vs. immersion time for a GC-hydrogel disk electrode. The higher apparent activity in comparison with PPF samples and GC plates is due to the fact that the entire electrode area is covered by the hydrogel in the case of the disk electrode. For the PPF and GC plates, the bare electrode area leads to a lower apparent CA. The CA of the GC-hydrogel disk electrode decreased by only ~ 30 % over 27 days and hence the orientation of the electrodes cannot account for the discrepancy. The most plausible explanation is that the better controlled curing times and temperatures used in the current work lead to more stable physisorbed hydrogels. The complete loss of enzymatic activity, observed by Barrière and coworkers over a 10 day period, would be expected for curing conditions that lead to low amounts of crosslinking.

7.4 Covalent Attachment of GOx Hydrogels

In the previous section, enzymatic hydrogels formed by depositing GOx/PEGDGE mixture on the carbon electrodes were shown to maintain significant enzymatic activity after 102 days immersion in PB, which suggests the physisorbed hydrogels are strongly adsorbed on the surface. Nevertheless, since some enzyme loss was detected, covalent attachment methods were investigated to explore whether the long-term stability of the hydrogels can be improved. The two covalent attachment methods have been discussed in Section 7.1 and are depicted in Schemes 7.3 and 7.4. The work described in the current section aims to determine whether these strategies lead to covalent immobilization of the GOx/PEGDGE hydrogel. Section 7.5 explores whether enhanced stability of enzymatic activity is obtained by covalent attachment of the hydrogel.

7.4.1 Covalent Attachment of Hydrogel using CP Films

The first strategy for covalently immobilizing GOx/PEGDGE hydrogels on carbon surfaces is depicted in Scheme 7.3 (n = 0). To briefly recap, GOx is covalently coupled carboxylic acid terminated films. Subsequently, the immobilized GOx is incorporated into the hydrogel matrix by deposition and curing of GOx/PEGDGE.

Two GC plate electrodes were modified with CP films via reduction of CBD as described in Section 7.2.5. Coupling of GOx was undertaken as described in Section 7.2.6.

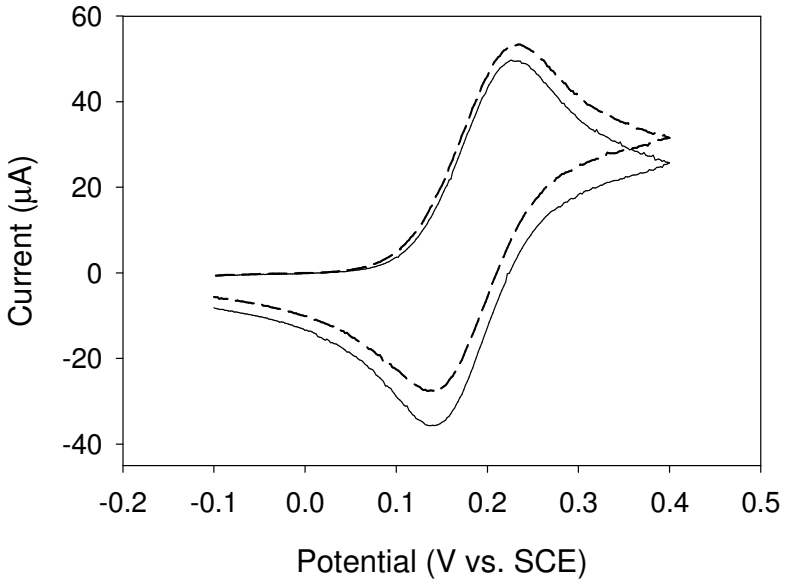

Figure 7.8. Cyclic voltammograms of GOx coupled to a CP film on a GC plate electrode recorded in 1.5 mM FcOH/0.1 M PB in the absence (—) and presence (---) of 0.2 M D-glucose. Initial potential = 0.1 V, scan rate = 5 mV s^{-1}.

To test for the presence of GOx at the surface, the electrodes were used to record cyclic voltammograms in 1.5 mM FcOH/PB, first the absence and then the presence of 0.2 M D-glucose, as described in Section 7.2.4. For both samples, a catalytic response was observed, with an increase in the FcOH oxidation current and a decrease in the corresponding reduction current (Figure 7.8) when D-glucose was added to the solution. This is consistent with the covalent coupling of GOx to the CP modified GC electrode. The coupling of GOx to diazonium derived films has been reported by a number of workers.[11, 22, 23] In the present work, it is expected that upon deposition and curing of a GOx/PEGDGE mixture, the covalently coupled GOx is incorporated into the resulting hydrogel matrix, rendering the hydrogel covalently bound to the surface.

7.4.2 Covalent Attachment of Hydrogel using AP Films

The second strategy for covalently immobilizing GOx/PEGDGE hydrogels on carbon surfaces is depicted in Scheme 7.4. Two GC disk electrodes were modified with NP films, which were reduced, as described in section 7.2.5. The resultant surface concentrations of electro-active AP groups, Γ_{AP}, were calculated as described in Section 3.3.3 to be 15.4×10^{-10} and 16.2×10^{-10} mol cm^{-2} for the two samples. After NP reduction, 20 µL of 2 mg/mL PEGDGE/H_2O mixture was spread (without mechanical contact with the surface) over the entire AP film area (0.71 cm^2) of one sample, which will be referred to as GC-AP-CL. 20 µL of H_2O only was spread in the same manner on the other reduced NP sample, which will be referred to as GC-AP-H_2O. Both samples were cured for 24 hours, and then sonicated in H_2O for 5 minutes.

Water contact angle measurements were undertaken on the samples before and after the deposition of PEGDGE/H_2O or H_2O. For GC-AP-H_2O, the contact angle did not change significantly (rising from 75 º to 77 º). However, for GC-AP-CL it dropped from 83 º to 48 º, indicative of a chemical change at the surface and consistent with the reaction of the AP groups with the epoxide functionalities of PEGDGE. Cyclic voltammograms were recorded of both the GC-AP-CL and the GC-AP-H_2O samples by cycling between 0.6 and 1.1 V vs. SCE in 0.1 M H_2SO_4 from an initial potential of 0.6 V (Figure 7.9).

The cyclic voltammogram of the GC-AP-H_2O sample (⋯) shows a broad oxidation peak at $E_{p,a}$ ≈ 0.9 V vs. SCE, which is assigned to the oxidation of AP groups present at the surface. In contrast, the GC-AP-CL sample (—) showed no distinct oxidation peak, indicating that the surface AP groups have reacted, presumably with the epoxide groups of the PEGDGE crosslinker. This result is consistent with the work of Pinson and coworkers who have reported the reaction of epichlorhydrin with an AP film produced via electro-reduction of NP films at GC.[24]

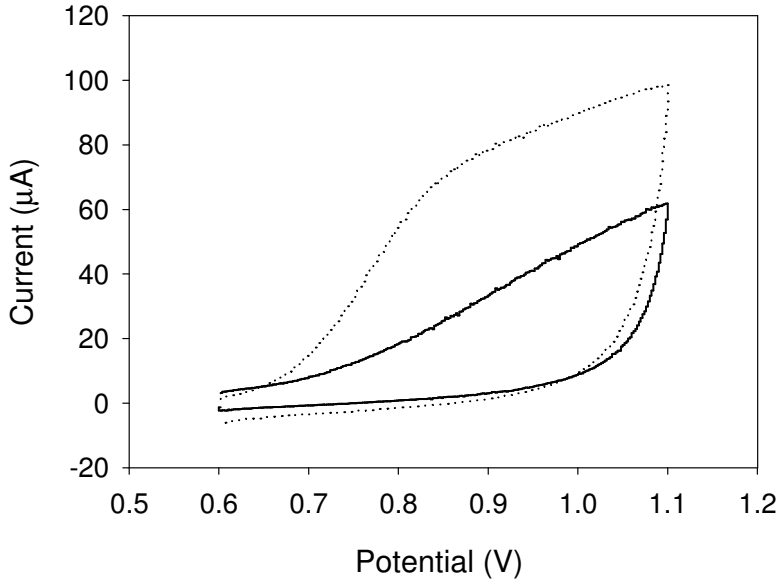

Figure 7.9. Cyclic voltammograms of GC plates modified after deposition of PEGDGE (—) and H_2O (···) on to reduced NP films recoded in 0.1 M H_2SO_4. Initial potential 0.6 V, scan rate 100 mV s^{-1}.

The work presented in the current section suggests that PEGDGE reacts with AP films on GC surfaces. Hence, the formation of a covalently bound hydrogel would be expected to result from the deposition and curing of a GOx/PEGDGE mixture on an AP modified carbon electrode.

7.5 Stability of Activity of Covalently Attached GOx Hydrogels

In the current Section the long-term stability of covalently immobilized GOx/PEGDGE hydrogels is investigated.

7.5.1 *Stability to Immersion*

Two GC plates were modified with NP films, which were electro-reduced, as described in Section 7.2.5. 10 µL drops of GOx/PEGDGE mixture were deposited on the resulting AP

modified electrode, and the samples were cured for 24 hours. The long term stability of the enzymatic activity of the samples was assessed by immersing the samples in PB, as described in Section 7.2.3, with the CA being determined approximately weekly.

The cyclic voltammograms of covalently immobilized hydrogel electrodes recorded in 1.5 mM FcOH/ PB showed currents and peak separations for the FcOH redox couple that were essentially the same as those recorded for physisorbed hydrogels at GC (Figure 7.1). This indicates that the AP film is not affecting the CA measurements by passivating the FcOH redox mediator response.

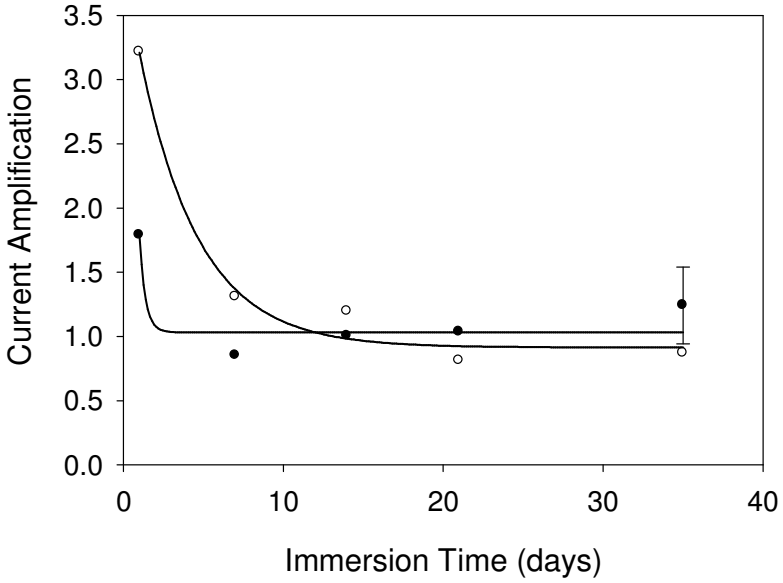

Figure 7.10. Plot of CA vs. immersion time for GOx hydrogels covalently bound to GC plates via an AP film. The hydrogels were prepared by curing for 24 hours.

Figure 7.10 shows a plot of CA vs. immersion time in PB for GOx/PEGDGE hydrogels covalently bound to a GC surface via an AP film. The trend is similar to that for physisorbed GOx/PEGDGE hydrogels at GC (Figure 7.7 (a)) and PPF (Figure 7.6) with the CA decreasing initially to relatively stable value. After 35 days the hydrogels retained ~33 % of their initial CA, again very similar to the results for physisorbed hydrogels under the same conditions. Hence there appears to be no increase in the stability of catalytic activity upon covalent immobilization.

The apparently lower CA activity of the covalent immobilized hydrogels compared to the physisorbed hydrogel can be attributed to sample to sample variations.

7.5.2 Stability to Sonication

The high stability of the physisorbed hydrogels to gentle agitation in PB suggests that more vigorous agitation might be needed to differentiate between the stabilities of the covalently bound and physisorbed systems. Hence, sonication was explored as another method of disruption.

Covalently bound hydrogels were prepared from GC plate electrodes modified with CP film, as described in Section 7.2.5. GOx was coupled to the modified electrodes as described in Section 7.2.6, then a 10 µL drop of GOx/PEGDGE mixture was deposited on the GC electrodes and cured for 24 hours. Physisorbed hydrogel samples were prepared by depositing a 10 µL drop of GOx/PEGDGE on GC plates and cured for 24 hours. Two samples of each type (physisorbed and covalently bound) were prepared and were immersed in PB prior to sonication experiments.

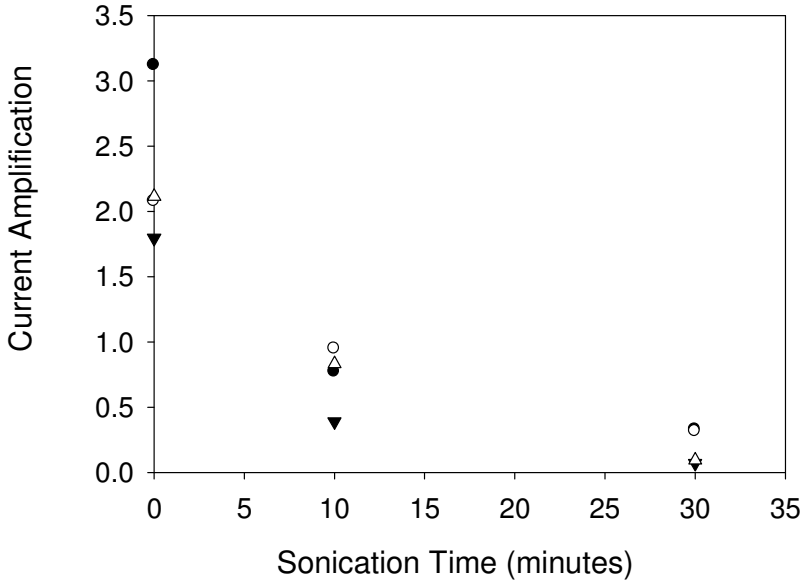

Figure 7.11. Plot of CA vs. sonication time at ~0ºC for covalently bound (○,●) and physisorbed (▼,Δ) GOx/PEGDGE hydrogels at GC.

Pre-sonication CAs of the samples was determined as described above. The samples were sonicated in cold PB ($T \approx 0$ ºC) for 10 minutes and the CAs of the samples were redetermined. The samples were then sonicated for a further 20 minutes and the CAs were determined for a third time.

Figure 7.11 shows the plots of the CA vs. sonication time. For both the covalently bound (○,●) and the physisorbed (Δ,▼) hydrogel samples, the CA was seen to decrease with sonication at approximately the same rate. Optical microscopy after the 30 minutes of sonication revealed no hydrogel remaining on the surfaces for either the covalently bound or the physisorbed hydrogel samples. The results indicate that the covalent attachment does not enhance the stability of the hydrogels to sonication.

7.6 Conclusion

The work described in this chapter was initiated with the aim of examining covalent attachment as a method for improving the adhesion of hydrogels to carbon surfaces. Initial experiments focused on the optimization of physisorbed hydrogls on carbon electrodes. A strong dependence of enzymatic activity on the curing time used to prepare the hydrogel was found, with the activity initially increasing with curing time, reaching a maximum after which the activity was seen to decrease with curing time. The physisorbed hydrogels proved to have good long term stability, maintaining significant activity after more than 100 days immersion in PB. This is inconsistent with a previous report where physisorbed hydrogels were seen to be stable for only 10 days immersion in PB. The discrepancy is attributed to insufficient control of curing conditions by previous workers. These results underline the need for tight control of curing times and conditions for the preparation of reproducible and stable enzymatic hydrogel electrodes. This appears to have been largely ignored in the literature.

Despite the high stability of the physisorbed hydrogel electrodes, further experiments were undertaken to determine if higher long term stability of the hydrogel activity could be obtained

by covalent attachment of the hydrogels to the electrode surfaces. Two covalent attachment strategies, based on modification of the carbon electrodes via reduction of aryldiazonium salts, were investigated. Initial experiments suggested that both attachment strategies would be expected to lead to covalent attachment of the hydrogels to the electrodes. However, the covalently immobilized hydrogels did not give higher long term stability of activity, to immersion or sonication, than physisorbed hydrogel electrodes in PB. The results suggest that the decrease in the catalytic activity of physisorbed hydrogels is not primarily due to poor adhesion to the surface, and that other factors, such as destruction of enzymatic activity by H_2O_2 are responsible for the observed decrease in activity.

7.7 References

1. Kim, J.; Jia, H. F.; Wang, P., Challenges in biocatalysis for enzyme-based biofuel cells. *Biotech. Adv.* **2006,** 24, 296-308.

2. Barton, S. C.; Gallaway, J.; Atanassov, P., Enzymatic biofuel cells for Implantable and microscale devices. *Chem. Rev.* **2004,** 104, 4867-4886.

3. Heller, A., Miniature biofuel cells. *Phys. Chem. Chem. Phys.* **2004,** 6, 209-216.

4. Mano, N.; Mao, F.; Heller, A., Characteristics of a miniature compartment-less glucose-O-2 biofuel cell and its operation in a living plant. *J. Am. Chem. Soc.* **2003,** 125, 6588-6594.

5. Chen, T.; Barton, S. C.; Binyamin, G.; Gao, Z. Q.; Zhang, Y. C.; Kim, H. H.; Heller, A., A miniature biofuel cell. *J. Am. Chem. Soc.* **2001,** 123, 8630-8631.

6. Mano, N.; Mao, F.; Shin, W.; Chen, T.; Heller, A., A miniature biofuel cell operating at 0.78 V. *Chem. Commun.* **2003**, 518-519.

7. Mano, N.; Mao, F.; Heller, A., A miniature membrane-less biofuel cell operating at +0.60 V under physiological conditions. *ChemBioChem* **2004,** 5, 1703-1705.

8. Barriere, F.; Ferry, Y.; Rochefort, D.; Leech, D., Targetting redox polymers as mediators for laccase oxygen reduction in a membrane-less biofuel cell. *Electrochem. Commun.* **2004,** 6, 237-241.

9. Gregg, B. A.; Heller, A., Redox Polymer-Films Containing Enzymes .2. Glucose-Oxidase Containing Enzyme Electrodes. *J. Phys. Chem.* **1991,** 95, 5976-5980.

10. Gregg, B. A.; Heller, A., Redox Polymer-Films Containing Enzymes .1. a Redox-Conducting Epoxy Cement - Synthesis, Characterization, and Electrocatalytic Oxidation of Hydroquinone. *J. Phys. Chem.* **1991,** 95, 5970-5975.

11. Pellissier, M.; Barrière, F.; Downard, A. J.; Leech, D., Improved stability of redox enzyme layers on glassy carbon electrodes via covalent grafting. *Electrochem. Commun.* **2008,** 10, 835-838.

12. Mano, N.; Kim, H. H.; Heller, A., On the relationship between the characteristics of bilirubin oxidases and O-2 cathodes based on their "wiring". *J. Phys. Chem. B* **2002,** 106, 8842-8848.

13. Mano, N.; Kim, H. H.; Zhang, Y. C.; Heller, A., An oxygen cathode operating in a physiological solution. *J. Am. Chem. Soc.* **2002,** 124, 6480-6486.

14. Mano, N.; Mao, F.; Heller, A., A miniature biofuel cell operating in a physiological buffer. *J. Am. Chem. Soc.* **2002,** 124, 12962-12963.

15. Boland, S.; Jenkins, P.; Kavanagh, P.; Leech, D., Biocatalytic fuel cells: A comparison of surface pre-treatments for anchoring biocatalytic redox films on electrode surfaces. *J. Electroanal. Chem.* **2009,** 626, 111-115.

16. Aoki, A.; Heller, A., Electron-Diffusion Coefficients in Hydrogels Formed of Cross-Linked Redox Polymers. *J. Phys. Chem.* **1993,** 97, 11014-11019.

17. Heller, A., Electrical Connection of Enzyme Redox Centers to Electrodes. *J. Phys. Chem.* **1992,** 96, 3579-3587.

18. Mano, N.; Heller, A., A miniature membraneless biofuel cell operating at 0.36 V under physiological conditions. *J. Electrochem. Soc.* **2003,** 150, A1136-A1138.

19. Kim, H. H.; Mano, N.; Zhang, X. C.; Heller, A., A miniature membrane-less biofuel cell operating under physiological conditions at 0.5 V. *J. Electrochem. Soc.* **2003,** 150, A209-A213.

20. Barrière, F.; Kavanagh, P.; Leech, D., A laccase-glucose oxidase biofuel cell prototype operating in a physiological buffer. *Electrochim. Acta* **2006,** 51, 5187-5192.

21. Martens, N.; Hindle, A.; Hall, E. A. H., An Assessment of Mediators as Oxidants for Glucose-Oxidase in the Presence of Oxygen. *Biosens. Bioelectron.* **1995,** 10, 393-403.

22. Bourdillon, C.; Delamar, M.; Demaille, C.; Hitmi, R.; Moiroux, J.; Pinson, J., Immobilization of Glucose-Oxidase on a Carbon Surface Derivatized by Electrochemical Reduction of Diazonium Salts. *J. Electroanal. Chem.* **1992,** 336, 113-123.

23. Liu, G. Z.; Paddon-Row, M. N.; Gooding, J. J., A molecular wire modified glassy carbon electrode for achieving direct electron transfer to native glucose oxidase. *Electrochem. Commun.* **2007,** 9, 2218-2223.

24. Allongue, P.; Delamar, M.; Desbat, B.; Fagebaume, O.; Hitmi, R.; Pinson, J.; Saveant, J. M., Covalent modification of carbon surfaces by aryl radicals generated from the electrochemical reduction of diazonium salts. *J. Am. Chem. Soc.* **1997,** 119, 201-207.

Chapter 8. Conclusion

The work described in this thesis concerns the modification of surfaces with thin (nanometer thick) films via both electrochemical and spontaneous reactions with aryldiazonium salts. The resulting films have been characterized by electrochemistry, atomic force microscopy (AFM), water contact angle measurements, x-ray photoelectron spectroscopy (XPS), scanning electron microscopy (SEM) and optical microscopy. Applications of the modification methods in the patterning of surfaces by microcontact printing (μCP) and improvement in the stability of enzymatic hydrogels have been investigated.

Initially, the suitabilities of several electro-active modifiers for film characterization studies were investigated by modifying glassy carbon (GC) in both aqueous acid and acetonitrile (ACN) via electrochemical reduction of the corresponding diazonium salts. The *p*-nitrophenyl (NP) modifier was determined to be the most suitable and was used most commonly for subsequent studies. It was found that films formed in aqueous conditions tend to be denser and have lower surface concentrations than those formed in ACN, in agreement with the conclusion reached by Downard and coworkers in an earlier study of NP films at pyrolysed photoresist (PPF).[1] The denser films formed in aqueous conditions are believed to inhibit electron transfer from the electrode to diazonium cations in solution more strongly than those formed in ACN, leading to lower surface concentrations.[1]

The modification of carbon (GC and PPF) and gold substrates via spontaneous reaction with aryldiazonium salts was investigated in both aqueous acid and ACN. The spontaneous reaction of *p*-nitrobenzene diazonium salt (NBD) with GC occurred in both aqueous conditions and ACN, but it was more facile in the former. As in the case of electrochemical modification, films formed in aqueous acid were denser than those prepared in ACN. At PPF substrates, modification occurred significantly and consistently in aqueous conditions but not in ACN. This can be attributed to the lower open circuit potential (OCP) relative to the NBD reduction peak of PPF in aqueous conditions. This is consistent with the proposal that spontaneous modification proceeds via electron transfer from the substrate to the diazonium salt in solution, leading to reduction of

the diazonium salt to an aryl radical. A possible alternative explanation for the sensitivity to the solvent would be the necessity for a physisorption step prior to modification. Physisorption is expected to be more effective in aqueous conditions than in ACN, and other workers have found evidence for such a step during modification of nanotubes using diazonium salts.[2] Nevertheless, further evidence for the reduction of the diazonium salt by carbon surfaces at OCP was found. In all three cases where significant modification was observed (aqueous conditions at GC and PPF, and ACN at GC) a large increase in OCP of the substrate upon addition of NBD, consistent with electron transfer to NBD, was observed. In the case where inconsistent modification and low surface concentrations were observed (PPF in ACN), only a small increase in OCP upon addition of NBD was observed. If the spontaneous reaction proceeds via electron transfer from the substrate to the diazonium cation, film growth should become self limiting at a thickness where the electron transfer is blocked. Plotting the surface concentration of NP groups, or the film thickness, against immersion time shows diminishing film growth at longer immersion times. However, the uncertainties and scatter in the data were too large to determine whether the films are genuinely self limiting. NP films formed by spontaneous modification of PPF show high stability, with no significant film loss of material, even after extended sonication in ACN. This is presumably due to the formation of strong covalent C-C bonds between the surface and the NP modifier. Further evidence of covalent bonding comes from the observation that the diazonium cation moiety reacts during modification.

AFM film thickness measurements determined that films grow up to 3.8 nm thick, consistent with the formation of multilayers of up to 3-4 layers of NP groups thick. The slope of a plot of the NP surface concentration vs. the film thickness gave a packing density of ~30 % of that for a closely packed monolayer on a flat surface. Hence, it can be concluded that the films are loose-packed multilayers. Loose-packed multilayers with a packing density of ~20 % were also observed upon electrochemical reduction of NBD at PPF by previous workers.[1] Hence, the films formed by the spontaneous reaction have a similar structure to those formed electrochemically.

Sensitivity of the spontaneous reaction of NBD with gold to solvent was also observed, with modification being successful in aqueous conditions but not in ACN. As with modification of carbon surfaces, an increase in the OCP of the gold electrode was observed upon addition of

NBD in aqueous acid. Furthermore, both of the surface concentrations and film thicknesses indicated that film growth is self limiting. This is strong evidence that the spontaneous modification of gold proceeds via electron transfer from the substrate to the diazonium cation in solution, despite doubts of previous workers that the gold substrate is capable of reducing the diazonium cations.[3] If the spontaneous reaction proceeds by this mechanism then diazonium salts with lower reduction potentials (e.g., resulting from electron donating *para* substituents) may not be reduced. Hence, the modification of gold by spontaneous reaction with *p*-carboxybenzene (CBD) and *p*-methoxybenzene diazonium salts (MBD) was investigated. In the case of the carboxybenzene derivative, modification was consistently observed, as expected by comparison between the reduction peak of CBD and the OCP of gold. However, with MBD, modification was observed on only a fraction of the duplicate samples. This is consistent with the variation of OCP values found for gold samples, spanning from within the range of the reduction peak of MBD to more positive potentials. Sample-to-sample variation in the OCP leads to modification for some samples but not others.

Gold substrates modified via spontaneous reaction with NBD were analyzed by XPS, cyclic voltammetry and AFM film thickness measurements. XPS indicated that ~30 % of the NP groups in the film have azo functionalities associated with them, similar to the azo content found previously at NP films prepared by electrochemical reduction of NBD at GC.[4] AFM film thickness measurements indicated the formation of films 2-3 layers of NP groups thick, at limiting film thickness. The packing density of the films was found to be ~50 % of that for a closely packed monolayer on a flat surface. This is higher than densities found for NP films formed electrochemically[1] and spontaneously (Chapter 4) at PPF surfaces.

The stability of spontaneously formed NP films was found to be much lower at gold than at PPF with ~80 % desorption after extended sonication in ACN. Films prepared electrochemically in aqueous conditions at gold also showed film loss of ~80 % after prolonged sonication in ACN, but those prepared electrochemically in ACN lost only ~60 % of the NP groups. Hence the modification medium (aqueous vs. ACN) rather than the modification method (electrochemical vs. spontaneous) dictates the stability of the films formed at gold. This may be due to the presence of more physisorbed film material in the films formed in aqueous conditions due to the

lower solubility of aryl dimers and oligomers in those conditions than in ACN. This could leave them entrapped in the film at the surface, preventing binding of aryl radicals to the surface. An alternative explanation is different rearrangements of the gold surfaces in the two media, leading to binding to different to surface sites with different bond strengths.

A major disadvantage of films formed spontaneously at gold, in comparison with those formed at carbon, is their poorer stability, making them less attractive for many applications where strong binding is required. Nevertheless, films formed at gold did show more reproducible surface concentrations and film thickness, presumably since gold surfaces are more homogeneous. This allowed us to demonstrate that the films are definitely self limiting, in strong support of the view that spontaneous modification proceeds via electron transfer from the substrate to the diazonium cation in solution. In terms of applications, the films formed spontaneously at gold are unlikely to be especially useful, since they offer no obvious stability advantage over SAMs formed at gold by thiol chemistry.

The weight of the evidence presented in this thesis supports the view that spontaneous modification using aryldiazonium salts proceeds via electron transfer from the substrate (at OCP) to the diazonium cation in solution. The fact that this will occur only if the OCP of the surface is sufficiently negative relative to the reduction potential of the diazonium cation presents a major disadvantage in comparison with electrochemical modification, where an appropriate potential can be applied. Furthermore, since the limiting thickness of the films is dictated by the OCP, and since sample-to-sample variation of the substrate OCP is observed, this limiting thickness is also expected to vary. Finally, since the OCP shifts during modification, and in a way that varies from one sample to another, preparation of reproducible surfaces is likely to be more difficult by spontaneous modification. In general, electrochemical modification is possible with a wider range of modifiers and is likely to give more reproducible films, and with a wider range of possible film thicknesses, than can be achieved by spontaneous modification. However, there are circumstances where spontaneous modification does have advantages. Firstly, no potentiostat is required. Secondly, it is a useful technique for modifying particles in solution (e.g., carbon powder and nanotubes). Thirdly, it allows for the possibility of microcontact printing (μCP) using aryldiazonium salts.

μCP was initially investigated by printing NBD on PPF substrates. Cyclic voltammetry confirmed the presence of NP groups and absence of the diazonium cation moiety (indicating that it has reacted) on the PPF surface after printing. Large sample-to-sample variations in the surface concentrations and film thicknesses were attributed to variable contact between the stamp and the surface. Printing on gold substrates gave more reproducible surface concentrations, indicating that the properties of the PPF surface also contribute to the variations in NP films formed by printing at PPF. However, films formed spontaneously at PPF have higher stability than those formed at gold. Hence, the majority of the printing work was carried out at PPF. CP films were printed on PPF and, after activation of the CP functionalities, coupling of *p*-nitroaniline to the modified surfaces was demonstrated. The ability to couple molecules onto printed films has potential applications in a range of areas. Two component surfaces with different chemical functionalities in different, well-defined, areas were also prepared.

One of the primary advantages of μCP with diazonium salts, as opposed to thiols and silanes, is that they are expected (and in part have been shown) to react at a large number of conducting and semiconducting substrates. Patterns formed by μCP using diazonium salts were imaged at PPF, Au, Si-H and Cu surfaces by SEM, thus demonstrating that μCP using aryldiazonium salts can serve as a general method for patterning conducting and semiconducting substrates with thin organic films. This is a significant result in the patterning of thin organic films.

A further application of aryldiazonium derived films was explored. This work was aimed at improving the stability of glucose oxidase (GOx) hydrogels (for use in bio-fuel cells) by covalent immobilization of the hydrogels on modified carbon electrodes. Two immobilization strategies were shown to result in covalent bonding between the carbon electrodes and the hydrogels. However, contrary to the results of other workers,[5, 6] , no advantage in terms of stability of hydrogel activity, in comparison physisorbed hydrogels, was seen upon covalent immobilization. The activities of the hydrogels are strongly dependent on tight control of curing conditions and physisorbed hydrogels prepared at optimized curing conditions are much more stable than has previously been reported.[5, 6] The discrepancy with the results presented by others is attributed to insufficient control of curing conditions in the earlier work.

Future work on the spontaneous modification of carbon and gold surfaces could focus on the effects of the solvent. By studying the spontaneous reaction in a range of solvents it should be possible to determine whether the sensitivity of the reaction to the medium is a result of an essential physisorption step or different substrate OCPs in different solvents. Other work could focus on the structure and stability of spontaneously prepared diazonium cation derived films on a range of substrates, since the stability and density of NP films prepared in this way appear to be substrate dependent. Detailed stability and characterization studies need to be carried out at a range of surfaces to determine the possible applications of the films on a case-by-case basis. The cause of the instability of NP films prepared at gold surfaces in aqueous acid is unclear, and hence, the exact nature of the interaction between the film and the surface (i.e., whether a Au-C bond is present) requires further investigation, possibly using spectroscopic techniques. It is worth noting that the instability of the films could be exploited to elucidate their structure; sonication of high-area modified gold would result in signifcant film material desorbing into the solvent, possibly allowing for NMR studies.

μCP using diazonium salts is an area that requires significant further work if it is to realize its potential. Optimization of the printing inks (both solvent and diazonium cation concentrations) may allow for better control of film thicknesses. The reduction of feature size on the stamps would increase the technique's relevance to a wider range of applications. Poly(dimethylsiloxane) PDMS alternatives can also be investigated for fabrication of the stamps. Hydrophilic materials would also allow printing with aqueous inks without the need for O_2 plasma treatment. In the build-up approach for multicomponent system preparation, the reactivity of the underlying film (in the patterned areas) to coupling reactions needs to be tested to determine the scope of potential applications. Other work could focus on developing techniques for printing on non-conducting surfaces. Since the spontaneous reaction appears to proceed via reduction of the diazonium cation by the surface, μCP using diazonium salt/solvent inks would not be expected at non-conducting surfaces. However, this limitation might be overcome by adding a chemical reducing agent to the ink. Applications of surface patterning by μCP with aryldiazonium salts also warrant investigation. Patterning on conducting substrates may allow the fabrication molecular electronic junction arrays, while tethering of biomolecules onto patterned surfaces could be used for the preparation of biosensor arrays.

As a final note, covalent attachment of hydrogels to surfaces appears to offer no advantage, in terms of stability of enzymatic activity, over physisorption. Since the physisorbed hydrogels exhibit excellent adhesion to the surface, optimization of the hydrogels should focus on other factors to improve their performance, such as eliminating degradation of the catalytic activity by H_2O_2.

1. Brooksby, P. A.; Downard, A. J., Electrochemical and atomic force microscopy study of carbon surface modification via diazonium reduction in aqueous and acetonitrile solutions. *Langmuir* **2004,** 20, 5038-5045.

2. Usrey, M. L.; Lippmann, E. S.; Strano, M. S., Evidence for a two-step mechanism in electronically selective single-walled carbon nanotube reactions. *J. Am. Chem. Soc.* **2005,** 127, 16129-16135.

3. Podvorica, F. I.; Kanoufi, F.; Pinson, J.; Cornbellas, C., Spontaneous grafting of diazoates on metals. *Electrochim. Acta* **2009,** 54, 2164-2170.

4. Yu, B. C.; Shirai, Y.; Tour, J. M., Syntheses of new functionalized azobenzenes for potential molecular electronic devices. *Tetrahedron* **2006,** 62, 10303-10310.

5. Pellissier, M.; Barriere, F.; Downard, A. J.; Leech, D., Improved stability of redox enzyme layers on glassy carbon electrodes via covalent grafting. *Electrochem. Commun.* **2008,** 10, 835-838.

6. Boland, S.; Jenkins, P.; Kavanagh, P.; Leech, D., Biocatalytic fuel cells: A comparison of surface pre-treatments for anchoring biocatalytic redox films on electrode surfaces. *J. Electroanal. Chem.* **2009,** 626, 111-115.